A Model for Cerebral Cortical Neuronal Group Electric Activity and its Implications for Cerebral Function

by

Fadi Nabih Karameh

Submitted to the Department of Electrical Engineering and Computer Science
in partial fulfillment of the requirements for the degree of

Doctor of Philosophy

at the

MASSACHUSETTS INSTITUTE OF TECHNOLOGY

February 2002

Author .....
Department of Electrical Engineering and Computer Science
January 11, 2002

Certified by....
.....
Munther A. Dahleh
Professor
Thesis Supervisor

Certified by..
.....
Steve G. Massaquoi
Assistant Professor
Thesis Supervisor

Accepted by .....
.....
Arthur C. Smith
Chairman, Department Committee on Graduate Students

A Model for Cerebral Cortical Neuronal Group Electric Activity and its Implications for Cerebral Function

by

Fadi Nabih Karameh

Submitted to the Department of Electrical Engineering and Computer Science
on January 11, 2002, in partial fulfillment of the
requirements for the degree of
Doctor of Philosophy

Abstract

The electroencephalogram, or EEG, is a recording of the field potential generated by the electric activity of neuronal populations of the brain. Its utility has long been recognized as a monitor which reflects the vigilance states of the brain, such as arousal, drowsiness, and sleep stages. Moreover, it is used to detect pathological conditions such as seizures, to calibrate drug action during anesthesia, and to understand cognitive task signatures in healthy and abnormal subjects.

Being an aggregate measure of neural activity, understanding the neural origins of EEG oscillations has been limited. With the advent of recording techniques, however, and as an influx of experimental evidence on cellular and network properties of the neocortex has become available, a closer look into the neuronal mechanisms for EEG generation is warranted. Accordingly, we introduce an effective neuronal skeleton circuit at a neuronal group level which could reproduce basic EEG-observable slow ($<$ 15 Hz) oscillatory phenomenon. The circuit incorporates basic laminar organization principles of the cortex. Interaction between neuronal groups is defined on three scales, namely the columnar (0.3mm), columnar assembly (1-2mm) and areal ($>$ 3mm). The effective circuit makes use of the dynamic properties of the layer 5 network to explain intra-cortically generated augmenting responses, restful alpha, slow wave ($<$ 1Hz) oscillations, and disinhibition-induced seizures.

Based on recent cellular evidence, we propose a hierarchical binding mechanism in tufted layer 5 cells which acts as a controlled gate between local cortical activity and inputs arriving from distant cortical areas. This gate is manifested by the switch in output firing patterns in tufted layer 5 cells between burst firing and regular spiking, with specific implications on local functional connectivity. This hypothesized mechanism provides an explanation of different alpha band (10Hz) oscillations observed recently under cognitive states. In particular, evoked alpha rhythms, which occur transiently after an input stimulus, could account for initial reogranization of local neural activity based on (mis)match between driving inputs and modulatory feedback of higher order cortical structures, or internal expectations. Emitted alpha rhythms, on the other hand, is an example of extreme attention where dominance of higher order control inputs could drive reorganization of local cortical activity. Finally, the model makes predictions on the role of burst firing patterns in tufted layer 5 cells in redefining local cortical dynamics, based on internal representations, as a prelude to

high frequency oscillations observed in various sensory systems during cognition.

Thesis Supervisor: Munther A. Dahleh
Title: Professor

Thesis Supervisor: Steve G. Massaquoi
Title: Assistant Professor

Thesis Reader: Emery N. Brown
Title: Associate Professor, Harvard Medical School-HST

To my loving parents,
Nabih and Nawal

Acknowledgments

Many thanks to God, *Alhamdu liLlah*, for everything.

I am deeply grateful to my Thesis Advisors Prof. Munther Dahleh and Prof. Steve Massaquoi. Munther has been simply a wonderful advisor: a constant beacon of intellect, encouragement, and support both at the academic and personal level throughout my studies at MIT. He is a role model for me, and I am forever indebted to him in foreseeing my seeds of intellect grow and in giving me the challenge, chance, and freedom to develop my research topic. I was also very lucky to have met and worked with Steve. His brightness, clarity of mind, support, endless energy, and patience with me were every bit inspiring to me and essential for this thesis.

I am also very grateful to Prof. Emery Brown for being on my committee. I greatly benefited from his deep insight and vast knowledge. Our discussions helped bring into focus essential parts of the thesis. I feel very fortunate and honored to have worked with those three bright scientists and trustworthy men.

This research would not have been possible without the financial support of the National Science Foundation. Early stages were also supported financially by Siemens AG. I am grateful for their support and especially the help of Dr Dragan Obradovic, and Dr Schurmann at Siemens in Munich for putting the diagnostic EEG problem forward.

To acknowledge what has contributed to this thesis means to take stock of a whole journey in a new world. The journey has come to end and its long winding roads have changed me. I have a vivid memory of when I first showed my college friends a reply letter from MIT. I remember Aida pronouncing MIT as met; she soon after realized what it meant, and she hugged me. I remember the anxiety of my parents of letting their child go; they soon after smiled and their faces were filled with hope.

The list of people who have lighted the tunnel for me is long. It starts in Lebanon, with my friends and professors at AUB, like Prof. Mounir Yehia, who helped and encouraged me to come to MIT, and continues here at MIT with Dr Marija Ilic and later with the many faculty, LIDS friendly environment, staff, and students.

My friends at LIDS have given me invaluable hours of support that aided me to get focused, being both a knowledge source and simply a sounding board. I want to especially mention my office mates Sean Warnick, Jorge Goncalves, Keith Santarelli and Ola Ayaso for the friendly happy environment in my office where almost anything funny can be said and many things can be done. Sean and Jorge were every bit helpful and cooperative even when pulling pranks. I am also grateful to the "extended office" people: Nuno Martins, Sridevi Sarma, Susan Beheshti, and Georgios Kotsalis for their friendship; and Fifa Monserrate for her smiling face and help over all those years.

The Lebanese bunch at MIT has provided for an invaluable social life, outlet, and distraction for which I am thankful, especially my friends Nadine Alameh, Hisham Kassab, Saad Mneimneh, Mahdi Mattar, Assef Zobian and Jamil Sobh.

Two people I am very indebted to for my sanity: Ibrahim Abou Faycal for being a good roommate and a true friend over all those years, and especially my girlfriend Jennifer Cardello for her love, unwaivering support in good and bad times, patience throughout my doctoral studies, and here ability to listen to me whining and to

laugh at my jokes. She has showed me the world through different, caring eyes and introduced me to the lovely italian culture and for that I am sincerely thankful.

Throughout my degree years, the invisible hand and unconditional support of my family have put me through my most difficult times. My younger sister Diana, who is a lovely image of myself, always reminded me of my beginings and made me smile. My sisters Olfat and Rola with Hisham and Rami along with my many happy little nephews and niece all fill my heart with comfort and incomparable joy.

My wonderful parents, to whom I owe it all, raised my ambition, will to search higher grounds and take challenges, the good man in me. My father's wisdom, insight, and morals; and my mom's love and prayers were always with me. I pray that your eagerness for science, dedication, and sacrifice to see me through this will always make you proud just as I am. I share this with you both.

Thank you and God bless you all.

Contents

1 Introduction **15**
- 1.1 Electroencephalography . . . 15
  - 1.1.1 Understanding EEG origins . . . 17
- 1.2 Electric activity of the brain . . . 19
  - 1.2.1 Relation between cellular firing and field potentials . . . 20
- 1.3 Modeling electric activity of the brain . . . 21
  - 1.3.1 Black box models . . . 22
  - 1.3.2 Neuronal group models . . . 27
- 1.4 A cerebral neuronal group electric activity model . . . 28
  - 1.4.1 Problem statement: realistic EEG modeling . . . 28
  - 1.4.2 Outline of the model and principal findings . . . 30
- 1.5 Thesis Outline . . . 34

2 Basic features of cerebral cortical neural anatomy and physiology **35**
- 2.1 The Neocortex . . . 38
  - 2.1.1 Neural phenotypes of the neocortex . . . 39
  - 2.1.2 Laminar structure of the neocortex . . . 41
  - 2.1.3 Major input and output pathways in neocortex . . . 43
  - 2.1.4 Hierarchical structures in the neocortex . . . 45
  - 2.1.5 Dominant synaptic organization in neocortex . . . 47
- 2.2 The Thalamus . . . 51

3 Oscillations in the Brain: Morphology and Cellular Basis **55**
- 3.1 States of vigilance associated with oscillatory EEG . . . 56
  - 3.1.1 EEG and Oscillations . . . 56
  - 3.1.2 Slow oscillatory states . . . 56
  - 3.1.3 Fast oscillatory states . . . 62
- 3.2 Cellular basis of Cortical Oscillations . . . 63
  - 3.2.1 Spindle oscillations . . . 63
  - 3.2.2 Delta Oscillations . . . 65
  - 3.2.3 Slow-wave oscillations . . . 66
  - 3.2.4 K-complex . . . 70
  - 3.2.5 SW seizures . . . 70
  - 3.2.6 Fast Oscillations . . . 73

3.3 Summary . . . 75

4 Hierarchical binding hypothesis **79**
4.1 Effective Skeleton Circuit . . . 80
4.2 Recent Findings in Cortical Neurophysiology . . . 83
4.2.1 Layer 5 pyramidal cells . . . 83
4.2.2 Layer 4 cells . . . 92
4.2.3 Inhibitory cells . . . 94
4.2.4 Synaptic organization . . . 99
4.2.5 Circuit dynamics . . . 103
4.3 Recent findings pertinent to the generation of certain cortical rhythms 105
4.3.1 Augmenting responses . . . 105
4.3.2 Alpha band oscillations . . . 106
4.3.3 Slow-wave Oscillations . . . 107
4.3.4 Seizures due to disinhibition . . . 107
4.4 A hypothesis . . . 108

5 Neocortical Circuit Models **117**
5.1 Cellular models . . . 117
5.1.1 General modeling scheme . . . 118
5.1.2 Layer 5 cells . . . 123
5.1.3 Layers 2, 3, and 6 Cells . . . 131
5.1.4 Layer 4 Spiny stellates . . . 132
5.1.5 Inhibitory Interneurons . . . 132
5.2 Connection Diagrams . . . 133
5.2.1 Synaptic connections within a minicolumn . . . 133
5.2.2 Synaptic connections within a column . . . 134
5.2.3 Synaptic connections within a columnar assembly . . . 134
5.2.4 Synaptic connections between areas . . . 135
5.2.5 Excitation sources . . . 136
5.3 Field potentials . . . 137

6 Simulations **141**
6.1 Augmenting Responses in Neocortex . . . 141
6.1.1 Main physiological observations . . . 142
6.1.2 Hypothesized circuit dynamics . . . 144
6.1.3 Simulations . . . 146
6.2 Alpha Rhythms . . . 155
6.2.1 Anatomical substrates of alpha rhythms . . . 158
6.2.2 Hypothesized mechanisms of alpha generation . . . 163
6.2.3 Simulations . . . 165
6.3 High Frequency Oscillations . . . 173
6.3.1 Physiological observations on induced gamma activity: . . . 173
6.3.2 Hypothesized mechanism . . . 176
6.3.3 Simulations . . . 178

6.4 Slow-wave Sleep Oscillations . . . 181
6.4.1 Hypothesized mechanisms . . . 182
6.4.2 Simulations . . . 183
6.5 Seizures due to Neocortical Disinhibition . . . 186
6.5.1 Main physiological observations . . . 186
6.5.2 Hypothesized circuit dynamics . . . 188
6.5.3 Simulations . . . 190
6.6 Discussion . . . 192
6.6.1 Control of layer 5 dendritic inhibition . . . 192
6.6.2 Scale limitations . . . 196

7 Conclusions **199**
7.1 Scenario of intracortical slow rhythm generation . . . 202
7.1.1 Sleep rhythms . . . 202
7.1.2 Awake rhythms . . . 202
7.1.3 Seizure-like states . . . 205
7.2 Prediction: The cognitive implications of alpha band rhythms . . . 205
7.2.1 Reorganization of local cortical assemblies . . . 205
7.2.2 Information transfer between cortical systems . . . 207
7.2.3 Synopsis on role of burst firing . . . 212
7.3 From neuronal group electric activity to EEG . . . 213
7.3.1 Layer 5 as a network oscillator . . . 214

A General Models of EEG generation **217**
A.1 Wilson Cowan models . . . 217
A.2 Alpha rhythm models . . . 218
A.3 Nunez Global model . . . 222
A.4 Signal processing techniques in EEG . . . 225

B Neural Diversities in Cerebral Cortex **227**
B.1 Neurons and Synapses . . . 227
B.2 Morphology . . . 227
B.3 Synapses . . . 230

C Simulation Parameters **235**
C.1 Notation . . . 235
C.2 Cellular currents . . . 236
C.3 Simulation scenarios . . . 236

List of Tables

2.1 Spatial scales of neocortical interactions 36

3.1 Summary table for main sleep/arousal EEG discussed 76

4.1 Summary of basic rhythms attributable to layer 5 dynamics 115

5.1 Neocortical cell model parameters 129
5.2 Distances of different cellular types from cortical surface used in computing surface field potential (per figure 5-14) 139

B.1 Common neocortical morphologies (adapted from Mountcastle [165]) 232

C.1 Model parameters for the slow wave (<1 Hz) oscillations simulation . 238
C.2 Model parameters for disinhibition-induced seizure simulation 239
C.3 Model parameters for Alpha Activity 240
C.4 Model parameters for Alpha Selectivity 241
C.5 Model parameters for Alpha Selectivity, figure C-1 242
C.6 Model parameters for Augmenting Responses 244

Chapter 1

Introduction

1.1 Electroencephalography

The electrocncephalogram, or in short EEG, is a recording of the electric activity generated by neuronal populations of the brain. Human scalp EEG is registered non-invasively with an array of electrodes which samples electric field potentials generated predominantly in the cerebral cortex and conducted through several layers of low conducting material, mainly the skull and scalp.

Scalp EEG recording has been long recognized as a clinical tool which monitors and reflects the vigilance state of the brain such as arousal, drowsiness, and sleep patterns (figure 1-1). It is also used to detect pathological conditions such as seizures, epilepsies and brain tumors, to calibrate drug action during anesthesia, to understand cognitive task signatures in healthy and abnormal subjects, and to study mental retardation, among other brain states.

Despite rivalry by newer imaging techniques such as functional MRI, the *real-time temporal resolution* of scalp EEG makes it an indispensable clinical tool in studying normal and pathological brain states; furthermore, its *noninvasivness* and low cost is attractive for continuous patient monitoring, such as to detect epileptic events, especially in children.

Clinical understanding of EEG involves manual or computer-aided identification of grapho-elements or signature waves whose appearance, reactivity, and spatial distribution over the scalp give indications of the current brain vigilance or functional state (figure 1-2). Such analysis of EEG signals is usually performed by a conventional spectral decomposition of individual channels, namely the following spectral bands with fuzzy upper and lower limits are considered:

Delta: below 3.5 Hz (usually $0.1 - 3.5$ Hz)
Theta: $4 - 7.5$ Hz
Alpha: $8 - 13$ Hz
Beta: $14 - 30$ Hz
Gamma: above 30 Hz

Different EEG observations have been linked to natural states of vigilance and tend to be either *localized* to specific areas of the head or more *globally-spread* across different areas. We will briefly describe the main rhythms of interest as subdivided, for our own purposes, into *low frequency oscillatory states* which include rhythms up to alpha range $< 14Hz$, and *high frequency oscillatory states* with frequencies higher than $14Hz$.

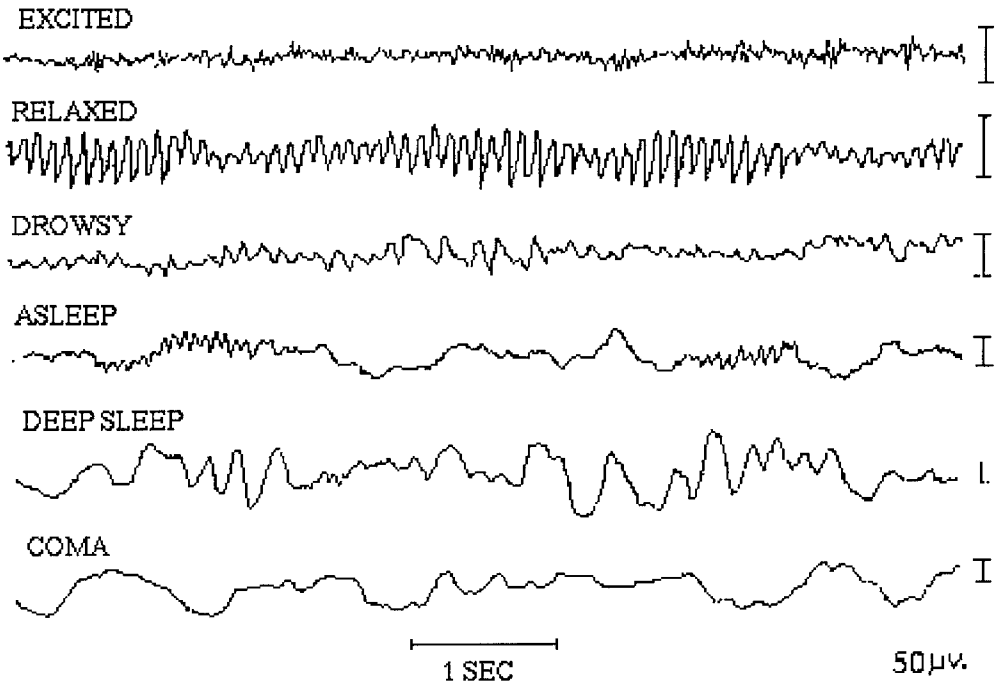

Figure 1-1: Sample scalp EEG recordings under several states of vigilance show different frequency content and amplitude (adapted from Nunez, 1995 [173].

Low frequency EEG rhythms: can occur either *locally* over specific recording channels, or *globally* over wide areas of the scalp.

Locally-induced low-frequency oscillations can be generated during specific awake states over spatially limited cortical structure. For example, alpha rhythms (8-13 Hz) are recorded primarily over the posterior regions of the head and are especially apparent during restful states with eyes closed. Such rhythms partially or completely block (disappear) when eyes are open or other afferent stimuli, mental activity is introduced. Similar alpha-band activity occurs over the motor cortex (electrodes C_3, C_4 in figure 1-2) and is known as rolandic mu rhythms.

Globally-induced low frequency EEG oscillations occur mostly in states affecting the general arousal state of the brain. Naturally-occuring sleep is one example where as a subject goes through drowsiness and into different non-REM sleep stages, EEG signals slow down to the delta-theta band and exhibit large amplitude waveforms

recorded over wide cortical structures. Characteristic signal templates can be identified in sleep progression. For example, posterior alpha starts mixing with slower rhythms as drowsiness deepens. In early sleep stages, a waxing-and-waning form of $8 - 14$ Hz activity termed *spindles* develop; this is then followed by increasing occurence of the slower activity termed *K-complexes* (< 1 Hz) which is a biphasic high-voltage event. Later stages of sleep (stages 3 and 4) are dominated by high-amplitude low frequency rhythms, mainly in the delta $0.1 - 4$ Hz range.

Globally-recorded rhythms can also be recorded under drug-controlled brain states, mainly anesthesia. In fact, some anesthetics such as barbituates produce spindle rhythms similar to those observed during sleep.

Finally, many pathological conditions produce abnormal slowing in EEG rhythms. Of interest are epileptic seizures and space-occupying lesions which can show either focally over specific cortical areas or generalized over both hemispheres. Although seizures can have varying morphologies and neural origins, they are generally vary large amplitude (spike-like) waves that occur at few cycles per second, sometimes with periods of fast runs (20 Hz).

High frequency EEG rhythms: Occuring in states of heightened arousal or mental activation, these fast rhythms (beta and gamma range) are usually localized over small areas of the cortex. The local nature of such rhythms is better understood when correlating fast activity recorded from different channels, where little or no coherence[1] between the different traces can be seen. The low pass nature of scalp recordings as well as the spatial scale of generation of these rhythms, mainly in spatially confined neural populations, drastically attenuates the appearance of fast EEG rhythms in standard measurements protocols. Note that fast EEG oscillatory activity is also recorded during periods or REM (Rapid Eye Movement) sleep.

Evoked EEG rhythms: Occuring over sensory areas such as motor and auditory cortices when appropriate stimuli are presented, these damped oscillations are usually referred to as event related potentials (ERPs). ERPs have been widely analyzed and help neurophysiologists diagnose various diseases of the central nervous system. For example, the latency of some visual response typically falls within some range for normal subjects; the absence of such response or extreme latency might indicate lesions in the sensory pathways. Also, evoked responses are used to study patients with cognitive and psychiatric disorders, such as amnesia, agnosia, schizophrenia, and depression.

1.1.1 Understanding EEG origins

Being a measure of electric field potentials generated within the cortex and sampled at a distance through high resistivity material, scalp EEG waves represent greatly

[1]The coherence between two channels is defined in engineering terms as a measure of similarity between the two signals. Frequency coherence describes how well the signal X correspond to a signal Y at each frequency.

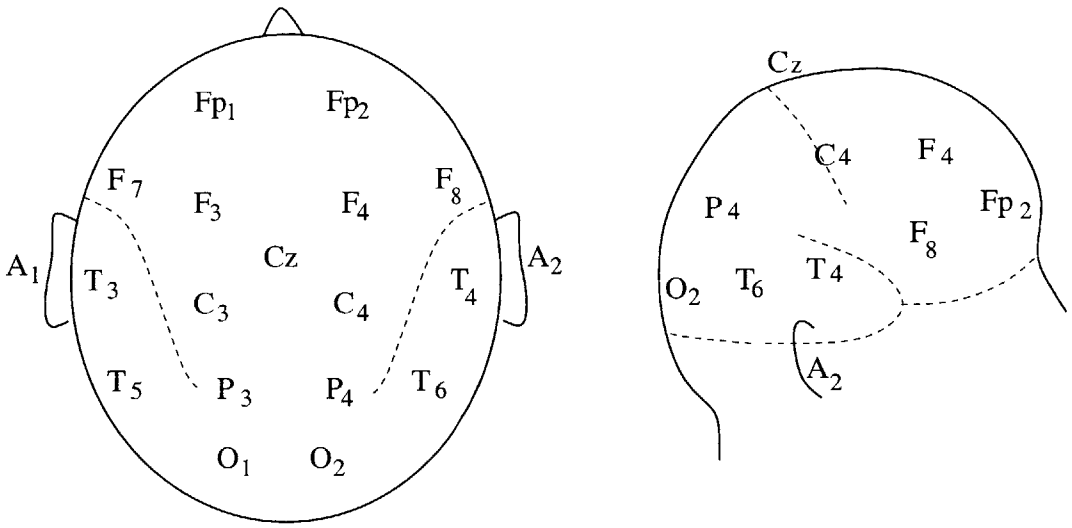

Figure 1-2: relative position of EEG electrodes on human head in the 10-20 channel system (Kandel 1991)

attenuated and spatially filtered versions of the inside-the-head or subdural counterpart. Accordingly, one expects that only highly coherent signal generators operating in close phase relationship within the neural substrate can be observable at the scalp. Thus, despite its excellent time resolution, the gross nature of scalp EEG imposes a limitation on the types of neural events that can be recorded and described.

While signal processing techniques have enriched the repertoire of successful EEG analysis stories (bispectral indices in anesthesia, for example), a fundamental gap in understanding the physiological implications of EEG in terms of brain functionality still exist (discussed in Karameh 2000, [109], see also appendix A). In fact, the correlation between EEG and brain functionality has traditionally been performed in terms of psychophysiological descriptions aided by computerized techniques (for example, alpha activity is correlated with restful states and disappears when the eyes are open).

A major challenge has been to go beyond phenomenological description into understanding the nature of neural activity that generates EEG oscillations, or what is known as the *forward modeling problem of EEG*[2]. Many skeptics dismiss the existence of such mapping citing the highly specific and complex operation of neural structures of the brain which provide for a high degree of variability in EEG origins across different brain regions and states. Although we contend that, in fact, while many cognitive events are unobservable at gross electric scale, forward models of many vigilance states can be obtained and could potentially become invaluable in providing a better understanding of vigilance states and its control, for example depth of anes-

[2]this contrasts with the inverse modeling problem, which usually involves, based on EEG multichannel recording, dipole localization within a three dimensional model of a human head (sphere or realistic, Kavanagh 1978 [113], Wang 1995 [251], Lopes da Silva 1996 [145], or recently intergrated with functional imaging as in Bonmassar et al 2001 [20]).

thesia and sleep, and in predicting and localizing pathological states such as seizures. Such forward models can also be the starting point in understanding the dynamics of evoked EEG in healthy and abnormal patients.

The forward modeling of EEG invariably requires a strong understanding of its neural origins, a fairly complicated task with the current knowledge in neural science. Our apprehension of such neural mechanisms has been drastically increased in the last decade or so, as more animal experiments are performed where electric activity of different isolated brain structures is probed in anesthetized and awake animals. Such experiments are usually carried out at the subdural level (surface EEG), intracortical level (electrocorticogram EcoG) and even intracellularly. A brief summary of these different scales will be presented next.

1.2 Electric activity of the brain

The scalp EEG recordings come at the coarsest spatial scale of measuring the electric activity generated by neural populations in the cerebral cortex.

The human cerebral cortex is a folded or convoluted layer of about 2 to $3mm$ thickness and total surface area of roughly 1600 cm^2. This layer is composed of about 10^{10} neurons that are highly interconnected and they compose what is known as grey matter. Each neuron receives as inputs to its dendrites and cell body around 10^3 to 10^5 connections or *synapses* which deliver electric currents from other cortical neurons and deeper brain structures such as the cerebellum (Nunez 1981 [171]). At its output, the neuron then transmits electric current through its output connections, usually to *dendrites* of other specific neurons. The neuronal interconnections (Fig 1-3) can be short, and hence occur within the grey matter, or they can extend over longer distances into other regions of the cortex and in this case occupy what is called the white matter which is immediately below the cortical grey matter.

With these connections varying between (i) immediate neighborhood (for example what is called a cortical column which is thought of as the smallest functional population), (ii) other functional populations (columns) in the vicinity, and finally (iii) connected regions at distant locations in the cortex, one can view the cerebral cortex as composed of several scales of interacting complex dynamic subsystems, whose activity comprises much of the conscious experience and cognition.

In studying neural substrates of spontaneous and evoked electric activity of the brain, the distinction is made in the recording process: (a) *single cell activity* both intra-cellular and extra-cellular, which give detailed description of neuronal firing and has seen drastic improvements and utility in animal experiments in the last two decades (b) *local field potentials* (LFP) within the cortex sampling the activity of a small neighborhood of several thousand neurons; this recording gained wide support with the study of cognitive relevance of gamma frequency oscillations , and (c) field potentials over the pial surface of the cortex also called *electrocorticogram (or surface* EEG); this is clinically utilized in localizing an monitoring epileptic foci in seizure-prone patients and has the advantage of circumventing the spatial smearing of the skull and scalp.

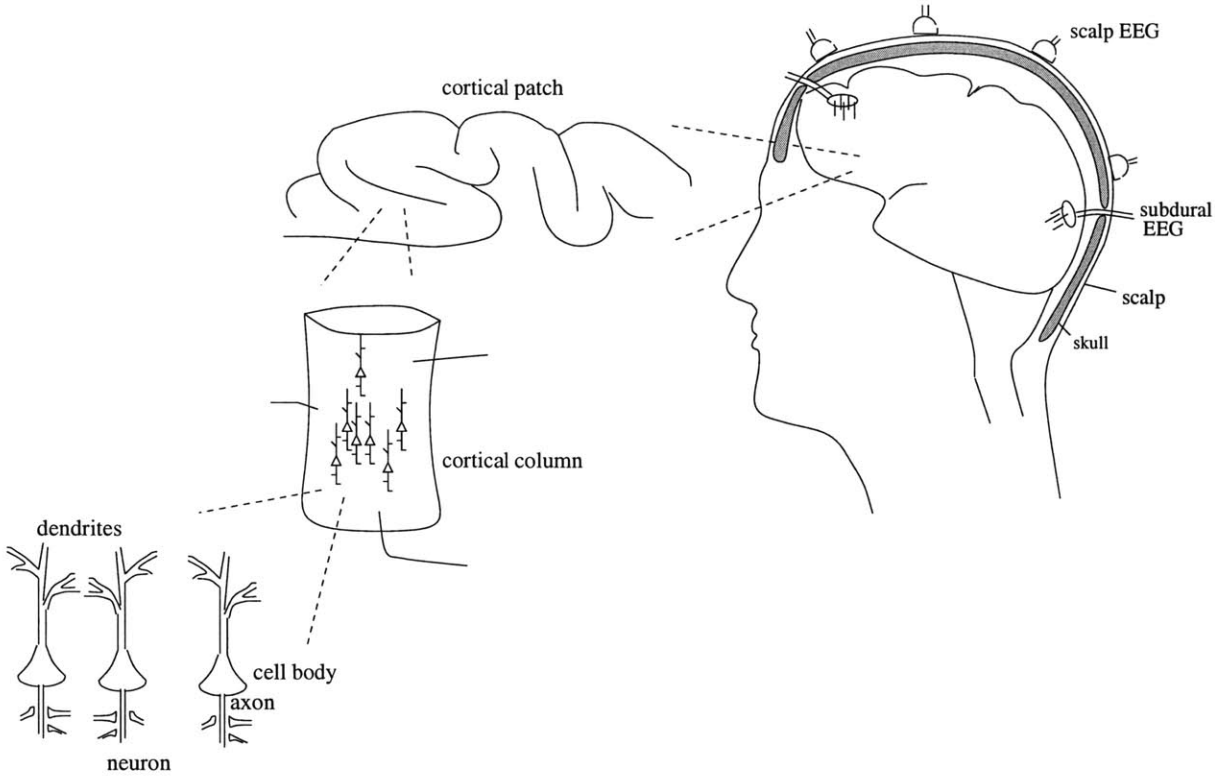

Figure 1-3: Several scales of recordings and activity

1.2.1 Relation between cellular firing and field potentials

While cellular recordings register the actual output of neurons in terms of action potential firings, local field potentials are recordings of the extracellular changes in voltage due to different currents transversing the medium and hence are more related to synaptic inputs to the cells (chapter 5). This has historically presented a question as to how local field potentials relate to neuronal output or action potential firing, since synaptic input to a neural population can originate both locally as well as due to long distance connections from other neocortical areas as well as deeper brain structures. Earliest relationships were drawn by Freeman on the direct correlation between firing of small isolated neuronal populations and the generated field potentials (Freeman 1975 [77]). The last decade has presented numerous evidence of the correlation between spike firing of neurons and the phase of local field potentials both at high frequencies (so called gamma oscillations, Singer 1995, [208]) and low frequencies (slow-wave sleep oscillations, Steriade 1993 [216]) and more recently in naturaly sleeping and awake animals (figure 1-4, Destexhe et al 1999 [62]).

A common feature in the above situation where field potentials reflect cellular firing is *the correlated or close-time firing of large populations of neurons* [3]. For ex-

[3] The ability of neuronal population in producing field potentials that is proportional to their firing can be explained by two factors, first the synchronized firing of recurrently connected neuron causes synaptic activity to summate thus creating large deviations in extracellular voltage, and second, the

ample, in high frequency oscillations of awake states, such correlated firing occurs among neurons lying within close spatial proximity and thus the resultant field potentials are low amplitude voltage oscillations that are well localized to the generating substrate. Low frequency oscillations of sleep, on the other hand, display correlations over larger distances and hence are of high amplitude and are observable over large areas of the cortex (figure 1-5).

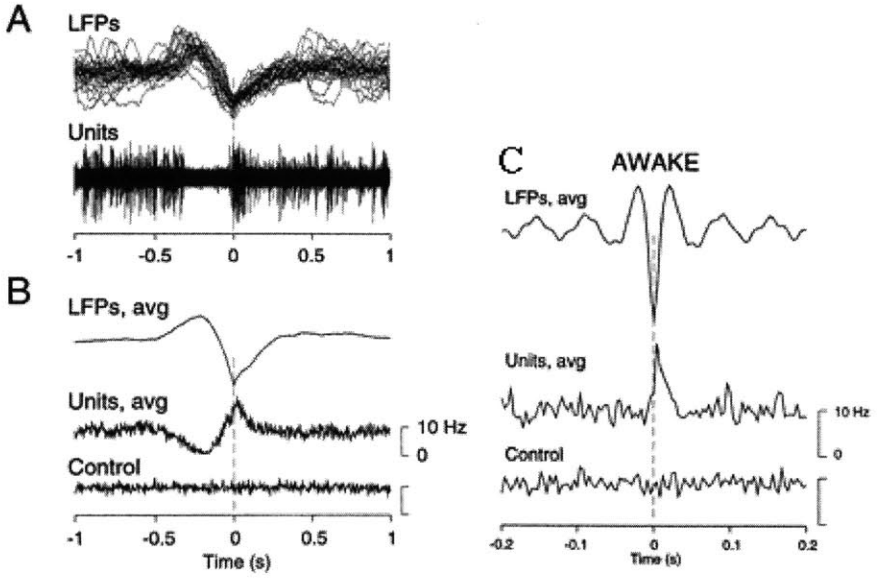

Figure 1-4: Correlation between local field potentials and neuronal firing in naturally sleeping and awake cats. A: traces of local field potential aligned at the maximum negative point and the corresponding multiunit firing in the same location of the cortex during slow-wave sleep. B. wave triggered average, which is obtained by averaging short windows of data selected by reference to the time of occurrence of a given trigger waveform (here maximum negative in LFP as in A) show direct relation between average unit firing and the LFP (control obtained by reshuffling the unit firing). C. Similar correlation is obtained during waking at a faster time scale. (Figure adapted from Destexhe et al 1999 [62]).

1.3 Modeling electric activity of the brain

The increasing evidence of the existence of a link between level of correlation in neuronal firing activity and field potentials provides a bridge between efforts to understand general EEG patterns and basic mechanisms of neural interactions at the cellular level. That, by understanding the responsiveness of neuronal groups, their basic dynamics and scale of interactions under specific input controls, one might be able to learn more about the origins of observed EEG under specific brain states. This will also help in developing specific experimental paradigms to test the model

spatial geometry of such cells, mainly that pyramidal cells are mostly aligned in a vertical direction, thus avoiding cancellation of generated field potentials from individual synchronized neurons.

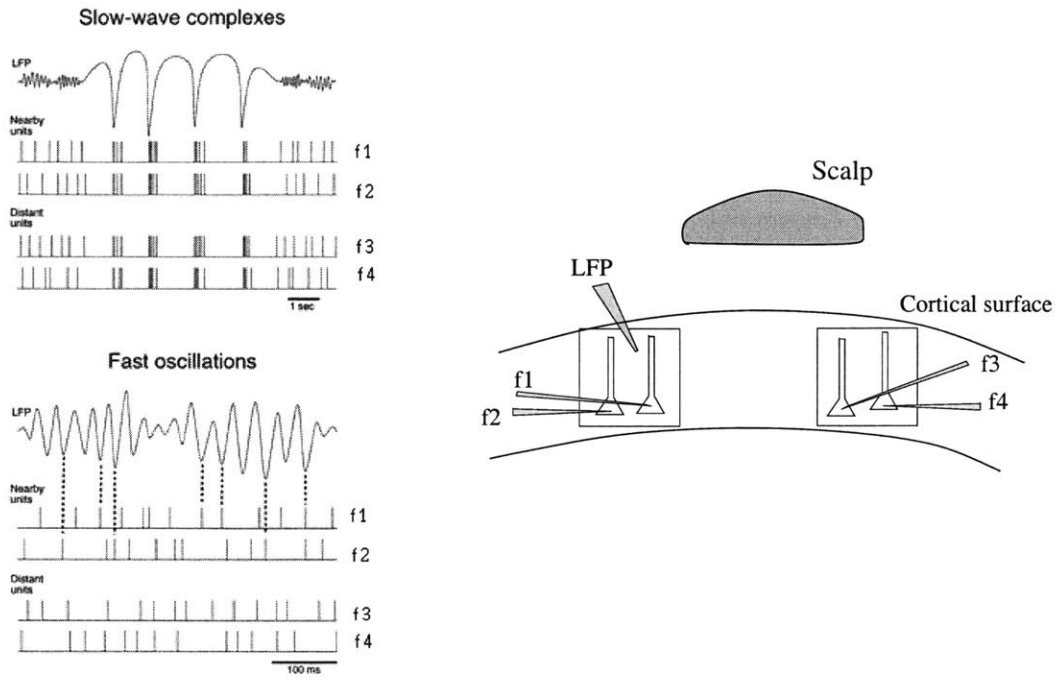

Figure 1-5: Schematic of correspondence between cellular firing and local field potentials. Low frequency oscillations (top left, slow-wave complexes) exhibited correlated firing at long distances (f1 through f4). On the other hand, high frequency oscillations (bottom left) show cellular firings correlated to LFP only in the local region (Adapted from Destexhe et al 1999 [62]).

predictions which is an essential closed loop interaction between experimental and theoretical models.

Theoretical treatments of EEG generation have surfaced at least as early as Wilson and Cowan models of neural group activity. Subsequently several black-box generic models of EEG generation were put forward. As our knowledge of cellular and network mechanisms increased in the past decade or so, several detailed neuronal group models have been developed which gather evidence from specific experimental work. We will present next a brief overview of different modeling schemes.

1.3.1 Black box models

These models are based on interactions among generic representations of excitatory and inhibitory populations with little if any details of the structure of the neocortex. By varying few model parameters, oscillatory phenomena can emerge which have several features of observed EEG patterns. Basic black box models are described briefly next.

Wilson-Cowan formulation: This model considers the average activity of two interacting populations of neurons: excitatory and inhibitory (Wilson and Cowan 1972 [259]). It is mainly based on the assumptions that the modeled neurons are

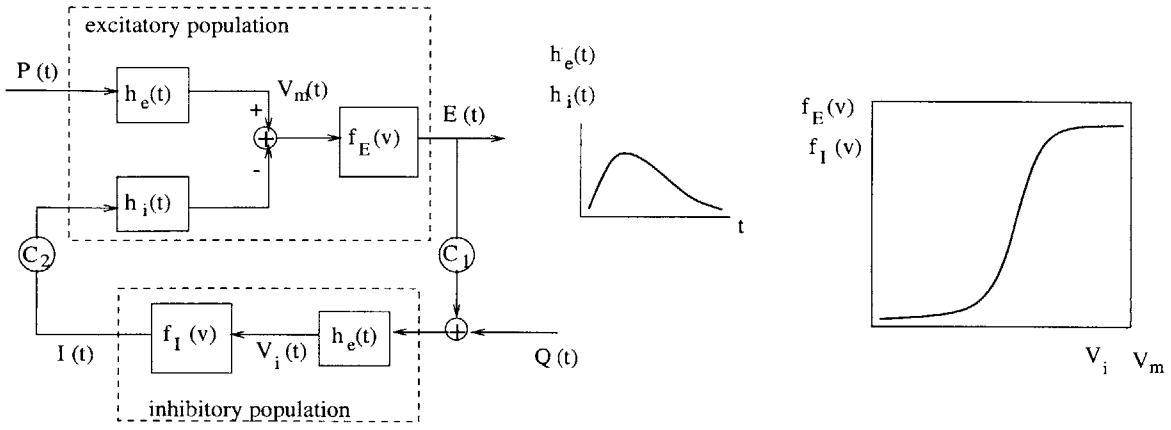

Figure 1-6: Schematic of Wilson and Cowan neural model formulation. $P(t)$, $Q(t)$ are input firing rate to excitatory and inhibitory populations respectively (modeled as Poisson arrival with some constant rate). $h_e(t)$ and $h_i(t)$ are rate to membrane potential functions (time trace shown). V_m is the membrane potential (proportional to EEG) and f_E, f_I are voltage to firing rate static nonlinearities. C_1 (C_2) is a connectivity weight between the outputs of excitatory (inhibitory) and inhibitory (excitatory) populations.

located within spatial proximity and that their connections are random yet dense enough for a path to exist between any two neurons within the population (either direct or via an interneuron). This leads to neglecting the spatial dimension and dealing with the temporal dynamics of the average activity. Briefly, the properties of the interacting populations are described by the behavior of two variables:

$E(t)$: the proportion of excitatory cells firing per unit time at instant t;

$I(t)$: the proportion of inhibitory cells firing per unit time at instant t;

which can also be interpreted as the average firing rates of these populations. E, I are dependent on the average excitation levels V_m, V_i arriving at the excitatory and inhibitory populations via sigmoidal nonlinearities $\mathcal{F}_e$ and $\mathcal{F}_i$ respectively.

$$E(t+\tau) = f_e[V_m(t)] \tag{1.1}$$
$$I(t+\tau) = f_i[V_i(t)] \tag{1.2}$$
$$\tag{1.3}$$

The average excitation V_m is also proportional to average cellular membrane potential and is related to input firing rates via a second order decay function $h_e(t)$ as shown in figure 1-6.

A generic neural model will then be represented by the two neuronal groups in a negative feedback configuration (inhibitory population decreases the membrane potential of the excitatory population). This nonlinear system could exhibit under specific connection both bistability and limit cycle oscillatory behavior (See Appendix A) and became the basis of many models to follow.

Alpha rhythm models: Lopes da Silva used a linearized form of Wilson and Cowan model to show that, for a particular choice of parameters, the linear system exhibits spectral peak at around 10 Hz or alpha oscillations (Lopes da Silva, 1974,[137]. He also arrived at a similar spectral characteristic by modeling a discrete set of interconnected excitatory neurons with feedback provided by another set of inhibitory interneurons. Since neural groups modeled are local in nature, Lopes da Silva argues, no propagation delays between different parts of the system are included. In this case, thus, a dominant spectral peak is network-generated by virtue of connection topology, and is not due to specific intrinsic properties of the cells[4].

The spatial propagation characteristic of alpha rhythms in the thalamus was later studied in a one dimensional chain of linearized interconnected cells (figure 1-7) with no connection delays. Fourier analysis of an equivalent two-dimensional linear filter showed that alpha rhythm propagates with minimum damping in such chain and that the model parameters correspond to physiologically acceptable values (see Appendix A for details).

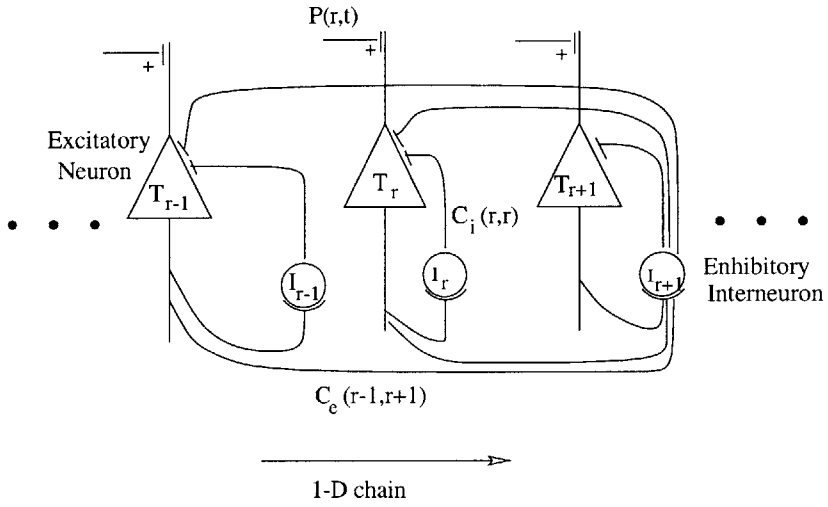

Figure 1-7: One dimensional chain of excitatory neurons and associated inhibitory interneurons. $P(r,t)$ is input firing rate and C_e (C_i) are connection strengths from excitatory to inhibitory (inhibitory to excitatory) cells. See Appendix A for details.

Nunez global wave model: Nunez and his group [171, 173, 172] developed over a decade an EEG model as a global resonance phenomena on the closed cortical surface due to inputs from deeper brain structure.The belief was that *"important features of EEG generation cannot be understood at the level of cortical column, regardless of the spatial scale "* and that boundary conditions were essential. Their "it global" theory demonstrates EEG as standing waves over large patches of cortex and simulate spatial patterns of EEG on one dimensional chain and on more complicated

[4]We will present later evidence and simulations which show that, in fact, some cells are intrinsically able to oscillate at alpha range for a specific set of intitial conditions.

spheroidal cortex-resembling surfaces. The theory represents the excitatory $l_E(r,t)$ and inhibitory $l_I(r,t)$ action densities (total number of active synapses per unit volume at time t) in a cortical macrocolumn by means of an *assumed quantitative relation* between these densities and action potential firings $g(r,t)$ (figure 1-8, right).

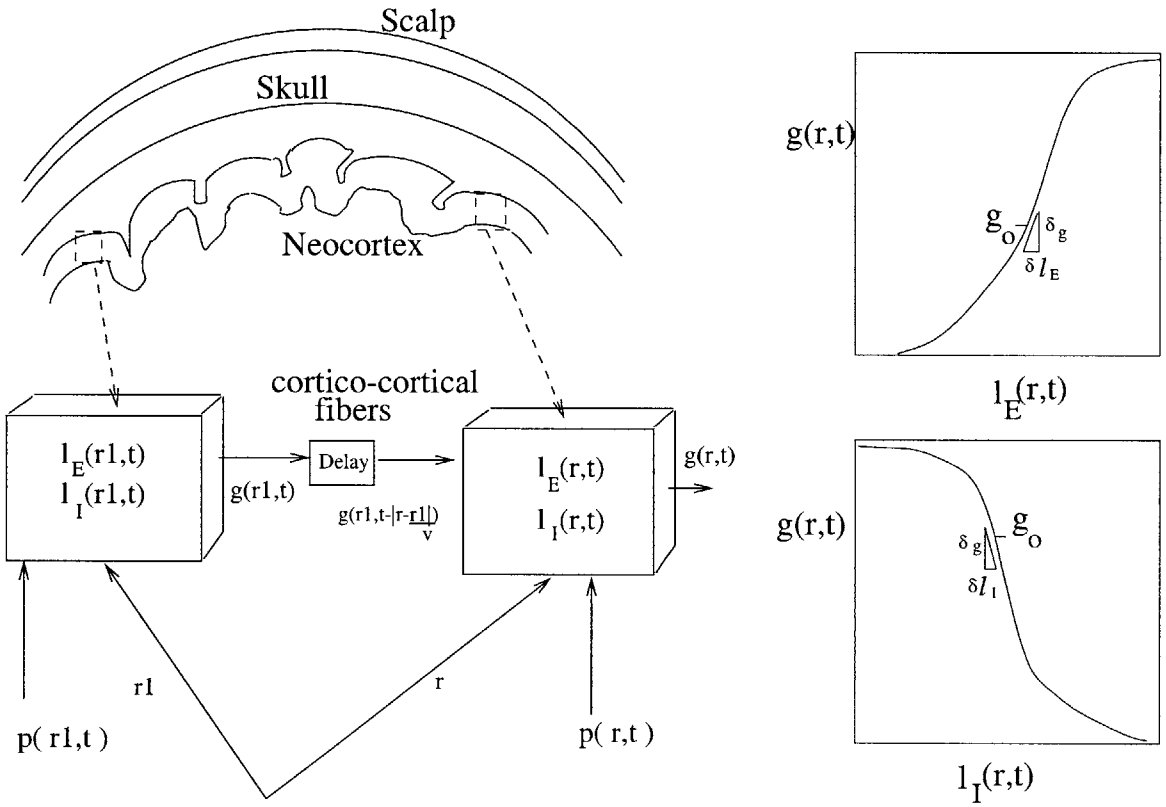

Figure 1-8: Nunez global model: *Left:* schematic showing relation between neuronal group at distant locations in the global theory setting. *Right:* assumed relation between the number density of action potential g(r,t) from a neural mass (such as a cortical column) and the excitatory (inhibitory) input to the mass. g(r,t) is in turn proportional to the recorded membrane potential (adapted from Nunez, 1995 [173]).

The main idea in this theory is that action densities at any neuronal group are related to the firing output of other groups possibly at earlier times. That is, delays between distant neural groups are incorporated.

$$l_E(r,t) = p(r,t) + \int_0^\infty dv \int_s R_E(r,r_1,v) g\left(r_1, t - \frac{|r-r_1|}{v}\right) d^2 r_1 \qquad (1.4)$$

$$l_I(r,t) = p_0 + \int_s R_I(r,r_1) g(r_1,t) d^2 r_1 \qquad (1.5)$$

where $p(r,t)$ is the excitatory input to the cortex at radius r and time t. The distribution functions $R_E(r,r1,v)$ describe the density of excitatory cortico-cortical fibers connecting locations r and r_1 which also have propagation velocity v creating delays. The distribution function of inhibitory intracortical fibers $R_I(r,r_1)$ has infinite

propagation velocities, as these connections are over short (local) distances. p_o is assumed to be a fixed inhibitory input to the cortex under a given physiological state. The formulation describes only surface interactions (integration over surface s), that is, neuronal groups are assumed as a thin sheet with static mapping between local excitation, inhibition and output action densities.

By linearizing the above integral equations about an operating point, a system solution over assumed surface topology can be computed. For a one dimensional loop standing waves of activity can be created with the lowest mode has a frequency of $6 - 18$ Hz (see appendix A for details). That is alpha rhythms can occur as a global wave phenomenon that corresponds to the first harmonic of the global system. By varying a control parameter of inhibition, different modes can be made to drop in frequency creating a parallel with what happens during sleep.

Freeman's model of olfactory EEG: Freeman's group has worked on understanding the olfactory EEG over the past two decades (Freeman 1975 [77], Freeman 1987 [76]). The basic neural population (so called KO set) is again described by generic coupled nonlinear differential equations) whose parameters are fitted to actual measurement of the input stimulus-output EEG relationship in slices of the olfactory bulb. Also, different known structures of the system were separately modeled and anatomically consistent pathways were incorporated. The resultant model simulates olfactory EEG oscillations as chaotic attractor patterns in a high dimensional nonlinear system of coupled equations.

Other models: utilize variations of the Wilson-Cowan formulation and to simulate general EEG wave phenomenon (Wright et al 1987, 1995 [263, 265], Kitazoe 1983 [118]) or specific cases (visually evoked potentials, Jansen et 1993[101]),will not be discussed here.

Summary

A main advantage of black box modeling to describe emergent neural oscillations is the utility of generic elements. This has provided useful insights through analytic and systematic manipulations of few control parameters of the system to model specific types of EEG oscillations. The limited success of such approach in EEG modeling however lies in its inability to sensibly account for the formidable array of oscillatory grapho-elements recorded across brain states. Thus, while a high dimensional system of nonlinear coupled differential equations can embed rich dynamics, the identification of clinically relevant parameters that correctly reflect (or model) changes in EEG states continues to be a nontrivial challenge.

For example, the alpha activity model provides a description of alpha activity emergence from network of generic neuronal populations [5]. Although an interesting

[5]New evidence, as we will see later, point to intrinsic currents within single neurons that allow sustainence of alpha-range firing in these neurons and hence alpha might *not* merely be a network-induced phenomenon

approach as a stand-alone application, this model does not provide a meaningful functional mapping of alpha activity, nor does it address the mechanism of switching to other oscillatory states. Nunez global theory addresses EEG as a global wave phenomenon and assumes a sweeping generality in the existence of static local maps for EEG generation without addressing local dynamics.

Finally, Freemans model of olfaction represents a systematic approach in constructing global olfactory dynamics from smaller constituent blocks coupled with preliminary experimental recordings (slice preparations). However, the tailored dynamics of this system, although attractive, is difficult to obtain for a complex highly distributed system such as the neocortex[6].

1.3.2 Neuronal group models

The increase in experimental knowledge on specific neural systems of the brain and the ability to manipulate and record cellular activity have prompted the development of more detailed models explaining the observed oscillatory behavior at the neuronal level. Here, individual neurons firing dynamics as well as their interactions are approximated with varying degrees of realism. A minimal network of interacting neurons, we call neuronal group, is then constructed whose dynamics could qualitatively reproduce observed oscillations. Examples of these models are given below.

Sleep spindles model: The underlying neural mechanisms for spindle oscillation have been recently attributed to the thalamus by virtue of experimental manipulations in animals which showed that the removal of the thalamus (thalamectomy) abolished sleep spindles in the cortex. Accordingly, by incorporating intrinsic firing dynamics of thalamic neurons and their connections in a neuronal group model, Steriade and coworkers have shown that, in fact spindles can occur in the thalamus when conditions similar to those occurring during early sleep stages are incorporated (Contreras et al 1997 [42]).

Thalamic seizure model: Experimental manipulation of inhibitory control in the thalamus results in so called 3 Hz spike and wave seizures. These again were replicated in neuronal group simulations of the thalamus where specific type of inhibitory synapses were explicitly modeled and varied to show the emergence of seizure oscillations as obtained experimentally (Destexhe et al 1998,1999 [57, 60]).

Computational models of cognition: A huge library of models has emerged in the last two decades explaining various computational phenomena observed in the brain at the cellular and network level which amount to "the computational neuroscience". These include the infamous gamma oscillatory activity in sensory systems

[6]Freemans success in describing olfactory oscillations were based on close approximation of a highly specific system. Thus, in order to address the problem at a cortical level, common features across the neocortex need to be retained and utilized

which is thought to provide a temporal binding mechanism for neural groups computing specific aspects of a task (visual feature integration, for example) in thalamocortical systems. Short term memory retainment in the prefrontal cortex is yet another example (Durstewitz et al 2000 [68]). Although few of these models address oscillations observed at the EEG level, they constitute a rich repertoire of basic ideas on how neural systems organize to produce globally-observed EEG.

Summary

The coupled experimental/modeling approach to decipher neuronal electric activity and oscillation in the thalamus have provided a deeper understanding to the role of the thalamus as a neural oscillator. By the same token, these results provided us with leads to what kinds of oscillations are generated in the neocortex itself. The complexity and diversity of neocortical structures have thus far been prohibitive of answering this question in both experimental and modeling paradigms.

1.4 A cerebral neuronal group electric activity model

In surveying the aforementioned approaches for modeling field potential oscillations in the brain, it becomes apparent that while generic neural populations modeling provide initial understanding of specific EEG states, a closer look at the neural origin is needed.

Neural group modeling and experimental efforts over the last decade have provided considerable insight to the role of the thalamus as an oscillator in punctuating some EEG rhythms and promoting synchronization among different cortical areas (Steriade and colleagues). However, such models fall short of explaining rhythms generated within the cerebral cortex itself since little attention if any has been devoted to the role of the cortex as an oscillator. Instead, the cerebral neural diversity and structure was overly simplified to generic neural populations passively reacting to thalamic-induced oscillations (Bazhenov 1998 [14], Destexhe 1999 [60]). Therefore, a potentially very valuable step forward would be attempting to understand neocortical origins of EEG.

1.4.1 Problem statement: realistic EEG modeling

The introduction of neocortical models of EEG synthesis entails understanding basic constituent neural elements, their anatomical connectivity and the dynamics of their functional interactions which could explain observed EEG phenomena. Skepticism over the existence of such a basic wiring diagram in the neocortex is very reasonable and in light of the ever-increasing diversity of known neocortical cellular types, response dynamics, and functional connectivity within cortical systems, as well as an increasing web of reciprocal connections among distinct cortical systems. Such neural

complexity, along with a current state in neural science, thus provide for a daunting, seemingly impossible task if one ventures into developing a do-all inclusive model.

Notwithstanding the problem complexity, this research follows an engineering reductionist approach: given the current knowledge at the cellular and neuronal network levels, formulate a minimal realistic model capable of explaining specific set of EEG phenomena while being consistent with known anatomical and functional constraints of the neocortex.

Our modeling premise is based on the simple observations that similar EEG oscillations are recorded across wide areas of the scalp despite the complexity and diversity of underlying neural structures. Furthermore, many oscillatory grapho-elements (or templates) are almost repeatable across different brain states, with distinctions noted in the amplitude and the spatial spread of such templates. For instance, slow wave sleep oscillations (< 1 Hz) are repeating cycles of neural activation and silence observed over wide scalp areas. Similar cycles can be seen under loss of inhibitory control, albeit with very high excitatory drives and synchrony across large neural populations. Also, 10 Hz oscillations are observed over visual, somatosensory and auditory areas of the brain.

Thus, *we conjecture in this thesis the existence of an* **effective neuronal skeleton** *circuit whose dynamics could be modeled to explain the main features of the EEG-observable brain states specifically global states such as sleep, and widely spread rhythmic states of wakefulness such as alpha band activity.*

From a neuroscientist point of view, the development of a model of such an effective skeleton of EEG generation would have many advantages, including

1. The ability to **explore** EEG generation mechanisms. This provides a better understanding of main vigilance state controls such as effects of neuromodulators, thalamic afferents, and other cortical pathologies that are reflected in EEG, such as seizures and delta slowing.

2. The ability to **incorporate** new knowledge of neurophysiology into the flexible neural structure offered by a reduced cortical framework. This allows rapid prototyping of simulated experiments where the effect of new mechanisms, cellular function on general EEG behavior can be tested.

3. The ability to **validate** ideas on how different organization principles in the neocortex within a single column and between areas might affect sharing information and recruitment into specific tasks. This includes, for instance, evoked potentials in the motor cortex where a hallmark template signal is seen upon movement.

4. The possibility of applying powerful **system theory** tools to a well defined structure of hierarchically-organized dynamical systems. With the surfacing of spatially-distributed control applications, and the increasing interest in complex large-scale system, this framework could readily lend itself to such analysis tools. Specific applications of system theory has surfaced over the last two decades, such as in the work of Freeman on the olfactory bulb (Chaotic attractors, [76].

This issue, in fact, opens the door for many clinical applications spurred by the availability of new tools to tackle the infamous EEG diagnostic problem.

1.4.2 Outline of the model and principal findings

The research conducted adopts several agreed-upon principles of cortical anatomical organization and builds upon basic ideas of cortical functional elements. By incorporating a large influx of recently reported experimental evidence on cellular properties, functional connectivity, network activity and modulation across different vigilance states, an effective skeleton circuit model of neuronal groups is proposed. The basic components of the model can be summarized as follows:

Hierarchy in neocortex

a. Cortical neurons are segregated into different (usually up to 6) *cortical layers or lamina* according to both intrinsic neuron properties as well as their connections within a layer and across different lamina. While very rich varieties of cell types and firing dynamics are reported, we restrict the model to well-known classes. In particular we will model regularly firing pyramidal cells in the superficial layers (lamina 2-3) and deep layers (layers 5-6), spiny stellate cells of the input layer in sensory systems (layer 4), and other interneurons. Finally, special emphasis is given to specific class of layer 5 cells known as *tufted layer 5 cells.*

b. The smallest functional circuit we considered is that of a *cortical column*, which extends up to around 300 μm and is the lowest scale of our model (figure 1-9). This circuit is comprised of several layers of neurons whose interconnections and firing characteristics are defined by earlier physiological studies along with new evidence. Of the major interaction pathways *within a column*, we focus on the reciprocal connectivity between superficial layer 3 and deep layer 5.

c. A functional column receives input from its immediate surrounding as well as from distant structures. Connectivity between functional columns within an immediate neighborhood exist via several pathways in both superficial and deep layers. We focus in particular on the network formed by connections within layer 5 and define the spatial extent of such a network as the a *columnar assembly* which is the second scale in our hierarchy.

d. Connectivity between functional columns belonging to distant cortical areas form the third scale of our model. In general, long range connections from distant cortical areas contact local functional columns over several input ports. Such ports are well characterized in sensory systems and are usually restricted to specific cortical layers [7]. We will adopt evidence showing a separation of ports for inputs to the middle layers of a functional column (feedforward inputs) and

[7] These input ports are more diffuse across all layers in higher order areas. We will not model such areas but draw parallels with sensory systems whenever possible

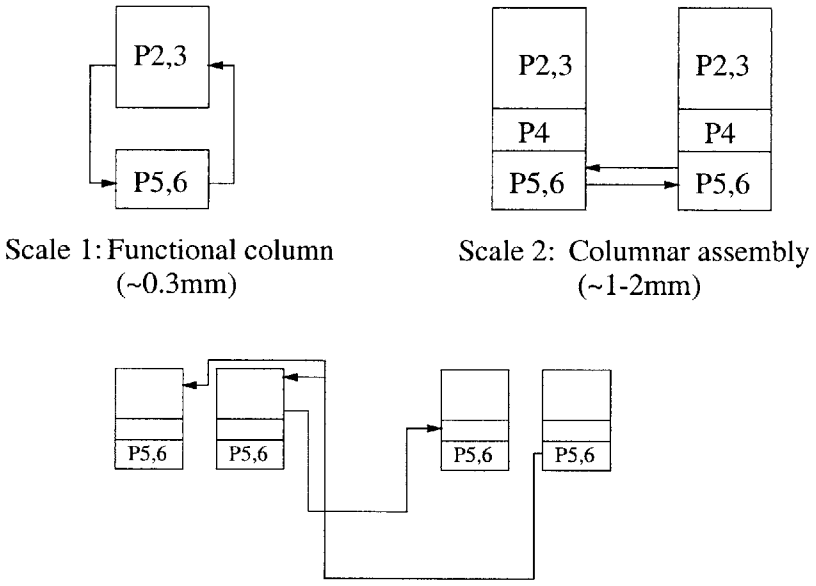

Scale 1: Functional column (~0.3mm)

Scale 2: Columnar assembly (~1-2mm)

Scale 3: Areal network (>2mm)

Figure 1-9: Three scales of interactions in an effective skeleton circuit.

those for inputs arriving to the superficial layers 1-2 (and possibly deep layer 5, so called feedback connections), as well as distinct functional characteristics of these ports. This separation provides distinct interaction gates of the neuonal networks at the current scale of hierarchy with lower order scales, and accordingly, has specific functional implications on information transfer between distinct cortical areas.

Layer 5 cells

The circuit model proposes a key role for a class of neocortical cells known as tufted layer 5 cells in binding the activity of the aforementioned three scales of neocortical hierarchy in a controlled fashion. This is based on the following

a. New evidence on the dynamics of these cells show the existence of two output modes of firing, regularly spiking and bursting. More importantly, a switch between these two modes is controlled by three input zones into a tufted layer 5 (TL5) cell.

b. The segregation of synaptic inputs arriving at superficial and deep layers of the neocortex imposes a distinction on which types of inputs are capable to drive and/or switch TL5 cells between the two firing modes.

c. The functional distinction between bursting and regularly firing regimes in TL5 cells could be understood mainly by changes in the intrinsic cellular properties as well as in the responsiveness of the cell synaptic targets. We argue that each

firing mode had different consequences in reorganizing connectivity pathways within and between cortical columns.

d. A large proportion of layer 5 pyramidal cells have a high input amplification gain under states of minimum excitation. This is due to both intrinsic mechanisms as well as to reduced inhibition of such cells. Consequently, tufted layer 5 cells can initiate firing activity more readily than other neural types.

The model also utilizes other intrinsic and network mechanisms in layer 5 cells to show how several oscillatory behaviors observed across vigilance states can be accounted for.

Principal findings

This research proposes a unified framework of hierarchical organization in the neocortex which explains the genesis of EEG signals over a wide range of frequencies. The resultant effective skeleton circuit is consistent with current knowledge of neuroanatomy and electrophysiology of basic structural elements of the neocortex.

The model is used to qualitatively show the emergence of slow (<14 Hz) oscillatory phenomenon observed in several states of vigilance and possible transitions into higher cognitive-related frequencies (beta and gamma range). Our key proposal in this regard is related to the role of connected layer 5 cellular network in driving neural activity, its reactivity, and functional properties under different neuromodulators and stimulus input levels.

a. Layer 5 network acts as an oscillator which drives other layers of the sensory cortex. This occurs during deep sleep (delta activity) as well as during restful awakeness of minimal attention (such as posterior alpha) and is based on intrinsic currents within layer 5 cells.

b. Under low excitatory input states characterized by periods of neuronal silence, layer 5 network can initiate activity and transfer it to other cortical layers. This occurs during later sleep stages (so called < 1 Hz slow-wave sleep) as well as after ictal events in disinhibition induced seizures.

c. Several sensory systems possess a resonance property in response to repetitive stimulus trains at 10 Hz known as augmenting responses which is thought to be important in spreading of excitation in local neural populations as well as increasing connection strength between cortex and thalamus. While layer 5 network has been implicated in this phenomenon, no specific mechanisms have been suggested. We argue, based on our simulations, that specific input ports of layer 5 cells are instrumental in initiating the observed resonance. Furthermore, such ports are also essential in linking local cortical activity to higher order systems.

d. The model builds upon augmenting response mechanisms and layer 5 properties to explain key interactions between local neural activity and inputs arriving from

distant regions. We present the functional implications of layer 5 network in light of the proposed hierarchy and based on new experimental evidence, most notably, on the cognitive role of alpha band activity. In this case, the layer 5 network initiates reorganization of local cortical activity in accordance with increased attention, higher order cortical input, or internal expectations. This reorganization is manifested by stimulus-specific oscillatory behavior of layer 5 network within alpha (10 Hz) band and precedes active cognition within local neural networks. Accordingly, we show how our model can account for the emergence of several alpha band oscillations over sensory systems that appear to be functionally relevant, in particular, the recently distinguished evoked, induced and emitted alpha oscillation.

e. The model proposes several possible mechanisms for transition between alpha- and activity and higher (gamma frequencies) after an input stimulus. It points to either intrinsic cellular or circuit mechanisms which are activated after the selected neural population are driven into a higher level of excitation, thus conforming to the temporal binding role of gamma band oscillations.

Contrast with existing models

The proposed model ventures into producing schematic diagrams of main effectors of EEG generation in neocortical tissue, a problem that has largely been absent in the literature due to both the complexity of neocortical systems and the humble knowledge of its workings.

The developed effective circuit surpasses the black box models devised by Lopes da Silva and Nunez by virtue of looking deeper into the neural tissue. In particular, while the alpha model of Lopes da Silva was able to produce maximal energy in the alpha band using generic neural populations of the thalamus, no specific mechanism of inducing and suppressing alpha activity were identified. The global theory of Nunez identifies static neural transfer functions in a continuous medium with no distinction of the heterogeneity in dynamics of subpopulations or their connection topology. Our model presents a framework where local activity can be understood at the columnar level due to laminar interaction and where a systematic framework of interaction between cortical columns (local connections) and across regions (global connections) is proposed.

While neuronal group models of Steriade and coworkers looked into oscillatory EEG patterns originating in the thalamus, this research addresses neocortically-generated oscillations and hence can explain these phenomena in more detail. Therefore, the model does not contradict previous work on thalamic oscillations but complements it with more explanatory models of the neocortical structure and dynamics. Although several hypothesis have addressed the role of layer 5 cells in cortical computations (Llinas et al, Koch et al), we are not aware of any general framework where new evidence and cortical structure is exploited in detail as in the current model. Furthermore, some researchers pointed to layer 5 cells to generating idling alpha rhythms as mechanisms of desynchronization between cortical visual areas in rest states, it is

argued, based on our model that, in fact, alpha band activity can have functional relevance during stimulus processing. This has various implications on information transfer and coordination between cortical areas, including those involved in attention as will developed later in the thesis.

1.5 Thesis Outline

This document has been written with two target audiences in mind: electrical engineers and neuroscientists. Accordingly, we attempt to strike a balance in introducing basic neural principles as well as advanced concepts derived from recent neural findings. In chapter 2, we present a brief description of the basic cortical structural principles, mainly laminar structure, columnar organization and connections between areas. Chapter 3 introduces main EEG oscillatory patterns and the current knowledge on their anatomical substrate. With this background in hand, we move in chapter 4 into outlining our basic claim , the "*Hierarchical Binding Hypothesis*" , upon which the model is based. We list the main component of the circuit and recent anatomical and electrophysiological evidence in its support.

Chapter 5 includes the mathematical formulation and schematic diagrams of our simulation model which are then utilized in chapter 6 to qualitatively reproduce several oscillatory phenomena of the cortex. We start by studying 10 Hz augmenting responses in basic neural models and highlight the role of layer 5 cells. This leads to studying different types of 10 Hz alpha band oscillations and their functional implications. Next, we present how layer 5 cells amplify inputs in slow-wave sleep and how this can progress into seizure like activity when inhibition is reduced. Finally, chapter 7 is synopsis of the framework, key ideas and predictions of the model.

Chapter 2

Basic features of cerebral cortical neural anatomy and physiology

This chapter is a very brief overview of basic anatomical structures and neurophysiological principles that are thought to hold with various degrees of modification across rodents and mammalian species. Since we will be sampling experimental data from different species, we are making a basic assumption about the basic principles of neural structures, both in terms of composition and the general rules of connectivity, which is fundamentally an evolutionary approach to neural processing. Nevertheless, our interest is to expose converging neural evidence on basic organizational principles and dynamic properties of the neocortex that could account for observable cortically-generated EEG states of vigilance.

There are several structures that contribute to the generation and modification of electric field potentials observed over the scalp. Since our interest is in scalp EEG measurements and underlying field potentials, it is reasonable to consider the neocortex as the primary source of such activity, modulated or modified by other deeper or lower brain structures whose activity is not observable from the scalp due to spatial filtering. That is, we will be looking at the cortex as a neural oscillator whose output measurements are observable and whose dynamics are shaped by different controllers. Of the main controllers is the thalamus which acts as a real-time relay station of sensory information into wide areas of the cortex. The oscillatory behavior of the thalamus has been extensively studied, as briefly mentioned in the previous chapter. Other input controls include brain stem nuclei whose inputs mainly on modulate the brain excitability and its vigilance state. These various controls act on several time scales to modify the resonance phenomena and response properties in the neocortex. Accordingly, only the end effect of such inputs on the neocortical function will be approximated in this thesis.

In what follows we will present the neocortex in generic organizational terms. That is, we will show a telescoping view of the cortex which is divided into increasingly detailed subsystems differentiated both by anatomy and functionality.

Starting with the minimal composition of a neocortex, one can describe a set of excitatory neurons mainly *pyramidal cells* that are oriented nearly orthogonal to the neocortical surface. These cells have long branching input arbors (dendritic tree)

Table 2.1: Spatial scales of neocortical interactions

Level	Typical diameter	Number of neurons	Anatomical correlate
Minicolumn	$30\mu m$	10^2	Spatial extent of inhibitory connections
Cortical column	$300\mu m$	$10^3 \sim 10^4$	width of arborizations of cortico-cortical afferents i.e, input scale for long-range connections
Columnar assembly (macrocolumn)	$0.5 \sim 3mm$	$10^5 \sim 10^6$	Extent of axon collaterals for single pyramidal cell, i.e, spatial scale for intracortical output
Regional level	$50mm$	10^8	Average length of cortico-cortical, fibers i.e, one spatial scale for long range output
Hemisphere	$400mm$	10^{10}	Longest cortico-cortical fibers

which tunnel activity to the cell body or soma. The soma then fires action potentials that are sent via its output wirings or axons (see appendix B). Axons are usually described in terms of their spatial reach. An axon which extends down out of the neocortex through white matter below and connect to distant cortical regions (possibly as far as across the cortical hemispheres) is called a *cortico-cortical fiber*. Such axons can also branch to contact closer or neighboring neurons and are then called *association collaterals or fibers* and are around $0.5 - 3mm$ in length.

Heavily intertwined with pyramidal cells are inhibitory interneurons which are of smaller sizes and irregular shapes arborizing in a smaller neighborhood ($25 - 30\mu m$) and help regulate pyramidal (and other excitatory) cells activity. Hence, based on this skeleton cortex, it has been inferred that a hierarchy of neocortical interactions could be derived based on the anatomical topology of neuronal populations and the electrophysiological constraints they impose.

Table 2.1 presents conventional neocortical scales of interaction. At the lowest end of the structure spectrum (larger than the neuron) is a *cortical minicolumn*, which is defined by the set of excitatory and inhibitory neurons interacting within the axonal arbors of an inhibitory cell extending in the lateral direction to about $30\mu m$ (figure 2-1). The minicolumn is thought to be the smallest functional unit in the neocortex, containing around 200 neurons that are heavily interconnected[1].

The next level is the *cortical column* and this is defined by the collection of minicolumns that share the same input connection from another cortical region or from sensory thalamic nuclei. Such connections usually diverge to contact minicolumns within a region of around $300\mu m$. Anatomic and physiologic data support the hypothesis that a cortical column is functionally subdivided into approximately 100

[1] A cortical minicolumn is thought to be the primary neural product of a neural plate during development (Jones 2000 [103])

minicolumns.

The spatial extent of a pyramidal cell association collaterals approximately defines the *macro-column*, or *hypercolumn*. This has been studied especially in sensory cortices such as the primary visual cortex where macrocolumns are collections of cortical columns thought to have specific feature representations of a scene geometry such as orientation. Specific stimulus properties, such as strength, determine neural action in pre-disposed subunits within a macrocolumn. Hence, a macrocolumn is commonly defined on the basis of functionality in sensory areas and its exact topological shape is not known, or at best nonuniform across sensory areas [2]. For our purposes, we will redefine this scale of conglomerates of cortical columns to be termed *columnar assembly*. Although of a similar spatial extent to a macrocolumn, this scale does not have a specific functional annotation except for its relevance in EEG generation, as we will see later. It is based on the extent of axon collaterals of a special neuronal class, the layer 5 pyramidal cells [3].

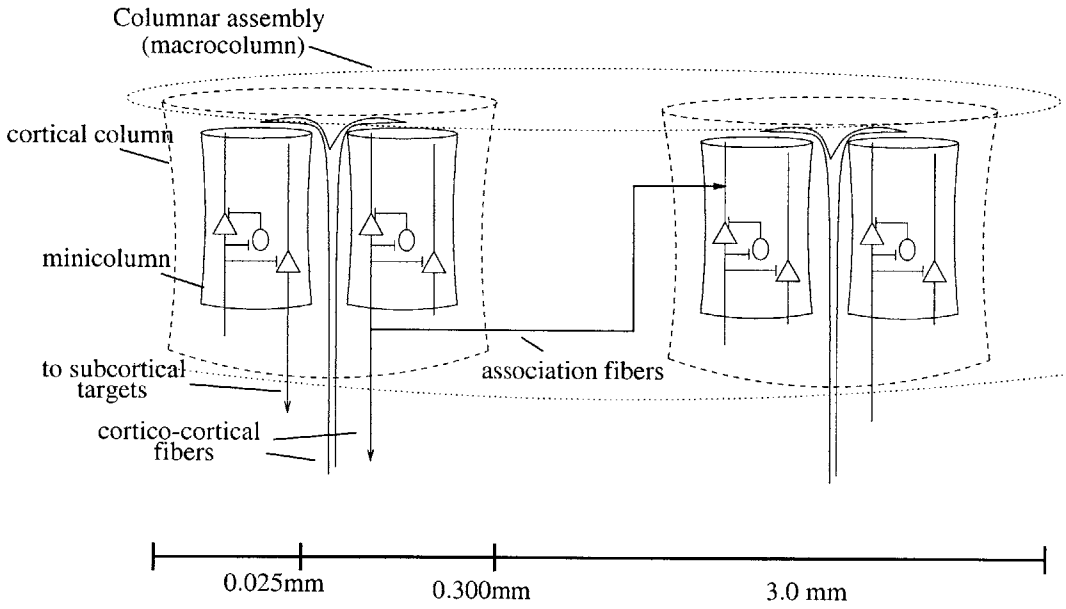

Figure 2-1: constituent structures at and below the columnar assembly level

The collection of columnar assemblies (or macrocolumns) which process the same aspect of a cognitive process form a region. In neuroanatomy these regions are called *broadman areas* and are characterized by similar cytoarchitectonics (structure) and can be several centimeters in diameter.

Higher scales involve collections of regions connected via cortico-cortical fibers and form according to spatial proximity different lobules (temporal, occipital, etc),

[2] An example of a macrocolumn in the primary visual cortex of cats is defined based on orientation and is thought to have an ice-cube shape (see Mountcastle 1998 [165], Braitenberg 1998 [22])

[3] This definition agrees with a study of EEG in the mouse cortex which concluded that the region of statistically homogeneous generator properties extends to $3 - 4mm$, which is the scale of a columnar assembly [173].

hemispheres, and finally the cerebral cortex. We will lump these spatial scales as defining the neocortex, with the understanding that there exists a set of inter-regional connections which essentially constitute the neocortical structure as a collection of about 50 broadman areas.

2.1 The Neocortex

The convoluted structure which covers internal brain structures has grown to symbolize the "brain" in everyday cartoons. Rightfully so, the neocortex is the dwell of our conscious behavior, sensory awareness, and thoughts. From an evolutionary viewpoint, the cerebral neocortex of the new world monkeys is known as the the latest and most powerful addition to their neural system. Accordingly, a survey of cortical tissue across vertebrates and especially mammalian species shows positive correlation between neocortical area and complexity of animal behavior.

The cortical thickness increases modestly over a wide range of animals; according to Mountcastle [165], thickness reaches an average value of 0.25-0.28 cm for brain volumes greater than about 3 cm^3. The increase in the size of the neocortex occurs mainly in the development of gyri or sulci, which are the folded tissue that extend deeper or perpendicular to cortical surface. The Mammalian neocortex has a basic ontogenetic unit or *minicolumn* which is repeated early during development which contains a chain of about 80 -100 neurons. In fact, "All major neural cell phenotypes of the mature cortex are present in each minicolumn " Mountcastle [165]. It is this statement that summarizes the foundation upon which any hope for a generic EEG-producing circuit lies.

The existence of a uniform structure in the neocortex has had both its supporters and skeptics. Nay-sayers such as Braitenberg [22] refute the idea of canonical circuits of computation except where these have been shown (such as the visual cortex), and argue through their experimentations that neural connectivity could resembles a "cloud" and that computation is very distributed among large neural populations so that no real geometry of connections could hold. Optimists, on the other hand, argue that minicolumns are repeatable across the neocortex and are part of a hierarchy of functional specification extending into columns and hypercolumns. While the reality might probably lie somewhere between the two extremes, our approach obviously depends on a certain degree of structural specificity. Accordingly we will be presenting hierarchical organization as is widely demonstrated and believed in the neural community.

We will next present basic cortical cell phenotypes, their firing properties and nature of their synaptic contacts. A detailed presentation is given appendix B for the less-familiarized reader. The laminar organization of major cell types will then be presented. The hierarchical organization of the neocortex will also be revisited in more detail.

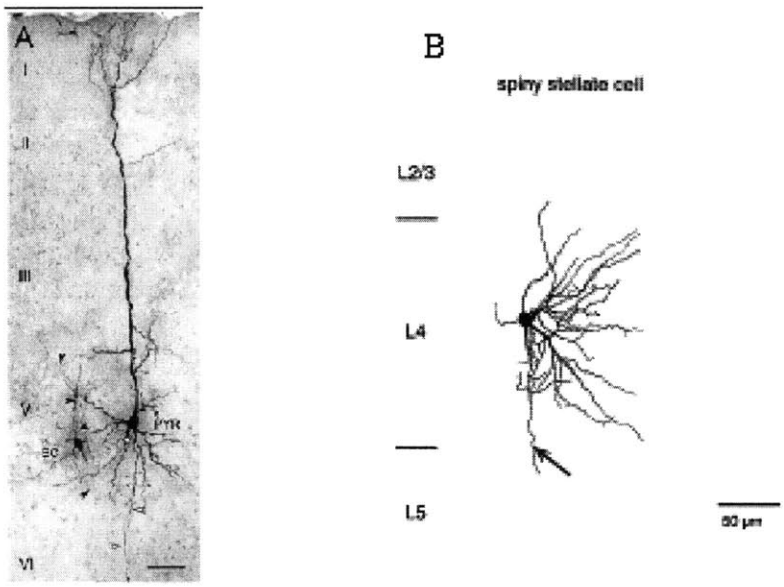

Figure 2-2: Sample of neural types in neocortex. Roman numerals refer to laminar location of cells. A: Layer 5 pyramidal cell (Pyr) and a connected basket cell (BC) (in rats motor cortex- from Angulo et al 1999 [7]) scale bar is 100 μm. B: Spiny stellate cell of layer 4 (rat- from Feldmeyer et al 1999 [70]).

2.1.1 Neural phenotypes of the neocortex

Cortical cells differ in their anatomical structure or shape, chemical mechanisms of producing action potentials (and hence internal dynamics of firing), synaptic effects and target specificity of their axonal proliferations or their output connectivity, and dendritic tree structure, or input connectivity. In general, neurons belong to major neuronal classes that appear across the neocortex in a fair degree of uniformity. Similar densities of the major classes exist in most areas of the cortex, with the striate (visual) cortex being an exception.

Morphology

Neocortical cells are classified according to the shape of the cell body, their dendritic trees and axonal targets. Cells that have spines on their dendritic trees are called spiny, while those that lack spines are called smooth cells, sparsely spiny cells have a low density of spines.

Spiny Pyramidal cells constitute about 70-80% of neurons in the mammalian neocortex and are called so referring to their somata shape (figure 2-2). They are the largest cells in the neocortex with long axonal connections, possibly leaving the grey matter (neocortex main) into the white matter.

Nonpyramidal cells can be spiny, sparsely spiny or smooth according to the density of spines on their dendritic tree. In general, these cells have local axonal ramifications [254], and hence, they tend to be part of the local cortical circuit without exiting into the white matter. Examples of these cells are : (a) *basket cells* which have form

nest-like axon structures on their targets within local cortical neighborhood and (2) *spiny stellate cells* which occur exclusively in middle layers of primary sensory areas of many species. Other varieties are presented in appendix B.

Synaptic Transmission

Excitatory connections form 75-80% of total synapses in the neocortex (Mountcastle 1998 [165]). The majority of these synapses are formed by pyramidal cells; other excitatory synapses are derived from spiny stellate neurons and extracortical inputs. The remaining synapses are inhibitory and are usually made by smooth nonpyramidal interneurons. In general, a synaptic input injects a current into a postsynaptic membrane which could be approximated by

$$I_{syn}(t) = g_{syn}(t - to)(E_{syn} - Vm(t)) \tag{2.1}$$

where g_{syn} describes synapse kinetics when an action potential occurs at time t_o and E_{syn} is the reversal potential of that synapse. The time constant of g_{syn} varies between different synapse according to the nature of the receptor (appendix B). Of these we mention the fast channels (AMPA which is excitatory and $GABA_A$ which is inhibitory) and the slow channels (NMDA which is excitatory and $GABA_B$ which is inhibitory).

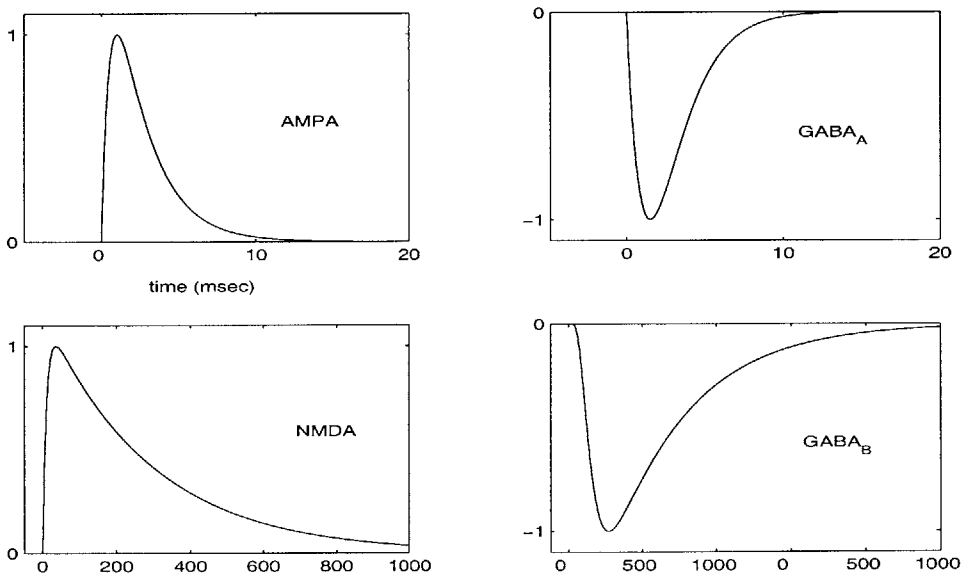

Figure 2-3: schematic diagram of the time profile of major synaptic responses

Neuronal firing properties

Neocortical neurons are customarily subdivided also by their intrinsic firing behavior, that is, the time profile of sequences of action potentials generated in response to a constant injection of input current to their soma. While this idea is being challenged

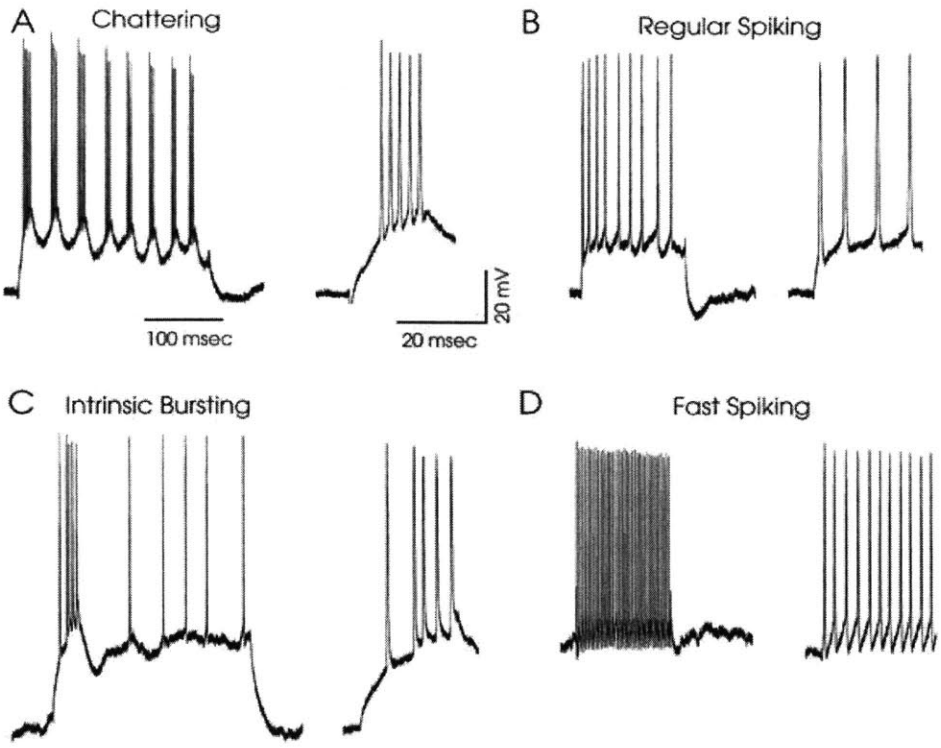

Figure 2-4: Major firing properties in neocortical cells (figure reproduced from Gray et al 1994 [92])

by an increasing diversity of firing characteristics of different neurons (especially interneurons), as well as within the same neuron under different stimulation patterns, few major firing patterns generally hold. These include *regularly spiking* (RS) cells, *fast spiking* FS cells, *Intrinsically Bursting* IB cells, and *Low threshold spiking* (LTS) cells (figure 2-4 and appendix B).

2.1.2 Laminar structure of the neocortex

The grey matter or neocortex in mammals is about $2mm$ thick and is divided into 6 layers in most cases (although some variations have been found). The distinction between layers is usually based on architectonic structure, that is types of neural populations observed. The horizontal separation between layers can sometimes be blurred due to the spread of axonal and dendritic trees from one layer to another. Still, it is common to look for the cite of the cell body as place of origin of a particular neuron and it is this horizontal homology within one layer that grants distinction in the vertical dimension.

(a) Layer 1 (L1): Descending inward from the surface of the cortex and extending to about $100\mu m$. This layer has very few cell bodies and consist mostly of afferent fibers (described later) and dendritic terminations extended from lower cortical layers. This layer also receives diffuse-type inputs from intralaminar nuclei of

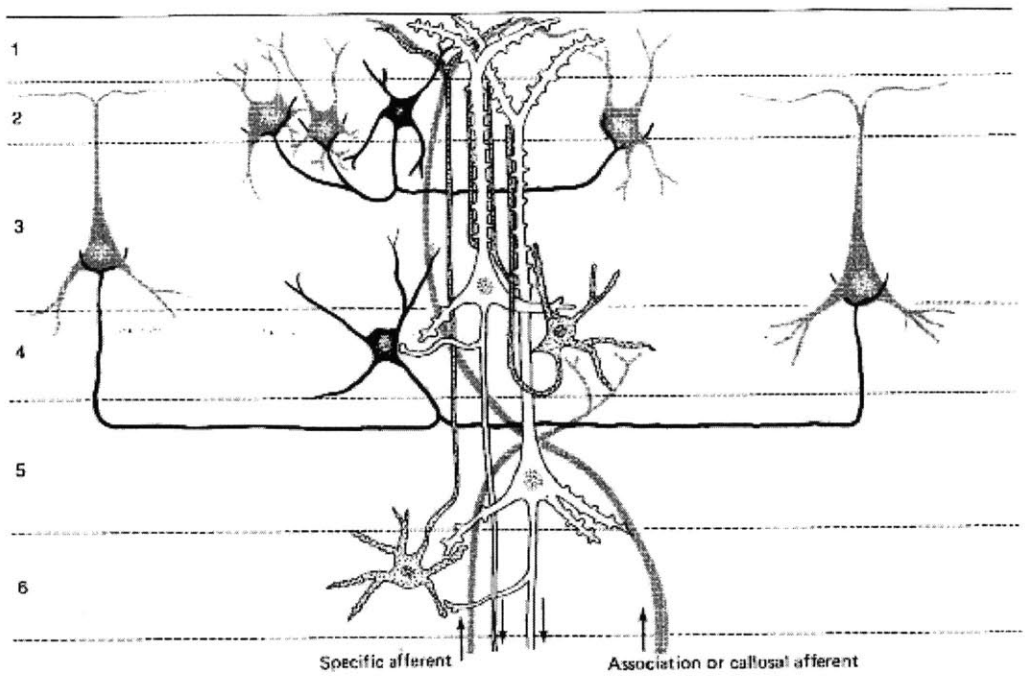

Figure 2-5: simplified diagram of the morphology of neocortex. The two large pyramidal cells (white) in layers 3 and 5 receive multiple contacts from the star-shaped interneurons (stippled) in layer 4. The inhibitory action of the basket cells (black) is directed to the cell bodies of cortical neurons (grey). Major input from specific thalamic relay nuclei (specific afferents) and is mostly directed to layer 4; association and callosal input is, in part, directed to more superficial layers (reproduced from Kandel, 1991 [105]).

the thalamus. At least one population of horizontally-extending interneurons have been found in this layer.

(b) Layers 2 and 3 (L2, L3): The distinction between these two layers is usually made between at least in terms of the higher density of neural bodies in layer 2 and the longer apical dendrites of pyramidal neurons in layer 3, as well as the size of these neurons (occasionally layer 2 has larger cell bodies, Braitenberg 1998 [22]). However, in the absence of a clear systematic functional and synaptic connectivity distinction between the two laminar populations, we will refer to the two layers in unison as $L2,3$. Accordingly, *The corresponding neural population to be termed* $P2,3$ *consists of a variety of excitatory pyramidal cells and an even richer populations of interneurons.* Pyramidal cells in $L2,3$ have been reported of the regularly spiking (RS) variety in many species [4].

(c) Layer 4 (L4): This is largely known as the input layer of the cortex where specific afferent input from the sensory thalamus is relayed. It also receive feedback

[4]Pyramidal Chattering cells (Ch) in $L2,3$ have been reported at least in the cat visual cortex.

inputs from other cortical areas, as we will see later. In humans, small L4 cells are generally well distinguished from large L3 cell. This layer is specially developed in sensory areas and inputs are topologically differentiated. For example, there is an interlaced or periodic input projections into layer 4 of the primary visual area $V1$ from left and right eyes. Also, in rats somatosensory cortex, layer 4 is referred to as barrel cortex due to the shape of neuron assemblies forming circular barrel-like structures around sensory projection inputs. *This layer contains star-shaped excitatory neurons called stellate cells or SS, and inhibitory interneurons or basket cells.* Spiny Stellate cells have dendritic arbors that are largely confined within layer 4 and are characterized with a high degree of synaptic fidelity and specificity. Other cells termed star pyramidals are also observed in this layer (rats, Feldmeyer et al 2000 [71]). The interneuronal population contains low threshold spiking (LTS) as well as fast spiking (FS) cells. (Gibson et al 1999 [88]).

(d) **Layer 5 (L5)**: starts approximately halfway in the vertical direction and is characterized by a less dense population and larger cells than those in layer 4. This area is known to contain at least two types of cells and hence further sublayers are not uncommon. *Neural population here includes large excitatory pyramidal cells termed P5 and two or more types of interneurons.* In particular pyramidal layer 5 cells are distinguished in terms of the extent of its apical dendritic tree and its size of the dendritic tufts. Large tufted layer 5 pyramidal cells (TL5) extend their apical dendritic arbor into upper layers 1 and 2 (figure 2-2,A), and have a thick dendritic tuft terminating in those areas. Smaller layer 5 pyramidal cells have a slimmer apical dendritic trunk and terminate shortly into layer 3 with a smaller dendritic tuft. Interneuronal varieties in rats include low threshold spiking (LTS) cells and fast spiking (FS) cells (Xiang et al 1998 [267]).

(e) **Layer 6 (L6)**: has denser populations of smaller pyramidal neurons than L5 does. Those pyramidal cells have apical dendrites extending into layers 4 and 5 and are thought to be actively connected with sensory inputs from the thalamus. Again, rich interneuronal populations exist in this layer.

2.1.3 Major input and output pathways in neocortex

We will provide a sketch of types of connections arriving and emanating from a local cortical area. These can be of cortical nature , either from/to a local neighborhood or distant areas, or of sub-cortical nature, from/to deeper brain structures such as the thalamus and brain stem.

cortico-cortical connections

These are long fiber tracts or axons which originate from one area, descend into the white matter and connect to different areas of the cortex over distances extending up to several cm in length. Cortico-cortical fibers are considered the main input

into a cortical area since other (deep brain) inputs form only a small fraction of it ($10 - 20\%$, hence the idea that a cortex is a reciprocating system). Also, cortico-cortical connections tend to form a point-to-zone connectivity map. That is, long fibers extending out of a local area in one zone form a wide arborization or connection to a wider area in another zone, an idea which is supported anatomically by the amounts of total wirings existing in the white matter (White 1989 [254]).

Intracortical connections

Before descending into the white matter, a long axonal tract of a pyramidal cell delivers local terminations of axon collaterals which extend over short distances within the cortical region of origin. These collaterals, also called association fibers, tend to arborize in patchy subregions and are thought to be important in forming neural assemblies of cognition in that area. Association fibers extend to 1-8 mm in some areas and can occur across all layers where pyramidal cells exist (mainly layers 2-3 and 5-6).

Specific thalamocortical afferents

The inputs from sensory stimuli arrive at the cortex via connections from the relay stations in the thalamus, called specific thalamic nuclei (described later). *Specific thalamocortical (TC) inputs deliver a spatially restricted, topologically defined arborization maps especially in the earlier cortical processing stages and provide quite powerful drive to the cortical region of interest, often synapsing in middle layers* (lower layer3, layer 4) and giving off collaterals into deeper layer 6. For example, visual inputs arriving from the lateral geniculate (LGN) of the thalamus synapse in layer 4 of the primary visual cortex and are organized topologically according to retinal receptive field and are interdigitated from both eyes. In this area, and despite the fact that specific thalamocortical afferents form only about 10 % of the total synaptic input onto spiny stellate cell of layer 4, they form a strong drive to these cells. Finally, the spatial precision of thalamic inputs organization falls off as it moves up the hierarchical stream into secondary and higher order areas of the cortex.

Nonspecific thalamocortical afferents

These inputs are derived from the intralaminar and midline thalamic nuclei and are characterized by a less-focused projection pattern into the cortex. Nonspecific thalamocortical inputs (nsTC) are excitatory and project densely into layer 1 of the cortex and possibly into lower layer 5. *Intralaminar nuclei provide for a widespread connectivity in the cortex and their disruption affect behavioral states such as sleep attentiveness and arousal.*

Brain stem afferents

In addition to the above inputs, the neocortex receives a wide repertoire of deep brain inputs from different systems. These systems deliver neuromodulators that affect the

excitability of the cortex. Examples are the raphe nucleus which provides serotonin (5-HT), the locus-ceruleus which provides norepinephrine (NE), and the basal nucleus of Meynert which provides acetylcholine (ACh). The projection patterns are usually much wider spread compared to thalamic inputs and act usually on a slower time scale. *These systems are involved in regulating waking/sleep cycles, memory, and even thoughts and actions.* Disruption of various neurotransmitters have been shown to produce a wide area of cognitive deficits and psychotic states. Specific systems will be mentioned later in the thesis upon need.

Cortical outputs

In addition to the recurrent connections within the neocortex between various areas, descending axons reciprocate and provide information to various deeper brain regions. Some of these outputs have a laminar specific origin. Mainly

1. Layer 5 pyramidal cells form at least two populations based on their subcortical outputs. Large tufted P5 cells extend axonal connections to spinal cord and basal ganglia. Smaller P5 cells lying deeper in that layer provide outputs to non-specific thalamic nuclei as well as send axons callosally to the opposite hemisphere of the neocortex (Kasper et al 1994a,b [110, 111]). P5 cells also provide a driving strength connection to the pulvinar (to be seen later).

2. Layer 6 pyramidal cells form a strong feedback pathway with the corresponding specific thalamic nuclei. This Cortico-thalamic connection is thought to modulate responses of thalamic neurons as well as reflect oscillations of the cortex back into these nuclei.

2.1.4 Hierarchical structures in the neocortex

Local cortical hierarchy

As mentioned earlier, the smallest assembly of tightly coupled neurons, appears to have a cylinder shape of few hundred neurons and have long been termed a minicolumn (table 2.1). It is thought to be the earliest cortical product of neural development (or so called migration from the neural plate see Jones et al 2000 [103]).

Neurons of a cortical minicolumn not only form tight coupling within themselves, but also interconnect with other neighboring minicolumns in laminar-specific manner. A group of interconnected minicolumns form the so-called cortical column which is a rather functional description of a cortical assembly which have access to similar input features, for example thalamic sensory input, which branches over $100 - 300\mu m$ and is also echoed in the spatial extent of layer 4 connections. This is often determined by dye-tracing of a particular thalamic afferent and displays blobs like staining which contours a cortical column.

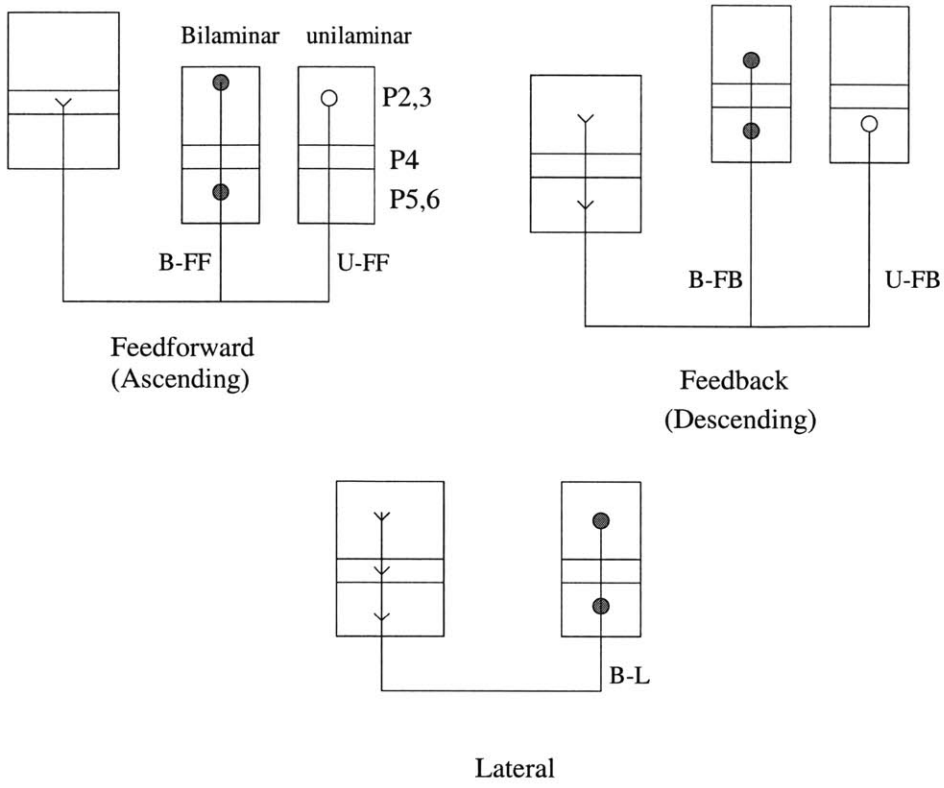

Figure 2-6: Diagram of possible connections between cortical systems. *Top left:* Feedforward connections ascend from a system of lower hierarchy to another of higher hierarchy and tend to synapse in the middle layers (P4). The origin of such connections can be either Bilaminar (B-FF, filled circles) or unilaminar (U-FF, open circles, primarily from supragranular layers P2,3). *Top Right:* A feedback connection (FB) occurs from higher to lower hierarchy systems. A major source for feedback connections occurs from infragranular layers (U-FB), although bilaminar connections are possible (B-FB). *Bottom:* lateral connections occur among systems where no clear hierarchy exists (e.g. association cortex). The interconnectivity in this case seems to involve all areas. Figure adapted from Fellman and Van Essen 1991 [72].

System hierarchies

The relationship between cortical areas involved in motor or other sensory tasks, although complex, is thought to obey certain general principles as first suggested by Fellman and Van Essen 1991 [72]. Of these, almost all relations are reciprocal, that is, fibers project to and from each area involved in information processing (Nunez 1995 [173]). Many such relations appear to be hierarchical; for example, the primary visual cortex has a reciprocal relation with the visual association cortex, and is lower in the hierarchy of information processing. Cortico-cortical fibers ascending up this hierarchy (conveying information from primary visual to association cortex) are called *feedforward* connections, while those that convey reverse information are called *feedback* connections (which will be further elaborated later).

Hierarchy also exists in a single sensory system and is usually defined both on

the basis of anatomical connection differences between subsystems as well as the functional specificity of a particular subsystem. According to this classification, "the functional properties of cortical neurons become more complex in transition from a lower to higher stages of the hierarchy. Such transitions include both increases in the size of peripheral receptive fields and a greater complexxity of dynamic properties" (Mountcastle 1998 [165]). Of the most studied hierarchy is that of the visual system. The primary visual cortex is usually referred to as area V1 which receives direct sensory input from the thalamus. Neurons in this area are topographically organized to respond to different regions of a single eye receptive field, and receptive fields of left eye are digitated with those of the right eye. Functionally, these neurons respond to basic features of a scene such as orientation. Up in the hierarchy, area V2 has more complex response features and has a feedforward input from area V1 and feedbacks to that subsystem in a laminar specific manner (figure 2-6).

It is important to note, however, that while such hierarchy is clear in the early stages of sensory processing, computation is more distributed as the signal goes up the pathway into more multimodal areas, such as the association cortex. Here, no clear hierarchy is apparent, both in functional terms as well as connectivity. Therefore, while reciprocal connections are observed in wide areas of the cortex, clear patterns of functional hierarchy among different systems become fuzzy shortly into the sensory processing pathway.

2.1.5 Dominant synaptic organization in neocortex

Despite the great degree of nonuniformity and specialization among various cortical areas, a fairly consistent skeleton of the neocortex is thought to hold upon which higher complexity organization are adapted. Cortical cell assemblies have access to different inputs and provide links to different outputs within the neocortex as well as in deeper brain structures. We will briefly mention major input/output pathways as well as intracortical synaptic dominance next.

Intralayer connectivity

Our knowledge about the spatial extent and synaptic specificity of connections within neocortical layers laminar circuits varies across species with few principles that are thought to hold.

1. *Superficial pyramidal cells in layers 2 and 3 are interconnected both locally through a horizontal association (or intracortical) system and over fairly long distances through cortico-cortical fibers.* The study of intracortical horizontal connections in many sensory systems demonstrated an intermittent arborizations of pyramidal cell collaterals in patches of several hundred micrometers and interdigitated with arborization-free regions of about the same size (Mountcastle 1998 [165]) and extending laterally over regions up to one or several millimeters.

   Many of these connections involve synapses that are commonly depressing, that is, the efficacy of synaptic connection between two superficial layer pyramidal

cells decreases when a high frequency train of presynaptic action potentials arrive at that synapse. The functional efficacy of synaptic connections in these layers, or the effective wiring diagrams which assembles neurons into subgroups is regulated with experience, possibly creating new subgroups that represent cognitive features. In fact these populations are sometimes thought of as *"the library cells"*, where basic computational features of the neocortex are stored. Not surprisingly, therefore, is the existence of specific long range connections that link superficial layer neurons over entire cortical hemifields or even across the two cortical hemispheres.

2. *Deep pyramidal cells* are connected intracortically via axon collaterals and could also form in sensory systems patchy connections over interdigitated areas just as superficial layers. An example is the existence of a network of interconnected tufted layer 5 cells which form reciprocal nonrandom connections up to distances of 1 mm (Markram 1997 [147]). In addition to being part of an intracortical network, these cells are thought of as the "*output cells*" of the neocortex since they project to deeper brain structures.

3. *Middle layer cells* or so called the cells of the granular layer are well developed in some sensory systems such as the visual and somatosensory cortex and are referred to as "*the input cells*". These cells interconnect over short distances which is often defined as the extent of a cortical column. For example, spiny stellates of layer 4 in the rat barrel cortex have dendritic arbors extending up to $100-300\mu m$ within that layer and degrade rapidly over longer distances. Thus, while the intracortical networks of superficial and deep pyramidals extend to include several cortical columns, middle layer networks are confined within the geometry of a cortical column.

Interlayer connectivity

Cortical neurons of different layers connect in the vertical direction in a non-random manner. In general, this cross-laminar connections serve to exchange information between different computational assemblies within a local cortical area as well as with distant cortical areas and deeper brain structures. Of the main features of such connections as demonstrated in different sensory systems of animal models are the following.

1. The pyramidal neurons of layer 3 send axons deep into the white matter, which before exiting branch into collaterals targeting deep layers pyramidal cells, especially a subpopulation in layer 5, mainly large tufted layer 5 pyramidals (Thomson and Bannister 1998 [237], Kaneko et al 2000 [107]).

   Pyramidal cells of layers 2,3 have their apical dendrites extending into layer 1 where afferent fibers are mainly axon collaterals of layer 5 neurons, feedback connections (cortico-cortical fibers) from other cortical areas, and nonspecific thalamic afferents.

2. Layer 5 pyramidal cells have contact across almost all layers within a cortical column. Axon collaterals from the smaller pyramidal cells in layer 5 are thought to contact superficial pyramidals in layers 2 and 3 (Callaway 1998 [26], Thomson and Bannister [237]) as well as inhibitory interneurons in these layers (Dantzker and Callaway 2000 [51]). Further, some collaterals of L5 pyramidals terminate in lower layer 5 /layer 6 where they form synaptic connections with L6 pyramidal cells.

3. Layer 4 network of the sensory areas has both excitatory (spiny stellate or SS cells) and inhibitory (basket cells) populations projecting into superficial layers 2,3 pyramidals. The afferents to this layer mainly come from the thalamus or as feedforward or ascending from other cortical areas. In general, inhibitory basket cells in this layer receive specific afferents from the thalamus and synapse upon layers 5 and 3 pyramidal neurons. In the primary visual cortex of cats, about 10% of the spiny stellate excitatory input come from the thalamus, 20% from feedforward connections, and 40% from layer 6 neurons and are mainly (90%) inhibited by basket cells (Shepherd 1998 [206]).

4. Layer 6 is also composed of several types of pyramidal cells, mostly sampling inputs via apical dendrites extending into lower to middle layers (5 and 4). The primary afferent inputs to this layer are from the thalamus as well as other cortical areas. The axons of at least one subset of L6 pyramidal cells form a focused connection to layer 4 as mentioned above. Others contact the basal dendrites of layer 5 pyramidals.

Interareal connectivity

The aforementioned connections tend to hold for horizontal intracortical connections extending up to one or few millimeters and where neural assemblies are part of a single system receiving similar (sensory) inputs and responding to similar features of such inputs. However, connectivity patterns across subsystems with distinct functional specializations changes especially when cortico-cortical fibers connecting distant cortical regions are involved. In this case some specificity in the laminar origin and termination of cortico-cortical connections exist, especially in the early processing stages of sensory systems, as mentioned earlier in the discussion of system hierarchies (figure 2-6).

Connection summary

The above basic connectivity patterns are summarized in figure 2-7. In it, we showed major excitatory connection patterns of interest within a cortical column. Not included in this figure are the different interneuron types existing in each layer and forming recurrent connections with pyramidal cells of that layer and possibly other layers. Two distinct connection patterns are to be noted:

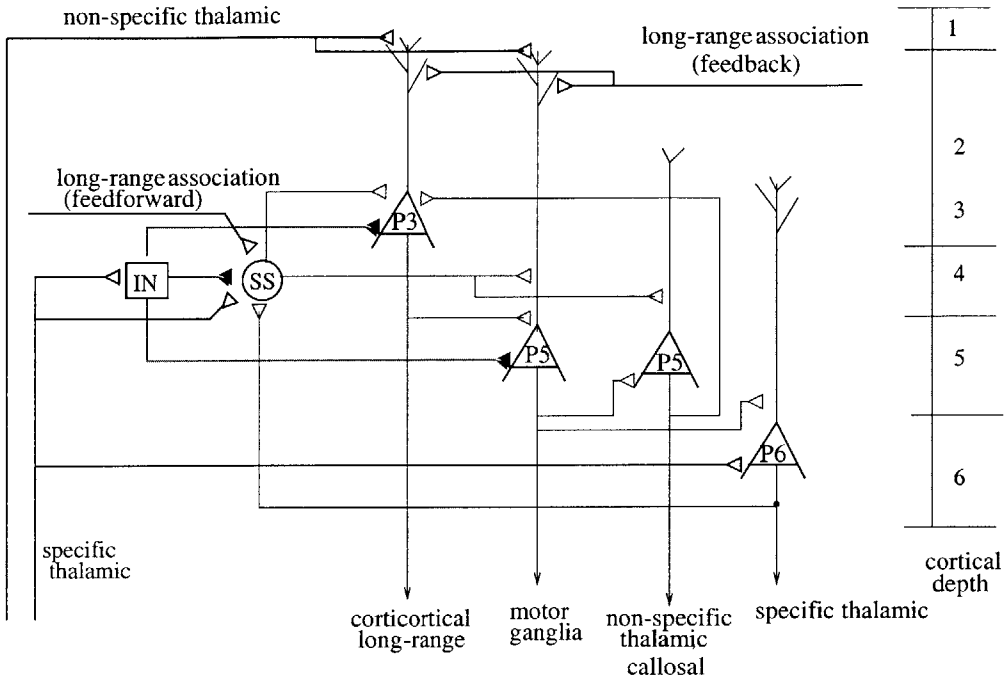

Figure 2-7: Basic connectivity patterns and main input-output pathways a generic sensory cortical circuit. It is assumed that layer 4 exists and provides for the main input layer (SS: spiny stellate, IN : inhibitory interneurons). Note that most inhibitory connections are eliminated for simplicity

1. The connectivity patterns of layer 5 cells with superficial pyramidals. This issue will revisited later upon discussing the new influx of evidence on layer 5 cells, especially on interneurons in this layer (chapter 4).

2. The overlapping patterns of input to a cortical circuit: feedback connections and nonspecific thalamic inputs on the one hand (so called modulatory), and feed-forward inputs and specific thalamic inputs on the other (so called driving). This will also be reemphasized later.

Early Canonical circuits Based on the above circuit outlines, shepherd at al [206] developed a canonical circuit of cortical function in the visual cortex which makes the distinction between superficial layers (2 and 3) excitatory population called $P2+3$ and the excitatory population of the lower layers (5 and 6) they call $P5+6$. The inhibitory population interacts with both, mainly with $P5+6$ and receives thalamic afferents, as shown in figure 2-8. They claim a wide generality of such circuit in tested cortical areas with site dependent variations.

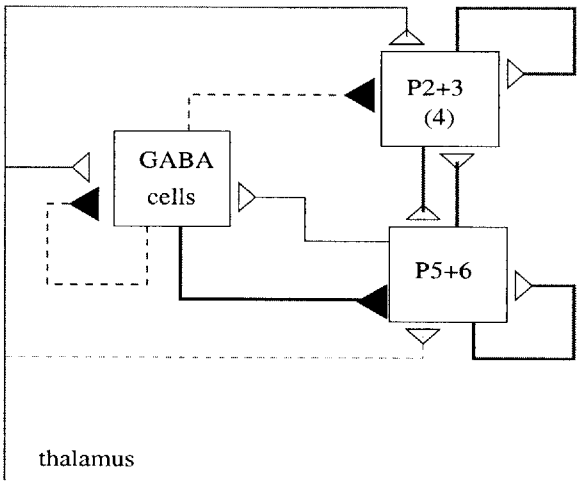

Figure 2-8: A canonical micro-circuit diagram for cat striate cortex. The thickness of connecting lines indicates the functional strength of the input. Note the dominant connection is between excitatory neurons, so that a relatively weak thalamic input can be greatly amplified by the recurrent excitation of the spiny neurons. (figure from Shepherd 1998 [206]).

2.2 The Thalamus

The thalamic structure is composed of different nuclei that receive input about different modalities such as vision, sensation and audition (Kandel 1991,[105], Miller 1996 [161]. It also transmits information from the cerebellum and basal ganglia to the motor cortical areas. The thalamus is also involved in deciding the level of consciousness of the cerebral cortex. It is divided into the dorsal thalamus, ventral thalamus and the epithalamus.

1 The *dorsal thalamus* has all the *specific relay nuclei.* These nuclei are reciprocally connected to specific sensory areas of the neocortex through cortical thalamic relay cells; the output of these nuclei synapse mainly in layer 4 of the neocortex, and, at a lower density, in layer 6. The dorsal thalamus contains non-specific or intralaminar nuclei. The output of these nuclei is diffusely distributed in the cortex, mainly in layer 1.

2 The *ventral thalamus* contains the reticular nucleus which connects to all relay specific and nonspecific nuclei of the dorsal thalamus, where it exerts an inhibitory action.

3 The *epithalamus*, which does not have efferents or afferents to the cortex, but rather connects to the hypothalamus.

Inputs

The dorsal thalamus receives extrinsic afferents that carry primary sensory information and are primarily excitatory (glutamatergic)and modulatory inputs from the

brain stem, cortex and feedback connections from the reticular formation. Cortical afferents are mainly from layer 6 pyramidal cells which form a strong excitatory feedback loop binding thalamic nuclei and cortical areas of the same type. The cortical-thalamic input usually follows maps established in the thalamus. Brain stem inputs are modulatory, releasing Acytelcholine (ACh) from the PPT nucleus, norepinephrine (NA) from the locus coerleus, and serotenergic from the dorsal raphe nucleus.

The thalamic nuclei can either be specific, which imply their direct involvement in sensory modalities with a topographic interconnections with specific cortical areas, or nonspecific, having a diffuse or multifocal connectivity character in the cortex and a role in the cortical level of arousal. It is important to note that this general dichotomy of specific vs non-specific nuclei have been recently challenged. Other hypothesis argue the existence of nonspecific projecting neurons forming a "matrix" extending throughout all nuclei of the thalamus intermingled with specific-projecting TC relay cells; it is only that intralaminar and other nonspecific nuclei lack relay cells (Jones 1998 [102]).

Synaptic organization

Thalamocortical relay neurons in the dorsal thalamus receive excitatory drive from the cortex on the distal dendrites, an inhibitory connection from the relay nucleus and another from local inhibitory interneurons within the relay nucleus, but do not have recurrent excitation (TC to TC) connections. Reticular formation neurons have recurrent inhibitory connections and receive inputs from relay nuclei, brain stem and thalamocortical neurons (figure 2-9).

Other nuclei, such as the intralaminar and midline, receive inputs from RE, and cortical layer 5, and their neurons project to apical dendrites in layer 1 of the neocortex (and some layer 6) and to basal ganglia.

Firing modes

Thalamocortical TC relay neurons could fire in two modes: tonic and burst firing. While tonic mode is more active during wakeful states and arguably functions in relaying information from the external world to the cortex, these cells switch into burst firing, also known as low threshold spiking (LTS), when they are hyperpolarized ($\approx$ 70mV). This is caused by de-inactivation of a low threshold calcium conductance and subsequent flow of an inward current called I_T, leading to bursting. The increase in intracellular calcium will cause Ca-dependent K^+ conductances to activate, causing an outward current which will repolarize the cell. Bursting in this mode occurs at low frequency (around 10 Hz), and is seen as an effective way to synchronize TC neurons, "detaching" them from sensory input during sleep (figure 2-10).

The reticular formation (RE) neurons receive a strong drive from the cortex and are fairly sensitive to this input. During early stages of sleep, these cells are hyperpolarized and are caused to burst fire. It has been demonstrated that the intact recurrent inhibition among RE neurons cause burst firings at 7-14 HZ frequency better known as spindles. The spindle cycle initiated in RE engages TC neurons in LTS

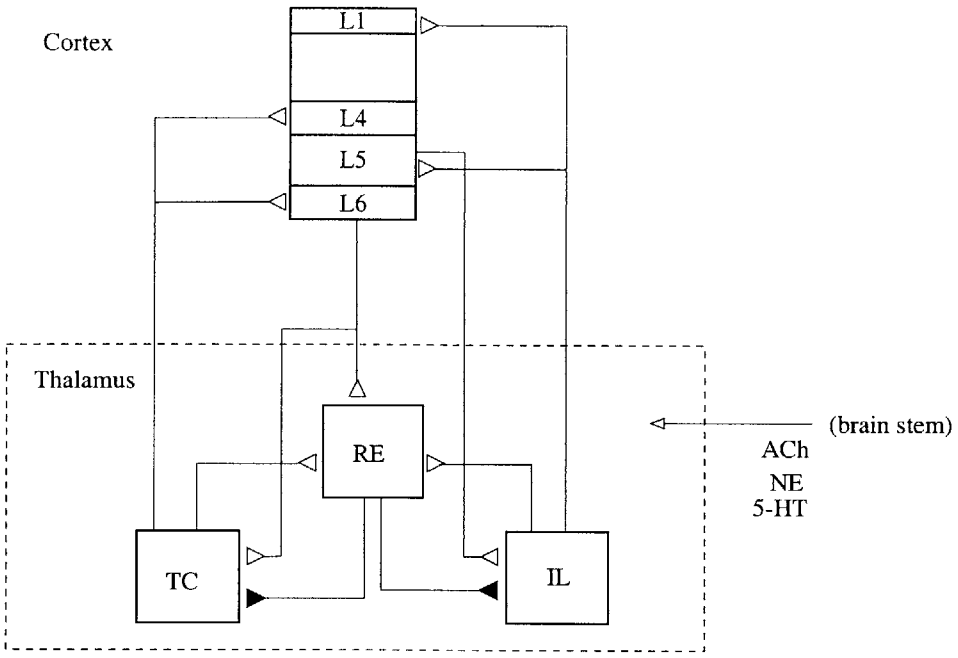

Figure 2-9: Schematic of major cortical-thalamic pathways. RE is the reticular formation which receives inputs from pyramidals in layers 5,6 and from thalamocortical relay nuclei (TC) as well as intralaminar nuclei (IL). In turn, RE inhibits TC and RE. Open triangles indicate excitatory connections, filled triangles inhibitory.

mode (due to their inhibitory effect on those cells) and is hence transferred to the cortex, as we will see later.

The switch between the two modes occurs due to mainly:

Brain-stem inputs: the PPT exerts an excitatory drive onto TC cells thus depolarizing them. PPT activation inhibits RE cells as well as local inhibitory interneurons, thus releasing TC cells from its inhibition with the net result of switching into tonic firing. Other modulatory neurotransmitters such as norepinephrine and serotonin have a similar effect.

Cortico-thalamic inputs cause long-lasting EPSPs in the TC cells, thus switching the cells into the tonic mode. This role is less obvious, and has been shown only by enhancing metabotropic glutamate receptors in TC cells, which is mainly driven by cortical afferents.

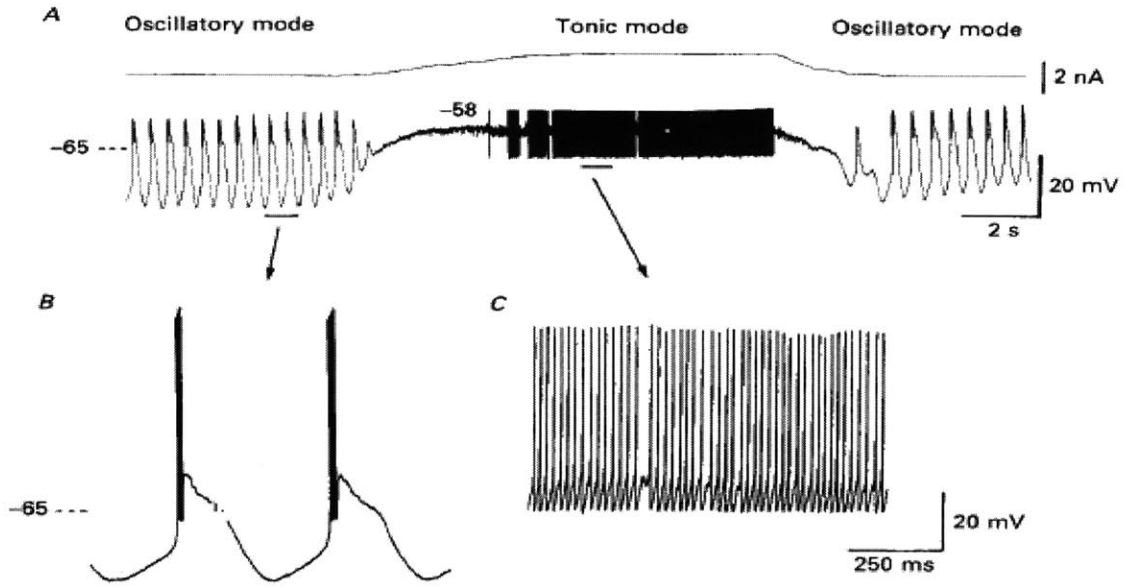

Figure 2-10: Switch in firing mode of thalamocortical relay cells when depolarized (LGN of cats). Upon depolarization, the 2 Hz burst firing mode (expanded in B) is switched to a tonic firing mode (expanded in C). Similar effects is brought about by neuromodulators such as Acetylcholine (PPT) during arousal (figure adapted from McCromick and Pape 1990 [152]).

Chapter 3

Oscillations in the Brain: Morphology and Cellular Basis

In this chapter, we will briefly present current knowledge of the basis and types of oscillations in the brain as resulting from coherent activity among different brain structures starting with minimal neural substrates and extending to large inter-areal coherence as well as involving lower brain structures especially the thalamus. Our aim in this exposition is to provide insight for the types EEG-observable activity and the experimental knowledge of its substrate. The descriptions are compiled from various experimental evidence in animals and humans. An excellent review of brain oscillations is given by one of the main workers in the field (M Steriade 2000, [227]).

As such, oscillations are observed under mainly (1) *globally-measurable states* where coherent activity is detected in large areas of the cortex and is generally related to the overall state of mental vigilance and (2) *locally-measurable states* which are related to specific sensory or cognitive state occurring in specific areas of the brain.

Many views of the relevance of brain oscillations exist, ranging from dismissing it as an epiphenomenon with little or no signatures of brain states to considering it as the basis of memory, dreaming, and even active cognition.

Of the main criticisms of the role of field potentials is that, first, spatial averaging of activity might lead to spurious conclusions about actual neural behavior especially that recorded potentials of a single electrode are influenced by the activity of both a large local underlying population (gross averaging) as well as interferences from other close structures (volume conduction), and second, that most experimental recordings of intracellular activity as it relates to field potentials are performed under anesthesia or in slices, which leaves much room for mismatch with neural behavior under naturally occurring states. As we saw in the introduction chapter, these criticisms have been fortunately increasingly refuted with the advent of recording technologies (figures 1-4 and 1-5) . Many experiments have demonstrated that most highly coherent states of vigilance such as sleep are usually linked to actual cellular activity, depolarizations and hyperpolarizations, as we will review in this chapter. Further, the effect of anesthesia appeared to be minimal in the general conclusions about sleep and awake states in the cat cerebral cortex after such states were recording in natu-

rally waking and sleeping animals and this includes both slow rhythms as well as fast oscillations related to cognition (Destexhe et al, 1999 [62]) .

3.1 States of vigilance associated with oscillatory EEG

3.1.1 EEG and Oscillations

Although EEG signals are mainly scalp measurements of undergoing brain oscillations in humans, it is worth mentioning at this point that such distinction is blurred in animal studies where many experiments actually have access to cortical surface field potential, termed *surface EEG* and intra-cortical field potentials, termed *depth EEG*. Hence, although many oscillations might be clearly observable in surface or depth EEG recordings, the low-pass nature of scalp measurements might smear fast or spatially-limited oscillations. This has been traditionally the case in human EEG where high frequency EEG was hardly observable or might even be dismissed as noise artifact. In contrast, these same oscillations have become a focus of attention in human EEG analysis ever since animal experiments reported intracortical recordings of the so called 40 Hz rhythms or fast oscillations arguably related to active processing in the brain. Therefore, although a distinction exists between what can be recorded on cortical surface and the scalp, most of the oscillatory types we will be discussing have been reported in scalp measurements, mainly due to there wide range spatial coherence (sleep or seizure rhythms), or their dominance over fairly large sensory areas (alpha rhythms over visual cortex). Accordingly, we will ignore for the moment distinctions between surface EEG and scalp EEG, and provide insights on any mismatches between the two measurements where need arises.

3.1.2 Slow oscillatory states

The spectral bands that were described earlier for clinical EEG practice still hold here. That is, we will refer to oscillations with less than beta frequency as slow. A main characteristic of such slow rhythms is coherency on fairly large areas of the neocortex and hence are possibly due to emergent properties of spatially distributed neural substrates or due to a common input or a modulator that drives the neocortex into a coherent rhythm. We will refer to such states as globally-measurable states. In the following, we will describe some of these rhythms and their clinical significance, and what is known about their neural origins.

Sleep rhythms

As the cortex progresses from a wakeful state into various stages of sleep, several hallmark signal templates are observable. In normal subjects, sleep consists of a periodic cycling between 4 non REM sleep stages and REM sleep. The nonREM sleep starts with appearance of low-voltage, high frequency activity with occasional

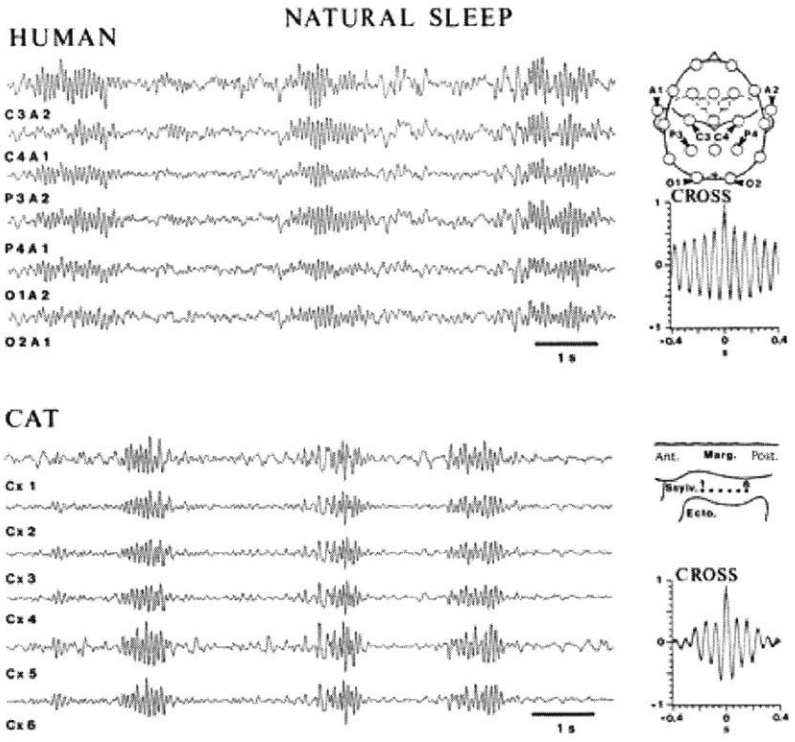

Figure 3-1: Spindle oscillations during natural sleep recorded from humans and cats show coherency over wide areas of the cortex. Right plots show location of recording and 14 Hz rhythmicity as displayed in cross correlation functions.(reproduced from Contreras et al 1997 [42])

spindles (or what is called stage 1 descending) followed by the dominance of distinctive $\approx$ 10 Hz waves called spindles (stage 2); delta and K-complex activity start in stage 3, and continue more pronounced in stage 4, finally REM sleep occurs after a 90 minute cycle and lasts for about 30 minutes (Sinton and McCarley 2000 [210]). In what follows, we will describe the main rhythms, these include

1. **Spindle oscillations:** These are 7-14 Hz waves that occur during natural sleep mainly at its early onsets (stages 1 and 2), but could also appear at later stages. It is recorded in short time windows at multiple electrode sites with a high degree of synchrony. Although this frequency band overlaps that of alpha band, they have quite different implications on consciousness, especially that alpha occurs during restful wakefulness. A possible source of spindle oscillations is the pacemaker effect of reticular formation of the thalamus where mutually inhibitory neurons burst at spindle frequency *in vivo* in naturally-sleeping cat experiments and in some *in vitro* manipulations. Still, the neocortex appears to play an important role in reinforcing this activity through cortico-thalamic feedback causing it to appear simultaneously and more coherently over multiple sites (figure 3-1), as has been demonstrated by Steriade, Contreras and coworkers (Contreras et al [42], Destexhe et al 1999 [62]).

2. **Delta oscillations:** These rhythms occur at 1-4 Hz and are observed mainly during later stages of sleep (stages 3 and 4). Two main patterns of delta activity occur during sleep: (1) highly stereotyped rhythmic delta which occurs in periods of relative silence in the neocortex and is synchronized with thalamic delta activity (hence might be of thalamic origin, as Steriade argues (Steriade 93) and (2) delta activity occurring in periods of high cellular activity and is present on the neural level as bursting in some cortical cells as well as membrane depolarizations in other cells in the delta range without a counterpart in the thalamus and hence might be of cortical origin (figure 3-2).

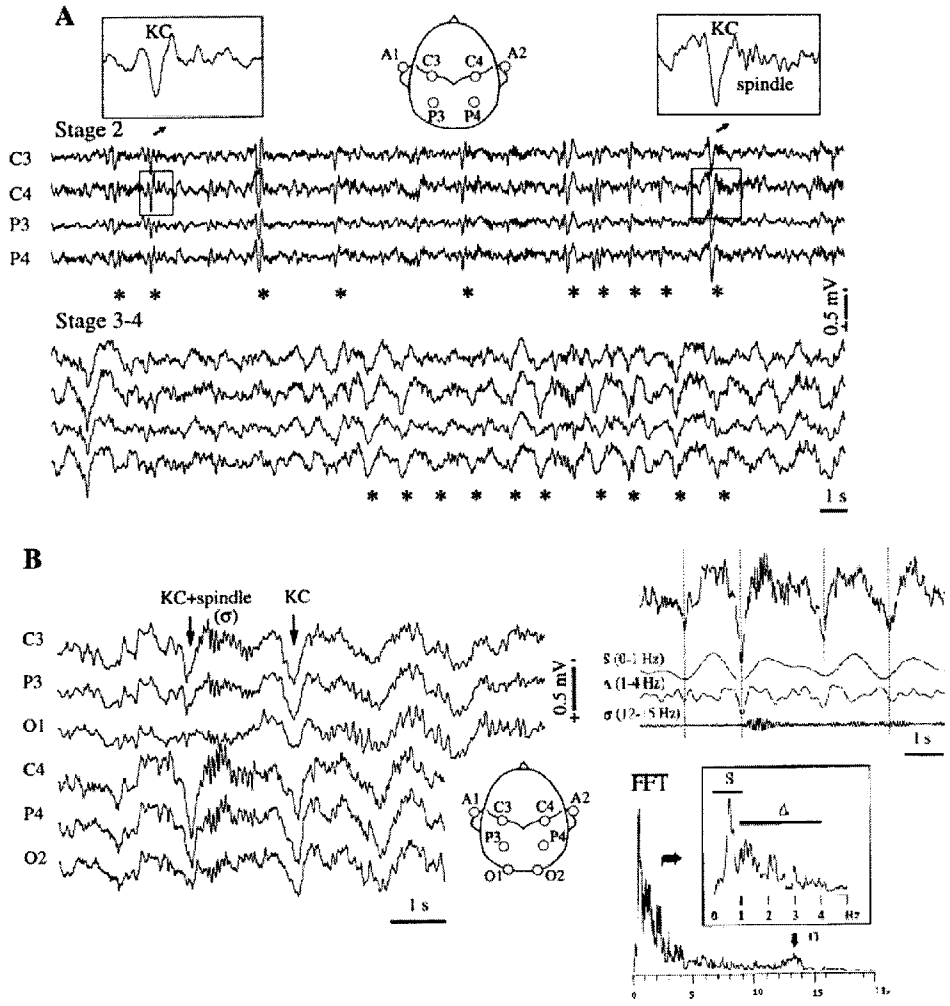

Figure 3-2: Human EEG recordings show progression of slow oscillations during sleep. A: K-complexes are repeated at a slow rhythmicity (0.7 Hz) as sleep deepens. Insets show occurrences of K-complexes that are occasionally followed by sleep spindles. B. Another example of K-complex rhythmicity with corresponding band wave decomposition (right upper trace) and frequency spectrum (right lower trace) (figures adapted from Amzica et al 1998 [5])

3. **Slow-wave sleep oscillations:** This refers to a very slow rhythmic grouping of other sleep activities in stages 3 and 4 and occurs at a rate of < 1 Hz ($0.7 - 1$ Hz). Although it has not been widely acknowledged in clinical literature, this slow rhythm, which was discovered by Steriade and coworkers under anesthesia, have been described in anesthetized cats and later reported in naturally sleeping animals as well as in MEG and EEG experiments in humans (figure 3-2). Slow-wave oscillations occur coherently in morphologically and functionally different areas. It is an intracortically generated rhythm since it survives thalamectomy, is absent in the thalamus of decorticated animals, and its synchronization is disrupted by disruption of intracortical synaptic linkages. It is characterized by an extended period of neuronal silence (0.3-0.4 sec) followed by an active periods of oscillations mainly starting with spindles and then followed by delta waves with occasional runs of high frequency. The spindle oscillations seem coherent between the thalamus and corticothalamic neurons and hence could be attributed to thalamic origin, as before. The slow-wave oscillation in humans is arguably the K-complex of sleep known to occur in stages 3 and 4 of nonREM sleep and has a hallmark 1 Hz periodic template of a large wave deflection followed by spindling.

4. **REM oscillations:** This is a period of high activation sleep where bursts of rapid eye movements and loss of muscle tone occur. It is characterized by desynchronized EEG patterns or fast oscillations similar to those present during alert wakefulness. REM sleep occurs after sleep stage 4 and repeats in periods of about 90 minutes, with the first episode being the shortest and occurring about 70 to 90 minutes after sleep onset.

5. **Alpha band oscillations:** Occur mainly over the visual cortex of humans and other mammals in restful wakefulness, eyes closed and are in the 8-12 Hz range. Alpha rhythms have traditionally been attributed to mental idling, but has recently been correlated with cognitive task performance and in cases of increased attentiveness in humans (Basar, Schurman [201] and and Klimesch [119]). In particular, a short period of time-locked alpha band activity has been demonstrated to be coherent over disparate visual areas only when upon successful recognition of an observed stimulus (Mima et al 2001 [162]). More on this rhythm will be detailed in view of our model in later chapters.

6. **Other signature waves:** such as rolandic mu rhythms over the motor areas and tau rhythms over the auditory cortex are observed and presumably related to cognitive aspects of respective tasks.

Seizures

The development of seizures in EEG have been reported as resulting from various pathologies in the neocortex and thalamus. Many slice experiments have demonstrated the ability of subpopulations of neocortical cells to produce excessive excitation leading to seizure-like activity. Among other conditions, seizures have been

reported to occur either as a natural progression from slow-wave non-REM sleep, after administration of anesthetics, or after injury. In what follows, we will briefly touch upon some of epileptogenesis experiments that might be of relevance for the current work.

1. **Spike and Wave seizures:** Steriade and co-workers have studied a type of seizure they termed *spike and wave (SW)* or *poly-spike and wave (PSW) seizures* (the distinction arising by the number of repetitions of spikes during an event). Their tests in cats have shown that such seizures might occur as smooth transitions from slow sleep oscillations, during quiet waking, drowsy or resting sleep, but not during REM (figure 3-3). This type of seizure, they argue, is similar to non-absence epilepsy in children.

   In their experiments, a SW seizure is a cortically-generated rhythm since the cortex has a leading phase in the generated waves. *It could also be artificially induced by repetitive* 10 *Hz stimuli or during anesthesia.* The spike and wave component occurs at 2 - 4 Hz and is often associated with runs of faster ($10-20$ Hz) EEG spikes. Spatially, spontaneous seizures do not occur suddenly over the whole cortex but could propagate between different foci, across hemispheres, with time lags for initiation of up to 50 msec. SW seizure could be induced during thalamectomy in cortex upon administration of the $GABA_A$ inhibitory blocker bicucilline in neocortical circuits, but this inhibitor when applied to thalamus, could only trigger spindles but not SW seizures in the neocortex. Several factors prompted the belief that similar circuitry might underly SW seizures and sleep K-complexes, with some distinctions that we are going to touch upon later.

   Other experiments induced seizures due to lack of inhibitory control. Castro-Alamancos showed that disinhibition in the neocortex of cats can produce starting from slow wave oscillations a 1 Hz seizure followed by several 10 Hz oscillations (Castro-Alamancos 2000 [32], figure 3-4).

2. **Injury-induced seizures:** Epileptogenesis under injury has been studied in cats and monkeys as isolated neocortical island (in vivo models). This type of seizure is cortically induced, mainly due to an increased excitability of neocortical cells via additional sprouting of axonal connections and increase in synaptic strength.

Anesthesia rhythms

At least two types of anesthetics produce slow oscillatory effect (< 1 Hz) similar to that seen during sleep. Ketamine-xylazine anesthesia produced slow rhythms at $0.6 - 0.9$ Hz and Urethane anesthesia oscillations have a frequency of $0.3 - 0.5$ Hz, with the difference assumed to be due a depressing effect of Ketamine, thus reducing cellular activation and the oscillatory cycle. Slow-wave inducing anesthetics were in fact the primary experimental preparations where < 1 Hz oscillations were first observed in cats.

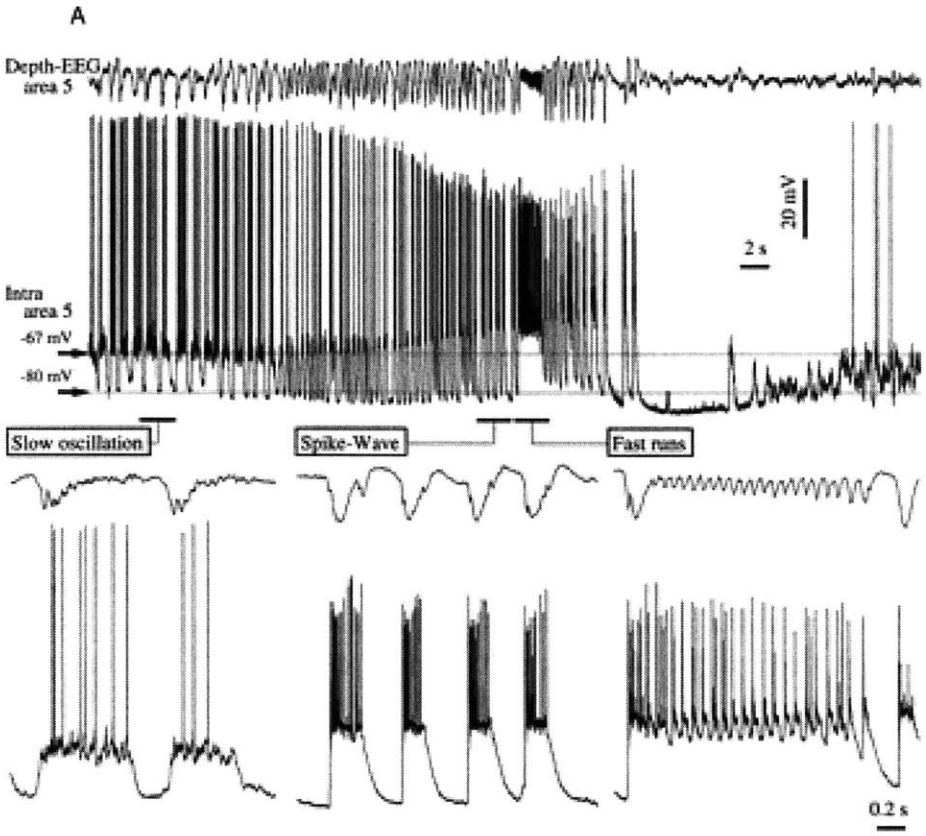

Figure 3-3: Spontaneous progression of slow wave oscillations into spike-and-wave seizures in cat. Upper trace shows intracortically recorded EEG. Middle trace is an intracellular recording from affected area. Lower plots show expanded views(from steriade et al 1998 [224])

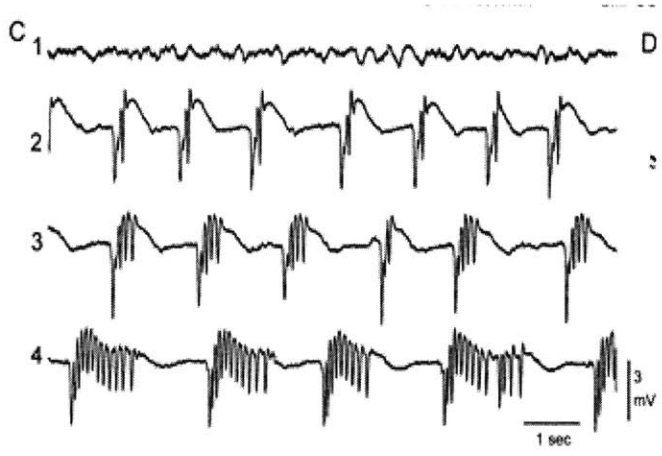

Figure 3-4: Generation of seizures in animal models under disinhibition. Top trace shows normal slow-wave oscillations; lower plots show evolving seizures under increased levels of disinhibition (from Castro-Alamancos 2000 [32])

Deep barbiturate anesthesia, on the other hand, produced overwhelmingly spindling activity ($7 - 14$ Hz waves) similar in shape to that occurring in sleep. Unlike natural sleep spindles, however, barbituate- induced spindles have incoherent foci of origin. This is understood by decreased cortico-thalamic interaction since barbituates depress cortical activity, leading to decreased excitability of neocortical pyramidal neurons (steriade). More on this will be presented later.

3.1.3 Fast oscillatory states

The slow oscillatory activities described above have a common characteristic of being coherent over fairly large areas of the neocortex and thus are reflected in EEG recordings with little or no change, hence our notion that they are *globally measurable states*. While such slow oscillations are confined to the non-REM sleep, anesthetic or epileptic response, they are replaced by low amplitude high frequency oscillations during active brain states, mainly alertness and REM.

High frequency oscillations were initially referred to as EEG desynchronization, with the name describing the contrast of low amplitude "jitter" with large coherent slow oscillations. With the advent of recording techniques, high frequency gamma oscillations, or so-called 40 Hz activity became an induced rhythm which seemed to correlate well with periods of high mental alertness, attentiveness, and response to sensory stimuli both in animal intracellular studies and in human EEG/MEG recordings. This has generated tremendous interest in the gamma oscillations as probably linked to representation of visual objects or even higher forms of cognition.

Fast rhythms have been recorded in the neocortex as well as lower brain structures, thalamus, basal forebrain, etc. These rhythms are seen under various states of vigilance including wakefulness, sleep and anesthesia. Of particular interest in the neural community, however, was the emergence of highly coherent fast oscillating field potentials in neural populations when under adequate sensory cues. Such coherence is also reflected at the cellular level in terms of synchronous spike discharges of involved neural populations.

Within one area of the neocortex, fast oscillations are in-phase throughout cortical depth, with short time lag between superficial and deep layers, and a dramatic decrease of fast activity in the white matter. Spatially, coherent activity occurs over limited proximity, with the intracortical connections which span areas up to 8mm of a single area possibly mediating this coherence. Further, fast oscillations were known to be coherent across areas over distances spanning the two hemispheres, possibly due to callosal fibers.

The emergence of synchronized gamma -range oscillations in sensory systems have spawned proposals that *such a synchronization might well mediate feature binding in lower visual structures and possibly higher cortical areas, or what became known as the temporal binding hypothesis* (Singer and Gray 1995 [208], Singer 2001 [209]) .

A growing body of experimental literature supports the role of oscillatory synchronization in visual feature binding (Usrey et al [243]). Stimulus-specific gamma has been recorded in the visual cortex of anesthetized cats and awake monkeys. The level of synchronization was higher in response to visually coherent moving bars than to in-

dependently moving bars. In human EEG/MEG experiments, an increase in gamma activity has been reported in the scalp EEG about 200 msec after the electrical stimulation of the finger in a sensory discrimination task. In an auditory task, differences in gamma power have been reported upon hearing standard tones compared to new tones (Tallon-Baudry and Bertrand 1999 [233]) .

Although high frequency activity has been attributed mostly to wakeful brain states, it has been observed across states of vigilance. In fact, fast oscillations are recorded not only in intense attention and response to stimuli, but also in diffuse arousal and occasionally in sleep and anesthesia. This may seem puzzling if one thinks of gamma oscillations as related to mental alertness. However, although high frequency activity appear to be part of the background activity of the neocortex, the level of coherence was maximal under adequate stimuli, and it at least seems to correlate well with perceived stimuli especially in visual perception experiments. Accordingly, the idea of synchronization of fast rhythms for feature binding under sensory stimuli continue to be valid and reinforcable with new experiments. For example, it was presented that neural synchrony could bias the way we percieve visual stimuli. In particular, neurons in different visual areas synchronize their response when responding to contours belonging to the same percieved surface but not when they responded to contours belonging to different surfaces (Castelo-Branco et al 2000 [28]).

3.2 Cellular basis of Cortical Oscillations

Many experimental studies have been conducted to elucidate the neural origins of brain rhythms, with varying degrees of success. The workers in the field usually analyze both intracellular activity as well as depth and surface EEG. In many cases, technical advances have allowed simultaneous recordings from many cells as well as from the associated field potentials *in vivo* in naturally behaving animals. As such, many workers hoped for a pacemaker role of subpopulations of cortical neurons and possibly lower brain structures, mainly the thalamus and reticular activating system. We will briefly survey a very small sample of these experiments which occasionally conclude with proposals as to what the role of different neural elements and properties were for generating the rhythm under scrutiny.

3.2.1 Spindle oscillations

The origins of rhythmic 7-14 Hz spindle waves have been fairly understood in a series of experiments involving the effect of thalamic circuitry in recruiting cortical populations in rhythmogenesis (Conteras et al 1997 [42], Steriade et al 1997 [221])). A group of mutually inhibitory neurons in the reticular formation (RE) of the thalamus in cats have been shown to generate, when hyperpolarized, a series of rhythmic bursts in the spindle frequency range in vivo, which would survive decortication. Computational studies have replicated this behavior, referring it to a complex interactions of ionic currents within the RE neurons themselves when hyperpolarized.

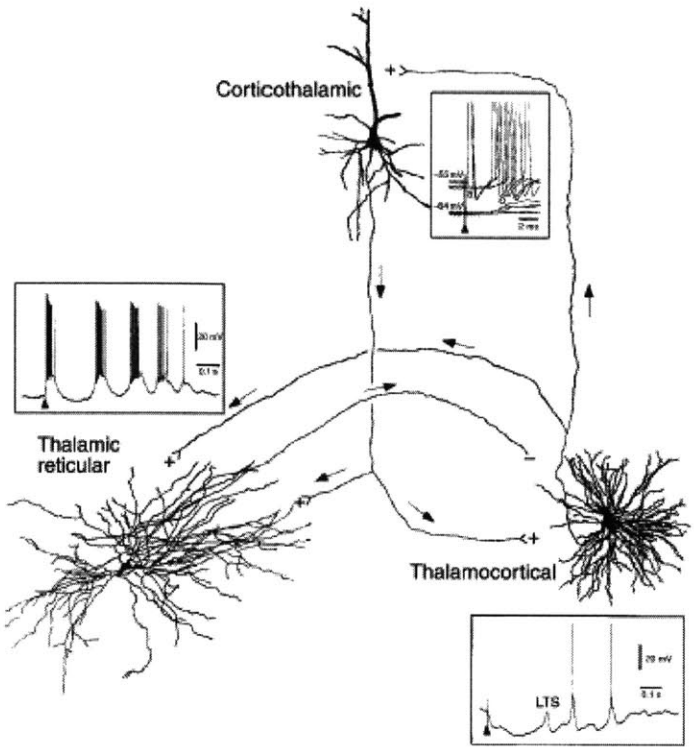

Figure 3-5: Spindle oscillations are an intrinsic response in RE of the thalamus under light sleep. IN response to cortical stimulation, an RE neuron generates a sequence of bursts at spindle frequency (7-14Hz). The same stimulation causes a net hyperpolarization in TC cells which leads to a post-inhibitory rebound in these cells which then transfer the spindling to the cortex (figure from steriade 1999 [226])

Using a repertoire of experimental evidence, Steriade and coworkers explain that spindle rhythmogenesis could probably be elucidated as follows. The transfer of spindling to the neocortex occurs via thalamocortical relay (TC) cells of the thalamus. These cells are inhibited by RE neurons (figure 2-9) . Hence, upon receiving a series of inhibiting bursts from RE neurons, TC cells will hyperpolarize causing to rebound from inhibition in a synchronous manner via an ionic rebound mechanism and thus follow the firing cycle of RE neurons. The synchronous firings of TC cells are then transfered to the cortex, which in turn becomes excited and returns the firing via neocortical cortico-thalamic cells (TC) into both RE and TC cells of the thalamus. With RE neurons poised as highly excitable the net effect is to cause these hyperpolarized cells to burst fire causing a net inhibitory effect on TC cells and the cycle essentially repeats (figure 3-5).

The cortex hence is seen as a feedback mechanism which reinforces spindle oscillations once they start in the RE and the TC cells act to synchronize spindles of the neocortex over wide areas due to the divergent thalamo-cortical synaptic linkages.

We have seen that spindle oscillations are generated in early phases of sleep. This, steriade explains, is partly due to a decrease of afferent excitation from the PPT

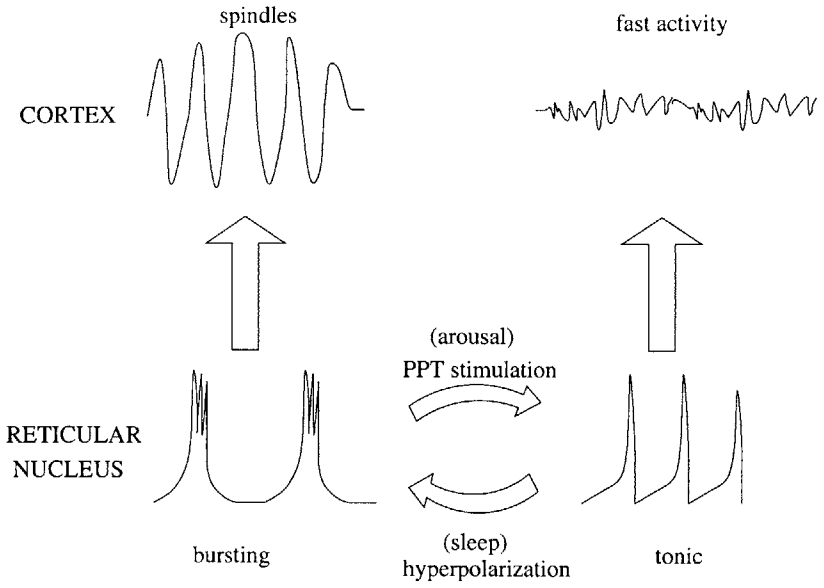

Figure 3-6: Schematic of how the switch in firing patterns in the reticular nucleus neurons (RE) is reflected in neocortex EEG. Arousal mechanisms (eg. PPT stimulation) switch firing to tonic of transfer mode. Sleep leads to hyperpolarization which switches RE neurons back to bursting at spindle frequency

and other structures which contact both thalamic nuclei and the neocortex. This withdrawal of excitation causes a cascading decrease and ultimately hyperpolarization in RE cells which initiate spindling and spread it to the neocortex (Figure 3-6) .

Under this mechanism, the neocortex acts as a reinforcement loop by virtue of strong intracortical connections, effective cortico-thalamic linkages, especially to the RE, and strong divergent thalamocortical connections. This could probably account for the near simultaneous appearance of spindle waves over wide areas of the cortex. In addition, the effect of barbituate anesthesia and other depressing factors on the neocortex in causing spatially incoherent spindles is explained. Essentially, the barbituate factor acts to reduce responsiveness of cortico-thalamic cells of the neocortex thus decreasing the gain of cortical feedback and producing an erratic generation of spindles within a loose initiation time and at a lower frequency (6-8 Hz) which is reflected in the neocortex. Computational models demonstrated this behavior and predicted the generation of epileptic discharges if neocortical pyramidal cells at 3 Hz when intracortical inhibition is reduced (Destexhe et al 1998, 1999 [57, 60]).

3.2.2 Delta Oscillations

As we have seen earlier, delta oscillations of the neocortex can be either (a)- highly rhythmic occurring in periods of neocortical silence, or (b) more random in initiation during periods of high neocortical activity.

a- Rhythmic delta activity could be generated in the thalamus if thalamocortical relay cells are hyperpolarized at more negative voltages than those required for

spindling to occur. That is, delta could be an intrinsic rhythm of TC cells due to an interaction between ionic currents (I_T and I_C). In vivo, this switch from spindle to delta could occur if NMDA receptors of thalamocortical (TC) cells are blocked, causing more hyperpolarization due to inhibition from the RE input. Similarly, with progressive hyperpolarization RE cells firing behavior is shifted from tonic mode (20-40 Hz) during arousal to lower frequencies (10-20 Hz) during drowsiness, and into rhythmic spike bursts during spindle sleep (figure 2-10) . At further hyperpolarization, RE neurons could generate delta–range activity which is possibly a slowed-down version of their intrinsic spindle rhythms (i.e. slower oscillatory frequency in figure 3-6). Such a scenario seems especially plausible given the dominance of delta activity during later stages of sleep when reduction of brain stem excitation is at its peak. In fact intracellular recordings of this delta pattern at periods of enhanced synchronization between the EEG and EthG (electrothalamogram) reflected a clock-like action potential firing in a group of neocortical cells at a frequency between 1-4 Hz.

b- EEG delta waves recorded from the neocortex tend to be less rhythmic than thalamic delta discussed above. In fact the irregular delta waves observed in EEG show that the neocortex is not passive under this rhythm, since *polymorphous delta waves can be generated in the cortex in the absence of the thalamus.* Intracellular recordings performed by steriade 1993b [217] shows that a group of intrinsically bursting (IB) neocortical cells (58/105 samples) followed a delta rhythm of 3-4 Hz on a 0.3-0.4 Hz slow wave sequences while other cells, possibly regularly-spiking cells did not synchronize with this delta rhythm (see figure 3-7).

3.2.3 Slow-wave oscillations

Slow wave oscillations are characterized by a long lasting depolarization superimposed with somatic action potentials and separated by periods of neuronal silence (figure 3-8). This rhythm appears to be neocortical in origin and resultant from intracortical connectivity. The emergence of slow-wave oscillations as a network property of the neocortical connections is demonstrated by multi-site recordings which showed that closely located cells in one area are also close in time, i.e. discharge with short time lags ($\approx 12msec$). Distant cells belonging to different areas, on the other hand, discharge with longer lags (mean $\approx$ 120 msec).

Looking at the depolarizing component in a 0.3-0.4 Hz cycle, regularly spiking (RS) cells fire for a period of 0.8-1.5 sec at around 5-30 Hz depending on the level of membrane depolarization. In cases that cells were hyperpolarized, action potentials seize; still ripples occur in these cells, possibly due to dendritic spikes (corroborating the idea that intracortical linkages mediate this activity). This depolarizing component decreases in length under ketamine which is an NMDA blocker, and is probably due to a persistent sodium current as well as NMDA receptors. An interesting observation is that, in the majority of neurons, hyperpolarization improved the amplitude of the depolarizing component, possibly due to reversed inhibitory synaptic potentials,

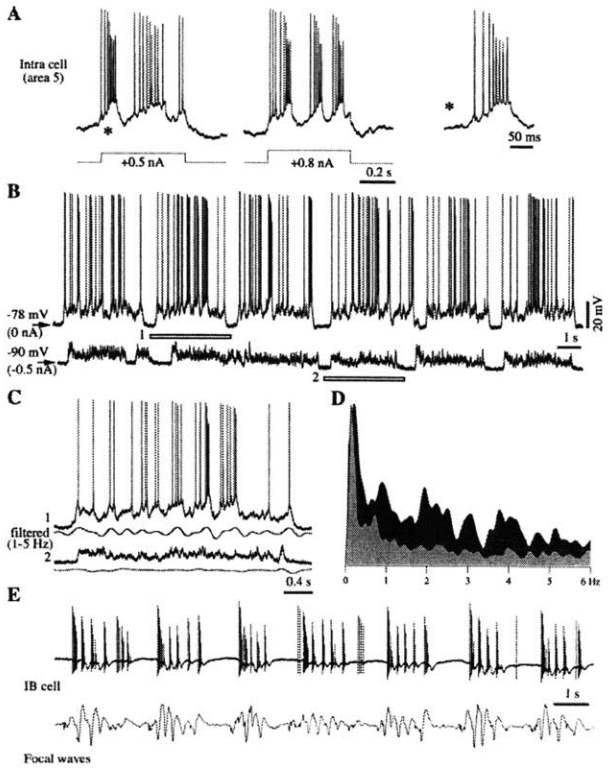

Figure 3-7: Delta oscillations are well reflected in intrinsically bursting neurons. *A* cell response to current injection shows low frequency oscillations that increase with input current (inset far right is a detail). *B:* same cell response during slow wave sleep shows delta component. Hyperpolarization stops burst firing and blocks the delta but not the general slow-wave profile. *C* expanded view of underlined segments and (D) corresponding power spectrum shows blockage of the delta band (light grey) compared to base line (dark grey). *E* correspondence between cell extracellular recordings (firing) and recorded field potentials (figure reproduced from Amzica and Steriade 1998 [4])

or non-NMDA receptors. Looking at the origin of the generated activity, Steriade noticed that the depolarization is reversed in the upper part of layer 2 of the neocortex, probably indicating a source if excitation in the apical dendrites in layer 1.

The origin of the long lasting hyperpolarization creating slow-wave rhythms is debated. Possible candidate for this are the following:

1. GABA-mediated inhibition, which is unlikely since no neurons were recorded firing in phase-opposition of the slow-wave template, rather it was a period of neuronal silence.

2. Hyperpolarizing effect of slowly developing Ca^{+2} dependent potassium ionic currents I_{AHP}. Upon stimulation of brain stem nuclei which are known to release Acetylcholine (Ach) into the neocortex, the hyperpolarized episode is suppressed, which could be explained by the blockage of Ca^{+2} dependent and other K^{+} current. Conversely, if a muscarinic blockers is applied the effect of brain

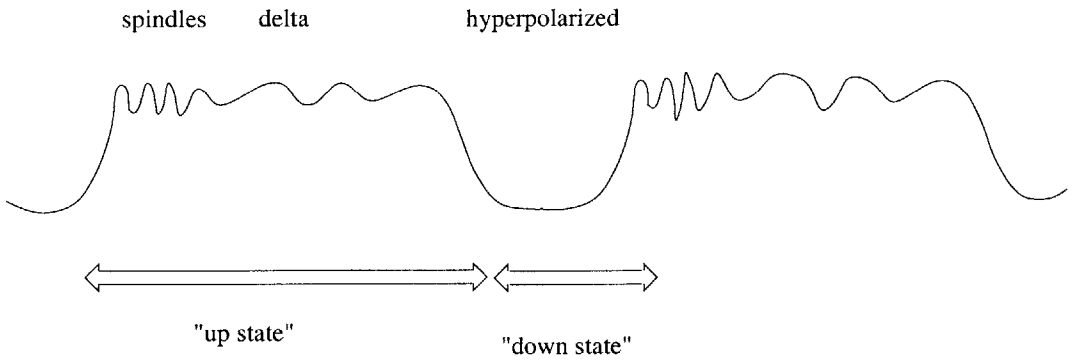

Figure 3-8: Schematic of a slow wave oscillation and possible constituent waves. During the depolarized or "up" state cells can entrain in a spindle rhythm followed by a delta band oscillation. Fast oscillations can also occur but have been omitted here for simplicity. The depolarized state eventually leads into a state of neuronal silence , hyperpolarized or down state.

stem activation is suppressed.

3. Effect of Adenosine in increasing K^+ conductances. Since it has been demonstrated that this neuromodulator is released during synchronous activity of neurons, the K^+ conductance increase will create sufficient hyperpolarization to shut of cell firing after some time.

4. Sudden withdrawal of activity throughout the cortical circuit, similar to what happens during burst suppression in EEG. In this case few afferent volleys after the withdrawal are sufficient to reactivate the cortico-thalamic network.

5. Recent experimental models (Sanchez-Vives and McCormick [193] showed that lack of excitability and increased hyperpolarization might be the main effectors in observed periods of neuronal silence (figure 3-9).

The thalamus reflects slow-wave sleep as follows: Neurons in the reticular nucleus (RE) displayed hyperpolarization coincident with the hyperpolarization of EEG. The depolarizing phase of cortical EEG preceded that of RE neurons by $\approx 0.3 - 0.4$ sec, which in turn responded with a sequence of spike bursts over a depolarizing envelope, and subsequently switching to a tonic firing mode (this is understood since firing mode of these cells depends on the level of membrane depolarization. The thalamocortical TC cells respond to RE spindles by low threshold spikes, thus following that rhythm and feeding it back to the cortex. This rebound firing contributes to time lags observed in the cortical EEG of different areas.

A recent experimental and computational model by Timofeev et al 2000 [238] demonstrated the emergence of slow oscillatory behavior in isolated cortical slabs in the cat as the size of the slab is increased. In the in vivo experimental setting, an isolated slab demonstrated long periods of silence in which the cells nonlinearly amplify low-amplitude depolarizing activity. Spontaneously occurring depolarizations interrupt periods of silence and occasionally led to action potential firing thus initiating a

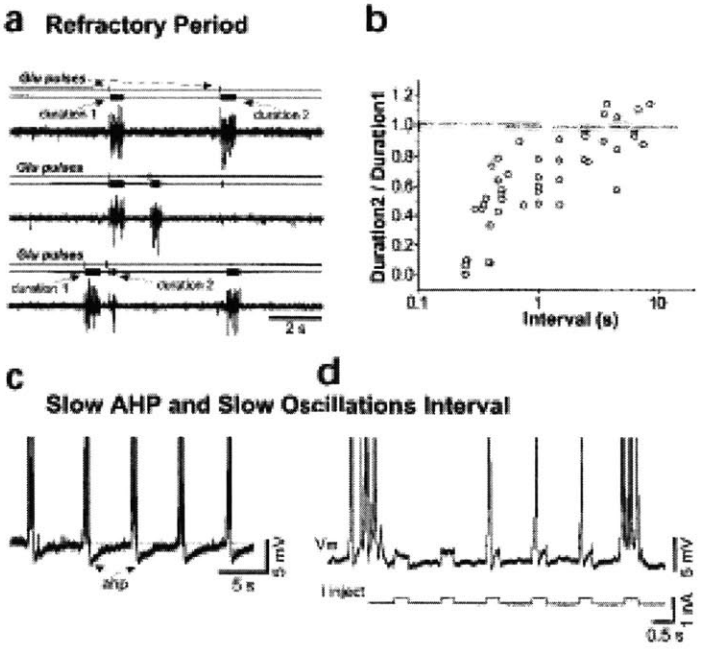

Figure 3-9: Slow oscillations in cortical slices have refractory periods where cell excitability is markedly decreased. A. Application of glutamate causes episodes of cell firing as those occurring spontaneously, the duration of which decreases if inter-application interval is decreased (plotted in B). C. After-hyperpolarization (AHP) occurs in cells after periods of firing. The combined effect shows marked decrease in cell response to current after periods of firing. (figure reproduced from Sanchez-vives and McCormick 2000 [193])

new cycle of the slow wave oscillation. During silent periods leading to a depolarization, small amplitude potentials were observed in cells and are thought to be miniature release events since no activity in the slice was recorded. In a network model, such mini- postsynaptic potentials leads to activation of a persistent Na^+ current $I_{NA^+(p)}$ which effectively lowers the threshold for action potential firing by about 10 mV, causing a more probable spontaneous action potential to occur. This phenomenon becomes more probable in a large enough network of interconnected pyramidal cells where spontaneously generated AP propagate in a slow avalanche effect within the slab and leading to a regular $0.5 - 1$ Hz oscillation in the network . This was consistent with their experimental recordings which showed emergence of slow oscillations as the size of the slab was increased. It is apparent that bursting behavior of cells played an important role in propagating activity within the slab (where incidence of IB cells is much higher than in vivo settings). In contrast to the necessity of large networks to generate slow waves, Sanchez-Vives and McCormick [193] demonstrated that when slices are placed in a realistic extracellular bathing medium, spontaneous slow-wave like activity (activated and silent states) can occur and is mostly initiated in layer 5 and propagated both superficial and deep layers. This experiment will be emphasized later in the thesis.

3.2.4 K-complex

K - complex is a major grapho-element of human sleep which recurs with a rhythmicity of less than 1 Hz. It is synchronously distributed over whole cortical surface and is transferred to the thalamus. During light sleep, it occurs in a regular spontaneous manner occasionally triggering spindles, but becomes more rhythmic at around 1 Hz as sleep deepens, to attain its highest level of synchrony just prior to REM sleep (figure 3-1). Like slow-wave sleep, K-complexes spatial synchrony depends on actual distance as well as functional distance between different areas. In fact, Steriade has argued that slow-wave sleep oscillation underly the genesis of K-complexes due to the similarity of wave profile and cellular discharges in both.

Being a well-characterized cellular oscillatory pattern, K-complexes have long been studied. They are cortically generated as they survive thalamectomy, could be recorded in functionally distinct areas (visual and motor, for example, both oscillate at less than 1 Hz), and are reflected in the thalamic nuclei including intralaminar nuclei.

K-complexes could also be evoked either by stimulating thalamic nuclei or by a synchronous volley to cortical tissue during slow-wave sleep. Stimulation of the ventrolaminar nucleus of the thalamus produced an initial excitation followed by a long period of hyperpolarization that ended with a rebound excitation (around 200 msec after) forming a K-complex. Similarly, stimulating the eye with an LED, initial excitation which exist in both waking and sleep states is followed during the sleep state by a K complex-like wave.

In studying the depth profile of KC in rats, it is seen that the potential reversed at around 0.3 mm (approximately layer 1). Current source density analysis demonstrated a massive sink between 0.3-0.6mm , which is about where layers 2,3 are located (Amzica et al 1998 [4]). This is consistent with intracortical linkages at this level which contact the apical dendrites of deep-lying pyramidal cells.

3.2.5 SW seizures

As we have seen before, a Spike and Wave seizure is an intracortically generated rhythm since most thalamic TC cells are hyperpolarized during its commencement and some other thalamic structures lag the cortical waves, and since it survives thalamectomy. A comprehensive review of the cellular basis and neural mechanisms of spike and wake and poly spike and wave seizures is given by Steriade series of papers (Steriade et al 1998a, Neckelman et al 1998, Striade et al 1998b [223, 167, 224]).

A SW seizure is characterized by a 2-4 Hz spike and wave component, often followed by fast runs of activity at 10-15 Hz, and ending with post-ictal depression (see figure 3-3). During a SW complex, the spike grapho-element is translated intracellularly to a paroxysmal depolarizing shift in membrane voltage which is crowned by action potentials and followed by hyperpolarization. As a seizure progresses, the cycle length of a SW seizure decreases and switches to the period of fast runs.

One can distinguish two types of firing dynamics in pyramidal cells. The first type is regular spiking (RS) cells which fire spike trains in phase with the depolariz-

ing component of the "spike" graphoelement and become hyperpolarized during the surface negative (hyperpolarized) wave. During the fast runs, RS cells were tonically depolarized and discharge single action potentials or doublets.

Another type of neurons that appear to be quite active in SW seizures are fast rhythmic bursting (FRB) neurons. These neurons have been described in many places in the neocortex including chattering cells in superficial and deep layers of the neocortex. FRB cells discharge vigorously with many more spike trains during a SW complex and they discharge spike bursts that are time locked with the depolarizing component of fast runs.

Spike and wave seizures can be induced by thalamic or intracortical stimulation as well as spontaneously. Electrically-induced seizures could reproduce the main pattern of spontaneous SW seizures upon stimulating various cortical areas (figure 3-10 and dorsal thalamic nuclei.

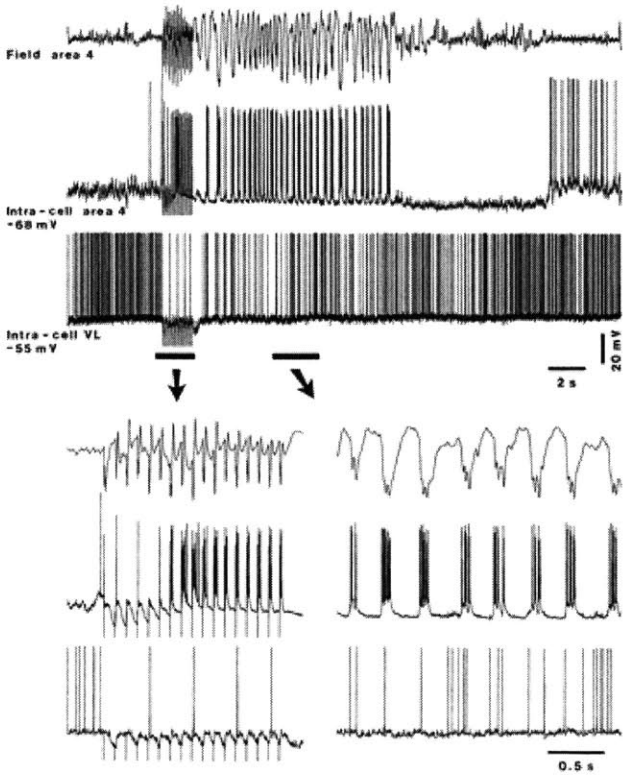

Figure 3-10: Cortically-induced seizures are possible with 10 Hz electrical stimulation in cats. Plot (top to bottom) shows depth EEG recordings in area 4, intracellular firing patterns of a FRB neuron in area 4 in response to 10 Hz stimulus and corresponding thalamic intracellular recording. Bar represents expanded segments. Not that during a stimulus train a short period of hyperpolarization occurs which gives was to busting following the stimulus at 10 Hz. Subsequently, a 3 Hz seizure develops, characterized by bursting at this frequency. (reproduced from Steriade et al 1998b [224])

Spontaneous seizure were seen to develop often (90%) from slow wave sleep of 0.9 Hz. In this case, about 16 seconds of SW elements at 2-3 Hz are switched to about 2 seconds of 15 Hz fast runs and then ended with depression. These seizures,

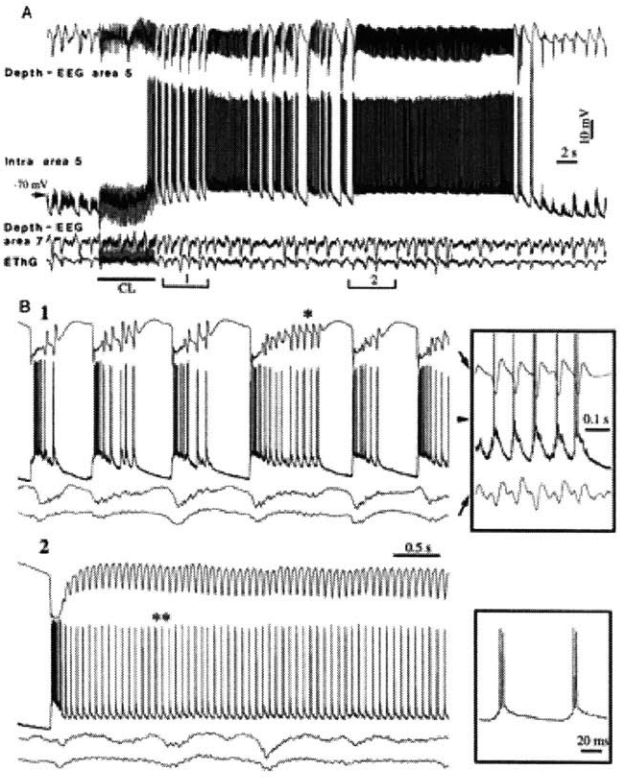

Figure 3-11: Thalamic-induced seizures in neocortex are possible with 7 Hz electrical stimulation of appropriate thalamic nuclei in cats. Stimulation of centro-laminar (CL) nucleus resulted in a long period of poly spike-and wave seizure (1.5 Hz) followed by period of fast runs (13 Hz). Plot (top to bottom) shows depth EEG recordings in area 5, intracellular recordings in area 5, depth EEG in area 7 and field potential in LP nucleus of the thalamus. Expanded traces show correspondence between EEG and firing of FRB neuron. During fast runs, the burst firing is replaced by doublet firing (inset), probably due to plateau depolarization in that cell (reproduced from Steriade et al 1998b [224])

Steriade argues, might be an exaggeration of sleep K-complexes since the depolarizing component appear to be mediated by cortical linkages, and reverses at 0.3 mm. Also, fast ripples in both phenomena appear during the depolarizing component which synchronize at distances over 3mm. However, the are important distinctions between the two, namely:

(a) Unlike sleep K-complexes, there is an increase in depolarizing envelope as the seizure progresses along with an increase in the corresponding hyperpolarizing component. This progressive membrane depolarization could be ascribed to the progressive entrainment of excitatory circuits through synaptic linkages. In fact, multi-site recordings showed progressive shortening of time lags between neurons during a seizure.

(b) The progressive depolarization of cell membrane voltage throughout the fast runs which result in partial inactivation of action potential firing.

(c) The sudden arrest of activity at the end of an episode is associated with a long lasting hyperpolarization.

cellular substrate Since there is a progressive recruitment of distant cortical structure into a seizure, it appears that both short-range as well as long-range connections mediate propagation of ictal (seizure) events, which aligns well with slow-wave sleep and other cortically-induced slow rhythms. SW seizures were also demonstrated in rats as intracortically generated and independent of the thalamus (Castro-Alamancos 2000 [32])

The rhythmic high frequency burstiness of FRB neurons appears capable of producing seizures locally and in related structures if stimulated rhythmically. In fact, Steriade notices that a 30-60 seconds of 10 Hz stimulation resulted in seizures when applied to FRB neurons but *not* to RS neurons.

Although intrinsically bursting (IB) cells of layers 4 and 5 were able to produce seizures in buciculline-infused slices (Chagnac-Amitai 1989 [35]), IB are found not follow frequencies greater than 4-6 Hz, and hence might not have mediated the faster 10-15 Hz runs. A recent experiment by Castro-Alamancos [32] , however, demonstrated a SW seizure in vivo in rats under cortical disinhibition, where the fast runs were in the 10 Hz range. Here, it was shown using current source density that the activity is mediated by lower layer 5-upper layer 6 neurons. Whether this population is different from IB cells (such as FRB) or is a variation of it is still unclear. Also, a form of IB cells have been recorded to fire at 11 Hz in awake behaving cats (Steriade et al 2001 [228]). In any event, it is possible that abolishment of both $GABA_A$ and $GABA_B$ inhibition was able of stimulating IB-like cells the high end of their bursting frequency.

3.2.6 Fast Oscillations

At the cellular level, fast oscillations could be evoked in many cortical and thalamic neurons by direct depolarization.

- Chattering cells which have been observed in the visual cortex in cats (Gray et al 1996) are superficial pyramidal cells that have intrinsic rhythmic firing in the gamma frequency band ($20 - 70$Hz) and are selectively oscillatory during periods of visual stimuli (but are largely absent during spontaneous activity).

- Thalamo-cortical cells in layer 6 of the neocortex discharged rhythmic ($20 - 40$ Hz), high frequency spike bursts (400 Hz) in response to depolarizing currents.

- High frequency oscillations occurred in sparsely spiny interneurons in layer 4 in guinea pig slices, and various neurons in layers 3-6 in motor and association cortical areas.

The preponderance of cells producing fast rhythms in various cortical areas and lamina makes it difficult if not impossible to implicate certain neurons in producing such rhythms. Based on his experimental results Steriade argues that voltage-dependent fast oscillations are not implicated by special cellular types, but rather is

generated by as many as $10-30\%$ of the total number of tested neurons. He demonstrated that some cells can display a continuum of spiking properties from single spike to spike doublets to high frequency spike burst and finally high frequency tonic firing. Hence, it seems that under the influence of brain stem neuromodulators and thalamocortical systems, cortical neurons may change their discharge patterns that were supposed to be otherwise invariant. Furthermore, synaptic activity may boost the intrinsic properties of cells discharging rhythmic spike bursts at high frequencies, such as during sleep spindles where certain cortical neurons discharge episodic burst with depolarizing slow oscillations. An interesting paper on the possible mechanism responsible for generating 40 Hz oscillations in chattering neurons as a ping-pong effect between somatic and dendritic action potentials and its implications on delivered activity into interneurons has recently been modeled by Wang ([253]).

Networked high frequency synchronization Fast rhythms in neural populations is observed to be coherent over short distances (up to $5mm$) unlike slow oscillations that characterize resting sleep and extend over a whole hemisphere. However, if one closely examines connected areas, large correlations of high frequency activity among distinct cortical and cortico-thalamic areas can be detected (Steriade 1997). Such a synchronization can be due to several mechanisms:

- Intracortical projections : these are horizontal connections that span up to $8mm$ in visual cortex. The recorded fast oscillations are usually in-phase through out the cortical depth with short time lag between superficial and deep layers, and are not due to volume conduction especially that there is a dramatic decrease of fast activity occurs in white matter.

  In his 1995 review, Singer and Gray commented on visual cortex work which showed inter-areal and interhemispheric synchronous firing occurring primarily, if not exclusively, during visual stimuli. In other experiments, high frequency synchrony is enhanced in amplitude in animals performing novel and complicated tasks, but suppresses, however, during trained movements (Singer and Gray [208], Nunez [173]). Such long-range interhemispheric synchronization can be supported by callosal projections that carry voltage-dependent fast oscillations. In fact an intact corpus callosum was required for interhemispheric synchrony, since its surgical sectioning reduces the probability of synchronous firing between the two hemispheres. Such experiment was first to demonstrate that cortico-cortical connections are critical for establishing synchronous firing.

  Therefore, high frequency synchronization is observable in both local circuit assemblies as well as between populations that are connected by long-range cortico- cortical fibers. New experimental evidence increasingly highlight the role of interneuronal networks in this synchronization, especially in *local circuit synchronization.* In particular, at least two *networks of electrically coupled interneurons* have been found (Gibson et al [88], Galarreta et al [84]). This allows for sharp synchrony of inhibitory tone in local networks which in tern promotes synchronization of cell firing into one coherent assembly reflecting in the observed fast (40 Hz) fluctuations in field potentials.

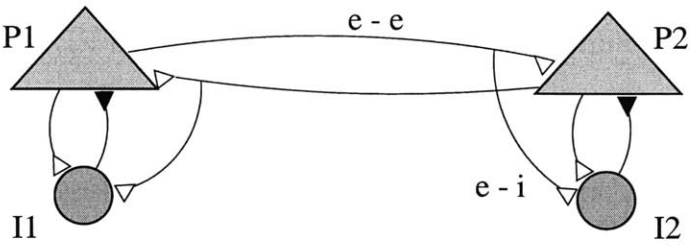

Figure 3-12: Long range connectivity contributing to high frequency synchronization in neural networks.

As for *long-range synchronization* which occurs over distances of several millimeters and even across hemispheres, suggestions as to how this might occur also points to inhibitory control of pyramidal cell firing by local interneurons (Traub 1996 [240], Traub et al 1999 [241]). Traub's basic idea is that local populations of interneurons sample input excitation arriving to associated pyrmidal cells (see figure 3-12). Accordingly a local interneuron (I_1) will fire based on excitation from local pyramidal population (P_1) as well as excitation from long-range afferents (P_2). The time difference between those two actions will code for the temporal delay between local pyramidal cell firing and that of distant pyramidal cell. Since a local interneurons inhibites local pyramidal cell, the net effect is creating a time-locked firing pattern between the two pyramidal cells thus synchronizing their firing into a single assembly.

- Intrathalamic synchronization: is argued to result mainly due to reticular nucleus as no cross talk occurs between thalamocortical cells.

- Cortico-thalamic synchronization: presumably caused by both specific thalamocortical loops (specific inputs) as well as connections through intralaminar and reticular nuclei. Neurons in the intralaminar region are of the chattering type (high frequency bursts) and project to superficial layers in association and visual cortices and may influence similar activity in these areas.

With high frequency oscillations occurring both in attentive as well as diffused arousal, steriade suggested that activation of thalamo-cortical circuits at 40 Hz upon arousal could set the stage for phase-locked fast oscillations between parietal and prefrontal areas when cognitive electrogenesis is initiated. Hence the issue is "development of behaviorally relevant oscillations on the basis of spontaneously occurring depolarization-dependent fast rhythms". Indeed, weakly synchronized fast oscillations become robustly coherent over $\approx 600msec$ after a sensory signal occurs.

3.3 Summary

The review presented above aimed at introducing common rhythms that are observable under different states of vigilance. A summary is given in table 3.1. We looked at

Table 3.1: Summary table for main sleep/arousal EEG discussed

Rhythm	Main effectors†	Possible neural mechanisms	Spatial scale
Slow-wave sleep (< 1 Hz)	Cortex (sleep stages 3-4)	Cortical networks undergoing recurrent depolarization and disfacilitation	Very wide cortical areas
Spindles (4-17Hz)	Thalamus (sleep stages 1-3)	Intrinsic bursting response of RE thalamic neurons	Wide cortical areas
Delta band (1-4 Hz)	Cortex and thalamus (sleep stages 3-4)	Intrinsic bursting response in thalamic and cortical neural populations	Wide cortical areas
Fast rhythms (> 20 Hz)	Cortex and thalamus (sleep, arousal)	Local circuits under appropriate depolarization and neuromodulators	Local regions
Alpha rhythms (8-12 Hz)	Cortex and thalamus (arousal)	Local circuits under specific cognitive correlates (e.g. resting, eyes closed)	Regional (occipital)
Seizures (2-3 Hz/10-15 Hz)	Cortex	Local cortical circuits under abnormal conditions (e.g. disinhibition)	Regional

† By default a rhythm is the property of intact cortico-thalamic system. Only rhythms that have been demonstrated to exist in one structure independently have been specific referred to that circuit.

slow rhythms of the brain mainly present under sleep, anesthesia, and few other spatially coherent oscillations. Such rhythms are present over large areas of the neocortex although they could originate from different foci within the neocortex (such as K-complexes and SW seizures), be driven by thalamic activity (spindle rhythms in early stages of sleep), or be a network-induced phenomenon which fails to exist in vitro, but rather requires intact in vivo cortical preparations such as slow-wave oscillations and alpha rhythms. We also looked at fast oscillations of the brain, mainly present during wakefulness, REM sleep, and occasionally intertwined with slow rhythms, These oscillations have a restricted spatial extent, and hence are locally-measurable, with field potentials corresponding to neural activity and showing varying levels of coherence over short-time windows and varying small spatial kernels, especially in natural non-anesthetized states (Destexhe et al 1999 [62]).

Looking at the morphology and cellular substrates of different rhythms, it is apparent that much of the basic circuitry is generating the slow rhythms is preserved;

that is, there is a local component of initiating the rhythm via shirt-range connections, a regional component of spreading the oscillation via long-range corticocortical connections and a global component via callosal fibers and the thalamus. Differences between rhythms could be due to modulators (Ach, Ketamine , buciculline, etc) leading to withdrawal or increase in excitation or inhibition, and intrinsic properties of basic neural elements (RE neurons, bursting neurons, etc). This leads to an optimism in formulating a basic generic circuit that could reproduce some or much of the above rhythms as seen in EEG recordings.

Chapter 4

Hierarchical binding hypothesis

In the previous chapters we provided a brief background review on the structure and organization of the cerebral cortex, its interaction with the thalamus, and classes of oscillatory behavior that are of interest in EEG problems, mainly sleep patterns, anesthetic effects, and seizure activity in the neocortex.

This chapter will include the formulation of a canonical skeleton cortical circuit based on basic principles of neural structure (Chapter 2) as well as new evidence on neuronal dynamics and network interactions. The circuit attempts to bridge the gap in ideas about local processing in the cerebral cortex at the level of a minicolumn, computations performed at the cortical column level, and longer range interactions between distinct columns either at the columnar assembly level. At its highest scale, the circuit discusses and provides anatomical correlates of hierarchical interaction between two areas connected via cortico-cortical fibers.

Although many of the basic operational ideas to be presented are not new per se, our interest has been in providing a unified framework of simple circuitry that could plausibly hold true in wide cortical areas and could explain EEG rhythms as implied by neocortical structure and dynamics. Although much work has been done by steriade school on EEG oscillations, a major emphasis has been placed on the role of the thalamus in promoting synchronization among different cortical areas with very little structure implied in the cortex itself, and hence falls short of explaining intracortically generated rhythms. As such, the cortical neural oscillator has been largely side-lined or overly simplified leaving it as a passive contributor to EEG signals, or at best as a feedback reinforcement of the thalamic oscillator, in most of the computational models developed so far. The hypothesis to be presented in this chapter goes a bold step forward in assembling a series of old experimental, computational ideas along with new influx of experimental evidence into a unified framework where large scale coherence of cortical rhythms could be explained. Such a framework has to address issues of vertical as well as horizontal organizations of the neocortex. To this effect, we will be utilizing, for the most part, a commonly agreed-upon skeleton of cortical wiring principles (outlined in Mountcastle 1998 [165]). In addition to the hard wiring problem, it also has to address issues of functional connectivity that allow a versatile recruitment or selection of neural populations participating in information transfer and coding. This will be based on a series of experimental and theoretical

work on cellular properties, synaptic dynamics and synchronization.

A very reasonable criticism of the existence of such a wiring diagram refers to the ever-increasing diversity of known cellular types, response dynamics, and functional connectivity within cortical systems, as well as an increasing web of reciprocal connections among distinct cortical systems. Our answer to such skepticism is given by our basic assumption on the nature of the problem we intend to tackle: *EEG signals are the gross recording of highly correlated field potential components over wide areas of the neocortex, and can be repeated across vigilance states (section 1.4.1); therefore, a unified* **effective neocortical skeleton** *of active cellular prototypes and connection topologies might very well exist under particular widely coherent EEG states.*

4.1 Effective Skeleton Circuit

To provide and overview of the chapter, we will put forward the main connectivity diagrams of the skeleton circuit we propose (figures) and its functional characteristics.

Circuit outline: The effective circuit has three scales of interaction, as follows:

1. The columnar scale is characterized by close synchronization across cortical layers provided by layer 4 inherent cellular population or inputs to this layer. Figure 4-1 shows major interlaminar connectivity pathways. A distinction is made between different neuronal populations in layer 5, namely large tufted layer 5 cells (TL5), smaller regularly firing pyramidal cells (P5) and low-threshold spiking inhibitory interneurons (LTS) which provide interlaminar inhibition. It can be seen here that TL5 cells have access to all layers in the model.

2. The columnar assembly scale is characterized by axon collaterals of lower layer cells forming a network of connections between different columns. Figure 4-2 shows inputs to layer 5 populations (TL5 and LTS) from different columns of a columnar assembly.

3. The areal scale is characterized by long-range or cortico-cortical connections arriving from distant systems into a particular area composed of different columnar assemblies. Such inputs have laminar specificity when connecting hierarchical related areas (figure 4-3). Feedback connections arrive in superficial layers and have a diffused nature while feedforward connections arrive in middle layers and are column-specific.

Circuit resonance: The network of layer 5 cells forms an oscillator of preferred resonance frequency with the alpha band ($\sim$ 10 Hz) which is able to drive other cortical layers at this frequency under minimal excitation. While this oscillator slows down during sleep stages (slow-wave sleep and delta), specific input patterns during wakefulness are able to excite this natural 10 Hz mode with maximal spatial spread and

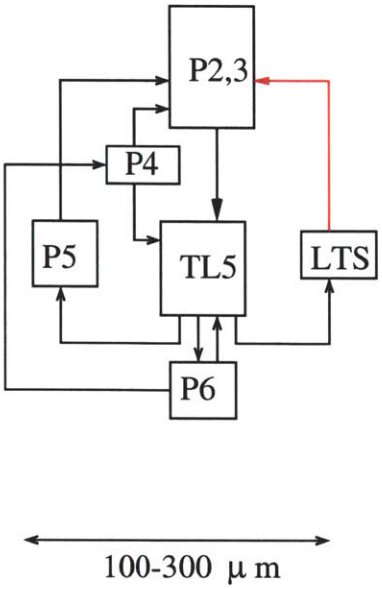

Figure 4-1: Block diagram of effective circuit at the column scale ($100 - 300\mu m$). Two major loops of excitatory connections are shown to include tufted layer 5 cells (TL5). These are P2,3-TL5-P5 and P6-P4-TL5. An inhibitory pathway between layer 5 and layer 3 (LTS cells) is also included.

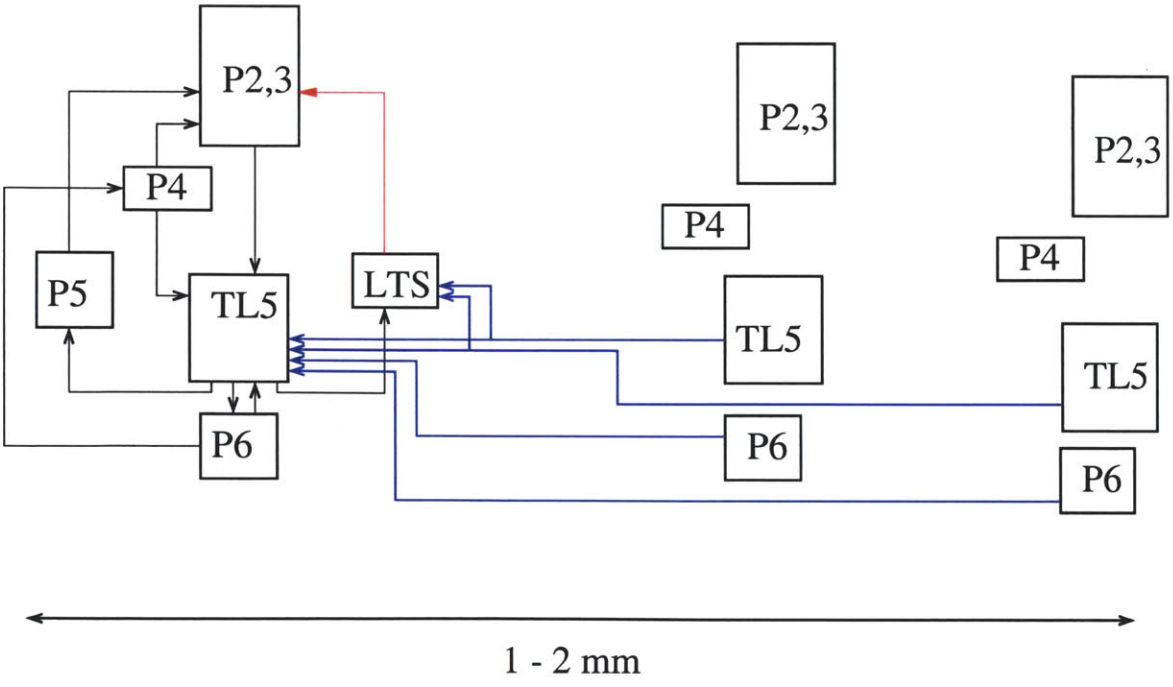

Figure 4-2: Block diagram of effective circuit at columnar assembly scale (1-2 mm). Shown are axon collateral inputs from lower layers of neighboring columns in a columnar assembly to TL5 and LTS cells.

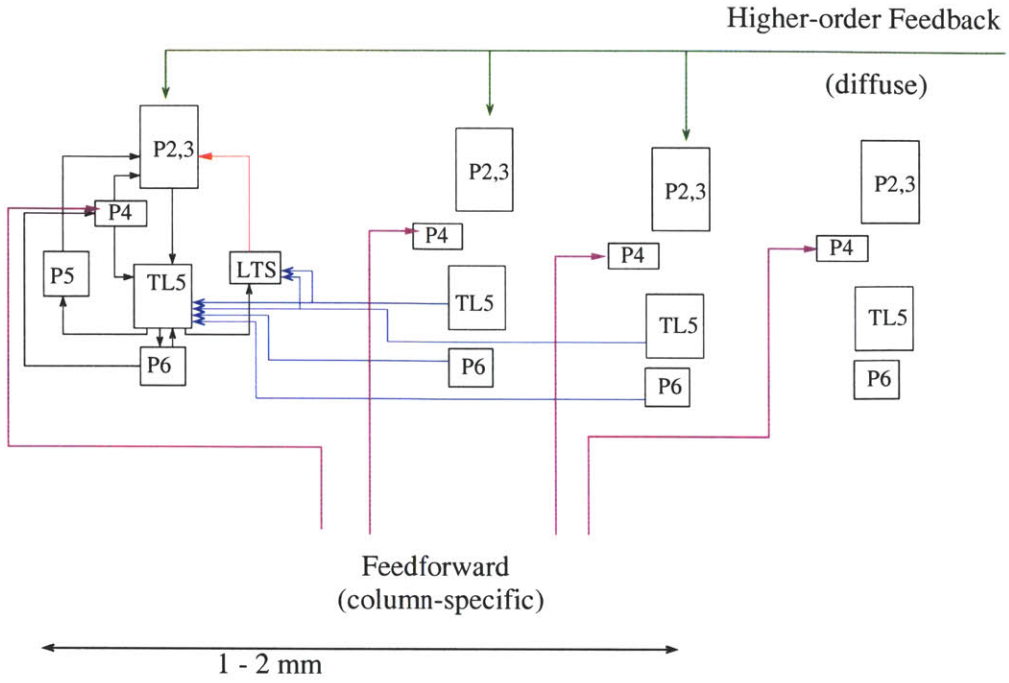

Figure 4-3: Block diagram of effective circuit in relation to long-distance connections. Inputs from distant cortical (cortico-cortical fibers) and thalamus are laminar specific in sensory systems. In this case, two forms can be distinguished feedforward and feedback.

thus activate cortical assemblies (or what is experimentally known as augmenting responses). Pathologic activation of such oscillator causes system instability, manifested experimentally as disinhibition-induced seizures.

Circuit role in "Hierarchical Binding": The interaction between the three scales of a skeleton circuit is provided by specific gating mechanisms in layer 5 cells which are able to modify activity at the columnar scale and reorganize columnar assemblies based on matching inputs arriving in the middle layers, such as specific thalamic inputs and feedforward cortical inputs from lower order areas, and those arriving in superficial layers, such as nonspecific thalamic inputs and cortical feedback from higher order areas.

The physiological manifestation of this binding mechanism is the ability of tufted layer 5 cells to respond preferentially to its inputs either in a burst or regular firing mode. The functional consequences of the two modes are different, that is, activity within a column is changed and so is its ability to organize into cortical assemblies. Finally, the binding of different hierarchies is modulated by levels of vigilance as well as by internal expectations and attention.

4.2 Recent Findings in Cortical Neurophysiology

In the following sections, we will first present a compiled list of experimental evidence on cortical neurophysiology that spans synaptic receptor types, ionic channels in cell membranes, firing dynamics of neural elements and their connection topologies and synaptic reliability. The evidence will be organized as follows:

1. A special emphasis will be placed on the cornerstone element of the circuit behavior which is *pyramidal layer 5 cells dynamics.*

2. Next, we will present evidence on the recruitment and synchronization properties within a cortical column as reflected in layer 4 cells.

3. An exhibition of inhibitory pathways in the neocortex, especially between different layers (layer 5-layer 3) is given.

4. Examples of circuit dynamics in response to input stimuli will be presented to validate interactions between different neural populations.

5. Rhythmogenesis of several EEG oscillations will be briefly discussed in the context of the given circuit. Simulation models will later verify the circuit role in generating such rhythms.

This collection of evidence will then be formulated into the main hypothesis on circuit dynamics that we believe plays an integral part in an effective neocortical skeleton of EEG generation.

4.2.1 Layer 5 pyramidal cells

The electrophysiology and connectivity properties of large pyramidal cells in layer 5 have been given a lot of attention in recent years. The size of these cells and their thick dendritic trunks have made these neurons been quite attractive for early intracellular experiments due to the relative ease of manipulations.

Several experiments aimed at understanding their role as integrative circuit elements, in addition to being output neurons, of the neocortex both to other cortical regions and subcortical structures, are found in the literature (Markram 1997 [147], Thomson et al [236, 237, 64]). In fact, the so called "layer 5 hypothesis" have been raised by (Connors and Amitai 1995 [40]) and its extensions to awareness by Koch and colleagues (Koch and Crick 1994 [124]) which explains these cells as basic for propagation and control of neural activity.

Earlier skepticism of the importance of tufted layer 5 cells has hinged on whether "intrinsically bursting" firing property has any functional relevance. With the apparent correlation of cognitive computation and high frequency (>30 Hz) firing, bursting behavior seemed to be uncorrelated since it occurs at lower frequencies (10-15 Hz). However, the evidence to be presented will ultimately lead to a formulation where bursting behavior is proposed to have functional consequence particularly in early responses to stimuli and preparatory states.

Recent discoveries regarding the synaptic mechanisms and their effect on the firing properties of these cells have given a new dimension for the function of these cells. In particular, we mention (a) The existence of three separate input zones to a large tufted layer 5 cell whose interaction largely dictates whether a cell will fire in a burst or a regular spiking mode; (b) the input amplification characteristic of these cells due to internal ionic current dynamics; and (c) the connectivity patterns of these cells. We will next present a detailed exposition of the characteristics of layer 5 populations.

Morphology and synaptic connections

Synopsis: Layer 5 pyramidal cells can be either large with thick apical dendritic tuft and (tufted layer 5 cells) or smaller with thin dendritic tuft. TL5 cells have three main input zones with the apical zone reaching layer 1. The axonal connections form an extensive network of connections between these cells. TL5-TL5 synaptic connections carry burst firing faithfully and are characterized by rapid signaling. Some experiments suggest that such connections are maximally facilitated when activated at 5-15 Hz frequencies, which is important in regard to the specific importance of bursting, rather than high frequency regular firing, in these cells.

L5-A. Layer 5 cells have been classified according to their firing characteristics in response to somatic current injection. These are the intrinsically bursting (IB) and the regularly spiking (RS) types (figure 4-4). In 1989, Changac-Amitai [35] reported this distinction and noticed that if inhibition (such as that of layer 4, denoted by IN) was decreased then stimulating IB cells of layer 5 causes a synchronous activity to spread to other layers in the vertical dimension and horizontally to other cortical populations up to several millimeters away in a seizure- like pattern. At the initiation of such synchronous event, RS cells were strongly inhibited but IB cells were not, suggesting that IB cells might be responsible for the generation of such events. Morphologically, IB cells of the lower layer 5 (layer 5b) were larger pyramidal cells whose apical dendrites reached layer 1, whereas the RS varieties were smaller pyramidals with thinner and fewer apical dendrites. Also, IB cells extended horizontally and connected extensively with each other and less so with RS cells, suggesting that IB cells receive inputs from each other and hence raising the hypothesis that under normal conditions, the strength of inhibition on IB cells allows them to operate relatively independently.

L5-B. Later Markram (Markram 1997 [147, 148]) studied IB cells (which he called tufted layer 5 or TL5 cells due to their morphology). A primary dendritic cluster of the TL5 cell extends horizontally to about $300\mu m$ in diameter (which falls into a functional column geometry). Their axonal arbors are long, extending up to several millimeters (Feldmeyer et al 2000 [71]) in both the horizontal and vertical directions. The primary axonal arbor in the local region is well clustered mainly in the horizontal direction. Vertical axon collaterals form contacts with different layer neurons, while horizontal connections mainly target neurons in the same layer, and in different cortical columns (Thomson et al 1998 [237]).

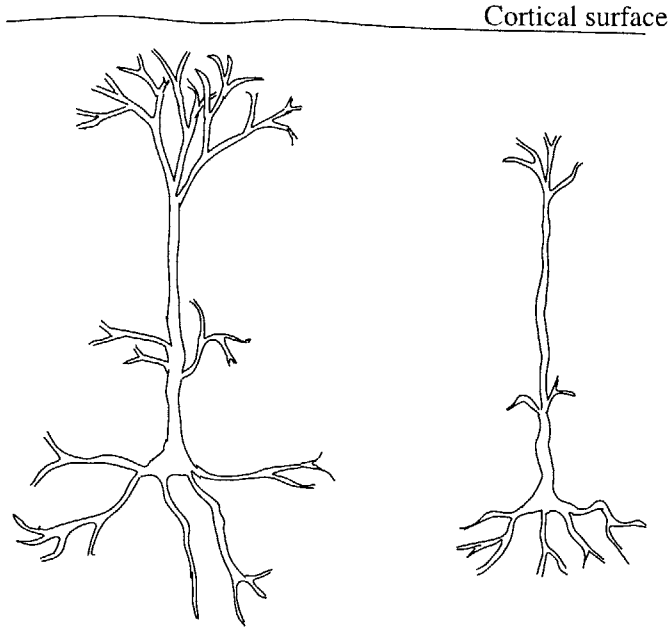

Figure 4-4: Schematics of layer 5 pyramidal Cells. While large cells have apical dendrites reaching upper cortical layers and form a rich termination, smaller cells have thin apical tufts with little arborization.

Although synaptic connections between layer 5 cells occur across all layers (1-5), the majority of synaptic contacts occur on the basal dendrites in layer 5 (63%of contacts, [71]), and it occurs within $100-200\mu m$ from the soma [147]. Markram noted that these cells form a connected feedback network with first, second, and possibly higher order recurrent feedback. Using statistical arguments, he argued that the connectivity patterns seemed nonrandom but obey a certain topology [147].

Connectivity between these cells have also been studied. Synapses between TL5 pyramidal cells are characterized by *rapid signaling* since most synapses are at a short electrotonic distance from the soma, and hence the transmission time from a presynaptic action potential to an EPSP onset is small ($\approx 1.7msec$). The rise time for EPSPs are typically $<$ 2msec, consistent with a large AMPA component of the EPSP (and a much smaller NMDA component). A unitary EPSP is 1.3mV on average and pairs of TL5 pyramidals have an average of 5.5 synaptic contacts (Feldmeyer et al 2000 [71]).

Frequency dependent synaptic transmission in layer 5 neurons was analyzed in a series of papers by Tsodyks and Markram (Tsodyks et al 1998 [242]) . In their experiments on young rats, they demonstrated that at high frequency burst of stimulus, synapses depress at high frequencies (20 – 40Hz), and transmission

seems more faithful or even facilitated at lower frequencies ($5 - 15$ Hz). This caused a flurry of arguments about neural code between excitatory cells, especially in terms of what features of presynaptic inputs are important, being at least in part temporal.

However, this constructed frequency dependence was recently challenged, with the demonstration by Reyes et al 1999 [187] that a developmental switch in fact occurs as rats grow older, when depression switches to facilitation in adult rats, at least up to the $40Hz$ range of input stimulus frequency. Also, other researchers (Angulo et al 1999b [7]) found that the synaptic transmission to inhibitory populations from layer 5 do switch from exclusively depressing in young rats into both depressing and facilitating in adult rats, thus increasing the range of integrative capabilities of a given excitatory connection. Whether the cut-off frequency of the EPSP response after development has shifted further upwards (say to $80Hz$) and the implications of such a change are questions yet to be answered. However, it became more apparent that synaptic responses are dynamically changed as a function of previous activity as well as balance between excitation and inhibition within neural populations (Varela et al 1999 [247]) and that the range of computation is increased in neocortical circuits as they become more mature.

During development, apical dendrites of layer 5 cells become thicker and their tufts increase 5 folds. The dendritic compartment switches from being electrotonically close to the soma to later forming an *isolated compartment* in mature rats (Zhu 2000 [269]).

L5-C. The experiments of Williams et al [256] studied the postsypantic consequences of burst firing in tufted layer 5 cells in more detail. During Bursting, later action potentials decreased in amplitude when recorded somatically. However, the action potentials are generated in the axon and are propagated down the axon with no decrement ($> 30\mu m$). The nature of EPSPs evoked by bursting layer 5 cells were studied by paired recordings from synaptically coupled layer 5 neurons indicated that each spike in a burst could cause transmitter release, although this release mechanism shows a use-dependent depression, voltage dependent postsynaptic amplification ensured that later EPSPs in a burst are amplified under sufficient depolarization (-60mV) counteracting synaptic depression. *Hence, both a presynaptic and postsynaptic mechanisms act in synergy to enhance synaptic coupling between layer 5 neurons.* Overcoming synaptic depression was also demonstrated by Galarreta et al [85] whose experiment showed that when combined with a low frequency ongoing activity, artificially simulated burst firing in layer 5 neurons causes a transient rebound in synaptic efficacy for 1-2 sec in both connections to other layer 5 cells as well as to fast spiking interneurons.

Firing dynamics and input coupling

Synopsis: Large tufted layer 5 cells can fire three or more action potentials in burst like

patterns at frequencies up to 15 Hz, or fire in regularly spiking manner[1].The switch between these two modes is controlled by three input zones (figure 4-5). Bursting is facilitated by near coincidence arrival of inputs to TL5 dendrites in lower layers (5 and 6) and in superficial layers (1 and 2). Inputs arriving at middle layers (4) is able to amplify or attenuate the ability of the cell to burst. Neuromodulators such as dopamine (Acetylcholine) also act on decoupling (coupling) apical and basal arriving inputs.

L5-D. The firing dynamics of large layer 5 cells have long been explored. It is now becoming apparent that the differences underlying burst and regular spiking patterns in these neurons might contribute to a redistribution of synaptic activity and a drastic increase in sensitivity to inputs arriving at the distal dendritic tufts of those cells. initialy, it was noted that brief current pulses into the apical dendrites of TL5 elicit little synaptic response unless a dendritic action potential was initiated (Thomson et al 1997, [236]). Once this happens, somatic depolarization of $\approx$ 2mV occurs, and the soma "listens" more closely to the dendritic inputs of sufficient duration (8-20 msec). Hence, despite the large electrotonic distance of dendritic tufts from the soma, layer 5 cells could amplify distal inputs in an intriguing fashion.

However, Stuart and Sakmann demonstrated that an Na^+ axonal action potential actively Initially to the dendritic region, where a dendritic Ca^{2+} AP could be generated under sufficient depolarization (Stuart and Sakmann 1994 [230]). These Calcium action potentials were restricted to the distal apical dendrites in TL5 neurons in rats ($540 - 940\ \mu m$ from the soma) and required co-activation of AMPA-NMDA receptors (Schiller et al 1997 [197], Schwindt et al 1998 [203]). Somato-dendritic backpropagating action potentials in layer 5 pyramidals were also demonstrated in awake rats by Buzsaki et al 1998 [25].

Further experimentation on this process lead to a discovery of a new coupling mechanism of inputs arriving in the somatic region and those arriving at distal dendrites (Larkum et al 1999 [131], Schwindt et al 1999 [204]). A layer 5 pyramidal neurons responds to low level of synaptic input at its apical dendrites, if the neuron had been stimulated at the basal dendritic zone within a time window of 5 msec a priori. Inputs at distant dendrites are usually greatly attenuated upon reaching the cell body or soma and hence large threshold must be achieved in the dendrite to generate a dendritic Ca^{2+} action potential leading to somatic depolarization and firing occurs at the soma. However, if a current was injected at the axon initiation zone (near the soma), then the back propagating Na^+ potential from the soma to the dendrite facilitates the dendritic role by decreasing such threshold by nearly 75% and the layer 5 neuron fires a burst of 2-3 spikes (Schematic in figure 4-5) . If the distal input arrives after more than $7msec$, then the threshold is increased.

[1] As seen above, bursting patterns allow facilitation in connections between layer 5 cells and hence possibly provide for propagating intermediate frequencies through the network.

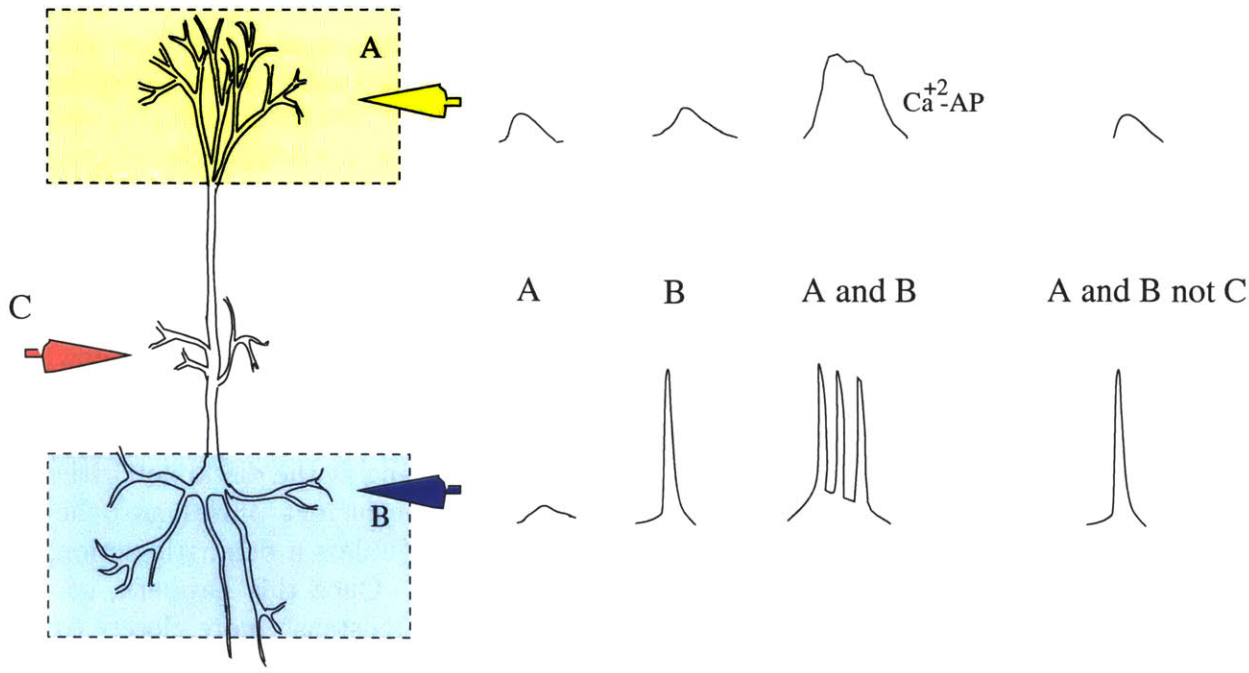

Figure 4-5: Activation of distinct zones in a tufted layer 5 pyramidal cell creates distinct firing patterns. Stimulation at the apical zone A will create a small voltage deflection at the soma. Stimulation at basal zone B could initiate a single action potential for a given stimulation strength. However, utilizing the same stimulation strengths simultaneously will initiate dendritic Ca action potential and a somatic burst. An inhibitory tone at C will prevent bursting

Hence, such a mechanism acts to couple inputs arriving at upper layers with inputs in the lower layers and signals for that by multiple spikes. That is, a near-coincident input to both the apical dendrites and the basal dendrites of L5 neurons will produce a burst firing which will not occur if the same sized inputs were introduced separately to each region.

Furthermore, inhibition of layer 5 pyramidals acts to dissociate this coupling by preventing the back propagating potential from reaching the dendrite, and hence places a " veto" action on burst firing which lasts about $400msec$.

Finally, Larkum et al noted that this bursting mechanism could possibly couple nonspecific thalamic input to layers 1 and 2 (which act on apical dendrites of some L5 pyramids) with specific thalamic input to layer 4 (which acts on the basal dendrites of L5 pyramids). Although his description remained at the electrophysiological level, it became apparent from these results that the two input ports to a cortical column, through superficial layers 1/2 and through infra/granular layers 4/5 have some mechanism of interacting and affecting the response of neocortical output cells in layer 5.

L5-E. The bursting behavior was further studied by Schwindt (Schwindt et al 1999 [204]). In addition to the above coupling behavior, increasing sustained den-

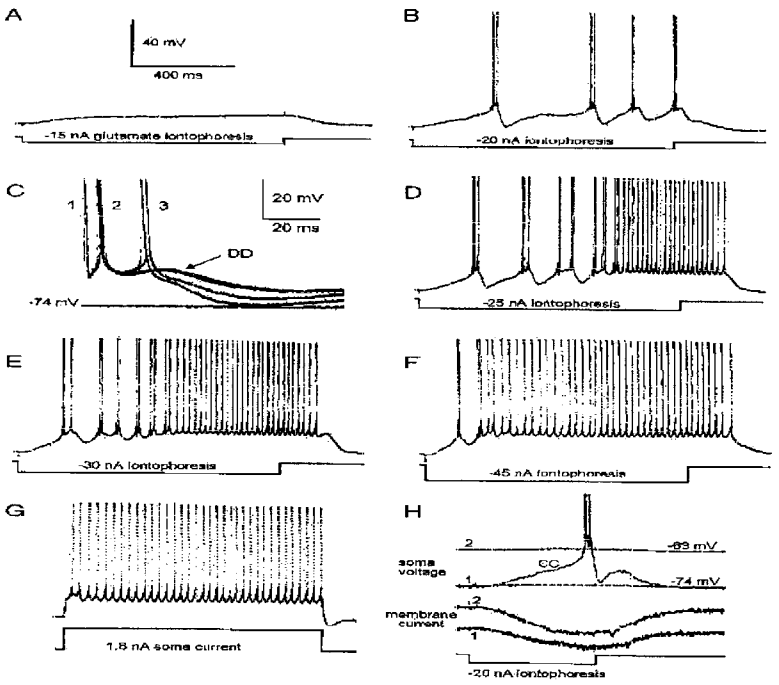

Figure 4-6: Firing characteristics of Layer 5 cell (Schwindt et al)

dritic injection could not only create dendritic Ca action potential (AP) but also generate a plateau potential in the dendrite which leads to switch of the cells firing back to regular spiking behavior (figure 4-6). This, he argues might be a mechanism to dissociate different compartments of dendritic inputs upon high activation, as new results from his lab indicate (Oakley et al 2001 [175]).

L5-F. Finally, the coupling between distal inputs ($400 - 700\mu m$) and somatic targeting inputs could be primed by the active history of the cell firing. Larkum et al 1999b [132] found that if somatic AP firing occurs above a critical frequency, ($90 - 100$Hz) dendritic Ca action potentials are generated even without any dendritic inputs. Again, inhibition prevented AP firing for a long periods ($400msec$). Hence, the dendritic efficacy could be redistributed once somatic AP firing rate is high, given the cell was released from inhibition for sufficiently long periods of time. It has been demonstrated that during whisker stimulation in rats, somatically recorded AP in layer 5 pyramidal cells of the barrel cortex fire 2-5 AP at 100-250 Hz, which could be a distal dendritic priming behavior. Similar experiments by Williams and Stuart 2000 [258] showed that action potentials trains occurring in vivo backpropagate several folds more effectively into distal dendritic zones. This behavior was voltage dependent, i.e, dramatically reduced by dendritic hyperpolarization and amplified by depolarization.

L5-G. The effect of neuromodulators on Layer 5 pyramidal cells has been reported in at least two experimental works of interest. Layer 5 neurons have a high density of serotonin (5-HT) receptors (5-HT_{2A}). In the frontal cortex of the rat, serotonin was seen to preferentially increase both the frequency and amplitude of

spontaneously occurring (not electrically evoked) postsynaptic currents in TL5 cells mostly on the apical dendrites in layer 1 (Lambe et al 2000 [129]). This is of interest since 5-HT was seen as highly up-modulated in vivo in animals under novel situations (ie zone A in figure 4-5 is upregulated) , and 5-HT receptors are rapidly desensitized under normal conditions.

Dopamine is seen to decrease the excitability of layer 5 pyramidal cells in the mouse prefrontal cortex in vitro (Gullegde et al 1998 [94]) and in motor cortex of anesthetized cats in vivo (Huda et al 2001 [98]). This was especially true for the distal dendritic region as is argued by Durstewitz (Durstewitz et al 2000 [68]) through reduction of dendritic Ca^{2+} spikes, but not in the proximal dendrites. Through a decrease in AMPA synaptic currents, and an increase in NMDA currents, dopamine results in lower amplitude, but longer lasting EPSPs. This could be a way of dissociating a local neural population that is sustaining high firing activity under a working memory task from layer 1 inputs (or zone A).

Input amplification

Synopsis: Tufted layer 5 cells are able to rebound from hyperpolarization due to internal currents (I_T). This phenomenon is manifested in many animals and is seen to contribute to augmenting responses which occur under ~10 Hz stimulation due to its internal dynamics and possibly synaptic facilitation of TL5-TL5 connections. Finally, TL5 cells appear to be much less readily inhibited than RS cells in layer 5 and are able to respond with action potentials for low levels of excitation.

L5-H In the rat sensorimotor cortex, layer 5 IB cells appear to contribute to rebound excitation after thalamic stimulation (figure 4-7) characterized by a period of high sensitivity to input stimulus followed by a long lasting depolarization.

In these experiments, an afferent spike arriving from the VL thalamus caused, after an initial short EPSP in the presumably TL5 cell (intrinsically bursting, long apical dendrites), a long lasting hyperpolarization mediated by $GABA_B$ type synapses which lasted for about 150-200 msec and is subsequently terminated by a long lasting depolarization which is also reflected in other cortical layers.

Interestingly, this hyperpolarization of IB cells due to an initial stimulus causes an over-sensitive period during which any thalamic input arriving could evoke a bursting response from these cells thus termed an "augmenting response". If a thalamic stimulus is delivered after the long lasting depolarization happens (after asterisk in figure 4-7, A), then no augmenting response occurs (no action potentials or bursting, figure 4-7,C). This sensitivity during the hyperpolarized state could possibly be mediated by low threshold calcium currents (I_T) as in vitro experiment showed a rebound depolarization in layer 5 IB cells subsequent to hyperpolarization. At least one study demonstrated the existence of such calcium current (I_T) in burst firing (but not regularly spiking) neurons of layer 5 (cat motor cortex, Chen et al 1996 [38]). An earlier experiment by de la Pena

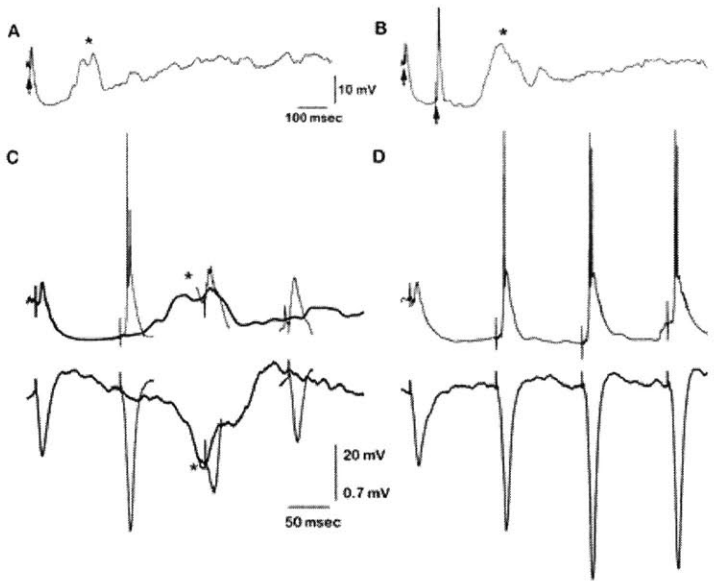

Figure 4-7: Augmenting response after thalamic stimulation occurs only before depolarization phase. See text for details. A and B: intracellular recordings durings a stimulus delivered to the VL thalamus which intiates a characteristic hypepolarization/depolarization in layer 5 cells. C and D: upper traces show intracellular potentials, lower traces are extracellular. In C, stimulus can intiate firing only when delivered before asterisk, but not after. Once firing is initiated, it can be sustained with subsequent stimuli as shown in D.

et al 1996 [54] showed that in the guinea-pig cortex, pyramidal cells having low threshold calcium currents are prevalent in layer 5/6 and that these cells have bursting firing characteristics. Similar rebound behavior after hypolarization in large layer 5 cells were recorded by Spain et al 1991 [212] in cat sensorimotor cortex, by Silva et al [207] and Thomson et al 1997 [236] in rats [2].

Similar form of augmenting responses during slow wave sleep have been demonstrated by steriade where it was shown that layer 5 cells, when stimulated callosaly at 10 Hz are able to generate *and sustain activity* at that rate (Steriade 1993b [217]).

L5-I In other experiments, Layer 5 cells are shown to be well positioned to receive thalamic excitation, due to relative lack of inhibition. In the rat auditory cortex slice preparation, it has been shown that while a thalamic stimulus results in a

[2]Using hindsight from newer experiments, we know now that since the VL thalamus synapse on both layer 5 and layer 1, bursting is a much more readily evoked phenomenon by activating the two layers simultaneously. It is possible that the non-responsiveness to thalamic input during the depolarized state is due to activation of GABAergic interneurons synapsing on the apical dendrite which will prevent bursting, as we have seen earlier.

combination sequence of excitatory and both $GABA_A$ and $GABA_B$ inhibition, TL5 cell response seemed more readily excitatory and occasionally triggered action potentials (Hefti and Smith 2000 [96]). Less than half of the TL5 cells examined received any identifiable inhibitory input, and stimulation usually caused an action potential or a burst even from rest. Also, unlike in the rat somatosensory cortex, no $GABA_B$ response in TL5 cells was recorded. It is not clear whether this discord is due to slice preparation limitation in this experiment, or it is a basic structural difference between the two areas.

These results resemble recordings from cat auditory cortex *in vivo* where some cells in layers 5,6 responded at tone onset but were actively inhibited thereafter, whilest other cells fired single spikes or bursts throughout the tone. Also, it is known in the cat visual cortex that RS layer 5 cells have sharp selectivity, while large layer 5 cells (TL5) have broader receptive fields and selectivity, implying a stronger inhibitory action in the former type.

L5-J Layer 5 cells appear to have the ability to augment their responsiveness in the rat prefrontal cortex in response to input stimulation thus contributing to short term plasticity (Hempel et al 2000, [97]). In these experiments, it was shown in slice preparations that, although layer 5 synapses might depress due to a high frequency input, their response is facilitated or augmented about 40-60% which lasts seconds to minutes and could possibly be mediated by intracellular Ca^+ influx. Such property might act to counteract the effect of depression and provide a pathway for sustainable recurrent excitation after input stimulus is extinguished, and important character known to occur to occur in prefrontal areas during temporary memory tasks.

4.2.2 Layer 4 cells

As we have seen before, the input layer 4 of sensory areas receives input excitation from thalamic afferents and feedforward connections from other cortical regions. The spatial selectivity and efficacy of this afferent control is therefore primarily dictated by the responsiveness and dynamics of neural populations in that layer. Of these, about 80% are excitatory neurons and 20 % are inhibitory interneurons (Fleidervish et al 98 [73]). Among the excitatory subpopulations, the dynamics of excitatory spiny stellate neurons and their synaptic properties appear pivotal since they employ strong recurrent excitation mediated by reliable synaptic connections innervating neurons within its axonal arbor domain. Another excitatory variety in layer 4 are the star pyramidal neurons (see chapter 2). Still, the major source of local excitation in that layer seems to be the spiny stellate neurons (Traczy-hornoch 1999 [239]).

Synopsis: Layer 4 excitatory cells have very reliable, NMDA receptor-mediated connections which allows fast recruitment of those cells within a cortical column.

L4-A. The dendritic arbor of spiny stellate neurons in layer 4 has a relatively short horizontal span, with a diameter of $< 200\mu m$ and is largely restricted to layer 4 itself in the rat somatosensory cortex (Feldmeyer et al 1999 [70], Feldmeyer

and Sakmann 2000 [71]) and in the cat visual cortex (diameter $100 - 250\mu m$, Traczy-hornoch et al 1999 [239]). In the somatosensory cortex, the dendritic tree is largely asymmetric and is oriented to the center of the cortical column termed "barrel" (hence the name barrel cortex). The axonal arbor of spiny stellate neurons in the barrel cortex is oriented almost exclusively vertically with contacts mainly to other layer 4 spiny neurons and layers 2/3 (figure 4-8).

Synaptic connections between spiny stellate (SS) neurons are found exclusively in layer 4, as the dendritic arbor is restricted to that area. More importantly, if a SS-SS connection exist, then it was restricted to the barrel of origin where the soma of the presynaptic neuron lies, and occurs about $50 - 200\mu m$ from that soma.

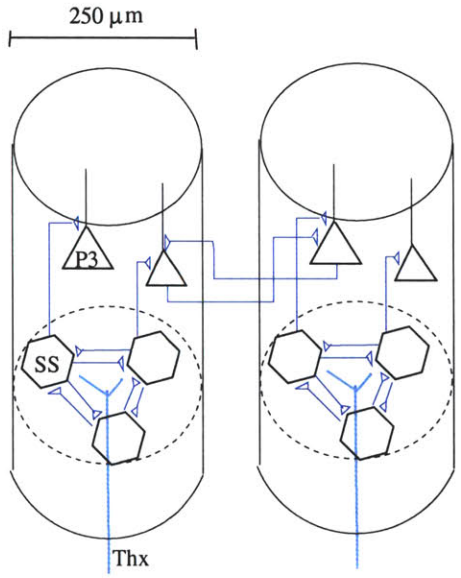

Figure 4-8: Spiny stellate neurons of layer 4 are confined to the dimensions of a cortical column

L4-B. The synaptic connections between spiny stellate neurons are very reliable as demonstrated in cat striate and rat barrel cortex (Traczy-Hornoch 1999 , Feldmeyer et al 1999). In rats, EPSPs occurring between two spiny stellate neurons are even faster and more effective than those between two layer 5 pyramidals: they have very short latencies (~0.9msec) and are mediated by very fast EPSPs (1.5 msec rise time, 2.9 msec decay constant) with high amplitude (~1.6 mV). The connections are very reliable (5.3 % failure rate), probably due to a high release probability. These intrabarrel connections thus seem to amplify and distribute the afferent thalamic activity in the vertical direction of a cortical column. In cats, connections between spiny neurons had large amplitude (> 1mV for unitary EPSP), and are very effective (0.69-0.98 release probability).

L4-C. The excitatory connections between spiny stellate neurons is dominated by NMDA type receptors, giving them an effective integrator role of input activity,

mainly via recurrent excitation (Fleidervish et al 1998 [73]). An intriguing NDMA subtype of receptors could be activated from resting membrane potential without depolarization (recall that for a typical NMDA receptor to activate, the Mg^{2+} block has to be removed via depolarization). This subtype was associated with recurrent connections between spiny stellates and not with thalamic input, which is associated largely with AMPA receptors and a small voltage dependent NMDA receptor subtype.

4.2.3 Inhibitory cells

The diversity of inhibitory cells in the neocortex is only beginning to be elucidated, as more experimental evidence is emphasizing the role of inhibition in synchronizing neocortical activity. Despite the lack or clear distinctions in the location, input and output targets of various inhibitory neurons (INs), few basic principles of classification according to morphology, response, output targets and laminar location hold.

Inhibitory interneurons constitute 20-30% of the total neural populations in the neocortex (Thomson and Deuchars 1997 [236]) and are 2- 10 % of the pyramidals axonal targets.

1. A simplified classification of interneurons could be according the location of its dendritic arbors and axonal ramifications. If a group of interneurons sample input from a particular laminar location, then it is not unreasonable to expect this group to be subject to all the axons targeting such area. Similarly, if IN axons target one cortical layer or proximal, somatic, or distal zones of pyramidal cells, then they probably participate in regulating the input or output behavior of such lamina or pyramidal cells. Accordingly, we mention

    - Basket cells (BC) which are recorded primarily in layer 4, have long horizontal axonal connections and synapse mainly on somata of target cells (Gupta et al 2000 [95]).
    - Small basket cells (SBC) which have short axonal segments that form dense clusters of axonal collaterals and have much higher bouton density (synapses) than BCs. These cells synapse mainly on somata of both pyramidal cells as well as other interneurons.
    - Martinotti cells (described earlier) and nested basket cells (NBCs) which are a hybrid between BCs and SBCs with dense soma clusters as well as long axonal and are most frequently found in layers 2, 3. NBCs have the most electrophysiological diversity.

2. Further classification depends on the intrinsic firing patterns of interneurons. With increased knowledge, the diversity of electrophysological properties have been thus far mapped into three classes (accommodating, non-accommodating and stuttering) and eight distinct subclasses (classical, bursting, delayed firing) described in Gupta et al 2000 [95] depending on response to sustained depolarization. Only a few of these subpopulations have been studied especially in terms of

their synaptic targets and connectivity, and for this, we will follow conventional classification reported in earlier experimental work (Thomson 1997). This firing classification includes

- classical fast spiking interneurons (FS), which generally innervate somata and proximal dendrites of pyramidal cells and elicit brief $GABA_A$ mediated IPSP in those cells. When these cells undergo prolonged high-frequency firing, the resulting IPSPs in targets generally increases and then decays to a plateau whose amplitude is constant, presumably caused by GABA-A receptor types. After 60-80 msec, another increase in amplitude occurs and lasts for extendend periods of time, possibly due to activation of GABA-B receptors.
- low threshold spiking or burst firing interneurons (LTS). These cells can generate bursts of spikes upon depolarization, although the interburst frequency is low. Associated with bursts are brief GABA-A mediated IPSPs in their targets with no slow components (no GABA-B type currents). These cells innervate mainly more distal portions of pyramidal cell dendrites and consequently, have a shunting effect which controls excitability due to inputs arriving at the distal locations of pyramidal cells.
- unclassified regularly spiking slow interneurons (Thomson and Deuchars 1997). These cells generate longer lasting GABA-A mediated IPSPs in their targets, which prevent their postsynaptic targets from firing for tens of milliseconds.

Synopsis: The general role of inhibition in relevance to the problem of oscillation generations is limiting the otherwise explosive effect of recurrent excitation in pyramidal populations as well as a strongly emergent property of synchronization in local cortical columns, possibly through electrical coupling between interneurons (figure 4-9). In addition, a subpopulation of interneurons in layer 5, known as low threshold spiking cells (LTS) are especially response to high frequency inputs (possibly arriving from TL5 bursting neurons). LTS cells also send axons into superficial layer 3 of a cortical column (figure 4-10).

IN-A Of the most studied interneuron classes, classical fast spikes (CFS) and low threshold spiking (LTS) interneurons have shown brief EPSP depolarizations at their input connections with their pyramidal counterparts. Furthermore, these INs have fast hyperpolarizing component after action potential firing (Thomson and Deuchars 1997 [236]). A study of Fast spiking INs in rats showed that pyramidal-FS connections are mediated mostly by fast AMPA kinetics with minor or no role for NMDA receptors at resting potential, the latter being active only at more depolarized levels (membrane potential >-50mV, Cecilia Angulo et al 1999 [6]).

Accordingly, efficient activation of these interneurons is usually based on either the close activation of many presynaptic pyramidal partners, or the bursting

behavior in some of these connections, due to the limited effect of single input spikes, that is, these cells have a more demanding integrative scheme of all the EPSPs arriving from different presynaptic cells as compared to that in pyramidal cells. In fact, Angulo et al demonstrates a linear summation of EPSPs elicited in FS interneurons at membrane potentials below action potential threshold. In these IN classes, many pyramidal-to-interneuron connections had low release probabilities in response to single action potential firings. However, transmission facilitated dramatically when pyramidal cells fired at high frequency (Gibson 1999 [88]) or in bursts (In Thomson 1997[236], second EPSP at interspike interval of 5-8msec are enhanced 4 to 10 fold, with 4th spike causing up to 30 fold enhancement when occurring within 60msec). Moreover, the decay time of this enhancement increased remarkably with more spikes (90 msec for two spikes, hundreds of msecs for 3 spikes). *Hence a given level of facilitation in LTS cells, once initiated by a burst of two or three input spikes, can be maintained at much lower frequencies.* This ties well with the fact that many pyramidal neurons either fire at high rate when activated and then adapt to lower rates, or with intrinsically bursting type cells which then shift back to regular spiking after a brief period.

IN-B Interneurons have a fixed limitation on the size of inhibitory events they can generate in the postsynaptic targets implicating a specificity in the action of different interneuron classes in modulatory or inhibitory control of pyramidal cell excitation or output. Ling and Bernardo found that fast inhibition was maximally recruited at certain extracellular stimulus levels and did not increase with stimulus intensity. In studying fast inhibition applied to layer 5 pyramidals, these authors demonstrated that layer 5 inhibitory population is maximally recruited or saturated by activation of deep layer simulation, and that stimulation of superficial layer of the neocortex will not increase the size of this inhibition which is maximal when an estimated 10-12 INs are engaged (Ling and Bernardo 1999 [135]). Therefore, inhibitory circuits might be restricted in both their control amplitude (size of inhibition) and its spatial extent (effective number of connections). In particular, layer 5 pyramidal cells might be able to elicit maximal inhibition from their postsynaptic INs partners without additional IN recruitment from layers 2,3 pyramidals.

IN-C At least two networks of interneurons mediating fast inhibition appear to be interconnected via chemical as well as electrical connections. The existence of gap junctions, or electrotonic coupling implies a fast synchronized response among different interconnected INs. This was earlier demonstrated by Bernardo in 1997 [18] where synchronous GABA-A mediated IPSPs occurred rhythmically in pyramidal cells and was associated with coherent activity in junction-coupled interneurons. More recently, networks of electrically connected FS cells were found in layer 5 of rat visual and somatosensory cortices (Galarreta et al 1999 [84], and Tamas et al 2000 [234]). Such electrical junctions coexist with GABAergic connections and help promote synchronous firing between coupled

interneurons in response to synchronous current injections as well as to in vivo operating conditions.

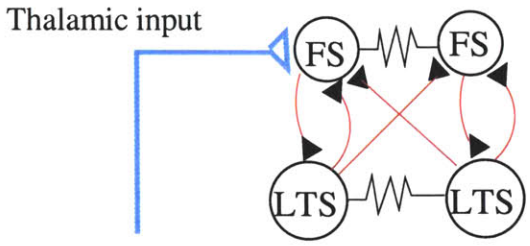

Figure 4-9: Two electrically coupled interneuronal networks mutually inhibit each other. Schematic based on finding in rat barrel cortex (Gibson et al 1999 [88]).

Moreover, Gibson et al 1999 [88] demonstrated the existence of two functionally distinct networks of electrically coupled interneurons in layers 4 and 6 in rat barrel cortex (figure 4-9). The first, an interconnected network of FS interneurons had electrical coupling and inhibitory chemical synapses between FS cells, and was specifically and strongly excited by thalamocortical synapses. The other network was comprised of LTS interneurons which were electrically connected but rarely inhibited each other, and was not directly excited by the thalamocortical pathways. In both experiments, the coupling was frequency -dependent and most effective at low frequencies presumably due to capacitive effects ($<$ 10-40 Hz). Finally, and similar to characteristics obtained in earlier experiments by Thomson [236], connections between regularly spiking excitatory neurons and the LTS variety facilitated dramatically at frequencies over 30 Hz. Thalamocortical to FS connections depressed fast and appeared to be a prominent feedforward pathway of thalamocortical inhibition which promotes sharp local synchrony in neural populations(a feature which was also observed earlier in layer 5 of rabbit somatosensory cortex by Swadlow et al 1998 [231]).

IN-D LTS interneurons have been recently demonstrated to produce synchronized inhibition in neocortical slices under noradrenergic modulation (Beierlein et al 2000 [15]). This network was able to produce synchronous oscillations that are independent of fast chemical, excitatory and inhibitory synapses and is not driven by action potentials, but is rather *intrinsic* and facilitated by metabotropic agonists. The oscillations can cause coherent LTS firings under sufficient depolarization which is synchronized within 100 μm and drives synchronized inhibition in local FS and regularly spiking pyramidal cells, the oscillations being either rhythmic (4-7Hz) or arhythmic.

Thus, it is possible that such LTS-network-induced inhibition can promote synchrony over recurrently connected local populations of neocortical neurons under activated brain states, while FS cells promote synchrony of thalamic inputs afferent into these cortical populations. Earlier studies by Deuchars and Thomson showed a class of burst firing LTS neurons contacting apical dendrites of layer 5 neurons arboring in layers 2,3. Further, these workers noted that small

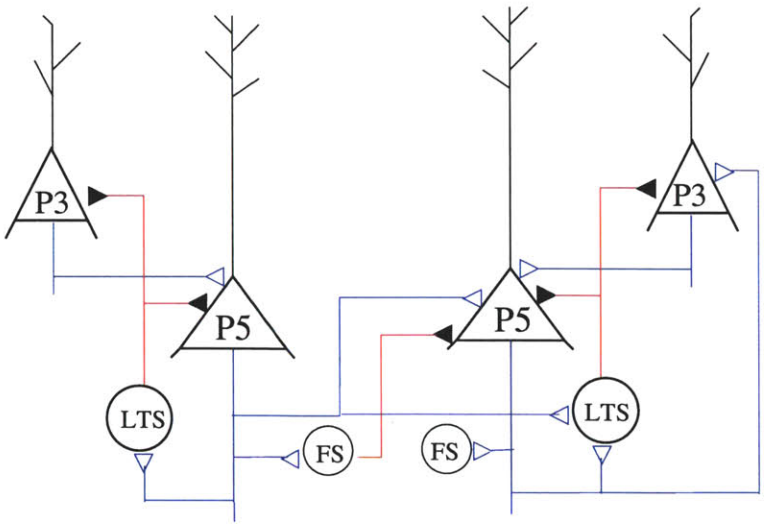

Figure 4-10: LTS and FS interneurons in layer 5 have different function. While FS is inhibited under cholinergic modulation, LTS are depolarized and can provide for intra-laminar inhibition (based on Xiang et al 1998 [267])

layer 5 pyramidal neurons have a distinctive innervation to the aforementioned LTS interneurons. Another study by Kawaguchi finds LTS cells with axonal innervations reaching layer 1 and layer 5 starting from their origin in layers 2,3 (Kawaguchi 1995 [114]) and, unlike FS cells, mainly target dendritic regions with a fairly constant synapse area across different dendritic arbors possibly implying a uniform tone-setting role for these cells (Kubota and Kawaguchi 2000 [127]). Also, LTS cells which project to layers 2,3 and 1 were found in layer 5 along with FS cells that are confined to that layer (rat visual cortex in Xiang et al 1998[267], rat frontal cortex in Kawaguchi et al 1997 [115] where these included martinotti and double bouquet cells). Interestingly, cholinergic modulation has different effect on these two classes: while FS cells are hyperpolarized, LTS cells are depolarized and might even produce action potential (Xiang et al 1998, [267]), providing a further segregation of functionality, with FS neurons possibly acting to limit spread of activity horizontally and LTS acting to synchronize activity within one column (figure 4-10). Hence, it is possible that layer 5 excitation has a pathway of interacting with at least one group of LTS neurons that might be a factor in promoting synchronous oscillations.

IN-E The fast inhibitory interneurons discussed thus far appear to contribute mainly through GABA-A type receptors. Slower kinetics GABA-B receptors are apparently recruited under different schemes or are associated with different populations of INs and at least several experimental works point to the necessity of abundant GABA release from the presynaptic neuron (possibly by bursting) for GABA-B receptor activation (Thomson 1997 [236], Destexhe 1998a [58]).

In his experiment on GABAergic synchronization, Bernardo noticed that the slow GABA-B component appears to be mediated by a different subset of INs

than those mediating fast IPSPs [18]. Recent immunoreactive labeling in monkey and human visual cortex showed low expression of GABA-B receptor types in layers 1 and 5, with higher expression in layers 2-4 and layer 6 and a use dependent regulation of GABA-B synapses in input layer 4 (Munoz et al 2001 [166]). Similar investigation by Shao and Burkhalter [205] showed *prominent slow inhibition in feedforward but not feedback pathways in the visual cortex of rats*, thus further corroborating the above finding.

4.2.4 Synaptic organization

Although some information on synaptic efficacy and interconnections appeared above, we will attempt to draw a clearer picture of specific interactions between different cortical layers and cortico-cortical connections which will be assumed in later discussions. The study of activity propagation and synaptic patterns in animal neocortex have been performed in vitro slices (dual intracellular impalements), in vivo (naturally behaving animals, [87, 163, 23]) and more recently using optical imaging [128, 125]. A review is given in Somogyi et al 1998 [211]. We will focus next on the interlaminar connections in the cortex, as connection properties between neighboring pyramidal cells have been fairly well established and discussed earlier.

Synaptic dynamics

The frequency dependent nature of synaptic connections has been a focus of attention of many researchers who argue that a depressing or facilitating connection essentially forms a filter of information transmitted between cells. Many variations of synapses which facilitate or depress have been reported. Very recently, the role of dendrites in integrating information and funneling it to the soma is becoming increasingly important with accumulating evidence of their non-passive nature. We have seen that by generating dendritic action potentials, distal inputs on layer 5 neurons become very facilitated at the soma. A more recent study showed that subthreshold AMPA-mediated EPSPs in layer 5 neurons can sum supralinearly when different dendritic locations receive simultaneous activity (Nettleton and Spain 2000, [169]). Also, EPSPs recorded in the soma of layer 5 neurons had the same time course as when they occur in the dendrite which was attributed to an increase of dendritic I_h with distance from the some (Williams and Stuart 2000 [257]). An even more striking experiment showed that in fact, in hippocampal CA1 pyramidal neurons, synaptic strength *increases* as a function of distance from the soma, giving a convincing answer as to how distal inputs could affect somatic potential regardless of cable filtering (Magee and Cook 2000, Spurston 2000 [146, 213]), and came to verify a theoretical treatment of this property by Cook and Johnston 1999 [46]. The recording method they used is expected to cause a flurry of experimentation regarding how dendritic information arrives at the soma, and it might further decrease the importance of accurately modeling dendritic attenuation in yet undetermined operating schemes. Synchronous arrivals of synaptic inputs has been a cause in lowering the threshold of spike generation in cat visual cortical neurons in vivo, thus providing further dynamic character

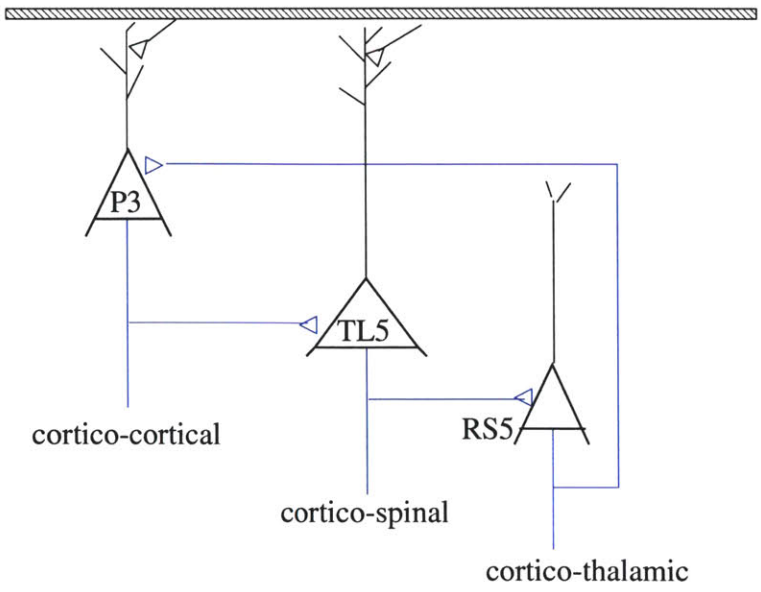

Figure 4-11: Dominant synaptic connections between pyramidal cells in layers 3 and 5.

to synapses that allow neurons to detect coincidence in inputs (Azouz and Gray 2000, [9]).

Hence, given the recent influx of information on integration of inputs, we will avoid making strong statements about absolute connectivity strengths unless have been demonstrated experimentally. Instead, a well accepted synaptic organization scheme, mainly known existing connections and their demonstrated relative strength, will be utilized. A recent review on the dendritic influence on the firing dynamics in neurons is given by Reyes 2001 [188].

SO-A Studies of interconnectivity between neighboring pyramidal cells of the superficial layers (layers 2, 3) have shown a wide range of EPSP amplitudes and durations. Many of those connections were NMDA receptor mediated, increasing in amplitude and duration as with postsynaptic targets depolarization. Connections exhibited postsynaptic depression unless some active voltage dependent mechanism was recruited. The recurrent connectivity in these layers are reported to be quite high (even higher than that between layer 5 pyramidals). Superficial layer pyramidal cells send long mylinated axons into the white matter that can travel for very long distances, including callosal and ipsilateral connections.

SO-B In studying the interlaminar connectivity patterns between layer 5 and superficial layer 3, Thomson [237] noticed in 1998 that the vertical innervation directed from layer 3 pyramidals into layer 5 is much more focused onto large layer 5 pyramidal cells. Quantitatively, within a tissue column of $250\mu m$ in a rat neocortex, a randomly selected layer 3 neurons have a probability of 1 in 4 of contacting an TL5 (IB) cells in layer 5 and only 1 in 40 in contacting a smaller (RS) cell. Also, all the IB cells had apical dendrites in layer 1 and they

usually intersected the apical dendrites of layer 3 pyramids, whereas the smaller RS cells had shorter dendritic arbors terminating in layers 2,3. Here again large layer 5 neurons were seen to have axonal arbors mainly in the deeper layers that extend horizontally (as in Markram 1997 [147]). Some axon collaterals ascended to layer 3 where it appeared to be less focussed innervation of neurons in that area. It is possible that layer 5 to layer 3 connection, however, is mediated by smaller RS cells as presented in the review by Callaway 1998 [26] on cat visual cortex as well as by caged glutamate application in rat somatosensory cortex (Schubert et al 2001 [200]). Hence, there is a strong descending connection from layers 1 and 3 to IB cells (corticospinal neurons, sending axons to motor systems), but not to RS cells in lower layer 5 (sending axons to non-specific thalamic nuclei and to the opposite hemisphere) or upper layer 6 (sending axons to specific thalamic nuclei), as was also suggested in another experiment in rat motor cortex (Kaneko et al 2000, [107]) where corticospinal neurons were four times more likely targets than corticothalamic neurons to layer 3 innervation and their response was of a monosynaptic (direct) nature. It is also apparent that an ascending feedback mechanism from the RS subpopulation of layer 5 pyramidals to layer 3 pyramidal cells. A summary is shown in figure 4-11.

SO-C A recent experiment in rat somatosensory cortex studied fully reconstructed synaptic connections of large layer 5 cells (IB) as well as smaller RS cells (Schubert et al 2001 [200]). A main finding was the strong connection between layer 6 and IB cells in layer 5 but not the RS variety. Unlike connections arriving from layer 3 to TL5 cells (which are confined to a column), connections arriving from layer 6 is more uniform and extend beyond the geometric boundary of a single column (figure 4-12). Also, this experiment demonstrated a synaptic innervation of layer 5 cells by layer 4 inputs which was thought to be absent before. IB cells had far more excitatory than inhibitory connections, which was not the case for RS cells in layer 5.

SO-D Cortico-cortical connections are thought to obey three main topologies depending on the nature of interaction between two regions, mainly lateral interactions, feedforward and feedback connections (Mountcastle 1998 [165]). Although the source and target specificity varies between areas and becomes more distributed especially in the lateral interaction scheme such as in association cortices, a clearer view can be drawn in the case of two interacting system within a hierarchy. In this case, it has been reported that feedforward or ascending connections tend to target the input layer 4 and feedback or descending connections target superficial layer 1. The origin of such connections can be either unilaminar, originating in either superficial or deep layers, or bilaminar, originating in both. A strong character of feedback connections is that they avoid the input layer 4 (figure 2-6 in Chapter 2). Studies of cortico-cortical connections have shown that feedforward connections are focused, feedback connections have both focused *and diffused termination patterns* (Callaway 1998 [26], also Cauller et al 1998 in rat somatosensory cortex[33]). Hence there appears

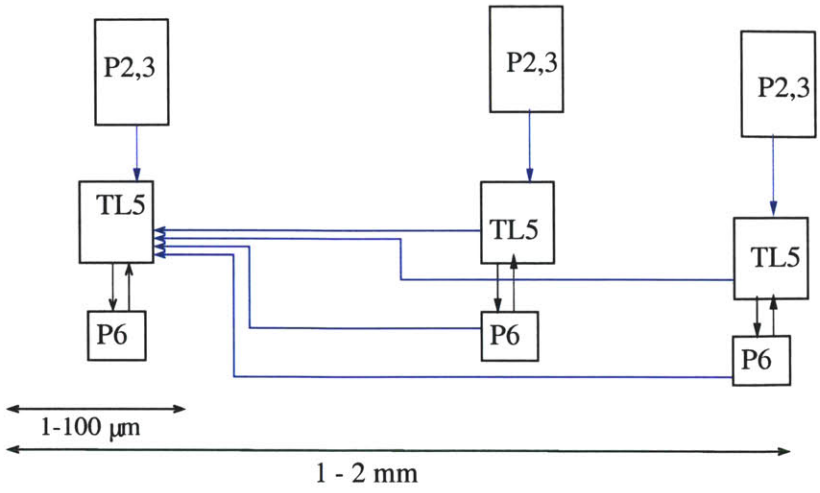

Figure 4-12: Superficial and deep pyramidal connections to TL5 cells have different spatial extent.

to be a separation of the information streams as dictated by the hierarchical connectivity patterns: ascending connections possibly assuming a role similar to thalamic input and descending connections possibly having a modulatory role for reinforcing and redefining activation maps in the target system. This is also noted by the nature of synaptic receptors accessible by each system: *feedforward pathways elicit strong ISPSs (slow and fast) in the target system (similar to thalamic effect) whereas feedback do not, but rather show strong polysynaptic EPSPs*, implying excitation of several local recurrent activation schemes in the target region (Shao and Burkhalter 1999 [205]).

SO-E Thalamic innervations of sensory cortical areas have been extensively studied, especially in the cat visual areas and rat barrel cortex. Although only about $5 - 20\%$ of the excitatory synapses in layer 4 neurons are thalamic in origin while the rest are intracortical, these are several times more effective than an average intracortical connection, mainly through a higher release probability and more release sites (Gil et al 1999 [90]).

The highly ordered specific thalamic innervation contrasts with the highly diffused projections of thalamic intralaminar areas. Due to the limited experimental data on the role of diffuse thalamic inputs, we will utilize the generally adopted organizing principles for these inputs, mainly into superficial layer 1 of the innervated area [3].

[3]The difference between specific vs nonspecific thalamic nuclei have been recently challenged, highlighting instead a focused vs diffuse afferents into the cortex that could originate in both relay and intralaminar thalamic nuclei, with the density of diffuse projections being much higher in intralaminar nuclei and focused input higher in specific relay nuclei.

4.2.5 Circuit dynamics

The potential for disparity between various cortical circuit diagrams and their dynamics appears daunting as more information become available about different neuronal types, cellular mechanisms and synaptic properties between populations of neurons, especially among the interneurons variety. Several sensory cortical areas have been more specifically studied than others in several animals due mainly to their proximity to input signals and the relative flexibility in controlling the afferent stimulus from its thalamic source. This includes visual areas and the somatosensory cortices of rats, cats and monkeys. While the specificity of cortical processes underlying information processing and neural representations appear to differ to some extent between these areas, we note that several basic principles of organization appear to recur across sensory cortices. A discussion and review of these similarities and differences is given elsewhere (see Mountcastle 1998, [165], White 1989 [254], and Shepherd 1998 [206]). In what follows we will provide a brief description of the dynamic responses of some cortical areas to stimulation both in slices and in vivo experiments in awake animals. *The main focus is, first, the greater excitability of layer 5 cells compared to layers 2,3; second, the spread of synchronous activation in layer 5 between cortical columns; and, third the ability of layer 5 cells to sustain oscillations around 10 Hz.*

Slice experiments

The study of synchronous propagation of oscillations generated in layer 5 in vitro has long been demonstrated. In earlier experiments, Changac-Amitai and Connors 1989 [35] studied excitation propagation in slices of the rat somatosensory cortex. Their results demonstrated that under minimal decrease in inhibition, intrinsically bursting (IB) populations of layers 4 and 5 produce synchronous activity that can propagate up to several millimeters. These cells have low amounts of inhibition, unlike the regularly spiking variety (RS) existing in layers 2-6. A stimulus delivered to layer 6 produced a small fast EPSP in RS cells followed by a sequence of IPSPs lasting for up to 200 msec. In IB cells however, the same stimulus strength had little inhibition and often lead to a bursting discharge.

Similar results were obtained in cat motor cortex. Slice preparations showed that inhibition in layers 2,3 seems more active at resting membrane potential than that in layer 5 pyramidals (Van Brederode et al 1995 [244]. While stimulating layers 2,3 always resulted in a fast EPSP followed by fast and slow IPSPs, those in layer 5 resulted only in EPSPs at resting potential, indicating the prominence of excitation in this layer. Stimulation of layer 5 after excitatory blockade showed fast $GABA_A$ IPSPs and less prominent slow $GABA_B$ IPSPs in this layer, which could only be activated with large release of GABA in this layer.

A consequence of the low inhibition in layer 5 is the ability of this layer to sustain emergent oscillations. Silva et al 1991 [212] showed that when a cortical slice was placed in increased excitability conditions (enhanced NMDA receptors via low Mg^{+2}), then 8-10 Hz oscillations emerged in the slice and were specifically caused by intrinsic bursting layer 5 cells. More recently, and under similar excitability conditions, 7-10

Hz oscillations were optically recorded in slices and shown as waves of propagating activity with limited spatial extent that travel over neural assemblies. Such dynamic ensembles could also be evoked under in vivo-like conditions (unaltered excitability) if a large enough number of neurons were simultaneously activated. Hence, the authors argue that such ensembles might also underly the 10 Hz oscillatory activity recorded in awake animals (Wu et al 1999 [266]).

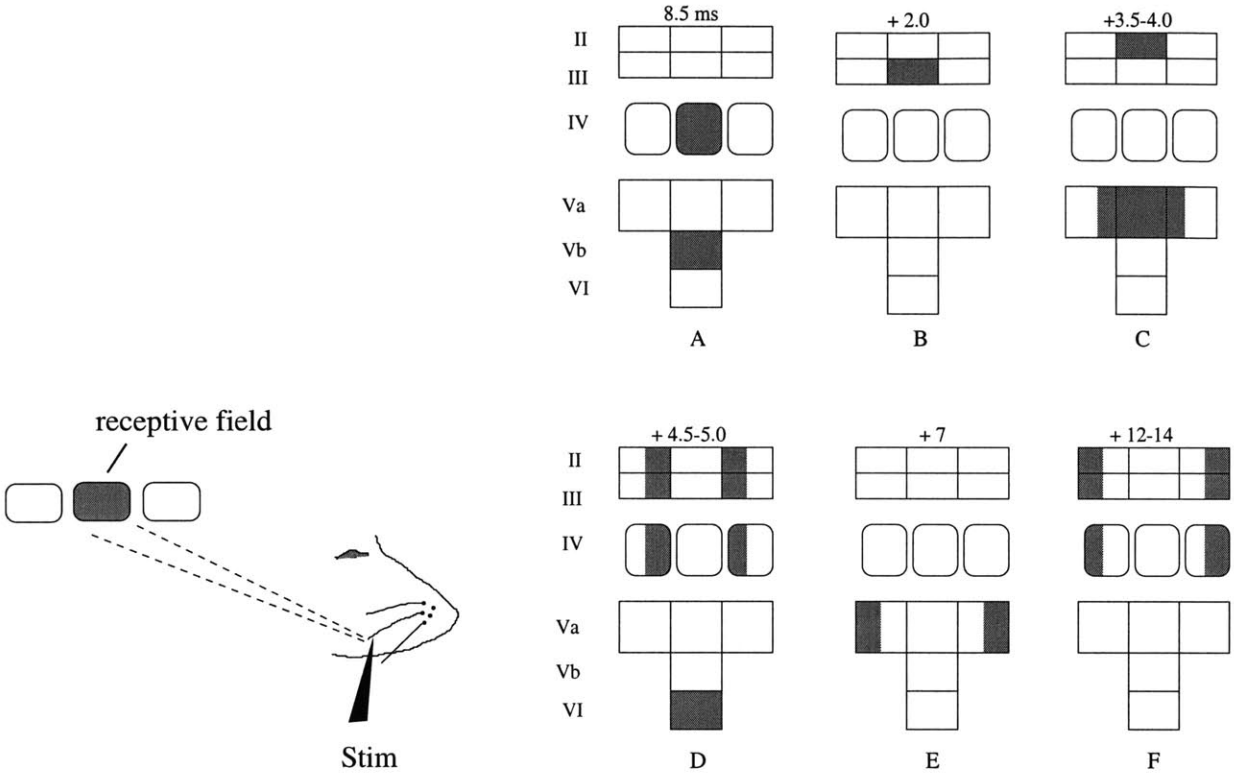

Figure 4-13: Temporal activation order in response to single whisker stimulation in rat somatosensory cortex. Three adjacent receptive fields are schematized by their layer 4 extent with the middle column representing the primary whisker projection. *A* Layer 4 is the first to respond in the columns of the main receptive field followed shortly by layer 5b. *B:* The excitation is then relayed to layer 3 after 2 msec. *C:* Cells in layer 5a are activated next both in the local column and first order neighboring columns 3.5-4 msec later. Also, layer 2 cells of the principal column become active in the same period. *D:* Subsequently, activation is relayed to superficial layers of the adjacent column (4.5-5 msec), at which time layer 6 cells are active. Similarly, layer 5a is activated in second order neighbors (*E*) and then in the associated superficial layers (*F*). (Adapted from Armstrong-James et al 1992 [8])

In vivo experiments

Experimental procedures in rats place qualitatively similar emphasis on the role of layer 5 cells in signal propagation. An interesting study of within-column and column to column transfer of activation was conducted in the somatosensory cortex of

urethane-anesthetized rats by Armstrong-James et al 1992 [8]. Here, a single vibrissa (whisker) is deflected and the magnitude and latency of response in different cortical layers was studied. The earliest response occurred in layer 4 and lower layer 5 (5b) of the corresponding cortical column (2-3msec later). Next, cells in layer 5a responded in both same and adjacent columns. Subsequently, layers 2,3 and 6 of the adjacent columns were activated (5 msec later) and this repeats to second order adjacent columns. A schematic is shown in figure 4-13.

The above experiment agrees qualitatively with newer manipulations in the awake rat barrel cortex, where in vivo recordings demonstrated fastest response in the barrel system in layer 4, followed by infragranular layers (0.92 msec) and then superficial layers (1.84 msec) (Brumberg et al 1999 [23]).

Hence, activation of layer 5 neurons appears to be not subject to the classical receptive field notion but is rather less spatially tuned[4] . In the awake rat primary somatosensory cortex, single whisker stimulation (sensory input) activated ensembles of layer 5 neurons well beyond a single cortical column (average of 5.6 columns, Ghazanfar et al 1999 [87]). Further, a layer 5 cell responded to different whiskers stimulation at specific times, hence indicating a spatio-temporal response specificity.

4.3 Recent findings pertinent to the generation of certain cortical rhythms

In this section we will present briefly some experimental evidence on the behavior of layer 5 cells under different cortical oscillation states which point to a natural role of these cells in initiating activity in a silent population of cortical neurons, in providing for a mechanism of cortical recruitment through augmentation, and in creating a common 10 Hz (alpha-like) rhythm in sensory modalities under higher order control. Finally, we mention the pathologic recruitment behavior of layer 5 cells under disinhibition which promotes a seizure-activity around the same characteristic 10 Hz frequency band. The present section attempts to provide a more complete list of evidence supporting the circuit models and hypothesis to follow. A more detailed presentation of rhythmogenesis is provided in Chapter 6.

4.3.1 Augmenting responses

An augmenting response refers to the increased depolarization in neuronal populations under repetitive stimulation. This is thought to be important for increasing local circuit activity and enhancing short term plasticity in cortico-cortical and thalamo-cortical pathways. Many experimental models showed augmenting responses (ARs) due to thalamic stimulation in cats (Bazhenov et al 1998 [14]), cortical stimulation in rats (Castro-Alamancos et al 1996 [29, 30]), and stimulation of callosally projecting

[4]By classical receptive field, it is meant that a particular group of cells respond primarily only to a prefered spatial location

layer 5 cells in anesthetized cats (Steriade et al 1993b [217] and Nunez et al 1993 [174]).

Although some workers considered a large portion of AR behavior to be thalamic in origin, others provided evidence for its initiation in cortex and its close link to layer 5 cells. In particular, augmenting responses (ARs) have been reported in the sensorimotor cortex in rats due to simulation of the corresponding thalamic nucleus (ventrolateral VL thalamus) as well as during electrical stimulation of the cortex itself (Castro-Alamancos et al 1996a, 1996b [29, 30]).

In this experiment, as the VL thalamus is stimulated repetitively at an alpha band frequency (10 Hz), increased levels of depolarization leading to cellular activity are observed in the connected cortical areas. Looking at current source density profiles and cellular firing in those areas, the augmentation seems to originate in layer 5 cells and is characterized initially by single spikes which lead to bursting-like behavior in this pyramidal population. Interestingly, this augmentation appeared to be maximally evoked in periods of sustained hyperpolarization in neural tissue, and since many of layer 5 cells have hyperpolarization activated conductances, it appears that this subpopulation of pyramidal cells might have a primary effect in inducing cortical ARs.

The above experiment appears to link well with now-known dynamic behavior of tufted layer 5 cells. First, looking at the laminar distribution of thalamic inputs from the VL thalamus, it has been reported that these projections avoid layer 4 and innervate layer 5 as well as layer 1 (just as the posterior nucleus (Po) and Lateral posterior LP). Also, feedback and callosal long-range connections terminate in superficial layers. Thus, it appears that stimulating such pathways is able to link apical zone A and basal zone B of large layer 5 cells which, when successfully coupled, induce bursting and provide for increased activity in cortical tissue.

The hyperpolarization apparently is a suitable mechanism of reenergizing the synaptic activity in layer 5 which tends to after initiation to increase its activity if operated at 10 Hz and spread it to other layers.

4.3.2 Alpha band oscillations

Alpha rhythms have long been observed as idling rhythms of the visual cortex in restful awakeness when eyes are closed and is blocked when eyes are open. They arguably have similar counterparts in other sensory areas such as the rolandic mu rhythm of the somatosensory area and tau rhythm of the auditory areas.

A functional aspect of alpha activity has recently surfaced however with the recording of these rhythms in animal experiments and more importantly in man. In visual cognition experiments in cats, it was observed that an increase in alpha band coherence between two visual areas that are known to be connected in a processing hierarchy, that is information is fed-back via long range connections from the higher order area to the lower (von Stein et al 2000 [250]). Hence, it appears that top-down information transfer might occur around 6-12 Hz, which is well within the range of bursting capabilities of layer 5 cells. Given the ability of tufted layer 5 cells to sample feedback excitatory activity in the superficial layers, this phenomenon might well be a reflection of the active coupling of feedback information and local information in

these cells, represented by bursting in the alpha range.

Functional correlates of alpha band oscillations were also observed in EEG recording in humans. One particular experiment demonstrated that during an object recognition task, there exists a transient increase in alpha band coherence between visual areas occurred only when subjects were able to correctly identify the objects. Further experiments were performed and will be dwelled on later as we discuss alpha oscillations in more detail (Mima et al 2001 [162], Basar el al 2001 [13]). We claim that all these experiments, the augmenting response properties of layer 5 cells, and other older intracortical evidence, such as the existence of a dipole source for alpha rhythms in layers 4/upper 5 (Lopes da Silva et al 1977 [141]), point to an active role of these cells in generating alpha activity both in functionally passive and active modes, as will be seen later.

4.3.3 Slow-wave Oscillations

The unyielding mechanism of slow wave oscillations ($<$ 1Hz) has long been debated and was thought to be a general excitability and disfacilitation property of cortical neurons. Recently a more direct locus has been highlighted where such activity might be originating, mainly layer 5.

In a slice preparation of ferret neocortex maintained in vitro, slow wave oscillations were observed when slices were placed in a bathing solution similar to ionic composition in situ (Sanchez-Vives and McCormick 2000, [193]). The oscillations were seen to originate in layer 5 and propagate to layer 6 and then superficial layers 2/3.

Slow oscillations were initially described by Steriade in a series of experiments in cats. There, IB cells were seen to respond fairly consistently over the depolarizing envelope of a slow-wave cycle (cf. Figure 11 in Steriade et al 1993, [217]). Interestingly, a 10 Hz callosal stimulation in cortical networks was able in few instances to increase slow wave frequency to the delta range (1.6 Hz) in a highly sustainable fashion, thus creating an augmenting response that outlasts thalamic input and carries the oscillation for 20-45 seconds (Figure 13B in Steriade et al 1993, [217]). This highlights the propensity of this layer 5 network in organizing cortical activity and sustaining it for fairly long periods of time in some instances.

4.3.4 Seizures due to disinhibition

The ability of layer 5 cells to organize synchronous activity in cortical networks might lead to pathological conditions if left unchecked. In fact, a recent experiment studies the origins of neocortical synchronized oscillations after disinhibition in vivo and could possibly further highlight a developing picture that we are trying to bring into focus. In this experiment (Castro-Alamancos 2000, [32]), slow wave sleep oscillations in rats were transformed into a large amplitude 1 Hz spike and wave oscillations after application of a $GABA_A$ receptor blocker (see figure 6-37 in Chapter 6). With stronger $GABA_A$ block, the 1 Hz discharges also contained lower amplitude discharges

at 10 Hz. Finally, applying $GABA_B$ blockers slows the 1 Hz oscillation to 0.5 Hz and increments the number of low amplitude 10 Hz discharges (actually 7-14 Hz).

Several important observations resulted from this experiment.

The oscillations are cortically generated since they persist with inactivation of the thalamus. While the initial large discharge can occur in either the upper of lower layers of the cortex (24% and 76 % of the time, respectively), only the lower layers (5,6) can trigger this discharge in the absence of the thalamus.

The subsequent 10 Hz discharges *always* originated in lower layer 5 /upper layer 6, and subsequently jumped to upper layers 2/3.

The lower layers are maximally sensitive prior to the initial discharge, since depolarization of cells in these layers produced enhanced activity immediately before each PDS. This ties well with the Vives-Sanchez and McCormick experiment on the origin of slow wave oscillations (above). Also, some layer 5 cells were shown to have strong propensity to burst (so called Low threshold bursters, accounting for about 10% of cells in layer 5 pyramidals in rat sensorimotor cortex (Schwindt et al 1997 [202]).

The propensity of layer 5 cells to discharge at 10 Hz ties well with their augmenting response at 10 Hz activation, further pointing to a preferred oscillatory frequency (resonance) of cells in this area. This was also demonstrated by Silva et al in 1991 where in an NMDA facilitated slice, layer 5 cells produced sustained bursts at 5-12 Hz *after* a brief hyperpolarization (Figure 1B in Silva et al 1991 [207]).

4.4 A hypothesis

The effective skeleton circuit for EEG generation was built based on the aforementioned evidence and is given in figures 4-1,4-2, and 4-3. We will now present a hypothesis on the functional consequences of cellular behavior, firing and network connections. While two authors have put forward what have become known as layer 5 hypothesis which implicate those cells in oscillation propagation and even neural awareness (Connors et al 1995[40], Koch et al 1994 [124]), the aforementioned neurological evidence has only recently became available and has not been fully incorporated to date. These aformentioned authors have assigned particular significance to layer 5 cells in promoting spread of activity in cortical tissue based on the size and the then-known connectivity of intrinsically bursting cells and electrophysiology in slices. However, the nature of oscillations supported by layer 5 cells, the corresponding intrinsic and network mechanisms, as well as a precise description of the consequences of such oscillations were not described. We now are at a position to consider in a clearer fashion the role of layer cells in coupling different afferent streams that arrive at superficial and deeper layers and in generating various cortical rhythms. We will first state our basic proposition and then detail its main points.

Conjecture 1: *In a sensory system, tufted layer 5 cells act as gates that provide a pathway for binding local cortical activity and higher order supervisory control. These cells initiate reorganization of local activity based on matching feedforward (driving) inputs with feedback (higher order control) inputs or internal expectations.*

Conjecture 2: *The slow oscillatory behavior of local neural populations (< 15 Hz), especially that observed over large areas and manifested in the EEG, is punctuated by the firing patterns of layer 5 cells, especially those cells acting as the neural gates of hierarchical binding.*

We base our conjectures on the following proposed effective skeleton circuit properties.

1. *Controlled interaction of input streams:* Large Tufted layer 5 pyramidal cells have two effective ports of cortical inputs with an active coupling mechanism controlling the degree of interaction between these inputs. As such, apical arriving inputs to the **distal zone A** can be selectively amplified or facilitated (figure 4-14) . These inputs are mainly thalamic afferents from intralaminar nuclei and long-range cortical afferents arriving from higher order systems (hence is a feedback signal from higher area in a sensory processing stream). The integrative ability of the apical system A is under neuromodulatory control, such as serotinergic modulation which increases its excitability and hence promote integration (motor cortex), or dopaminergic modulation which decrease its excitability, and hence allows the local circuit to sustain its current state (prefrontal cortex, for example).

   Afferents to **basal zone B** have a direct driving capability of the somatic region of integration and hence can initiate firing on a large layer 5 cell. Furthermore, if coupling between zones A and B is enabled (zone C enabled), then basal inputs can selectively define which relevant apical zone A information to integrate based on its own afferent inputs (e.g., thalamic) as well as local circuit constraints (e.g., Layers 3 and 6 inputs). The mechanism of integration is a back-propagating action potential which, when successful, creates a burst firing at the soma. This is an active mechanism which not only changes the firing pattern of a layer 5 cell, but also initiates, via active Ca^{2+}-mediated action potentials in the apical region, an increased sensitivity state in which afferents in the distal zone A are accommodated.

   Synaptic connections to the middle-apical regions (**control zone C**) of layer 5 cells have a supervisory or control role of the coupling level between zone A and zone B. As such, inhibitory afferents to this zone can decrease the coupling or eliminate it for elongated periods of time. Evidence suggest that the main input in this layer comes from input layer 4 (Schubert et al 2001 [200]).

2. *Role of bursting:* The binding mechanism is manifested by bursting in tufted layer 5 cells. The functional significance of bursting is in reorganizing local activity pathways and can be traced in changes in activity transfer:

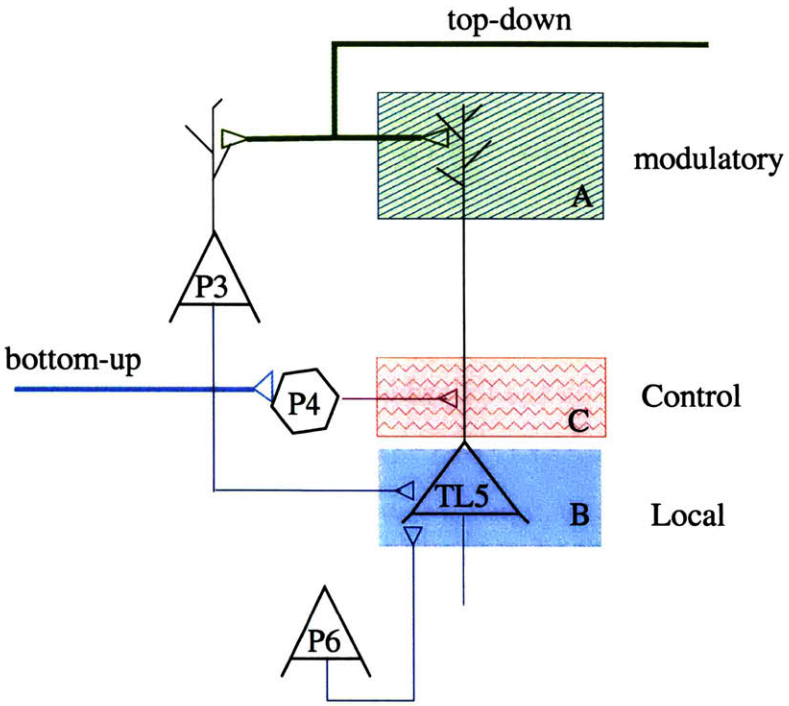

Figure 4-14: Tufted layer 5 cells provide a controlled binding gate between local cortical activity which affects lower layers of the cortex and higher order modulatory input which arrives in superficial layers. A control zone in middle layers acts to facilitate or prohibit this binding

a- Bursting transmits reliably across layer 5 cells in different cortical column, allowing for horizontal spread of activity. As we saw earlier, only burst firing activates both presynaptic and postsynaptic mechanisms at synapses within layer 5 to enhance synaptic coupling and overcome depression, an effect which is not observable under regular firing (Williams et al 1999 [256]).

b- Bursting activates layer 5 to layer 3 inhibition, thus controlling the vertical spread of activity within a column. A specialized form of interneurons provide for this interlaminar inhibition. Connections of inputs to these cells, plausibly of the low threshold spiking (LTS) variety, enhance by several folds under high frequency inputs and hence could respond strongly to bursting in TL5 cells. Accordingly, LTS cells are capable of selectively shunting (inhibiting) excitatory inputs arriving at the target pyramidal cells in superficial layer 3 (figure 4-10)[5]. This phenomenon is mostly observed during alpha-like oscillations observed at initial stimulus response stages.

[5]Hence, although LTS inhibit pyramidals in layer 3, there effect is negated in those columns with bursting layer 5 cells mainly due to strong excitatory feedback from layer 5 pyramidals as will be seen later

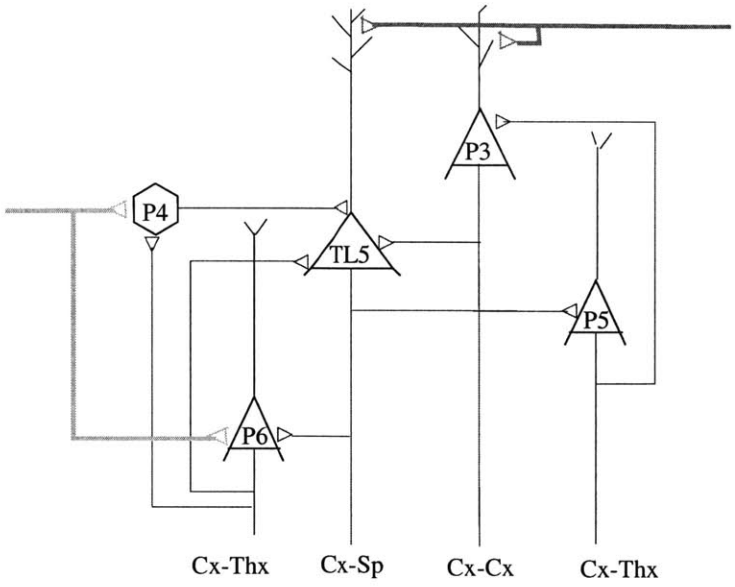

Figure 4-15: Major local excitatory connection of TL5 cells. While inputs from layers 2-4 are within a column boundary, those from layers 5-6 can be across columns, and hence are at a columnar assembly scale

3. *Role of layer 4:* Layer 4 cells are the main input port of a local cortical circuit and are able, by virtue of their strong recurrent connections, to amplify input activity and spread it vertically to layers 2, 3 and to layer 5. Activity is transferred to layer 6 via axon collaterals of layer 5 cells branch. Layer 6 pyramidals, which is the main cortico-thalamic feedback output, have a strong feedback connection with layer 4 and large tufted layer 5 cells, which could create a positive feedback loop reinforcing selective activation maps.

4. *Role of Layer 3 input:* Tufted Layer 5 pyramidal cells receive strong inputs at the basal dendritic zone B descending from the superficial layers pyramidal populations P2/3. When the latter population is sufficiently active, therefore, TL5 cells can be driven by the basal input and thus could fire in the regularly spiking (RS) mode. Hence, while thalamic input effect on layer 5 cells might be modulatory, as implied by the broad receptive fields of thalamic inputs in the visual cortex, superficial layers can activate basal system B, possibly creating a precise map of (regularly spiking) firing patterns in these cells, which supports the known role of TL5 cells as output terminals of the neocortex[6].

5. *Layer 5 network:* Pyramidal neurons in layer 5 fall into possibly three classes (figure 4-16) with each contributing to the EEG oscillatory behavior under different conditions. At least a subset of large layer 5 pyramidal cells have the propensity to oscillate in the alpha frequency band ($\approx$ 10 Hz). At the

[6]In this case, TL5 cells could fire in RS mode due to either (a) modulation by brain stem neuromodulatory inputs or (b) activation of GABAergic inputs to zone C of these cells.

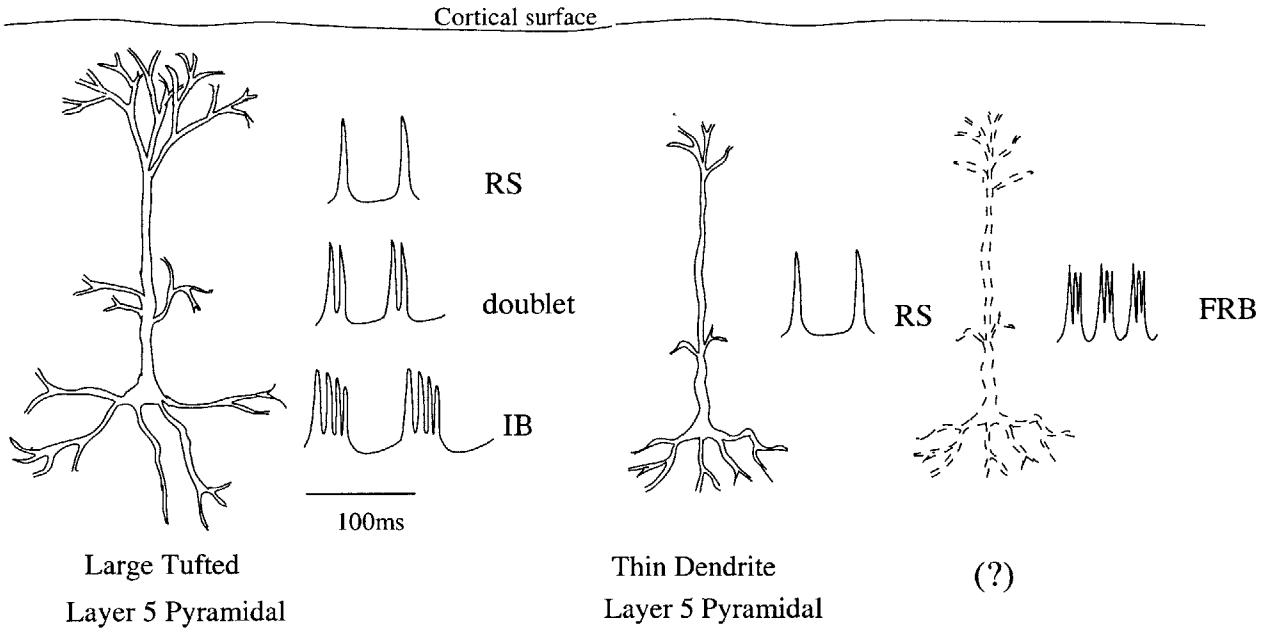

Figure 4-16: Possible firing characteristics of layer 5 pyramidal cells. *Left,* Large tufted pyramidal cells could fire in regular spiking, doublet or intrinsically bursting modes. *Middle,* Thin dendrite pyramidal cells are of the regularly spiking variety. *Right,* A layer 5 cell class could fire fast burst sequences (termed FRB by steriade)

cellular level, such resonance is possible by virtue of rebound depolarization mechanisms which are active at low levels of excitation or upon dominance of a strong inhibitory tone in layer 5 (leading to hyperpolarized membrane potentials of these cells). Hence, a cortical augmenting response is created by exciting the natural frequency of layer 5 network based on specific input configurations. Specifically, basally-arriving inputs in layer 5 (such as from thalamic nuclei) can create initial hyperpolarization in layer 5 cells. When coupled with high sensitivity to apical-arriving inputs, rebound depolarization in large tufted layer 5 cells can lead to burst firing patterns with subsequent propagation of depolarization into other layers in the same column and other columns within a local region.

Under disinhibition, recurrent excitation could, if left unchecked activate specific fast rhythmic bursting cells in a runaway excitation mode such as in seizures. Therefore, we think that similar resonance frequencies appears under many conditions, such as augmentation, alpha rhythms, and disinhibition-induced seizure conditions.

6. *Role of interneurons:* An integral part of network synchronization is mediated by local inhibitory neurons. In particular, long-range synchronization is made possible possible at high frequency via fast spiking interneurons which observes both local excitation levels as well as input excitation from distant cortical structures (a Traub like mechanism as presented in chapter 3). The action of

these INs is mediated mainly via fast $GABA_A$ receptors, or at slower rates via $GABA_B$ receptors. Synchronization within a local circuit could also be attained by gap-junctions (direct electrical coupling) between GABAergic populations.

7. *Rhythmogenesis:* Although the thalamus initiates some of the cortically recorded rhythms such as sleep spindles, a large repertoire of EEG rhythms are cortically generated. Accordingly, we conjectured that specific circuitry in the neocortex produce signature waveforms in EEG that are observable under several vigilance states (table 4.1). In particular, we argue that many rhythms such as slow wave sleep (K complex, polymorphous delta), 10 Hz augmenting response, alpha-like activity, and seizures, could either be initiated or sustained by affective local cortical circuits that interact within a large network to produce the observed signals. In particular we mention.

   a- Although several experimental and modeling efforts demonstrated augmenting responses as generated at by thalamocortical interactions, augmenting responses can be generated in local neocortical populations under specific input patterns to large layer 5 cells. In particular, the network of TL5 cells is maximally recruited to create augmentation when apical inputs to local TL5 cells are activated.

   b- The augmenting behavior of layer 5 cells to 10 Hz stimulation is a simple manifestation of more general resonance characteristic in this layer, possibly involved in information transfer between cortical hierarchies or facilitation of thalamocortical systems. In particular, induced alpha activity is a case where many layer 5 cells resonate at around 7-9 Hz due to minimal levels of feedforward excitation (restful wakefulness, minimal sensory input). Further, 10 Hz oscillations are observed in many cognitive conditions over visual areas (alpha rhythms), motor areas (rolandic rhythms) and auditory areas (tau rhythms). As will be shown in chapter 6, such rhythms, which are related to cognitive task performance, might reflect early initiation of the task: specific activation patterns of layer 5 cells, especially TL5, explain experimental data of many alpha activity patterns observed and reflect interactions between higher order structures and local processing cortical circuitry. On a larger network level, 10 Hz range oscillations might be contributing to long-term potentiation in thalamo-cortical pathways which appears to increase at this frequency and reverse at 1 Hz (Castro-Alamancos 1999 [31]).

   c- Gamma frequency activity is related to active processing in the local neural populations. Therefore, in this frequency range (> 30 Hz), one expects system-specific local mechanisms to be dominant and will not be dealt with in detail here. However, two general principles might hold. First, inhibitory interneurons might play an essential role in providing local and long synchronization between pyramidal cells (locally: electrical coupling, long-range: Traub-like mechanisms). Second, several experiments point to an increased alpha-range synchronization in early stages of cognitive

processing (100-300 msec post-stimulus). We claim that such activity is essential to providing local reorganization of cortical assemblies and provide two scenarios on how such alpha will switch to higher frequencies based on layer 5 cells properties.

d- Slow oscillations originate in lower cortical layers due to rebound activity in layer 5 cells which have the highest sensitivity after long periods of hyperpolarization. This rebound is then transferred to other layers and across regions and is sustained for a long period of time before another cycle of hyperpolarization begins. Other sleep rhythms that ride on slow wave sleep include spindling, delta and fast oscillations. While spindling appears to be a characteristic behavior of thalamic circuitry, it might be well reflected in cortical layer 5 cells which have a tendency to oscillate at similar frequencies. Although spindling does not necessarily evoke burst responses in tufted layer 5 cells but rather regular firing patterns, such cells are capable of bursting at spindle-range frequencies (awake cat experiments showed bursting at 11 Hz -Steriade et al 2001 [228]). More importantly, however is that these cells take over as sleep deepens and there is a far higher incidence of bursting in TL5 at 3-4 Hz (delta range) attributable to higher levels of hyperpolarization and decreased levels of excitation in the neocortex, necessarily deactivating control zone C of TL5 in this state.

   Since K-complexes are arguably manifestations of slow-wave oscillations in humans (Steriade et al 2000 [227]), such grapho-elements could be explained by the same mechanisms as above. In particular, the rebound activity of a K-complex and its transformation to spindles and delta waves.

e- Intracortically-generated spike-and-wave seizures as seen by cortical disinhibition appear to be exaggerations of the activity under slow-wave sleep in which large portions of 10 Hz oscillating circuits are recruited. Under such conditions, it is also possible that large populations of fast rhythmically bursting cells (FRB) are recruited in a bursting mode, a condition which only occurs pathologically . The in vivo experiments of Castro-alamancos trace a similar qualitative contribution for layer 5 cells in its generation. Paroxysmal depolarizing shifts observed in seizures start with a large spike and transform to 10 Hz discharges, much the same way as observed in K-complexes.

In the next chapter we will present circuit models of cortical neurons, column and interactions across columns. Utilizing these minimal models, simulation experiments capable of generating the aforementioned rhythms are given in chapter 6. Further insights to specific cellular mechanisms that might be active under different states will be discussed accordingly.

Table 4.1: Summary of basic rhythms attributable to layer 5 dynamics

State	Major cell types and firing patterns
Slow wave sleep (< 1Hz)	initiated by L5 rebound mechanisms, propagates to other layers transferred between regions by superficial layers
Polymorphous sleep delta	initiated by TL5 under strong hyperpolarization, characterized by low frequency bursting (3-4Hz)
10 Hz Cortical augmentation	initiated by L5 rebound mechanisms under repetitive stimulus trains sustained and transferred by TL5 in bursting mode
10 Hz alpha activity	Layer 5 mechanisms
- induced	rebound under inhibitory tone of restful wakefulness (7-9 Hz) wide scale
- evoked	TL5 in bursting mode, influenced by feedforward feedback (10-12 Hz) limited (local) scale
- emitted	TL5 in bursting mode, driven by feedback (10-12 Hz) medium scale
disinhibition-induced seizures	Layer 5 cells, IB, and FRB

Chapter 5

Neocortical Circuit Models

After outlining the main components in an effective skeleton circuit in the previous chapter, we will develop models of basic neural elements and their interaction schemes at a column, columnar assembly and regional scales. This chapter aims at both providing a brief outlook on possible cellular models as well as introducing the building blocks to be utilized in the following simulations.

In studying the dynamics of neural activity a wide spectrum of scales and levels of complexity in modeling the underlying phenomena are possible. Biochemical processes of synaptic receptors, ion concentration pumps and highly detailed structural models of cells are at the one end of the modeling spectrum. These have been well developed since the initial Hodgkin-Huxley equations of ion concentrations changes in neural elements and Rall's dendritic cable theory of current propagation were put forward, and accuracy was improved with the ability to image fine structure of neurons and isolate ionic currents in well-controlled experiments.

Still, other researchers utilized wide range of approximations including simple integrate-and-fire neuron models and static input/output firing rate characteristics of large neural systems (Nunez 1995 [173]) with the level of detail arguably adjusted according to computational requirements to demonstrate the phenomenon under study.

We will present in this chapter two types of neural models that aim to mainly reproduce the firing characteristic of major cell classes, especially the firing dynamics of tufted layer 5 cells. We will also show a schematic wiring diagram among model neurons within different scales. We will finally present a way to compute field potentials and surface EEG based on cellular activity.

5.1 Cellular models

In this section, the computational models of several cellular classes are presented. Since these cell types are believed to be of a general nature and present in many cortical areas, our aim is to study the possible interaction schemes within an "effective skeleton circuit". The simplest individual cells are modeled as *single compartments* with basic ionic conductances necessary to generate the firing dynamics of a particular class of cells. Synaptic inputs to a neuron are described mainly as exponentially

decaying second order impulse responses (with occasional nonlinear dependence on input frequency or voltage, as will be seen later).

Given the special emphasis we placed on the role of layer 5 neurons and their intrinsic dynamics, we attempt a detailed phenomological representation of these cells. Other cellular subtypes were regular spiking (RS) cells of the superficial areas, layers 2 and 3; the input layer cells or spiny stellate excitatory cells of the granular cortex whose regular firing is governed by a high fidelity transmission; the layer 6 RS cells which are also represented as generic population; and the inhibitory interneurons (fast spiking or Low threshold spiking) whose ability to fire at high frequencies is modeled.

5.1.1 General modeling scheme

Our purpose is to develop *phenomological models* of neuronal input-output maps, that is, models which will approximate the firing dynamics of different generic cell types in a faithful manner and which will allow us to assemble a network of such cells, governed by approximate synaptic responses and realistic propagation delays, and subsequently to study using a minimal network topology emergent behavior under the imposed cellular constraints.

We will first address the cellular soma-axonal dynamics and the action-potential generating mechanisms there. We will then discuss synaptic connectivity, and then interconnect such models.

The soma

Two types of approximations of somatic dynamics were utilized. In the first neurons were represented by an integrate-and-fire soma whose time constants, (leakage conductances and membrane capacitances) were matched to anatomical evidence. The second is an adaptation of Hodgkin-Huxley equations that accurately describes action potential generation mechanisms and is derived by Wilson in 1999[260].

In general the somatic firing characteristics were based on the compartmental modeling techniques, namely that the change in the somatic voltage is related to leakage, ionic, and synaptic currents in the soma as follows:

$$C_m \frac{dV_m}{dt} = g_l(E_l - V_m) + \sum I_{syn} + \sum I_{ion} \tag{5.1}$$

where C_m is the membrane capacitance, g_l is the leakage conductance of the soma, E_l is the leakage equilibrium potential, and I_{syn} is the synaptic current flowing into the somatic compartment from the dendrites (figure 5-1).

The ionic current component is usually composed of a combination of ionic flow through several membrane channels; examples of these ionic currents are voltage dependent Na^+, K^+, Ca^{2+} currents, Ca^{2+}-dependent K^+ currents. The ionic current dynamics could be fast, slow, concentration dependent, or voltage dependent. The interaction among these subtypes create general firing characteristics of neurons, such as depolarization, action potential firing, afterhypolarization, and bursting. The detailed representation of a particular ionic current requires knowledge about the existence,

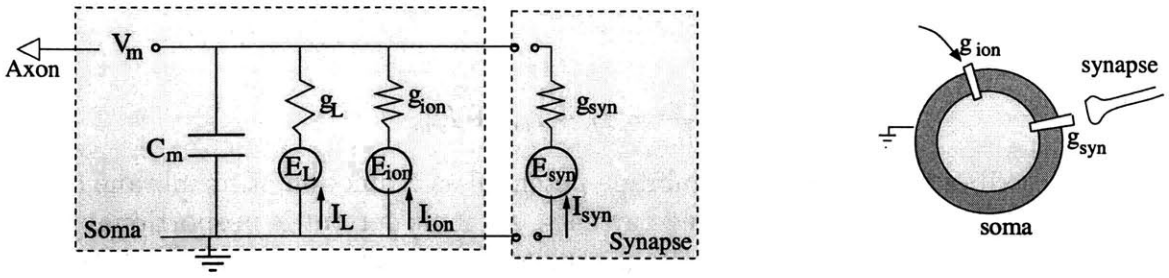

Figure 5-1: Compartmental model of a cell soma. *Left*, equivalent circuit. V_m C_m, and g_L are the membrane voltage, capacitance and leakage conductance, respectively. Ionic currents have equilibrium voltage E_{ion} and conductance g_{ion} (which can be voltage and time dependent). Synaptic currents are modeled similarly with g_{syn}, E_{syn}. *Right*, schematic of a soma with synaptic and ionic channels. Note that the extracellular voltage is taken as reference.

density and dynamics of the corresponding ion channels, and hence, experimental manipulations such as blocking and isolation of subtypes of channels.

Subsequently, mathematical models can then be used such as Hodgkin-Huxley models, calcium concentration pumps, and the like, to fit and describe the ionic current dynamics (Koch et al 1989 [122], Bower et al 1998 [21]). However, despite the abundance of detailed models of many known cellular types (regular spiking of layers 2, 4, bursting, etc), the dynamical characteristics of layer 5 neurons that we are interested in, namely the temporal binding mechanism between apical and basal systems and the switch between bursting and firing modes, are generated by yet unknown ionic mechanisms at the time this research is conducted. Therefore, we will attempt to minimize ionic current representations, and, instead, resort to a phenomological model of the cell.

We think of a *phenomological model* as an *input-output description* of a neuron soma which matches closely the experimental behavior of the recorded cell under prespecified operating regimes. The input to the cell is thus an injected somatic current and its output is the membrane voltage, including action potential generation.

Two levels of approximation were utilized: a simple integrate-and-fire model with a refractory period for firing (given in Appendix C), and a lower order Hodgkin-Huxley type model (developed by Wilson [260, 261]), described next.

Wilson Models: These are lower -dimensional approximations of the Hodgkin-Huxley equations which will preserve changes in the membrane potential as it depolarizes (or hyperpolarizes) under injected currents, thus preserving the essential dynamics underlying action potential generation including action potential duration, firing rate, and adaptation under sustained moderate input current injection. Such models have the advantage of maintaining biophysical significance in that Ohm's law and the dependence on Na^+ and K^+ equilibrium potentials is made explicit. In general, a Hodgkin-Huxley formulation describes the membrane potential by the following equations which includes basic ionic currents that replicate neocortical cell

firings.

$$C\frac{dV_m}{dt} = I_L + I_{ion} + I_{syn} \tag{5.2}$$

which describes the change in membrane potential as a function of membrane capacitance C, leakage, ionic and injected currents. An ionic current is proportional to the change in ionic conductance and voltage gradient between ionic reversal potential and membrane potential

$$I_{ion} = g_{ion}(t, V_m)(E_{ion} - V_m) \tag{5.3}$$

The ionic conductance $g_{ion}(t, v)$ activates (corresponding to ion channels opening) and inactivates (channels closing) at different rates that are measured experimentally and fitted to Hodgkin-Huxley formulations, namely that

$$\begin{aligned} g_{ion}(t, V_m) &= n^x h^y g_{max} && (5.4)\\ \frac{dn}{dt} &= \frac{n_\infty(V_m) - n}{\tau_n(V_m)} && (5.5)\\ \frac{dh}{dt} &= \frac{h_\infty(V_m) - h}{\tau_h(V_m)} && (5.6) \end{aligned}$$

where n, h are the activation, inactivation variables respectively and x, y are integer exponents designed to fit experimental data. $n_\infty(V_m)$, $h_\infty(V_m)$ are activation, inactivation levels at membrane voltage V and are approached according to time constants $\tau_n(V_m)$ and $\tau_h(V_m)$ respectively.

In a Wilson type model, few ionic currents are utilized to replicate firing properties of regularly spiking (RS), fast spiking (FS) and bursting (BS) neocortical neurons.

$$C\frac{dV_m}{dt} = I_L + I_{Na} + I_K + I_X + I_{AHP} + I_{syn} \tag{5.7}$$

I_{Na} is fast activating depolarizing Na^+ current, I_K is the medium activating K^+ hyperpolarizing current, I_X is low threshold Ca^{2+} depolarizing current activating at relatively hyperpolarized voltage levels, and I_{AHP} is a slow afterhyperpolarizing Ca^{2+}-dependent K^+ current.

$$\begin{aligned} C\frac{dV_m}{dt} &= m_\infty(E_{Na} - V_m) + 26R(E_K - V_m) + g_X X(E_{Ca} - V_m) && (5.8)\\ &\quad + g_H H(E_K - V_m) + I_{syn} \\ \tau_R\frac{dR}{dt} &= -R + R_\infty(V_m) \\ \tau_X\frac{dX}{dt} &= -X + X_\infty(V_m) \\ \tau_H\frac{dH}{dt} &= -H + 3X \end{aligned}$$

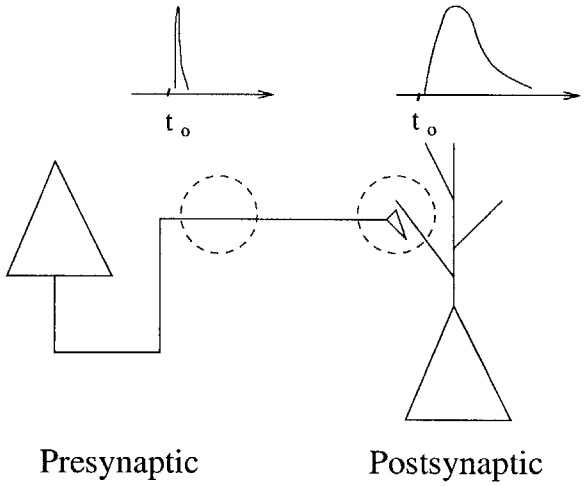

Figure 5-2: Schematic of postsynaptic potential generation in a neuron dendrite. The change in membrane conductance is often approximated by a decaying exponential.

which utilizes fourth order equations compared to eighth order in a classical Hodgkin-Huxley model.

Here the first equation describes the change in membrane potential as a function of membrane capacitance , ionic currents and synaptic input current. $m_\infty \in [0, 1]$ is the Na^+ activation function; E_{Na}, E_K, and E_{Ca} are reversal potentials for Na^+, K^+, and Ca^{2+} respectively. The second equation describes dynamics of the recovery variable R which corresponds to K^+ channel activation as a function of the time constant τ_R and equilibrium state R_∞. The third equation describes calcium current, while the last equation corresponds to I_{AHP}.

Although the modified integrate-and-fire models assume simpler form and reproduces much of the essential dynamics as in Wilson-type models, the switching behavior renders the solution numerically sensitive to integration techniques, especially when many cells are interconnected. Therefore, while such method were used in some simulations which will be appropriately marked, Wilson models were the method of choice due to continuous behavior.

Synapses

Following compartmental modeling techniques, a synaptic input causes an influx (or efflux) of ionic current though the cellular membrane (Appendix B). The amount of ionic current flow can be modeled by a simple relationship between the membrane voltage, the reversal potential of the synaptic channel, and the conductance of that channel:

$$I_{syn} = g_{syn}(E_{syn} - V_m) \tag{5.9}$$

In general, a synaptic input arrival is either due extracortical inputs or due to a firing of a presynaptic cell. In the latter case, a synapse is activated when the presynaptic action potential reaches a specific level of depolarization V_{pre} (effectively

releasing neurotransmitter into the synaptic gap and causing postsynaptic potential in the receiving cell membrane).

The synaptic conductance g_{syn} of direct transmission synapses can be modeled as a second-order filter which is activated upon arrival of an input pulse at that synapse:

$$g_{syn}(t) = A_1 e^{-\frac{t}{\tau_1}} + A_2 e^{-\frac{t}{\tau_2}}. \tag{5.10}$$

The above equation applies to fast activating synapses (AMPA, $GABA_A$). Slower activating synapses (such as NMDA and $GABA_B$) have additional mechanisms for activation. An NMDA receptor is normally blocked by Mg^{2+} ions at resting membrane potentials and will be effectively activated only upon removal of this block at more depolarized levels.

For NMDA, AMPA and $GABA_A$ synaptic currents, models and values given in (Durstewitz et al 2000 [68]) were used.

$$\begin{aligned}
g_{\text{AMPA}} &= g_{\text{AMPA},max} \cdot K_a \cdot [e^{-t/\tau_2} - e^{-t/\tau_1}], && \tau_1 = 0.55ms, \tau_2 = 2.2ms \\
g_{\text{NMDA}} &= g_{\text{NMDA},max} \cdot S \cdot K_b \cdot [e^{-t/\tau_2} - e^{-t/\tau_1}] && \tau_1 = 10.6ms, \tau_2 = 285ms \\
S &= 1.50265/(1 + 0.33e^{-60V_m}) \\
g_{\text{GABA}_A} &= g_{\text{GABA}_A,max} \cdot (t/\tau_1) e^{-t/\tau_1 + 1} && \tau_1 = 11.5ms
\end{aligned} \tag{5.11}$$

where $g_{i,max}$ is the maximal conductance of the i channel, and K_a, K_b are chosen to give $g_i = g_{i,max}$ at peak. S is the voltage dependent Mg^{2+} block of the NMDA channel.

Unlike other synapses which reach maximum activation for each input spike, GABA-B synapses are maximally activated with an input train of high frequency (burst-like), modeled as in Destexhe et al 1998 [58], by a two state model.

$$\begin{aligned}
\frac{dr}{dt} &= K_1(1 - r)[u] - K_2 r \\
\frac{ds}{dt} &= K_3 r - K4s \\
g_{\text{GABA}_B} &= g_{\text{GABA}_B,max} \frac{s^4}{s^4 + K_d}
\end{aligned} \tag{5.12}$$

where $K_d = 100\mu M^4$,$K_1 = 9 \times 10^4 M^{-1}s^{-1}$, $K_2 = 1.2s^{-1}$,$K_3 = 180s^{-1}$, and $K_4 = 34s^{-1}$. A single presynaptic spike corresponds to a pulse of neurotransmitter release $[u]$ of 1mM in 1 msec. Example profiles of postsynaptic conductance changes of these four receptor types are given in figure 5-3

Although other subtypes do exist and further detailed models of synapses account for facilitation and depression of synapses, equation 5.10 will be utilized in our models.

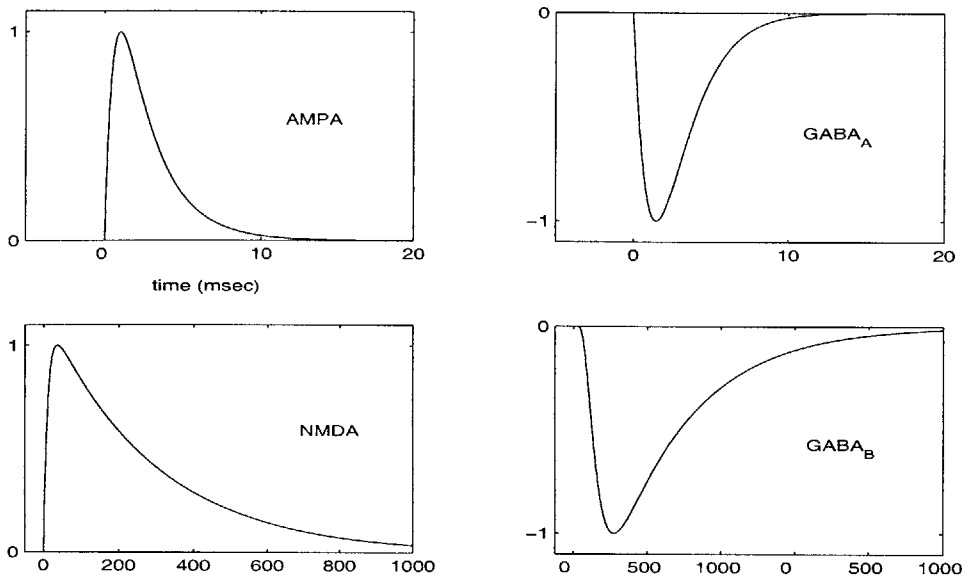

Figure 5-3: Time profile of the conductance change under different receptor channels. Note that the magnitude was normalized to the maximal conductance change and that its sign exemplify the current direction from a resting membrane potential (hence the inhibitory synapses are represented as negative). $GABA_B$ mediated conductance change results from a presynaptic burst (11 spikes at 200 Hz).

Dendritic models

Earlier studies of dendrites focused on the passive behavior of these processes in receiving synaptic input and funneling it in an attenuated form into the soma based on cable theory. This however, is becoming increasingly challenged by new experimental evidence, showing an active role for action potential generation in neocortical layer 5 cells for example, and differentiation of separate dendritic input sites by virtue of ionic currents. Furthermore, distal inputs in hippocampal slices appear to affect somatic firing far more effectively than dictated by dendritic attenuation dictated by cable theory (see chapter 4).

Therefore, and while more accurate modeling of dendrites awaits clearer experimental answers, we will simply consider dendritic process as input terminals which reliably transmit synaptic currents to the soma of a neocortical cell. We will, however, make use of known properties of layer 5 distal dendritic system, as presented next.

5.1.2 Layer 5 cells

Soma dynamics

The main dynamical characteristics of Layer 5 cells are derived from experimental recordings of Larkum et al 1999, Sakmann et all 1999, and Schwindt et al 1999. These are repeated here for convenience.

(1) A Layer 5 cell has two systems of inputs: basal inputs, which presumably cause

the cell to spike in a regular fashion if isolated from the apical system; and apical inputs which, although become greatly attenuated significantly before reaching the soma, can interact with basal currents to generate a bursting behavior. The burst was found to be optimally induced if a basal and a dendritic input arrive within a short time window of 5-10 msec (Larkum et al 1999 [131]). A third system of input (oblique dendrites, system C) control the degree of interaction between the two former systems.

(2) As dendritic input is increased, the cell will switch from a regularly firing mode to bursting mode. A further increase in this input will create a plateau calcium action potential in the dendrite and the cell will switch back to regular spiking after some time (Schwindt et al 1999 [204] Oakley et al 2001b [176]).

(3) Layer 5 cells have a low-threshold type current which is characterized by a rebound depolarization upon release from inhibition, sometimes leading to rebound-like firing of these cells (Castro-Alamancos et al 1996 [29]. Spain et al 1991 [212], delaPena et al 1996 [54]).

The developed model accounts for the above three properties.

(1) we replicated a "window of facilitation" for the generation of bursts (and calcium action potentials in the dendrites). In their paper, Larkum et al 1999 [131] described that dendritic current injection which replicated postsynaptic current (double-exponential) with maximum amplitude of I_o will generate bursting behavior if $I_o > 2.28\bar{+}0.14$ nA. The magnitude of current needed to generate Ca-Ap in the dendrites, and therefore bursts in the soma, is decreased when this input is coupled with a back-propagating action potential (BAC) within a time window of Δt. To replicate this behavior, we computed the net voltage change that dendritic current injection of I_o will cause in a passive dendrite, that is

$$C_d \frac{dV_d}{dt} = (E_{L,d} - V_d)/R_d + I_o A(e^{-t/\tau_1} - e^{-t/\tau_2}) \tag{5.13}$$

where C_d is the dendrite capacitance, R_d is the membrane resistance of the dendrite, and A is a normalizing time constant. In layer 5 cells, we assumed $C_d = 0.02084 F/m^2$ and $R_d = 0.7042 \Omega m^2$ (based on Bush and Sejnowski 1995 [24]), giving a time constant of 20 msec. For $I_o = 2.29$ nA, the peak of voltage change will be $V_d = V_{th,Ca}$ which causes Ca^{2+}-AP generation. Therefore, for synaptic inputs, one can compute corresponding dendritic voltages and compare with the threshold $V_{th,Ca}$ necessary for bursting to occur. When coupled with back-propagating action potentials, however, this threshold is adjusted according to the time difference Δt between time of somatic current occurrence t_s (which causes BAC) and the time dendritic current arrives (t_d) , that is $V_{th,Ca} = f(\Delta t)$ where f is the approximate experimental map given in the paper (figure 5-4). A schematic of the interaction between soma, basal system and apical dendritic system is shown in figure 5-5.

The inhibitory control provided by system C in decoupling basal and apical inputs is approximated, to a first order by a veto-type action which greatly attenuates the magnitude of back propagating action potentials over a period of 300 msec as observed by Larkum et al 1999 [131].

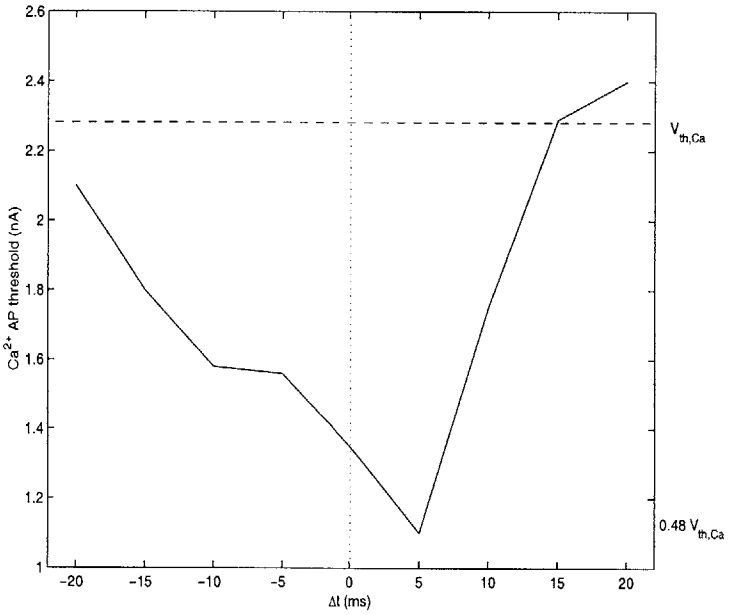

Figure 5-4: Threshold for generation of Ca- action potential in dendrite depends of coupling between somatic and dendritic inputs. Here, the x-axis plots the time difference between input arriving at the soma (zone B)and apical dendrites (zone A), respectively (adapted from Larkum et al 1999).

(2) The dendritic current range of Schwindt et al was approximated to switch between bursting and regular firing at similar times[1]. The modeled neuron response is shown in figure 5-6..

For the modified integrate-and-fire model, the passive electrical characteristic of the cell soma were taken from models by (Bush and Sejnowski 1995). In particular, the cell has a per unit capacitance of $C_M = 0.0284F/m^2$, membrane resistance of $R_M = 0.7042\Omega m^2$, giving a time constant of $\tau_m = 20msec$, and a somatic area of $1.233e^{-9}m^2$, giving a total capacitance of $35.14pF$ and $Rm = 571M\Omega$. The cell regular spiking firing characteristics were matched to a GENESIS simulation of layer 5 large-tufted regular spiking cell by the same authors, which is the same type we are interested in.

For the Wilson-type model, a layer 5 soma has, in addition to Na^+ and K^+ current providing for regular spiking; two ionic currents, I_X and I_H providing for bursting

[1]Although this latter author reported ionotopheresis experimental values, we approximated the corresponding synaptic current after matching firing threshold reported in his earlier experiments (Schwindt and Crill 1998 [203]) to synaptic currents in other references (Larkum)

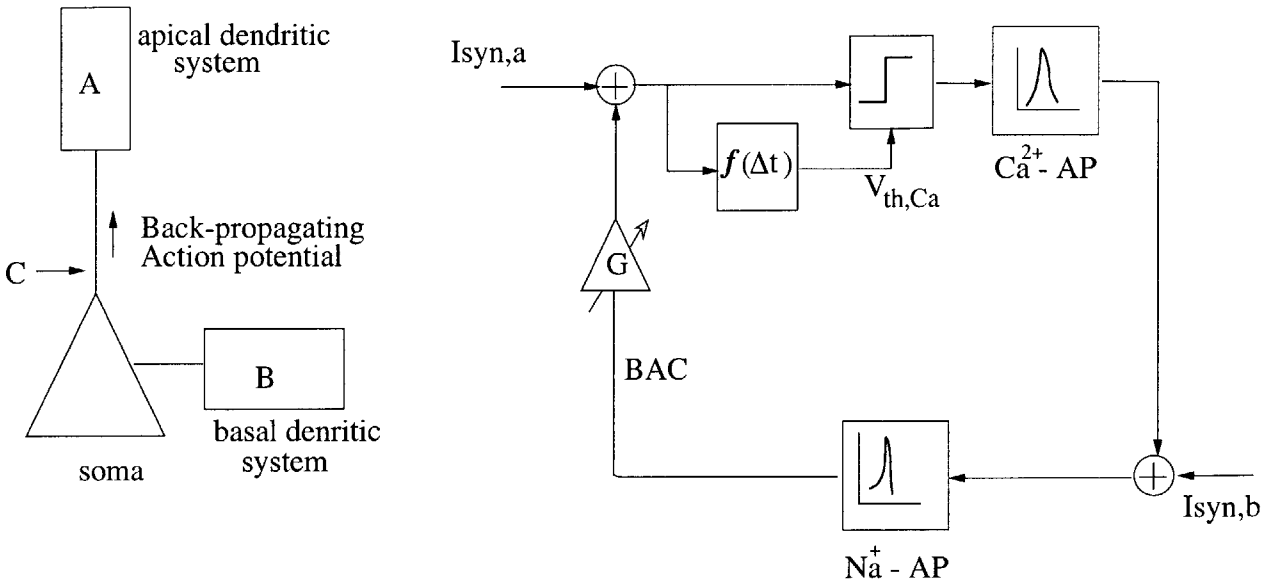

Figure 5-5: Diagram representing basic synaptic inputs to a large layer 5 pyramidal cells and the arising mechanisms of interaction between these inputs. *Left,* the two synaptic regions considered funnel inputs to the soma. *Right,* Back propagating action potentials (BAC) interacts with apical input $I_{syn,a}$ to lower the threshold for generation of Ca^{2+} - action potential in dendrites (based on function $f(\Delta t)$-see text). This Ca^{2+}-AP invades the soma and results in generation in burst-pattern of Na^{+}-AP

behavior; inward current I_h and low threshold activated current I_T providing for rebound depolarization, as given below

$$\begin{aligned}
\frac{dV}{dt} &= m_\infty(E_{Na}-V)+26R(E_K-V)+g_X X(E_{Ca}-V) \qquad (5.14)\\
&\quad +g_H H(E_K-V)+I_h+I_t+I_{syn}\\
\tau_R\frac{dR}{dt} &= -R+1.24+3.7V+3.2V^2\\
\tau_X\frac{dX}{dt} &= -X+8(V+0.725)^2\\
\tau_H\frac{dH}{dt} &= -H+3X\\
m_\infty &= 17.8+47.6V+33.8V^2
\end{aligned}$$

Voltage amplitudes are scaled to units of 1/100 V, and thus, $E_{Na}=0.5$, $E_K=-0.95$ and $E_{Ca}=1.2$. Current activation time constants are $\tau_R=3msec$, $\tau_X=12msec$, and $\tau_H=35msec$.

The inward rectifying current I_h and the low threshold currents are modeled as in (Huguenard and McCormick 1992 [99], McCormick et al 1992 [153]).

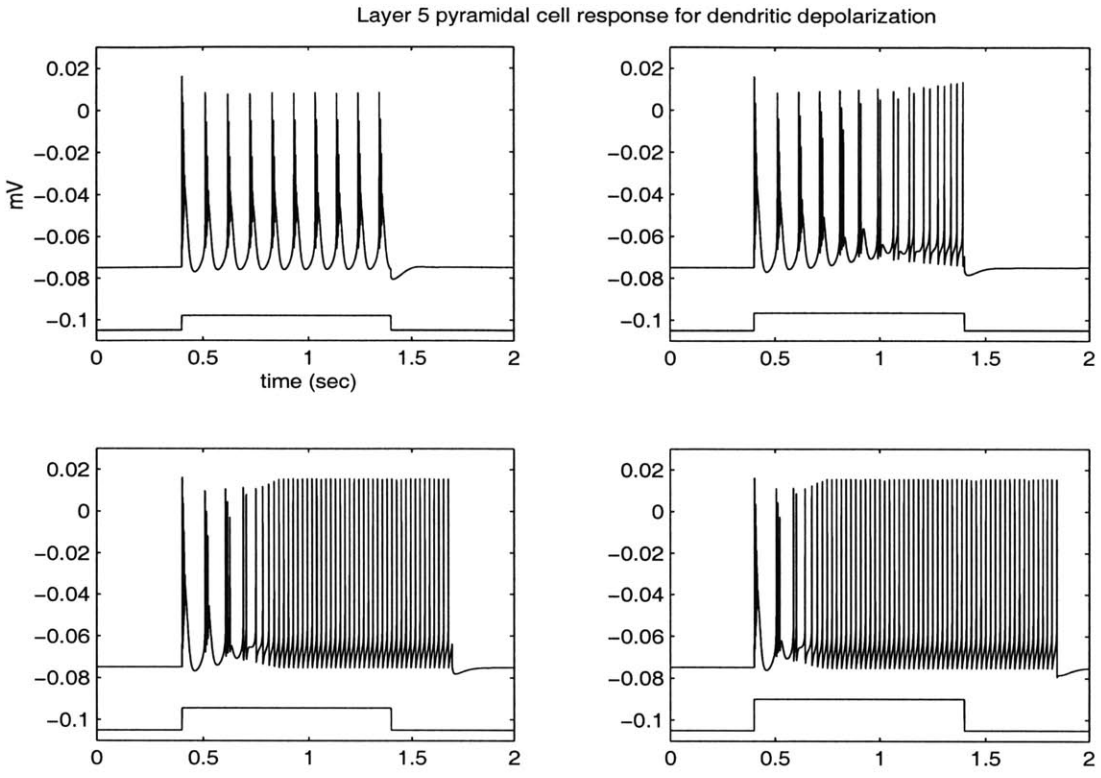

Figure 5-6: modeled Layer 5 cell response for dendritic depolarization

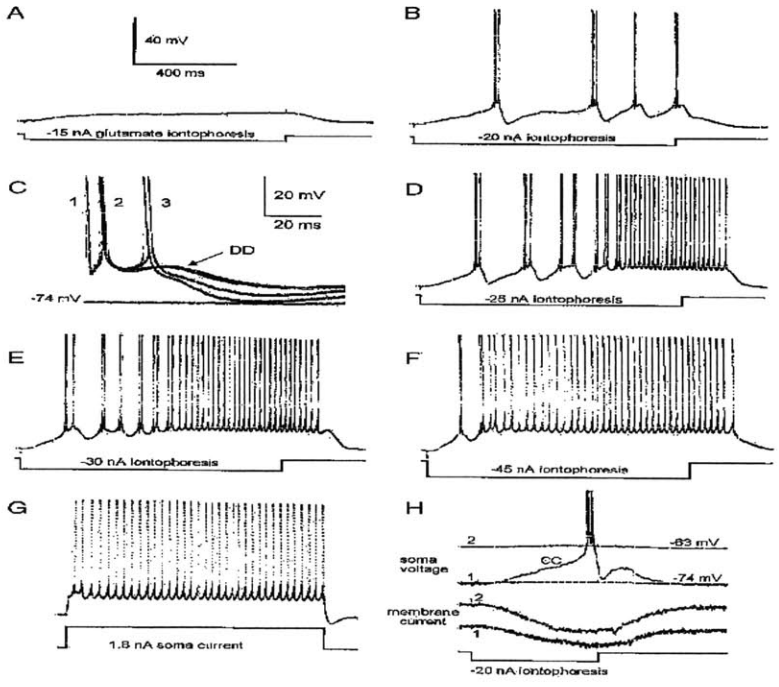

Figure 5-7: Firing characteristics of Layer 5 cell (Schwindt et al 1999 [204])

$$
\begin{aligned}
I_h &= g_h n(E_h - V) \\
\frac{dn}{dt} &= \frac{n_\infty(V) - n}{\tau_n(V)} \\
n_\infty(V) &= \frac{1}{1 + exp(\frac{V+0.75}{0.055})} \\
\tau_n(V) &= \frac{1}{exp(-14.59 - 0.086 * 10^{-2}V) + exp(-1.87 + 0.0701 * 10^{-2}V)}
\end{aligned}
\tag{5.15}
$$

with $E_h = -0.43$ (in 1/100 volts).

$$
\begin{aligned}
I_T &= g_T n^2 h(E_T - V) \\
\frac{dn}{dt} &= \frac{n_\infty(V) - n}{\tau_n(V)} \\
\frac{dh}{dt} &= \frac{h_\infty(V) - h}{\tau_h(V)} \\
n_\infty(V) &= \frac{1}{1 + exp(-\frac{V+0.57}{0.062})} \\
\tau_n(V) &= 0.612e^{-3} + \frac{1}{exp(-\frac{V+1.32}{0.167}) + exp(\frac{V+0.168}{0.182})} \\
h_\infty(V) &= \frac{1}{1 + exp(\frac{V+0.81}{0.04})} \\
\tau_h(V) &= \begin{cases} 0.028 + 0.001 * exp(-\frac{V+0.22}{0.105}) & V > -0.8 \\ 0.001 * exp(\frac{V+4.67}{0.66}) & V < -0.8 \end{cases}
\end{aligned}
\tag{5.16}
$$

with $E_T = 1.2$ (Calcium equilibrium potential).

In the above equations, the calcium current I_X and the afterhypolarization current I_H play a dual role in the cell behavior.

1. In the regularly firing mode, the contribution of I_X is negligible ($g_X = 0.1$) and I_H allows for adapting behavior of the cell ($g_H = 3$) replicating regularly spiking cell behavior as reported in Wilson 1999 [260].

2. In the bursting mode, the I_X contribution increases ($g_X = 2.7$) causing fast spiking behavior of the cell (burst-like) which is terminated by I_H, also of larger amplitude ($g_H = 9.25$). In this case, the interaction between these two currents provide for a low frequency repetitive bursting (up to 10Hz) of the cell. One can thus think of the I_X contribution in this case as a "fictitious" Ca^{2+} action potential generated in the dendrites and propagated to the soma to cause repetitive burst firing (I_X effect is terminated by I_H, since I_X in this model does not inactivate).

3. Upon application of sustained high amplitude current to the dendrites, the cell

Table 5.1: Neocortical cell model parameters

Cell type	g_X	g_H	g_T	g_h	τ_R	τ_T	τ_H
Layer 5 pyramidal							
(Burst mode)	2.7	9.25	5	1.5	3	12	35
(RS mode)	0.1	3	5	1.5	4.2	12	35
Layer2,3 pyramidal[†]	0.1	8	–	–	4.2	14	45
FS interneurons	–	–	–	–	2.1	–	–

switches from bursting to regularly spiking (plateau Ca^{2+} currents). This effect is replicated qualitatively by decreasing g_X, g_H back to regularly spiking values such that the overall behavior resembles that obtained experimentally (figures 5-6 and 5-7)

4. When the cell membrane is hyperpolarized, I_T exhibits a rebound activation upon release from inhibition, causing a rebound depolarization in the cell voltage[2]. It is further amplified by I_h which is activated at hyperpolarized levels, contributing to further rebound in cell membrane voltage. Note that the latter current does not contribute to cell activity above resting potentials (non-hyperpolarized conditions). An example of this rebound is given in figure 6-5 in section 6.1.3.

Synaptic inputs

We assume that the two synaptic input systems occur at (1) distance apical dendritic region (about $700-900\mu m$ from the soma) which is the main focus of dendritic action potential generation in the aforementioned studies, and (2) a basal region which extends almost horizontally above and below the cell soma. The apical obliques of system C were only modeled as having an inhibitory $GABA_A$ type synapse since we will only account for the veto-type action caused by inhibition.

NMDA, AMPA and $GABA_A$ conductances were added (as given in equation 5.11) to both apical and basal integration regions. Based on anatomical evidence, NMDA

[2]In some cases, only I_X was utilized as the low-threshold calcium current and no additional I_T was added, as used by Wilson. In this case, rebound depolarization only occurs during a fast release from inhibition which causes a fast switching of the equilibrium point of nonlinear dynamic system (see Wilson et al 1999b [261]).

receptors were more focused in the basal regions (Durstewitz et al 2000 [68]). Also, $GABA_B$ receptors were only added to the basal region (Shao et al 1999 [205], Eder et al 2001 [69], Princivalle et al 2000 [184]). Unit synaptic values conductances were $g_{AMPA} = 15.1nS$, $g_{NMDA} = 0.0912nS$, and $g_{GABA} = 8.4nS$.

Dendritic-somatic interaction

The dendritic input regions were not modeled as separate compartments. However, and since we are trying to approximate the apical region of interest, we need to approximately account for the dendritic attenuation of inputs from the distal apical regions as they enter the soma, as well as account for the effect of depolarizations caused by backpropagating action potentials from the soma into the dendrites and which might lead to generating calcium action potentials (in case of bursts), and also modify the effect of synaptic current in these dendritic regions.

To carry this approximation, we adopted experimental recordings by Sakmann et al for the level of attenuation of backpropagating potentials, and results from a study by Koch et al on attenuation of dendritic currents in the soma.

(1) The recordings of Schiller et al 1997, Larkum et al 1999a,b demonstrate the Calcium action potentials (Ca APs), when formed in the dendrites due to the back propagation of somatic AP or due to large local dendritic current, are of a slower time course (time constant $\approx 20msec$) than the somatic Na action potential, and slightly exceeds 0 mV when fired from rest ($-65mV$). Furthermore, in the event that no Ca AP are generated, the back-propagating somatic Na APs are greatly attenuated when reaching the dendritic region (about $20mV$ depolarization). Therefore, for our modeling purposes, and since Ca^{2+} action potentials are associated with bursting behavior in the soma, we accommodated for dendritic voltage changes according to whether a cell bursts or not by creating slow, large depolarizations when Ca^{2+} AP occurs, or smaller, faster depolarizations when no Ca^{2+} APs are initiated (which is the non-bursting, or passive back-propagating mode).

(2) The effect of post-synaptic potentials arriving at the apical system A are attenuated as the propagate towards the soma. Since we are not using a multicompartmental model to accurately represent dendritic filtering, this degree of attenuation is approximated from a study by Koch et al 1990 [123]. In this work, the somatic current Is due to a synaptic input in channel i at a point d_i in the dendrite is given by:

$$I_s = \frac{K_{d_i s}}{K_{ss}} \cdot \frac{g_{d_i}(E)}{1 + g_{d_i} K_{d_i d_i}} \tag{5.17}$$

where the terms are the following: g_{d_i} is the synaptic conductance for the channel i, $K_{d_i d_i}$ is the input impedance at point d_i, K_{ss} is the somatic input impedance, E is the reversal potential of the synaptic channel i at point d_i relative to zero resting potential, and $K_{d_i s}$ is the transfer impedance between d_i

and the soma, given by $K_{d_i s} = K_{d_i d_i} e^{-\lambda/x}$ for an infinite cable, and λ being the electrotonic attenuation factor. Recalling that synaptic current at d_i is given by$I_{d_i} = g_{d_i}(E - V_{d_i})$, the steady state attenuation for synapse i at d_i is given by

$$A_{ss,i} = \frac{I_s}{I_{d_i}} \tag{5.18}$$

Using values of measured Layer 5 neuron somatic impedance in (Koch et al 1990 [123]), $K_{ss} = 164M\Omega$. Data from Durstwitz et al 2000 on the layer 5 axial and membrane resistances is used to compute the input impedance at apical $d_i \approx 900\mu m$ of $K_{d_i d_i} = 223.18M\Omega$, and at basal location $d_b \approx 150\mu m$ of $K_{b_i b_i} = 146M\Omega$. For synaptic conductances in section 5.1.2, the attenuation factors for system A input located at 900 μm arriving at the soma become:

$$A_{ss,AMPA} = 0.14, \quad A_{ss,NMDA} = 0.61, \quad A_{ss,GABA} = 0.21 \tag{5.19}$$

5.1.3 Layers 2, 3, and 6 Cells

Superficial layer cells of the regular firing variety were assumed. To model regularly spiking cells, Wilson model was utilized with the following dynamics:

$$\begin{aligned}
\frac{dV}{dt} &= m_\infty(E_{Na} - V) + 26R(E_K - V) \\
&\quad + g_X X(E_{Ca} - V) + g_H H(E_K - V) + + I_{syn} \\
\tau_R \frac{dR}{dt} &= -R + 1.24 + 3.7V + 3.2V^2 \\
\tau_X \frac{dX}{dt} &= -X + 8(V + 0.725)^2 \\
\tau_H \frac{dH}{dt} &= -H + 3X \\
m_\infty &= 17.8 + 47.6V + 33.8V^2
\end{aligned} \tag{5.20}$$

The main distinction from burst firing patterns is in the dynamics and effect of Calcium current I_X, since its contribution is minimal ($g_X = 0.1$). Also, medium levels of afterhyperpolarizing current I_H ($g_H = 5$) produce adaptation in the firing pattern as observed in neocortical RS cells (Wilson 1999 [260]. This current essentially produces a long-lasting outward current which reduces effectiveness of sustained depolarization, and hence firing rate. Table 5.1 summarizes the relevant parameters [3].

[3]In integrate-and-fire schemes, cellular models of layer 2 pyramidal cells utilized in (Bush and Sejnowski 1995) were approximated, again using simple integrate and fire models. The firing rate characteristic for various injected currents were matched to the aforementioned data in a GENESIS simulation. Passive cell characteristics were $R_m = 0.678\Omega m^2$, $C_m = 0.0295F/m^2$, giving $\tau_m = 20ms$.

Unlike layer 5 cells, and since no special dynamic character for these cells is modeled, we assumed no difference in stimulation of basal or apical dendrites of these cells, and hence only a somatic compartment was considered with the sole function of the dendritic processes acting as input integrators.

A single RS cell receives synapses mediated by AMPA, NMDA and $GABA_A$ and $GABA_B$ receptors presented in section 5.1.2.

5.1.4 Layer 4 Spiny stellates

The firing characteristic of spiny stellate (SS) neurons of the input layer are assumed similar to those of layers 2 and 3 ($\tau_m \approx 20ms$). AMPA and GABA synaptic conductances were of the generic type used above. However, according to recent information on spiny stellate (SS) cells in the cat barrel cortex (Fleidervish et al 1998 [73]), some NMDA receptor types were found to be non-voltage dependent, and could be evoked by intra-layer 4 recurrent excitation. Hence, the NMDA model of equation 5.11 is adjusted here to have $S = 1$.

5.1.5 Inhibitory Interneurons

Fast spiking interneurons :

FS cells were modeled using only fast Na^+ action potentials it without adaptation. Hence, only the first two equations of Wilson model are utilized[4]. The fast spiking behavior is due to shorter action potentials, and accordingly the recovery variable time constant τ_R is set to 2.1 msec (Wilson 1999 [260]).

Although (Durstewitz et al 2000 [68]) reported the existence of NMDA receptors on layer 5 interneuron (IN) connections, a study by (Cecilia Angulo et al 1999 [6]) argued that excitation of IN is mediated mainly by AMPA receptor type of fast kinetics, although NMDA receptors might activate at $Vm > -50mV$. Therefore interneurons received inputs mediated only by fast kinetics receptor types (AMPA, $GABA_A$).

Layer 5 interneurons:

Although, the inhibitory population in layer 5 is known to be of at least two types, a fast spiking type (FS) and a low threshold spiking type (LTS) (Deuchars and Thomson 1995 [64]). We only made the distinction between the two types in terms of their target connections, mainly that FS are confined to layer 5 and LTS target pyramidals in layer 3.

[4]In an integrate-or fire scheme, the membrane time constant of an interneuron was $\tau_m \approx 10ms$, and the firing characteristics were approximated to experimental data from (Fuming Zhou et al). For example, Layer 2-3 Fast spiking interneurons fire at $100Hz$ for $0.8 - 1nA$ current injection, etc.

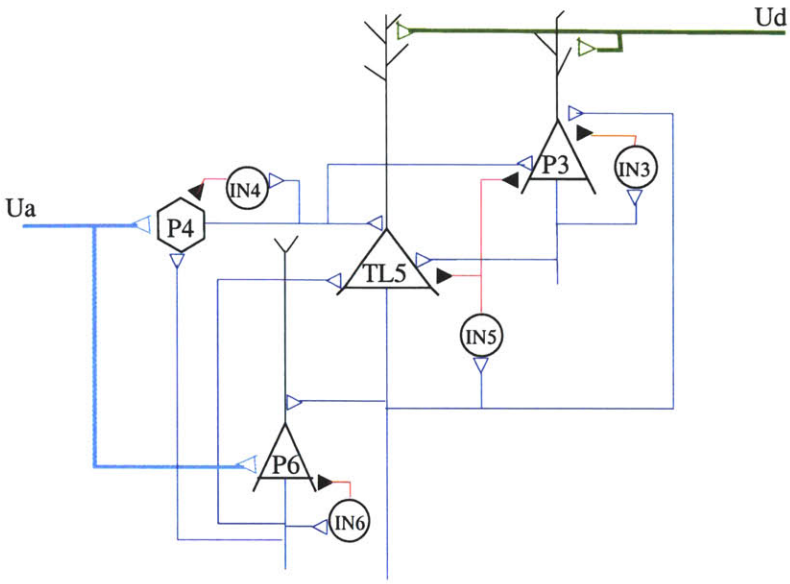

Figure 5-8: Vertical connections within a cortical minicolumn/column

5.2 Connection Diagrams

5.2.1 Synaptic connections within a minicolumn

The vertical connections within an effective skeleton circuit are derived from neurophysiological evidence presented in the hypothesis chapter. For the purpose of these simulations, we are assuming that single neurons of each layer are representatives of the specific class of neural population within that layer. Layers 3, 4 and 6 had pyramidal neurons (RS cells) that are reciprocally connected with inhibitory interneurons in the same layer (FS cells). E-I connections included AMPA synapses where as I-E connections had both $GABA_A$ and $GABA_B$ synapses. A diagram of connections considered between layers in a minicolumn is given in figure 5-8. The strength of synaptic connections is assigned to comply with known connection strategies. That is, strongest connections exist between a pyramidal cell and associated interneurons within the same layer. The excitatory pathways P3-P5 and P6-P4 have the strongest terminations followed by the P6-P5 and P5-P3 feedback (Shepherd 1998, Thomson and Deuchars 1998 [206, 237]). Connections P4-P5 forms the least focused excitatory pattern (reports of its existence in Shubert et al 2001 [200]). Connection delays were on the order of 1-1.5 msec.

L5-L3 inhibition: This cross-laminar inhibitory pathway can have two forms: interneurons in layer 3 receive excitatory connections from ascending layer 5 axons (Dantzker et al 2000 [51]); alternatively, interneurons of layer 5 may send collaterals into layer 3 (Xiang et al 1998 [267]). For our simulations, we will assume the former (IN5 to P3 connections).

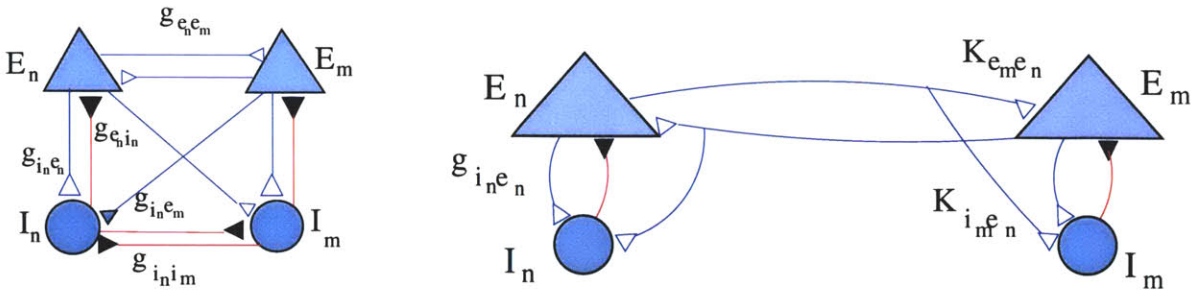

Figure 5-9: Generic connectivity patterns. *Left*: Within a cortical column, reciprocal connections in a layer involve E-E, I-E, E-I, and I-I synapses. *Right:* Over long distances, such as at the columnar assembly scale, I-I connections do not exist since these axons are local to a region.

5.2.2 Synaptic connections within a column

Several minicolumns are interconnected to form a column. Since our canonical circuit does not provide any functional distinction between the two scales, a minicolumn serves as a representative of a cortical column. In some instances, a cortical column is modeled explicitly as a collection of minicolumns, mainly for the purpose of amplifying local dynamics such as for simulating slow-wave oscillations and inhibition induced seizures. In this case, vertical connections patterns between minicolumns follow similar pathways as those within a minicolumn. Also, recurrent all-to-all connections within a single layer are utilized:

1. Within a single layer, reciprocal E-I, I-E, E-I, and E-E connections exist (see figure 5-9, Left). This can be seen in layers 3,4, 5 and 6 and is essentially a conservative diagram of how interconnections within a single layer in column (spatial spread 200-300 μm) are organized (figure 5-10).

2. The cross laminar connections between two minicolumns are less focused than those within a minicolumn (that is, $g_{in_{e_m}}$ is smaller than $g_{in_{e_n}}$). This decay could be described by a geometric weighting function. For the purpose of our minimal model, the relative weight is around 50 %. The connection delays across columns was on the order of 2-3 msec.

5.2.3 Synaptic connections within a columnar assembly

This scale is distinguished by the absence of cross columnar inhibition since connections occur at distances beyond a single column scale ($> 300\ \mu m$). Connectivity within a single layer originate from pyramidal cells (P3, 5, and 6) and target a pyramidal cell as well as its local interneuron (figure 5-9). Connectivity across lamina is maximal in the deep pyramidal layers (P6-TL5 and TL5-P6) with minimal P3-TL5, TL5-P3 connections (figure 5-11).

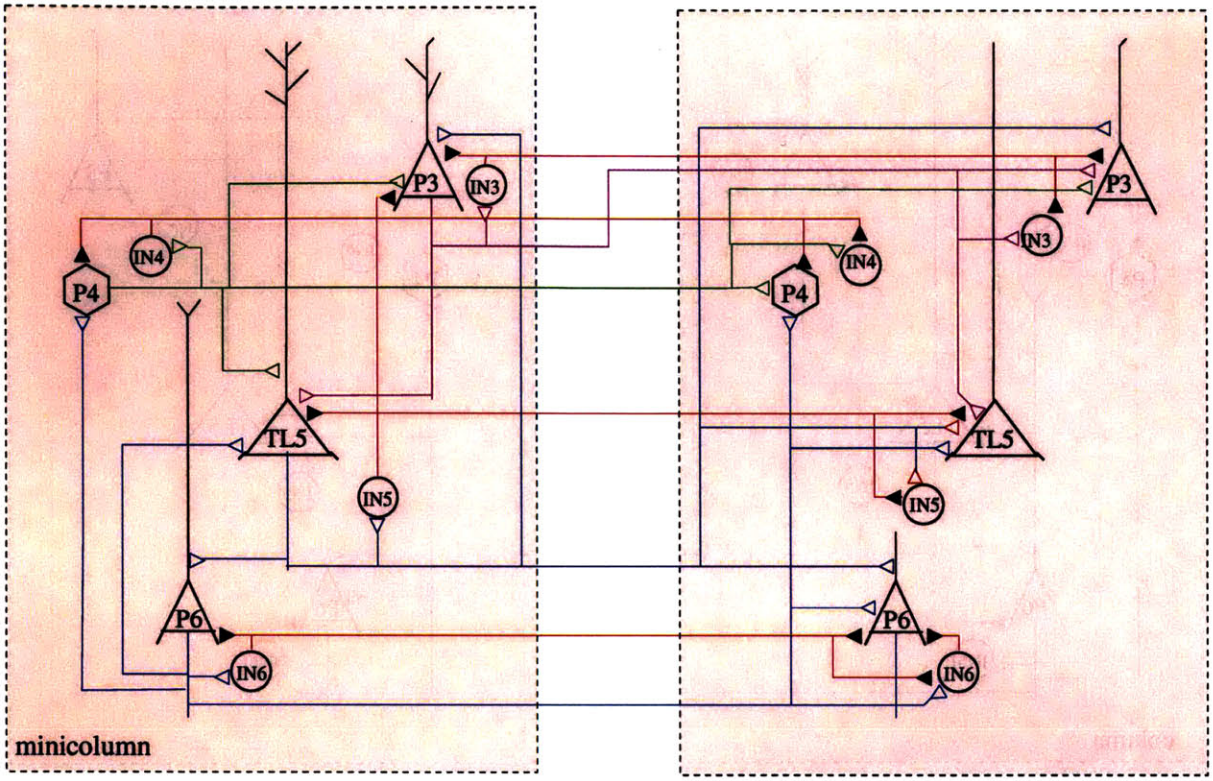

Figure 5-10: Connections within a cortical column (100-300 μm). Horizontal connections are reciprocal (although one direction is shown) and are strongest with the same layer, especially layer 4.

5.2.4 Synaptic connections between areas

We will follow the connection topology of a hierarchical information stream, that is, two areas are connected in the ascending/descending pathway topology discussed earlier. Still, in some instances no hierarchical precedence was assumed (e.g, seizure and slow wave sleep simulations).

In either situation, connecting axons between two spatially-separated areas have considerable delays (5-10 msec). Only axons of pyramidal neurons formed these types of long-distance connections. Main connectivity principles followed were:

1. In general, a pyramidal cell axon travels through the white matter to the target area and synapses on both pyramidal and interneuronal populations in the arborization zone (figure 5-9, Right). This follows the general hypothesis that interneuronal subpopulations in an area have access to the excitatory input arriving to the pyramidal subpopulations, which has been argued to contribute to synchronization between areas over large distances, especially at high frequencies (see section 3.2.6).

2. Two columns belonging to the same hierarchy were connected through both superficial and deep layers (P3, P5 and P6). Columns belonging to different hierarchies followed a general principle: ascending connections originated from

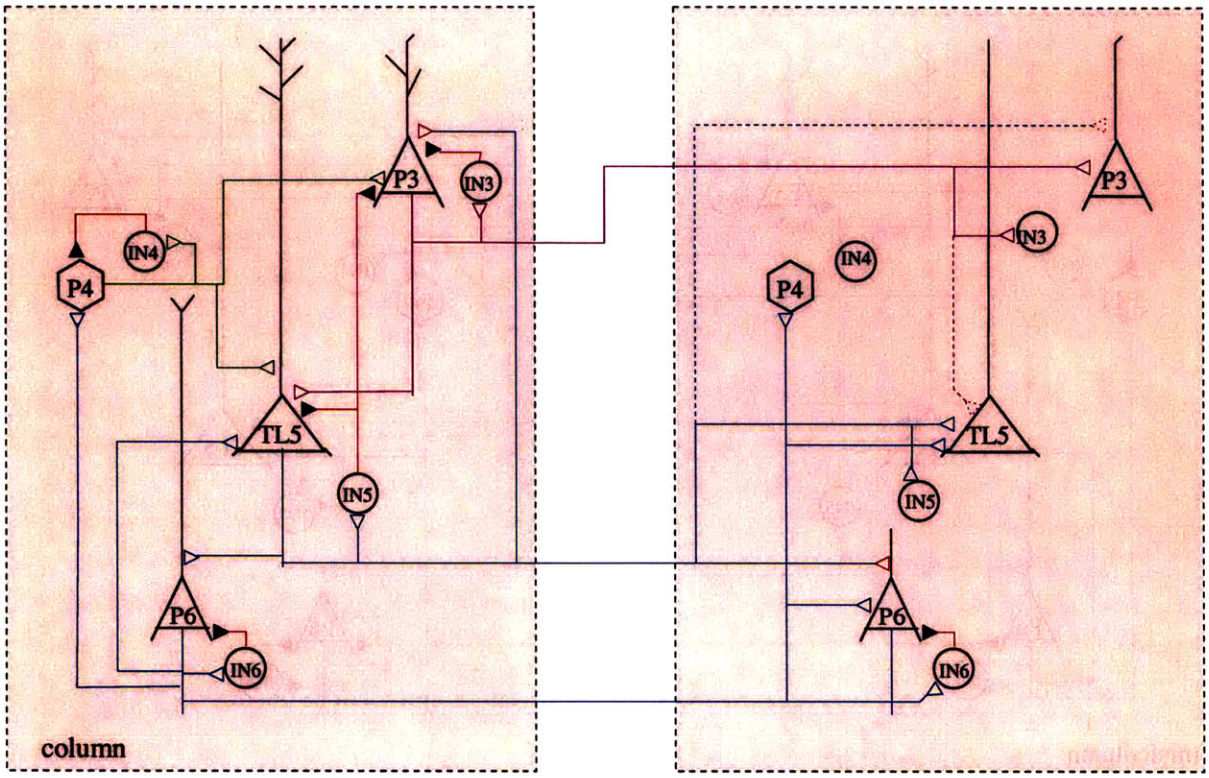

Figure 5-11: Connections within a cortical columnar assembly (0.3-2mm). Horizontal connections are reciprocal (although one direction is shown) and are strongest with the same layer. Note that deep pyramidal layers form cross laminar connections at this scale. Also, layer 4 cells do not interconnect beyond a single column.

superficial layer 3 and the terminations were focused in the middle layers similar to thalamic input patterns; descending connections originated from deep layers (both layers 5 and 6) and arborized in superficial regions of the target area (see figure 5-12).

5.2.5 Excitation sources

The minimal model presented is in reality part of a much larger circuit. Accordingly, it can be argued that the small populations of cells at hand receive afferent input excitation from unmodeled external connections, either intracortical or thalamic in origin. In all simulations, each cell in the model (pyramidal, spiny stellate, or interneuron) was independently stimulated either by (1) injecting a random uniformly-distributed current into the soma (creating random fluctuating membrane potential) or (2) subjecting input synapses to a afferent spike train with a Poisson arrival rate of 150 Hz. In either situation, the cell had a baseline excitation which will allow 1-2 action potentials per second. The strength of baseline excitation (injection current

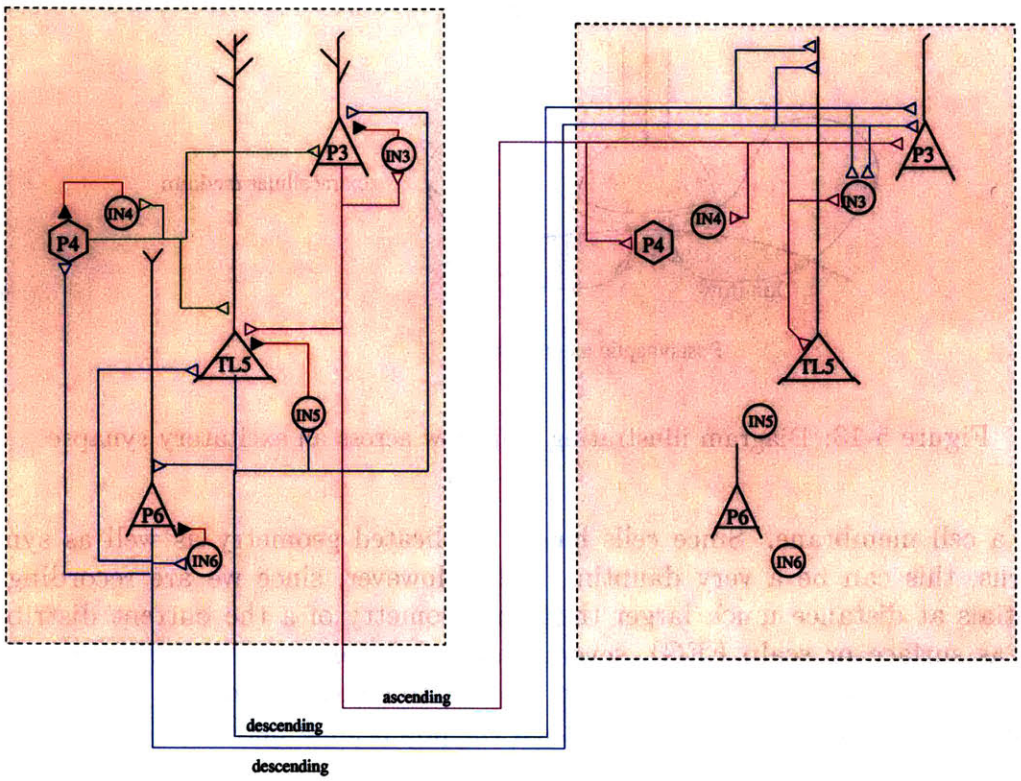

Figure 5-12: Connections across hierarchies. Note that ascending connections are assumed to start from layer 3 (superficial layers) only, while feedback includes tufted layer 5 cells as well as layer 6 RS cells (which, in this case can also be though of as RS cells of layer 5). Note that all connections are drawn from the left to the right circuit for illustration.

or synaptic strength) was identical to all cells[5].

5.3 Field potentials

The computation of field potentials is based on the voltage generated in the extracellular space due to currents flowing into and out of cell membranes. As shown in figure 5-13, occurrence of an excitatory postsynaptic potential (EPSP) at an excitatory synapse causes an influx of positive ions through the cell membrane and hence acts as a current sink. Conversely, an inhibitory postsynaptic potential (IPSP) is a local source of current. Current laws then necessitate that each of these currents to leak back in (or out) at more distal locations.

Consequently, an accurate modeling of the generated field potential in the extracellular medium requires knowledge of synaptic input patterns and their distribution

[5]In cases where neuronal silence dominates such as during slow-wave sleep, synaptic input was insufficient to create firing in RS cells of layers 3 and 6; only layer 5 was able to initiate firing by virtue of internal mechanisms. In this case, baseline excitation is assumed to simulate spontaneously-occurring synaptic potentials

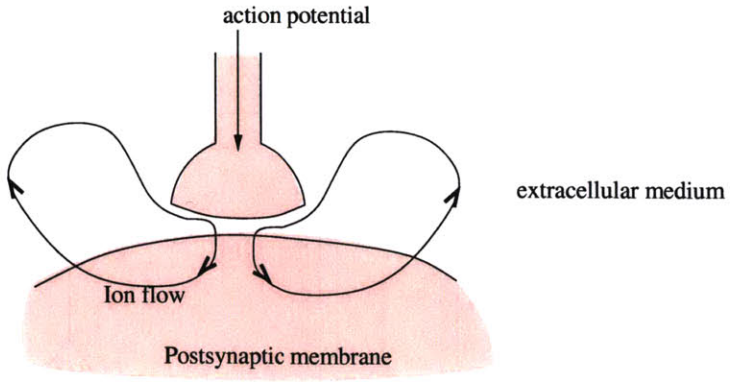

Figure 5-13: Diagram illustrating ionic flow across an excitatory synapse

along a cell membrane. Since cells have complicated geometry as well as synaptic patterns, this can be a very daunting task. However, since we are recording field potentials at distance much larger than the geometry of a the current distribution (such as surface or scalp EEG), several approximations can be performed (Nunez 1981 [171]). In particular, a common method is to consider synaptic inputs as point sources in a homogeneous conductor, then the potential Φ becomes:

$$\Phi(\vec{r},t) = \frac{1}{4\pi\sigma}\sum_{i=1}^{n}\frac{I_i(t)}{R_i} \tag{5.21}$$

where n point sources are assumed. Point source i is located at R_i meters from the field point $\vec{r}$ and $I_i(t)$ is the total current flowing from i into the medium of conductivity σ.

The contribution of a particular neuron to the field potential is in general dependent on the geometry of a cell. In particular, since pyramidal cells are oriented orthogonal to the cortical surface, scalp and surface EEG have a maximal contribution from these cells. Interneurons have radially distributed branches whose contributions are minimal (see Nunez 1981 [171], chapters 3-4).

For our purposes, we will utilize the approximation of a large current sink in the cell body (due to a large number of EPSPs) which causes current sources distributed along the dendrites above and below the cell (as well as the axons). This is represented schematically in figure 5-14.

For the simple case of computing potentials on a vertical axis above the cell, then the field potential is given by (Nunez 1981)

$$\Phi(y) = \frac{I}{4\pi\sigma}\cdot\frac{d}{y^2}\left[\left(\frac{y}{d}\right)^2\log\left(\frac{y+d_2}{y-d_1}\right)-\frac{y}{d}\right] \qquad y > d_1 \tag{5.22}$$

Where I is the total current at the soma I_s due to synaptic inputs. The above approximation was used for pyramidal cells in layers 3 and 6 with soma located at 0.7mm and 1.6mm below cortical surface respectively. For tufted layer 5 cell assumed located at 1.2 mm depth, an apical sink (system A) and a basal system of synaptic

Table 5.2: Distances of different cellular types from cortical surface used in computing surface field potential (per figure 5-14)

Cell type	y_0 (μm)	d_1	d_2	d
Layer 3 pyramidal	700	600	250	850
Layer 5 pyramidal				
(basal system)	1200	400	300	700
(apical system)	1200	1100	300	1400
Layer 6 pyramidal	1500	800	100	900

sources were considered separately. Table 5.2 shows distances of each cell from the cortical surface used. Finally, assuming that all cells in a cortical minicolumn lie vertically under the recording electrode, the total potential is the sum of individual contributions.

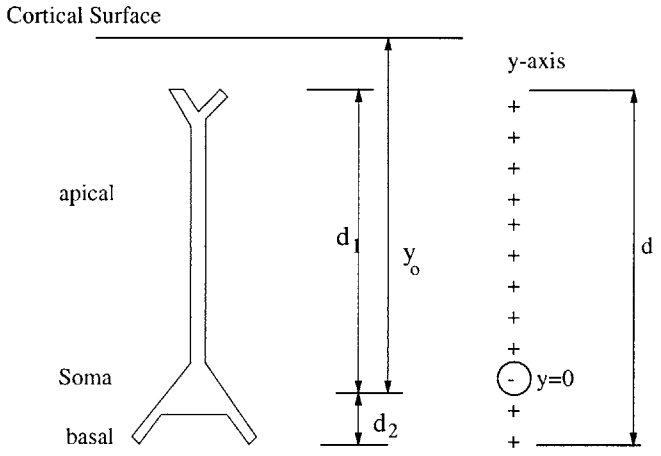

Figure 5-14: Approximation of a pyramidal cell with a distributed line source and single sink at the soma. The vertical y-axis has origin at the soma

Chapter 6

Simulations

In the previous two chapters we outlined an effective skeleton circuit that we claim could account for several basic rhythms observable in the EEG and is at least compatible with known properties of high frequency synchronization in neural systems associated with cognition. In this chapter we will describe how few basic features of EEG can be realized using a minimal model of cortical interaction. Starting with the idea that layer 5 cells have the propensity to resonate at a preferred frequency of 10 Hz, we simulate a simple system where augmenting responses can be attained mainly through rebound depolarization in layer 5 and successive recruitment of bursting cells in this layer. Next, we build upon this resonance property to describe the genesis of different types of alpha rhythms: those that appear in cases of mental idling (conventional alpha) as well as functionally-relevant alpha band activity. For this, the model describes coupling between systems at disparate orders in sensory processing stream and emphasizes the role of tufted layer 5 cells as providing such link. The transition from alpha frequency to higher frequencies during cognitive states is then discussed briefly. Slow oscillations are qualitatively described as initiated in layer 5 during hyperpolarization, propagated to other layers and finally terminated by disfacilitation and ionic currents. Finally, the same model of slow oscillations is shown to go into a spike-and-wave type seizures when inhibition in the system is decreased.

6.1 Augmenting Responses in Neocortex

An Augmenting response refers to the increasing amplitude of a cortical field potential under repetitive stimulation. Augmenting responses have been reported to occur in several cortical areas by delivering stimulus trains to some connected thalamic nuclei in the 10 Hz range, as well as by stimulation of the white matter or callosally projecting cortical fibers in athalamic animals. The importance of augmenting responses arises from their potential role in promoting short-term plasticity in thalamocortical systems as well as promoting sustained activity in cortical networks.

A form of augmentation was seen earlier by Steriade in anesthetized cats in vivo where stimulating intrinsically bursting (IB) L5 cells via trans-callosal connections at 10 Hz was able to entrain these cells into a sustainable oscillation which out-lasted

the stimulus duration (Steriade et al 1993 [217] and Nunez et al [174]). Augmentation at layer 5 synapses (but not at layers 2/3) has also been described in primary visual cortex and are even more pronounced medial prefrontal cortex where it might be attributed to the properties of the synapses themselves (Hempel et al 2000 [97]).

While Steriade and colleagues have attributed cortical augmentation partly to thalamic networks (Bazhenov et al 1998 [14], Gernier et al 1998 [86]), the intrinsic neocortical mechanisms that generate this behavior are less obvious. In understanding the underlying cortical cellular and network mechanisms of augmenting responses, Castro-Alamancos and Connors conducted a series of experiments in the sensorimotor cortex of rats which showed augmentation due to stimulation of the ventrolateral (VL) thalamus at 7-14 Hz (or simply termed "10 Hz"). Here, augmentation seemed to originate in layer 5 cells and is manifested by bursting-like behavior in this pyramidal population and is maximally evoked in periods of sustained hyperpolarization. A similar response was evoked by cortical stimulation (Castro-Alamancos et al 1996a, 1996b [29, 30]).

The authors argued that synaptic enhancement in layer 5 could be due to hyperpolarization -activated conductances in layer 5 pyramidal cells. Further, current source density analysis showed a large sink in layer 5 and a source in the superficial layers during augmenting response, which is a consistent picture with the origin of this phenomenon. Also, maximal spatial spread of augmentation occurred in layer 5.

Interestingly, this augmenting response might be linked to a recently reported form of presynaptic long-term potentiation in cortico-thalamic pathways (Castro-Alamancos and Calacagnotto, 1999 [31]). Such LTP was seen to occur at 10 Hz and is reversed at 1 Hz. Since spindle oscillations are generated in the thalamus, they cannot contribute to this enhancement which is entirely presynaptic. Instead, an alpha rhythms at 10 Hz were seen in animals during awake immobility just as an animal prepares for attentive processing and is abolished soon after active exploration. Hence, and since we know that alpha rhythms are produced in neocortex, it is possible that augmentation in cortical circuits might be manifested as a resonance phenomenon at alpha frequency and is a intracortical mechanism for attentive preparation that depends exquisitely on layer 5 IB cells.

6.1.1 Main physiological observations

Following a stimulus delivered to ventrolateral thalamus, cortical circuits in the reciprocally connected areas (sensorimotor cortex) respond with an initial EPSP followed by a strong hyperpolarization possibly due to GABA-B synapses. This is followed 200 msec later by a long-lasting depolarization (figure 6-1). In the time period when cells are hyperpolarized, layer 5 cells amplified subsequent VL stimulus delivered and had a suprathreshold response starting with single action potential. The same stimulus will not illicit firing, however, when delivered after the long-lasting depolarization occurs. If a train of stimulus was delivered at 10 Hz starting prior to the long-lasting depolarization period, then layer 5 cell firing is augmented from single spike to 2 or 3 spikes that will follow the frequency of the input and will only stop about 200 msec after the stimulus is terminated. Subsequently, the long-lasting depolarization will

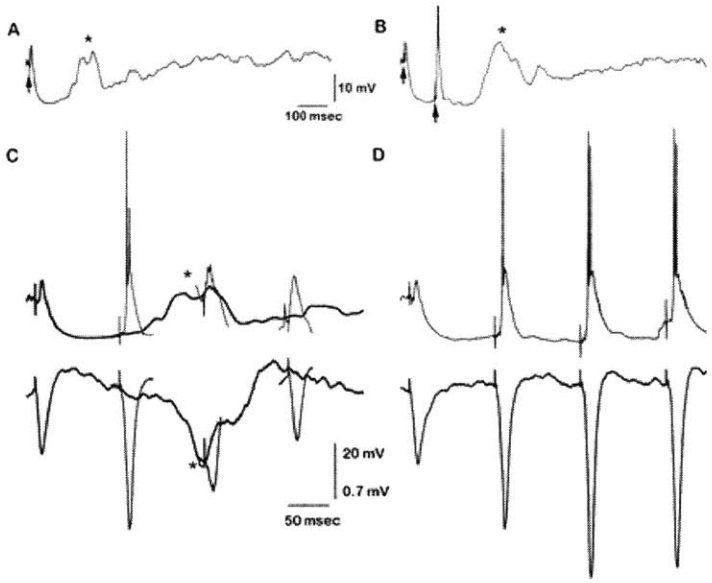

Figure 6-1: Augmenting response after thalamic stimulation occurs only before depolarization phase. *Top left*, response of sensorimotor cortex to a single stimulus delivered to the VL thalamus. Asterisk indicates the initiation of depolarizing wave beyond which augmentation cannot occur. *Top right* delivering a stimulus before the asterisk causes firing in layer 5 cells. *Bottom left* Schematic showing that stimuli delivered before the depolarization cause cell firing, but not after the asterisk (a window of 200 msec). *Bottom right* delivering a 10 Hz train of stimuli starting before the asterisk will cause augmentation and increase in cell firing

occur about 200 msec later. Castro-Alamancos noted that such cells had a rebound characteristic when released from hyperpolarization and this could be the mechanism that defines such amplification during hyperpolarization.

Similar work was performed by Steriade and co-workers and the noted that the long-lasting depolarization after a thalamic stimulus is actually initiated by post-inhibitory rebound firing in thalamocortical cells (Gernier et al 1998 [86]). Further, those authors noted that a cortical slice devoid of long-range cortical connections and thalamocortical inputs will not exhibit such rebound depolarization. Still, intracortical recordings demonstrated the ability of cortical circuits to sustain oscillations for periods longer than that in thalamic networks. Deep layer pyramidal cells had a higher propensity to generate augmenting responses than superficial layers pyramidal cells and were a precursor to the augmenting activity generated in the latter. Their experiments, however, failed to reproduce augmentation in isolated cortical slices (which, we will argue later, is due to lack of stimulation of apical inputs to tufted layer 5 cells).

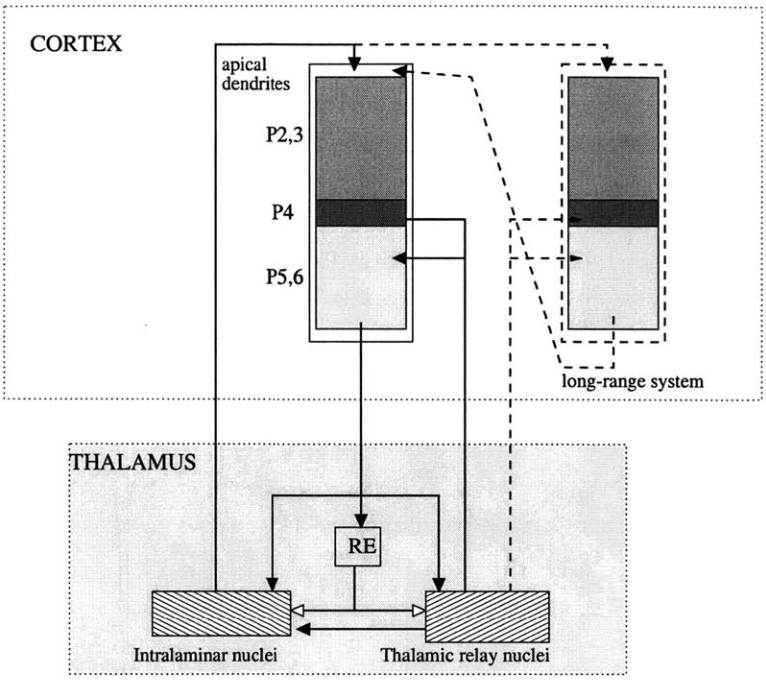

Figure 6-2: Main players in generating augmenting responses in neocortex. The thalamic circuitry is able to produce augmentation by virtue of rebound depolarization in thalamic relay neurons, which is then transfered to the cortex. The cortex is also able to produce augmentation via long-range connections between coupled areas by virtue of rebound depolarization/ coupling of input streams in layer 5 cells

6.1.2 Hypothesized circuit dynamics

Based on the above experiments and our previously mentioned cortical circuitry dynamics, a scenario as to how cortical rebound occurs is as follows. The schematic in figure 6-2 shows the main player in generating augmenting responses in neocortical tissue. The thalamic component will not be emphasized here since this has been well studied and modeled earlier (Bazhenov et al 1998 [14]).

1. A cortical column receiving feed-forward excitation from a specific thalamic source has a main input port in middle layer 4. Such input, under certain conditions such as ketamine anesthesia, elicits strong response in interneuronal circuits that promote GABA-B inhibition in pyramidal cells, especially those in layer 5. The net effect is a long lasting hyperpolarization in the cortical column (Figure 6-3).

2. During hyperpolarization, many layer 5 cells have strong amplification characteristics due to low-threshold calcium currents in the soma, which promote rebound depolarization. While such currents might not be able to generate rebound firing under slow release from inhibition in cortical slices (slow GABA-B inhibition), these cells are able to generate large depolarizations upon receiving excitatory inputs (EPSP) from afferent sources, due to long-range cortical connections or

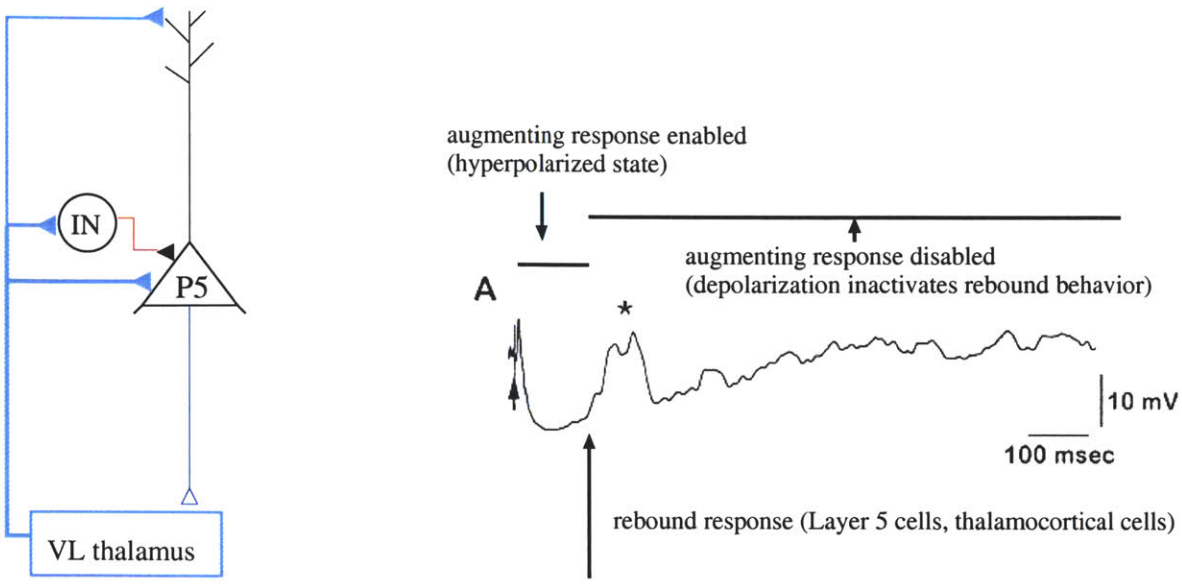

Figure 6-3: Basic mechanisms effecting augmenting responses in neocortex. *Left:* stimulation of the VL thalamus causes marked hyperpolarization due to activation of inhibitory interneurons in layer 5. *Right:* Response to VL stimulus consists of initial period of hyperpolarization followed by rebound depolarization.

thalamic inputs.

3. Artificial cortical stimuli delivered trans-callosally (or in large enough cortical slices) are able to generate strong enough excitation in layer 5 cells to generate single action potentials (figure 6-4). *The recurrent connections into layer 1, from long range feedback connections or from non-specific thalamic nuclei have an essential role in generating augmenting responses since these promote apical dendritic depolarization, a mechanism essential in promoting burst firing in these cells.* Hence, one can see how recurrent connections can augment layer 5 cell responses from single to multiple spikes.

4. The long-lasting depolarization ensuing after a thalamic stimulus is initiated by rebound firing of thalamo-cortical cells which then impinge upon deep layers in the cortex to generate subsequent activation of different cortical layers. While this response is observed in intact thalamocortical networks in vivo, cortical circuits could in principle generate similar responses if sufficient excitation occurs during the hyperpolarization period to generate rebound activity in layer 5 cells. Accordingly, layer 5 cells rebound mechanism is not as dominant as that of thalamocortical relay neurons, which could be argued based on cellular responses to hyperpolarizing pulses.

5. The lack of augmentation seen after the occurrence of long-lasting depolarizations is due to activation of dendritic inhibitory mechanisms which reduce layer 5 cell propensity to burst, and hence eliminate their non-linear amplification characteristics observed prior to the depolarization period (Figure 6-3).

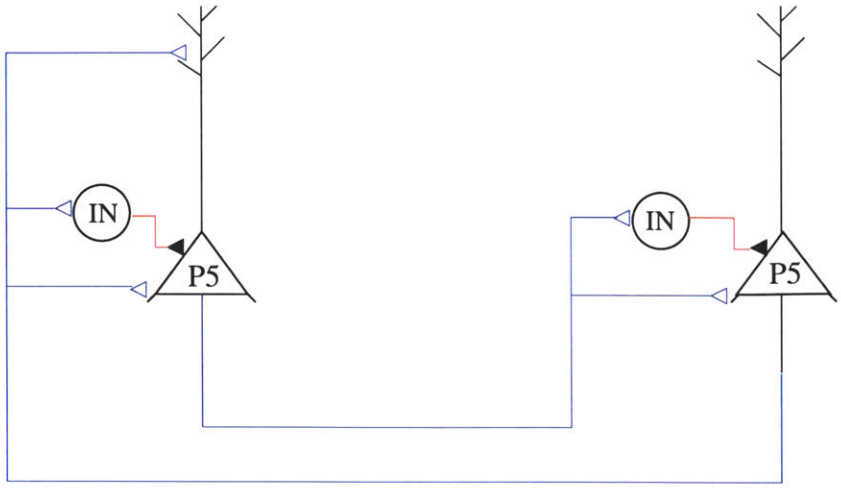

Figure 6-4: Hypothesized circuit involved in augmenting response generation due to cortical stimulation. We here assume that long-range connections obey feedforward-feedback topology. In general, afferent activity to superficial layers allow maximal recruitment of tufted layer 5 cells, causing bursting.

6.1.3 Simulations

The main result of this simulation is the ability of layer 5 network to produce augmentation when appropriately stimulated at 10 Hz. In particular, activation of apical system of tufted layer 5 cells can produce strong augmentation of the type observed experimentally (ketamine anesthesia, NMDA receptors blocked). Finally, The augmentation can outlast an input stimulus if slow NMDA receptor are active. We will detail these results next.

Rebound behavior in L5

The rebound response of layer 5 cells after periods of hyperpolarization was modeled based on low threshold Ca^{2+} currents I_T. Replicating data obtained by Castro-Alamancos in 1996 (figure 6-5) shows a tufted layer 5 response to brief hyperpolarizing pulses. In a network setting, a layer 5 cell can amplify subthreshold synaptic inputs, to generate suprathreshold activity (firing) after a prolonged period of hyperpolarization (Figure 6-6). This is approximately replicated in our layer 5 cell model[1].

[1]For the current simulations, a layer 5 soma model had only I_T current without explicit activation/inactivation properties, as modeled in Wilson [260]. Accordingly, although the time window over which amplification in the model is smaller than that experimental setting (50-100 msec). This is mainly due to the approximation of low-threshold calcium currents in the model, which rebounds only after sufficiently large sudden jumps in membrane potential (which occurs in the model only when input stimulus occurs in the period after the cell is released from hyperpolarization). More accurate modeling of I_T current, as well as inclusion of hyperpolarization sag current I_H might correctly model the amplification nature of hyperpolarizing periods.

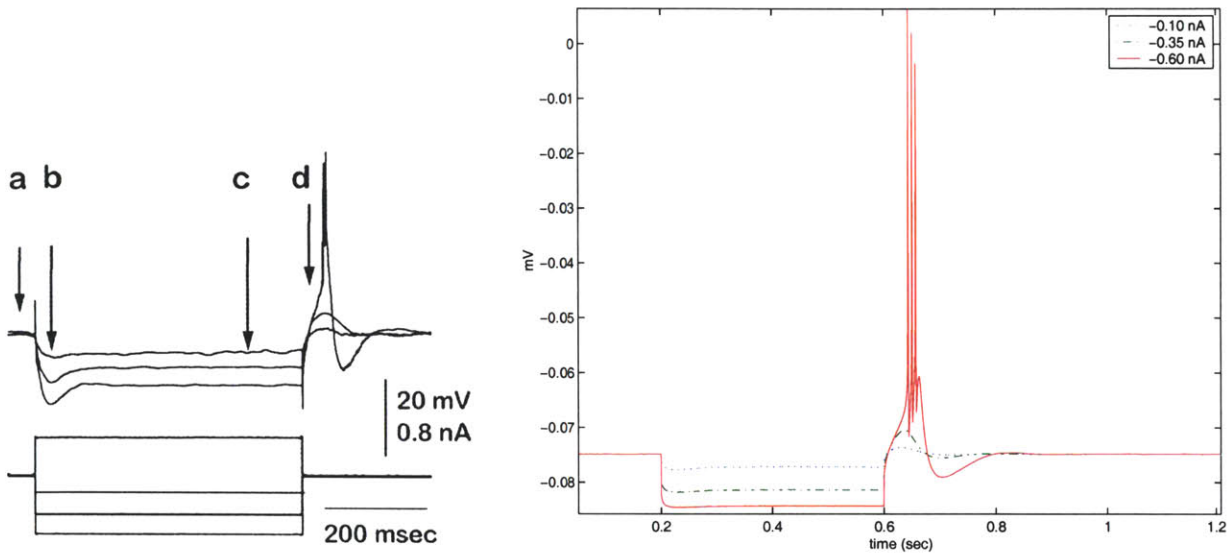

Figure 6-5: Post-inhibitory rebound behavior of Layer 5 cells in rat sensorimotor cortex in vitro. *Left*, experimental data (from Castro et al 1996). *Right*, simulated layer 5 cell.

Augmenting response in Layer 5

In this simulation, we utilized a minimal model of a cortical region, namely only three tufted layer 5 cells were reciprocally connected and subject to interneuronal inhibition (figure 6-7). A presynaptic cell contacts a postsynaptic IB cell on its basal dendritic system, forming both NMDA and AMPA type excitatory connections (NMDA synapses will be removed later to simulate effect of ketamine anesthesia). Each cell is contacted by an input system representing thalamic afferents. The thalamic stimulus is approximated by a train of bursts (intra-burst frequency 200Hz) occurring at inter-burst rate of 10 Hz. The minimal model demonstrates that a network of interconnected layer 5 cells can generate an augmenting response similar to that observed in vivo, as shown in figure 6-8.

As observed in experiments (such as in Steriade et al 1998 [222]), thalamic inputs contact the cell itself as well as inhibitory interneurons which in turn provide a strong long-lasting inhibition . Thus, a thalamic stimulus has a net effect of low amplitude initial EPSP followed by stronger EPSP (due to afferents from thalamic relay cells that undergo rebound bursts) and subsequently followed by a long lasting GABA-mediated IPSP (action of interneuron).

Thalamic excitatory input depends on the of thalamic nucleus being stimulated, and hence could either terminate in layer 1 contacting apical dendrites of layer 5 cells, or in middle layers, hence contacting the basal dendritic system. In the simulation, we assumed that thalamic input contacts the apical system only through AMPA receptors, while inhibition acts mainly through GABA-B type receptors of 100 msec duration (as given in Gernier et al 1998 [86]). Similar results could be obtained if excitatory thalamic input reaches the basal system. The main findings of these simulations were the following.

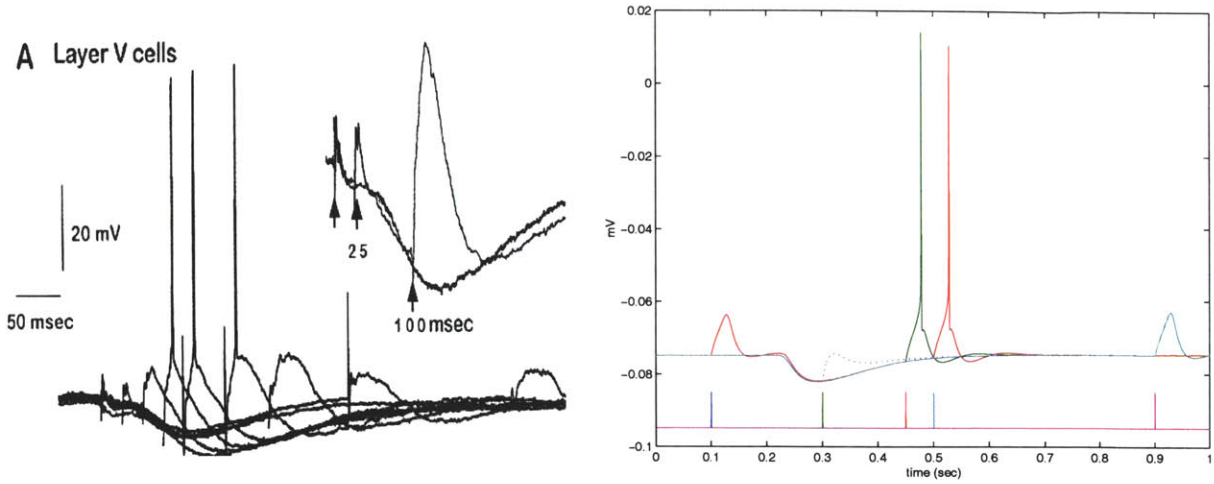

Figure 6-6: Layer 5 cells amplify synaptic input after a brief period of hyperpolarization. *Left*, experimental data (from Castro et al 1996) showing cell response to coupled stimuli, on delivered at the onset of the trace, resulting in long lasting hyperpolarization, and another delivered after a period of delay (indicated by vertical lines). *Right*, simulated layer 5 cell behavior under qualitatively similar settings(differences are due to approximated behavior under of hyperpolarization activated currents -see text). Lower trace vertical bars indicate time of second stimulus

1. The hyperpolarization incurred in layer 5 cells after the first thalamic input amplifies subsequent EPSPs due to rebound behavior, as observed in individual cell setting.

2. The augmenting behavior occurs after the second stimulus from a single spike to 2 spikes by the third stimulus and an increased depolarization of the cell afterwards which is similar to results obtained by Steriade et al 1998 and Castro-Alamancos (figure 6-8).

3. Augmentation is generated intracortically. In general, a thalamic stimulus delivered to layer 5 could generate weak augmentation in these cells (Figure 6-9) when such cells are minimally connected at their basal system *and* the dendritic system is not excited. However, increased recurrent excitation in the reciprocally connected L5 network is expected to further amplify such responses, especially when these cells are able to burst, since bursting behavior is able to recruit larger populations in the neocortex and hence enhance cellular firing.

4. While the aforementioned intracortical connections were made onto the basal dendritic system L5 cells, it is expected that contacts on apical system will further enhance the cells ability to augment its number of spikes as the stimulus train progresses, since apical system is found to prone the cell to burst at even smaller somatic depolarizations. Accordingly we formed a hypothetical intracortical connection between layer 5 cells both on the basal system as well as the apical system. As a consequence, stimuli delivered at the basal system (thala-

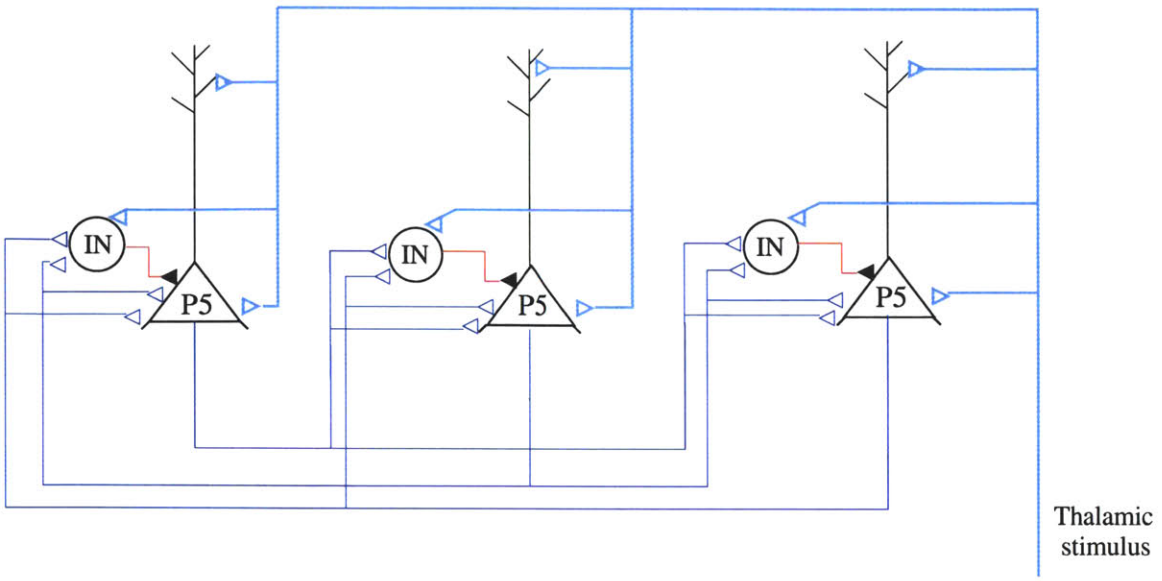

Figure 6-7: Connection diagram of simulated minimal model of a cortical region stimulated by external (thalamic) afferent

mic or otherwise) are greatly enhanced under an excited dendritic system. This is qualitative demonstration of the effect of stimulating callosal or long-range connections, since many of these fibers contact the apical dendritic system. In this case, stimulating callosal fibers at 10 Hz is found to greatly augment L5 cell activity and to even generate sustained oscillations for long periods of time (figure 6-10). The subsequent termination of such activity could be attributed either to synaptic disfacilitation (decrease in extracellular calcium) or increases in depolarization possibly by inward currents such as Ih which will prevent rebound activity in cells when hyperpolarization is decreased, or a combination of these factors[2].

5. The apical dendritic system is contacted by intralaminar thalamic nuclei (CL, for example). This connection acts in a similar manner to long-range feedback intracortical connections. Consequently, it is very plausible that while the thalamus is undergoing 10 Hz oscillations, a recurrent thalamic relay -thalamic intralaminar-cortical excitation will serve to amplify layer 5 cell ability to burst and hence assist in cortical augmentation.

Augmenting response in L5 under Ketamine Anesthesia The simulations presented above had NMDA receptors active which would provide an incremental excitation to pyramidal cells once they are active that lasts for 100s of milliseconds, hence allowing for augmentation to be easily attained. However, augmenting responses have been reported under *ketamine anesthesia which blocks NMDA receptors*

[2]This was only qualitatively simulated in the model by including an equivalent hyperpolarizing current which integrates the calcium concentration in a cell-see chapter on circuit models

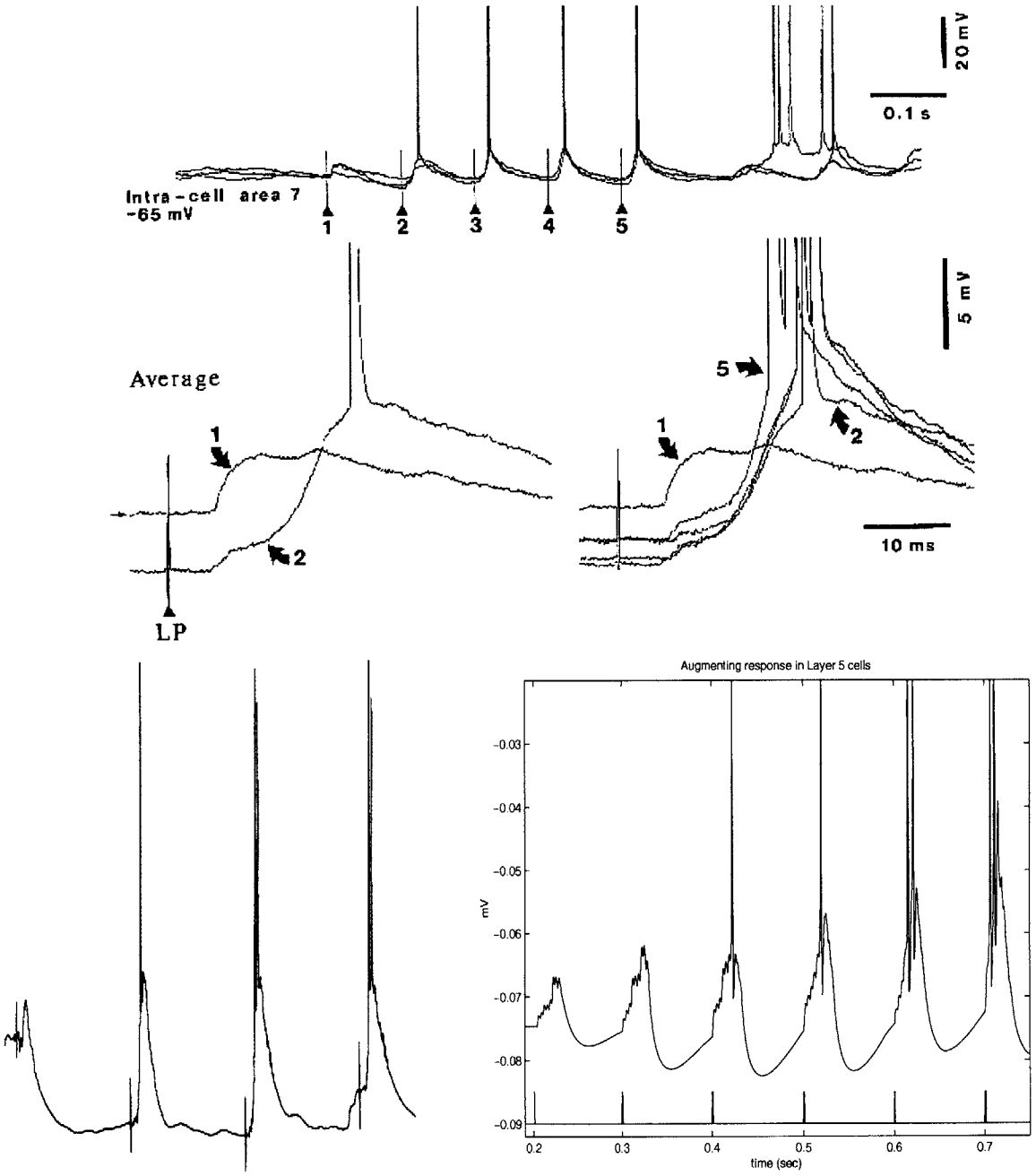

Figure 6-8: Increased depolarization in cortical cells under repetitive stimulation leads to augmenting response. *Top,* intracellular recording from cat area 7 under LP stimulation at 10 Hz. *Middle* expanded view of the same cell showing increased depolarization with stimuli. Numbers correspond to the stimulus number in the top trace (from Steriade et al). *Lower left,* intracellular recording from layer 5 in rats under $10Hz$ stimulation of VL thalamus (from Castro-Alamancos et al 1996 [29]). *Lower right,* simulated layer 5 cell shows increased depolarization at $10Hz$ stimulation.

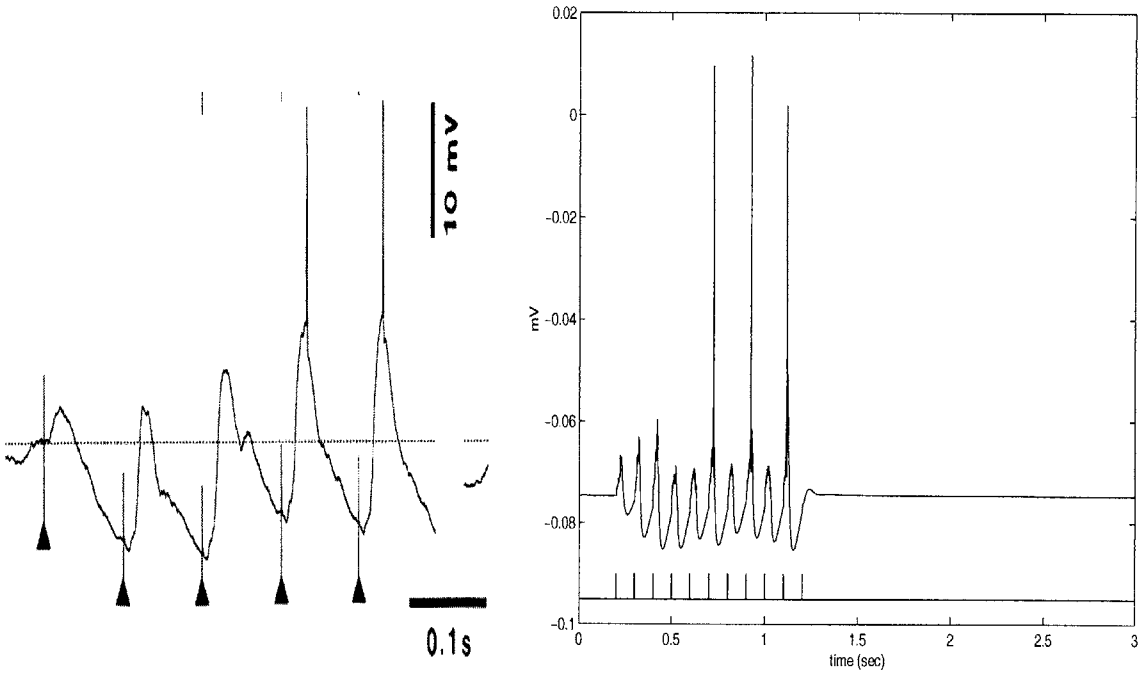

Figure 6-9: Augmentation in layer 5 cells under 10 Hz thalamic stimulation. *Left*, LP-evoked augmenting response in area 5 (Cats, ketamine anesthesia- from Steriade el al 1998). *Right*, simulated layer 5 cell response to 10 Hz burst train stimulus, minimal intracortical connections.

(Steriade et al 1998 [222]). Hence, it was necessary to demonstrate how layer 5 cells could attain an increasing depolarization without NMDA receptors. To this extent, the simulation model included the following

1. According to experimental records (Castro-Alamancos and Connors 1996 [30]), augmentation spreads from the initial site of activation into fairly large areas (several millimeters) in layer 5. Further, callosal connections provide augmentation (Steriade et al 1993, Nunez et al 1993 [216, 217, 174]). Therefore, we assumed that initial stimulus (thalamic of cortical) affects a subpopulation of Layer 5 pyramidal cells $PL5_1$ at the site of activation, causing characteristic hyperpolarization and rebound behavior and initiating firing (Figure 6-11, also figure 6-4). These cells subsequently activate second-order layer 5 cells $PL5_2$ through basal dendritic connections as well as their GABA-B interneurons, since cortical stimulation also creates a characteristic hyperpolarization (Castro-Alamancos 1996, Fig 5).

2. With subsequent impulses arriving to the initial site, the second-order activated cells $PL5_2$ are now capable of enhancing their own excitatory input via their rebound mechanisms, initiating firing activity. This activity is then transfered back to $PL5_1$ causing further depolarization and hence augmentation into bursts.

3. Although sufficiently high depolarization of basal dendrites in $PL5_1$ can initiate

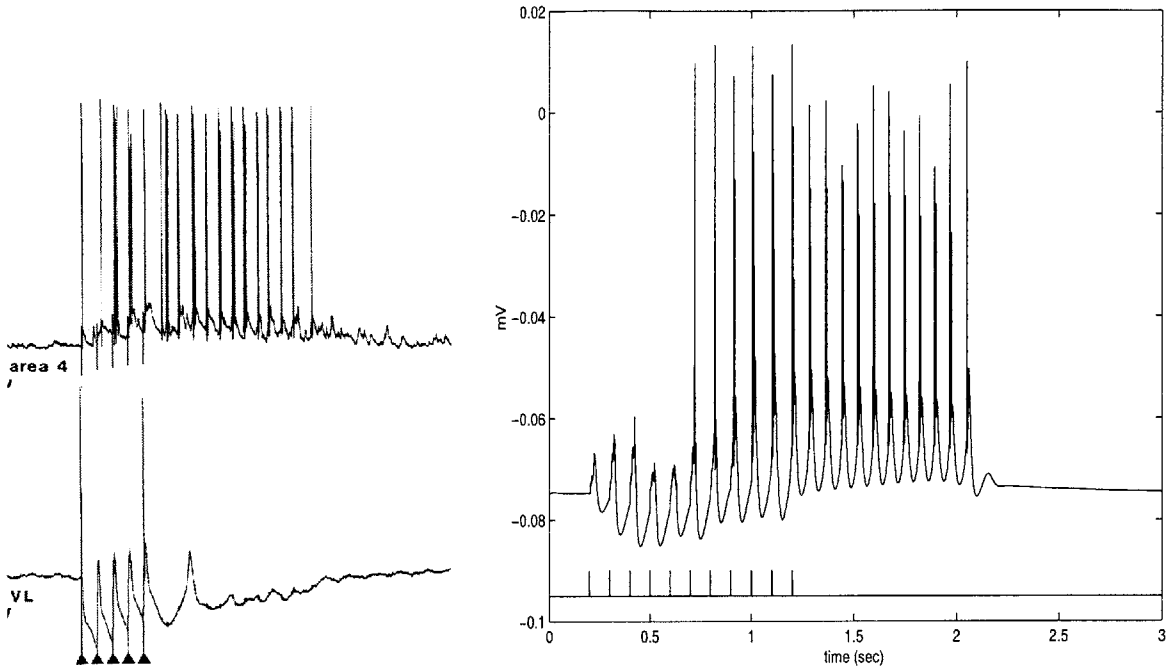

Figure 6-10: Augmentation in cortical neurons can outlast thalamic stimulus. *Left*, recordings from cat area 4 to VL-evoked stimulus at 10 Hz (Cat, Barbituate anesthesia- from Steriade et al 1998). *Right*, simulated layer 5 neurons can develop long-lasting recurrent excitation when apical dendritic system is activated, generating bursting behavior in these cells.

bursting, recurrent activity from $PL5_2$ to $PL5_1$ is especially especially effective when connections are made onto apical dendritic compartments of $PL5_1$. Hence, one could see how a feedback projection of $PL5_2$ to layer 1 of the initiation site will cause bursting in $PL5_1$ cells. This scenario might well be the reason why callosally projecting cells are so effective in providing augmentation between two areas, since many of these projections are known to make synapses in both deep layers as well as layer 1.

According to the above scenario, we simulated 6 representative layer 5 cells, 3 in each region along with their reciprocally connected interneurons. Synaptic connections were scaled highly due to the limitations of such scale. Still, figure 6-12, demonstrates the obtained augmentation in the system. A sample of layer 5 cells from both regions $PL5_1$ and $PL5_2$ is shown in figure 6-12 illustrating the recruitment. Although the augmenting response is terminated with the stimulus in this simulation, we believe that sustained oscillations could be attained if the system is scaled to a realistic size network, in which case recurrent excitation between large cell populations can provide necessary substrate for such oscillations to outlast the stimulus.

Finally, Steriade et al reported the absence of the characteristic hyperpolarization after an initial stimulus when applied to cortical slices deprived of thalamic and long-range cortico-cortical connections. Further, it has been reported that thalamocortical

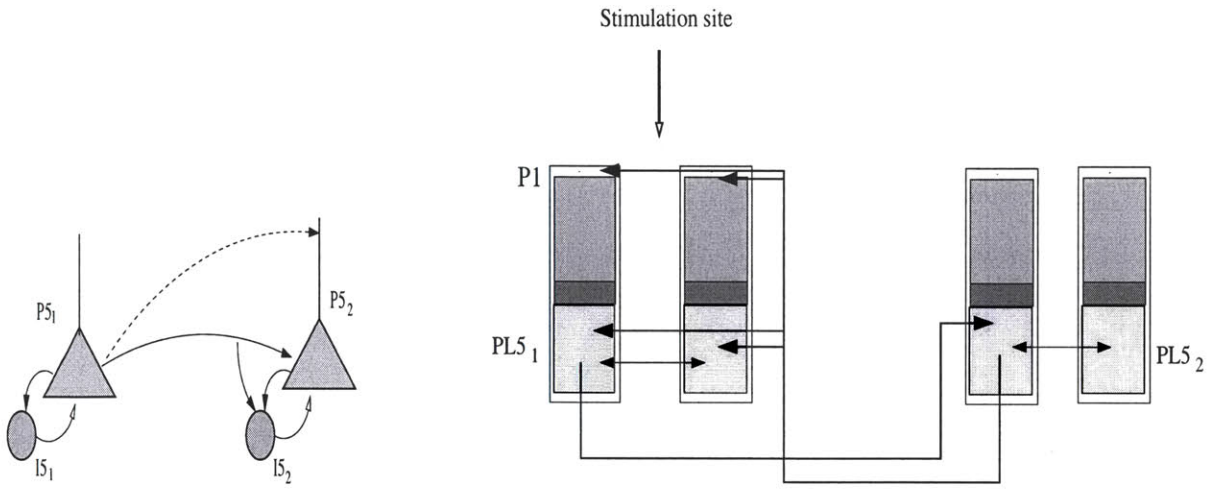

Figure 6-11: Recruitment of layer 5 populations. *Left:* connection diagram between two layer 5 cells and their interneurons. filled arrows are excitatory, empty arrows inhibitory. Dashed line indicate possible dendritic connections which could be found for long-range feedback connections. *Right:* distant connection can provide recruitment starting from an initial site of stimulation to cause augmentation. Apical connections are especially effective in causing bursting

afferents activates feedforward inhibition more effectively than intracortical afferents (Gil and Amitai 1996 [89], Gil 1999 [90]) and that the latter could evoke inhibition at higher stimulus intensities.

Therefore, it is possible that activation of inhibitory mechanisms affecting layer 5 require converging afferents from large populations of synchronized neurons. Also we believe that a more attractive alternative is that long-range cortico-cortical connections are capable of recruiting the main local circuit mechanisms that thalamic pathways utilize in initiating feedforward inhibition.

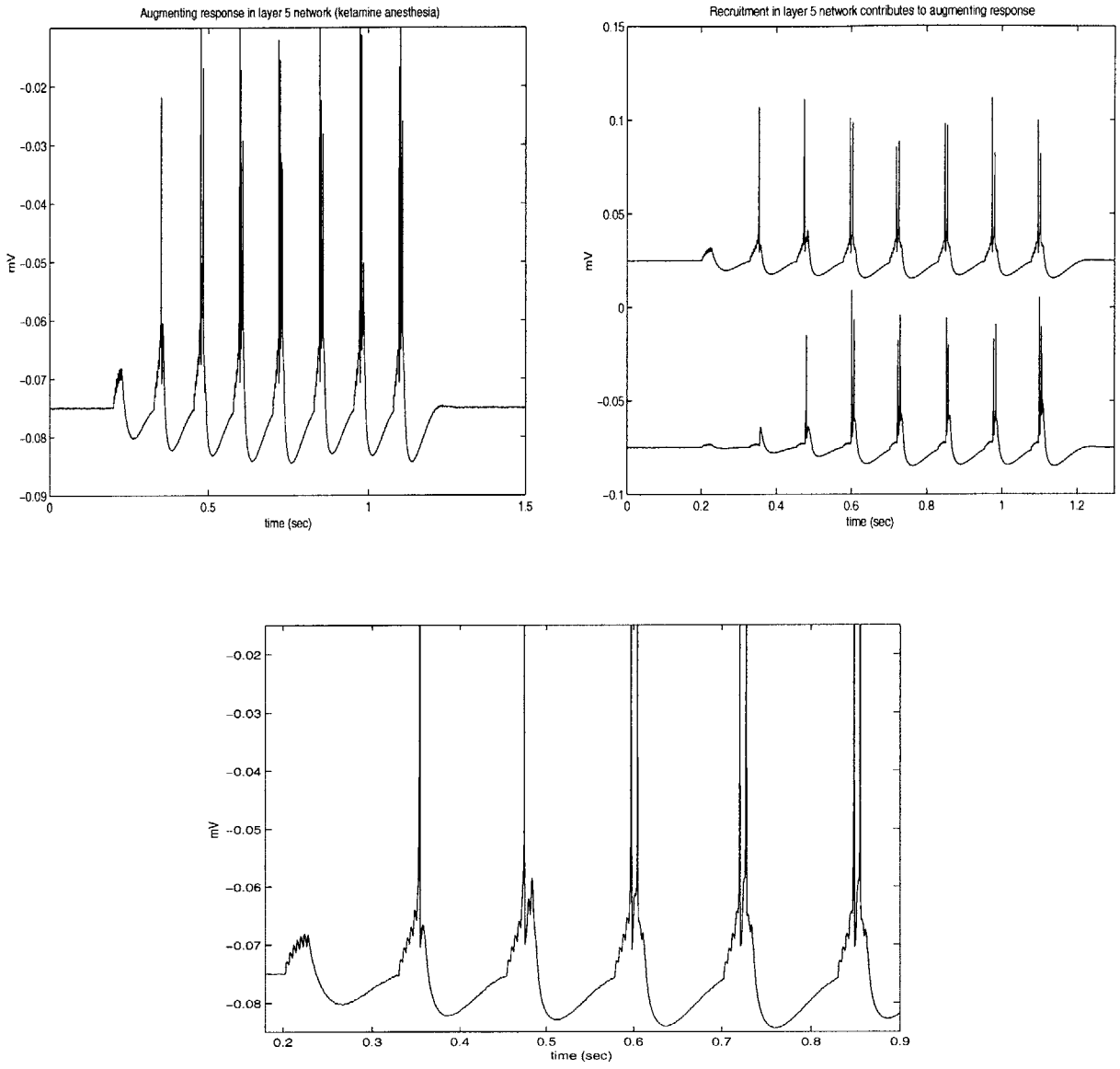

Figure 6-12: Augmentation in layer 5 network under ketamine anesthesia (no NMDA mediated excitation) is enhanced by apical dendritic excitation. *Upper left:* layer 5 cell at stimulus initiation site. *Upper right:* recruitment of a distant layer 5 (lower trace) by virtue of its connection to stimulated local layer 5 cell. *Bottom:* increased depolarization in a layer 5 pyramidal cell (compare with experimental plots).

6.2 Alpha Rhythms

Oscillations in alpha frequency range (10 Hz) have long been observed in states of restful awakeness over the visual cortex, eyes closed, in the scalp EEG over the posterior cortex of humans and other mammals. This rhythm was until recently associated with a state of mental idling, as it is seen to desynchronize when eyes are opened or when cognitive behavior resumes. The term *alpha desynchronization* refers to the reduction in the power content of the alpha frequency band and increase in that of the higher (beta, gamma) bands. It is contrasted with synchronized alpha which describes the existence of high alpha power in a relatively wide spatial area: EEG signals recorded over that area show close phase relation ships in the alpha band and hence are "synchronized".

Comparable $\approx$10 Hz rhythms have been observed over other sensory areas and suggest that such rhythms might not be restricted to visual areas. For example, alpha band activity is registered over the somatosensory cortex-blocked by movement and tactile stimuli (so called mu or rolandic rhythms), and over the auditory cortex (tau rhythms)- blocked by auditory inputs (reviewed in Schurmann and Basar 2001 [201]).

Recent studies, however, have demonstrated that alpha activity might actually have important functional correlates. The implications of alpha activity, nevertheless, seems paradoxical and at best confusing in view of available experimental data. We will make the distinction between induced alpha activity related to preparatory attentional processes and evoked alpha band oscillations which are event-related, as explained next.

A. Induced alpha as suppressive mechanism: Synchronized alpha activity have been demonstrated in anticipatory or preparatory states where inter-modal attention is required[3]. For example, in a combined auditory-visual task, subjects were cued to attend to one component of the task (beep or flash) that will follow 1 second later. In the post-cue pre-stimulus period, alpha activity appears over occipital-parietal (visual) areas when the subject was cued to attend to the auditory component of the next stimulus (Foxe et al 1998 [74]). This alpha activity is described in terms of increase in alpha-band power in the EEG and is *not time-locked*[4] *to a particular stimulus*, but rather shows a broad band around the 10 Hz frequency peak with little phase locking (figure 6-14).

In another visual experiment where subjects had to focus attention onto a spatially localized target (e.g left) while ignoring a distractor in the opposite hemifield (right), it was seen that alpha activity is sustained over the scalp region corresponding to the distractor (figure 6-13) while the band power decreased over the scalp area corresponding to the target (Worden et al 2000 [262]). Further,

[3] An inter-modal task refers to the combination of two or more sensory modalities

[4] The cortical activity induced by a stimulus is usually measured with respect to the stimulus onset: time-locked activity is a consistent initiation of the same phasic activity after the stimulus onset over repeated trials; hence, we say that the activity is phase-locked to the stimulus

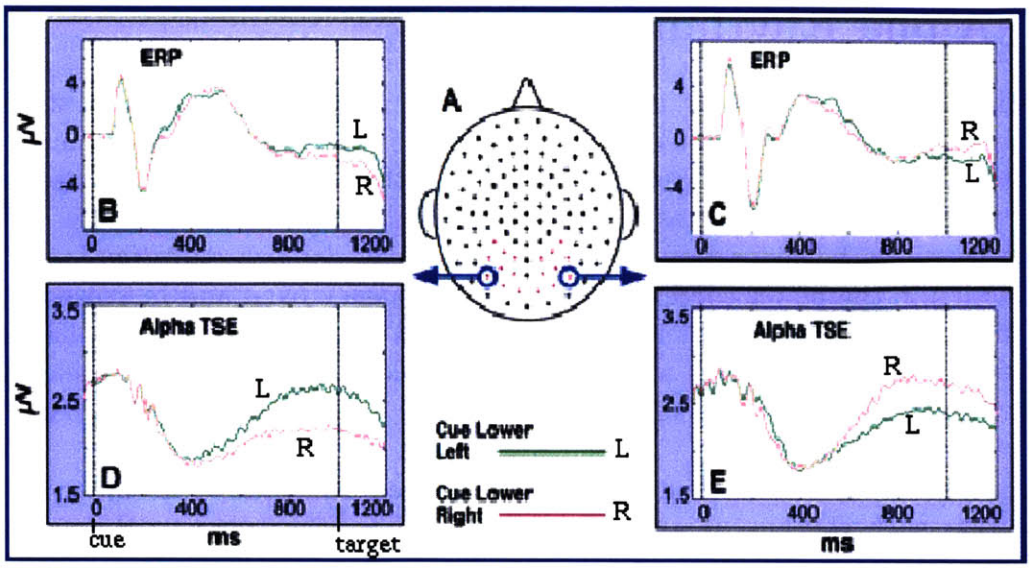

Figure 6-13: Effect of anticipatory state on alpha band power during delay periods in visual attention experiment. upper plots show event related potentials (ERP) recorded from the electrodes shown during experiment. Time zero refers to appearance of cue as to where the target is going to occur (L or R) after 1 sec (vertical line at 1000msec). Lower plots are alpha Temporal spectral evolution (which is alpha-band filtered EEG signals that are full-wave rectified and squared) . These signals indicate that under attend left condition (L), the right electrode, which corresponds to the left visual hemifield, has reduced alpha band power (but not under attend right condition (R)). Adapted from Worden et al 2000.

in an experiment where subjects have to judge visual stimuli and give a motor output, Klimesch and Pfurtscheller demonstrate that during visual stimulation, alpha activity desynchronizes over occipital (visual) areas while it synchronizes over motor areas. The opposite happens during the motor response.

Hence, it was suggested that alpha activity might have a suppressive attentional or "gating" role to parts of the system that are not involved in the immediate task. Support for this hypothesis also comes in memory tasks designed by Klimesch 1998 [119] which related alpha oscillations to cognitive and memory performance in humans. These authors noted that while long-term memory tasks cause alpha desynchronization, a 'paradoxical' synchronization was seen in a task which maximizes short term memory while minimizing long-term memory demands, and thus attributed this synchronization to inhibition of long-term memory mechanisms (Klimesch et al, 1999 [120]).

B. Evoked alpha as cognitive mechanism: Although alpha desynchronization has long been considered as a sign of cognitive processing, it appears that transient increases in alpha band activity may have relevance to cognition as well. The latter idea was put forward by Basar and coworkers (reviews in Basar et al 2001 [13], Schurmann and Basar 2001 [201]) who recorded evoked alpha activ-

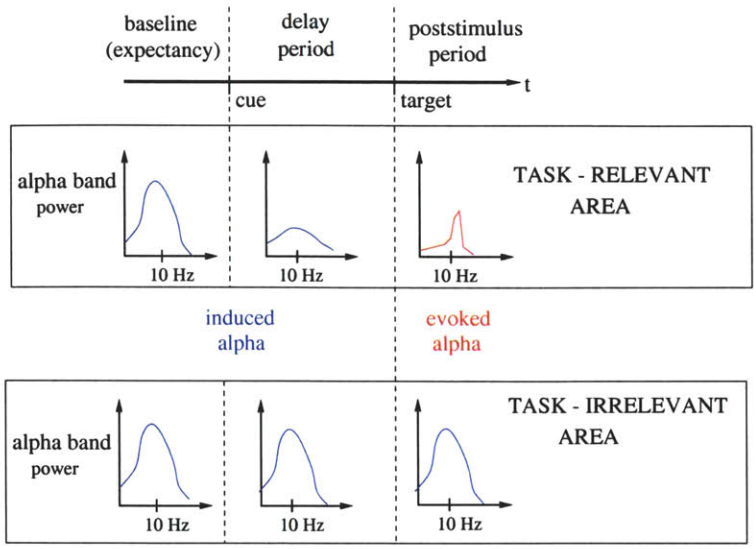

Figure 6-14: Alpha band activity recorded over a task relevant area is modulated by attention. During baseline periods, large alpha band power is recorded over both task relevant and irrelevant areas. After a cue is presented as to which part of the following stimulus is a target, alpha band power (induced) decreases. Post-stimulus evoked activity, however, exhibits phase-locking over a transient period (100-500msec).

ity under cognitive tasks and observed synchronization. In partial contrast to the aforementioned experiments which observed that alpha synchronization is related to inhibition of task-irrelevant areas, these authors noticed that alpha band oscillation is synchronized over the task specific area *and not* over task-irrelevant areas (Schurmann and Basar 2001 [201], figure 1 in cat, and figure 2 in humans). This *evoked alpha is time locked* to the stimulus, shows a narrow band at around peak frequency (10 Hz) and lasts for about 100-500msec prior to alpha desynchronization (figure 6-15, Left).

A very recent experiment in human subjects found a transient EEG increase in alpha band coherence over occipital-temporal regions of the left and right hemispheres when subjects recognized meaningful objects spanning the visual mid-line (Mima et al 2001 [162]). This coherence, which lasted up to 370msec post-stimulus did not occur with meaningless objects or in states of passive viewing, and therefore possibly correlates with conscious recognition of the attended stimulus (meaningful object).

Finally, evoked alpha appears to be functionally related to the cognitive processing demands associated with the occurrence of the template P300 wave in event related potentials or ERP in short [5] (Yordanova and Kolev 1998 [268]). In

[5] An event related potential is a measure of recorded electric activity as the task-related area responds to a given stimulus. Auditory ERPs have long been recorded and are characterized by wave occurring at distinct times after a stimulus. For instance, P300 is a positive wave occurring 300 msec post-stimulus.

their experiment, ERPs were recorded during a task of counting specific auditory tones. The task involved mentally counting auditory targets (20%) among distractors (uncounted non-targets 80%). It was found in these experiments that a target illicited larger and more phase-locked high range alpha (10-14 Hz) at frontal locations and reduced non-phase locked low-range alpha (7-10 Hz) at the parietal electrode when compared to non-targets, which is a similar sensitivity to that observed in P300 waves.

In summary, while it may seem that alpha activity desynchronizes over task-relevant areas in cognitive experiments, there is transient period (up to 500 msec post-stimulus) when alpha band phase locking occurs (although band power might be small). In contrast, alpha band power occurs during preparatory attentional stages and usually sustained over task-irrelevant areas although phase locking is small (figure 6-14).

In addition to evoked and induced alpha activity, Schurmann [201] distinguishes an **emitted alpha activity** which is an expectancy signal: well trained subjects show phase-locked bursts of alpha energy for up to 1 second before an expected target, or what is called "internally-induced alpha activity". In an auditory prediction experiment, subjects heard 800 msec tones repeated every 2600 msec. Every third or fourth tone was omitted and subjects were asked to predict the time of occurrence of omitted stimulus. As the subjects learned the task, their attention capability and predictions of omitted tones improved. Comparing pre-stimulus EEG at the beginning of the experiment (untrained subjects) with that at end of experiment (trained subjects, good predictions) showed an increase in phase ordering in the alpha band towards the end of the experiment which did not occur initially (figure 6-15, right). Again, this shows an association between alpha-band power and increased levels of attention and cognition performance.

6.2.1 Anatomical substrates of alpha rhythms

Earlier experiments on mechanisms of alpha activity generation were performed in dogs (Lopes da Silva et al, 1973a [138]). Alpha waves could be recorded in the visual cortex and the visual thalamus (LGN and pulvinar). Later experiments recorded alpha activity and mu rhythms in cats (Chatila et al 1992 [37]). Basic results are summarized as follows

1. The alpha waves in the cortex were generated by cortical neuronal elements forming an equivalent dipole layer corresponding to cortical layers 4/5 (Lopes da Silva and van Leeuwen 1977 [141]).

2. Alpha signals appeared to be generated in "epicenters" in the cortex and spread in different directions by cortico-cortical connections. Coherence drops to 37 % of its maximum within about 300 μm which corresponds to the dimension of a cortical column (Lopes da Silva 1996 [145]).

3. While coherence between cortex and specific thalamic nuclei (such as LGN) was of intermediate value, it seemed that cortico-cortical connections were the main

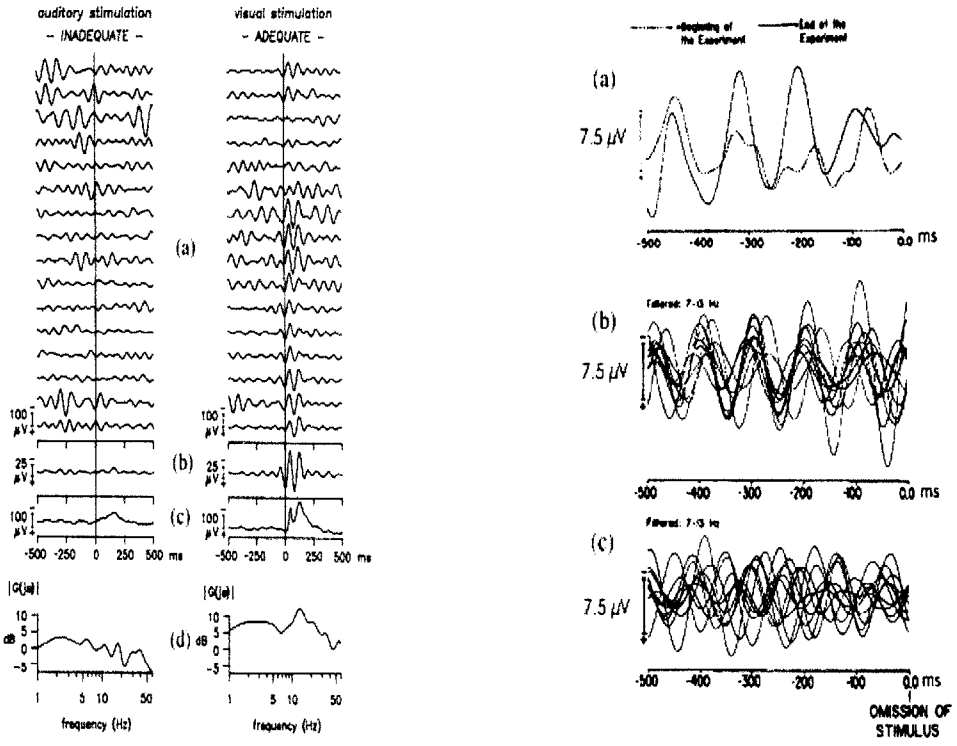

Figure 6-15: Evoked and emitted alpha activity. *Left*, visual stimulation evoke phase locked alpha activity over visual cortex in cat (intracranial recording); no such response is observed during an auditory stimulus. *Right*, Emitted alpha activity becomes more synchronized towards the end of an experiment (a and b) as subjects learn to predict omitted auditory stimuli starting from a naive or unlearned state (a and c)

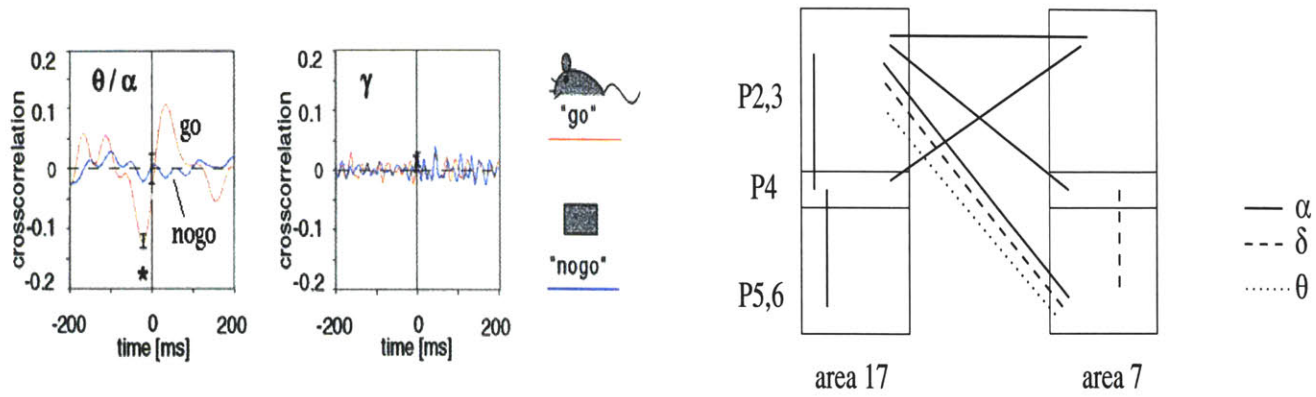

Figure 6-16: Top-down information transfer may be mediated by middle frequency ranges. *Left*, correlation between area 17 and area 7 is maximal in the α, θ frequency band when a go-stimulus is observed but not when a no-go stimulus appears. *Right*, laminar profile of increase in correlations in the α, θ, and δ frequency band, Lines indicate increase in computed correlations and comply with a feedback nature from area 7 (higher order) to area 17 (primary visual or lower order). Figures adapted from (von Stein et al 2000[250]).

contributors [6] to the observed alpha activity (Lopes da Silva 1974 [137]). Of all thalamic nuclei studied, the pulvinar seemed to have the strongest influence in determining alpha activity in the neocortex (Lopes da Silva 1991 [144]): a study of partial coherence of alpha activity in two distinct sites of the neocortex of a cat showed that removing the pulvinar contribution significantly reduced coherence of alpha between the two sites (Lopes da Silva et al 1973a [138]) thus indicating a possible pathway for alpha activity propagation through the pulvinar in to different cortical areas.

4. Although they occur in comparable frequency bands, alpha activity and barbituate spindle sequences are fundamentally different; whereas the former is recorded in awake animals and exhibits modest forms of cortico-thalamic coherence, the latter is recoded under dissociated states and exhibits strong thalamic influence that spreads over large regions of the cortex (Lopes da Silva and Van Lierop 1973b [139]). Therefore, we expect that the mechanism of generating alpha activity (cortical) to be different from that generating spindles (thalamic).

Since trying to identify the exact neuronal mechanisms of alpha activity generation requires intracellular recordings in awake animals, earlier experimentation was limited due to technical difficulties . While recent experiments, which can provide in vivo awake recordings, have not addressed alpha activity per se, several studies have looked into the neuronal synchrony between cortical areas and within cortical lamina and observed alpha band synchrony. These experiments were mostly done in attentive animals during visual tasks and will be presented next.

[6] The contribution of a thalamic nucleus or a cortical site is studied by partial coherences

1. In a vision experiment in cats, a dominant top-down information transfer between different vision hierarchies was seen in the middle frequency ranges (theta and alpha, 4-12 Hz). The cat was attending to two objects displayed on a computer screen, one representing a go-stimulus (push a lever) and the other is a no-go stimulus. Intracortical activity recorded in the primary visual cortex (area 17) and a distant area in association visual cortex (area 7) showed prominent correlation in the 4-8 Hz range (von Stein et al 2000 [250]). Interestingly, the behavioral significance of the stimulus showed different correlation patterns between go/no-go stimuli. Where as the go-stimulus showed significant correlation between area 17 and area 7 in the 4-12 Hz range, no such correlation was found during the no-go stimulus. Furthermore, the laminar profile of this correlation showed a feedback pattern of information transfer which is also dominant in the 4-12 Hz range (area 7 up in the hierarchy, area 17 lower in hierarchy). This association between behavioral goal and middle frequency synchronization suggests that when top-down interactions do not contribute to processing, inter-areal synchronization in the middle frequency range is well reduced.

2. In studying inter-modal selective attention in monkeys, Mehta et al 2000 [156] observed that the first robust modulation of neuronal activity by attention occurred around 100-300 msec after stimulus onset. This was maximal and first observed in V4 and is delayed and attenuated in systems of lower hierarchy (visual areas up-stream, V2 and V1), and fairly unobserved in the corresponding thalamic nucleus, LGN. Laminar distribution of attentional modulation showed increased firing in supragranular and infragranular layers, but not in layer 4. This experiment provided further evidence for feedback or top-down attention mechanisms and suggested that attention works by decreasing the refractory period in local neuronal pools by virtue of disinhibition. Accordingly, Mehta et al suggest that perceptual suppression of irrelevant stimuli is due to the *passive nature of cortical physiology, i.e. that the net cortical response is conservative and largely mediated by inhibition*[7]. Attention thus acts to reduce the effect of this inhibition, possibly by increasing net excitation to neuronal pools by feedback mechanisms (100-300 msec later). This delay in modulation might correspond to observed evoked alpha activity in scalp recordings in humans (which lasts up to 500msec).

3. When looking at the effect of selective attention on local neuronal assemblies, Fries et al 2001 [78] demonstrated that in cortical V4 of macaque monkeys, neurons that are activated by the attended stimulus showed an increase in gamma frequency (35-90Hz) synchronization and a reduction in low-frequency (<17 Hz) synchronization (post-stimulus period). This intracortical recording corresponds well with observations of alpha desynchronization in task-relevant areas which only now was shown as possibly corresponding to increased gamma

[7] That is, a default state of a local neural population is passive (possibly inhibited) and that it does not respond vigorously unless attention mechanisms provide necessary excitation to overcome the inhibitory dominance

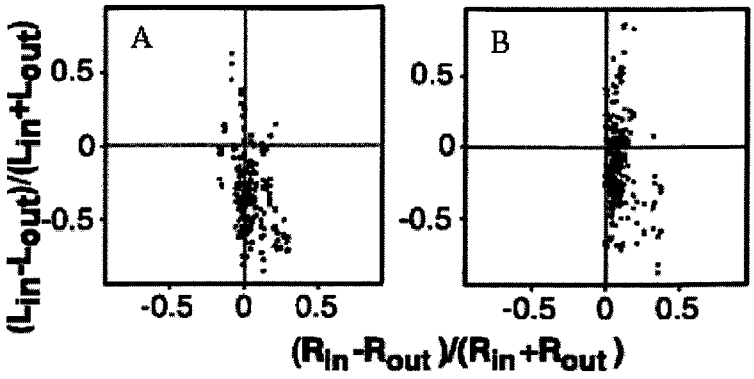

Figure 6-17: Change in spike frequency coherence under different attentional states Each dot represents one pair of recording sites. The x and y axis are attentional indices defined as AI(P)= [P(in)-P(out)]/[P(in)+P(out)]. Here P is either low frequency synchronization L, or firing rate R. P(in) is the value of a parameter with attention directed into the receptive field of a recording site. P(out) indicates attention outside the receptive field. **(A)** occurs during the pre-stimulus delay period. **(B)** occurs during the stimulus period itself (reproduced from Fries et al 2001 [78]). Note the higher percentage of increases in both low frequency synchronization (L) and firing rate (R) for attended spatial location (receptive field) during the stimulus period (plot B, 1st and 4th quadrants) compared to pre-stimulus/post-cure period (plot A).

synchronization. Although the authors did not specifically define alpha activity, we can look deeper to the results of their experiment on cellular substrates for the difference between induced alpha activity (post-cue) and evoked alpha activity (post-stimulus). In their statistical analysis, the level of coherence between firing of various neurons and the local field potential was computed. This is called spike-field coherence SFC which measures phase synchronization between spikes and local field potential oscillations. SFC was determined for low frequency oscillations for both attended and unattended stimuli (figure 6-17). It was seen that in the delay period (post-cue/pre-stimulus), the SFC at low frequency in the attended stimuli was reduced on average by about 51 % compared to unattended condition (160 decreases, 23 increases). In contrast, in the post-stimulus period the SFC of low frequency at the attended stimulus was only reduced by 23% (142 decreases 42 increases). The net increase in SFC in the post-stimulus period compared to the delay period corresponds well to the previous idea that while in the delay period induced alpha activity is reduced in power over task-relevant areas, evoked alpha activity increases and is more phase-locked in the post-stimulus period.

6.2.2 Hypothesized mechanisms of alpha generation

Based on the aforementioned experimental data, we summarize the three basic types of observed alpha band rhythms as follows

- Emitted alpha activity is an expectancy signal which precedes stimulus and seems to become more time-ordered with task familiarity or learning.

- Induced alpha rhythms appear as sustained band power over task irrelevant areas while alpha desynchronization dominates over task-specific areas, presumably associated with a higher facilitation of the latter, or sustenance of inhibition in the former.

- Evoked alpha rhythms seem to correspond to the shift of oscillatory behavior in a task relevant area into a highly ordered, topologically-specific and cognitively-relevant signal.

In trying to understand the network mechanisms underlying different alpha rhythms, we will consider intrinsic properties of cortical columns as well as their main inputs that act to modulate and possibly change such properties.

Intrinsic mechanisms

1. Many layer 5 pyramidal cells have a post-inhibitory rebound mechanism which amplifies their depolarization after a hyperpolarizing input.

2. Layer 5 pyramidals are able to fire in a bursting mode at around 10 Hz if sufficient, but not excessive, drive is available at their apical dendritic system.

3. At least two varieties of inhibitory interneurons are available in layer 5 the activation of which seem complimentary under cholinergic input (Xiang et al 1998, [267]). Some fast spiking cells (FS) cells in layer 5 are hyperpolarized under cholinergic modulation; with layer 5 pyramidal cells being their main inhibited targets, this modulation has a net effect of decreasing intra-laminar (5 to 5) inhibition in layer 5. In contrast, low threshold spiking cells (LTS) are depolarized by acetylcholine and hence could be actively involved in inhibiting their targets. Since the axonal arbors of LTS cells cross into layers 2,3 and presumably inhibit pyramidal populations there, this condition contributes to inter-laminar (5 to 3) inhibition. Another possibility for intralaminar inhibition is through excitation of adapting interneurons in layers 2/3 by a strong pathway from deep layers (Dantzker et al 2000 [51]).

Cortical inputs:

1. Feedback and tonic modulating inputs arrive at superficial layers 1 and 2 as well as layer 5. These inputs have the dual role of modulating activity in the cortical column both during active processing (information transmission among

hierarchies of a sensory system) and during selective attention tasks (tonic activation)[8].

2. Feedforward and driving sensory inputs arrive at middle layers and interact with top-down feedback inputs to enhance specific cortical neural assemblies.

Rhythmogenesis of different alpha bands :

Based on the aforementioned electrophysiological observations, we claim that alpha rhythms evolve, based on our canonical circuit dynamics, as follows.

A. Induced alpha range oscillations are characterized by a decrease in bottom-up sensory stimuli in lower order systems (such as V1 and V2), and a minimal top-down facilitation mediated by either higher order systems or deeper brain nuclei , such as non-specific thalamic (Figure 6-18). These feedback inputs have a modulating effect which, while unable to generate strong activity in superficial layers of the cortex, are capable of driving a network of layer 5 pyramidal cells at 8-10 Hz by virtue of (a) low threshold currents in these cells, which contribute to augmenting responses in these cells and (b) low levels of inhibition in layer 5. This condition we believe corresponds to cases of induced alpha activity where eyes are closed. In this case, and while layer 5 pyramidals oscillate at alpha range, the synchronization is rather loose and hence a propagating type of activity occurs in cortical tissue (observed "epicenters" of activity).

During a cognitive task, the drop in induced alpha band power over task relevant areas (figure 6-13) is attributed to increase in attentional and arousal modulation of those areas. Such modulation, possibly mediated by arousal mechanisms (cholinergic inputs) results in further excitation of cortical layers, particularly layer 5 cells where depolarization will reduce the effects of low threshold currents, thus reducing after-hyperpolarization rebound properties, in many of those cells. Thus fewer cells are oscillating in the alpha range, and the total band power decreases.

B. Evoked alpha range oscillations are characterized by a time-locked recruitment of a specific layer 5 neural assembly or topology. A cortical column is generally passive in responding to a sensory input. This is seen by dominant inhibition upon stimulation of a specific thalamic afferent arriving into medial layers. Hence a sensory stimulus (or feedforward input) will create sufficient drive in those layer 5 cells whose apical system is primed (by higher order system) to generate a bursting behavior. This bursting activity, in turn is sufficient to reorganize local columnar activity (by activating LTS cross-laminar inhibition in layer 3), thus increasing signal-to-noise ratio in the system. This activity re-organization is expressed in a time-locked alpha activity (10-12 Hz

[8]The distinction in activation between active processing and attention assumes that attention could possibly rely on deep brain inputs such as afferents from the pulvinar and striatum while processing involves interaction between cortical systems

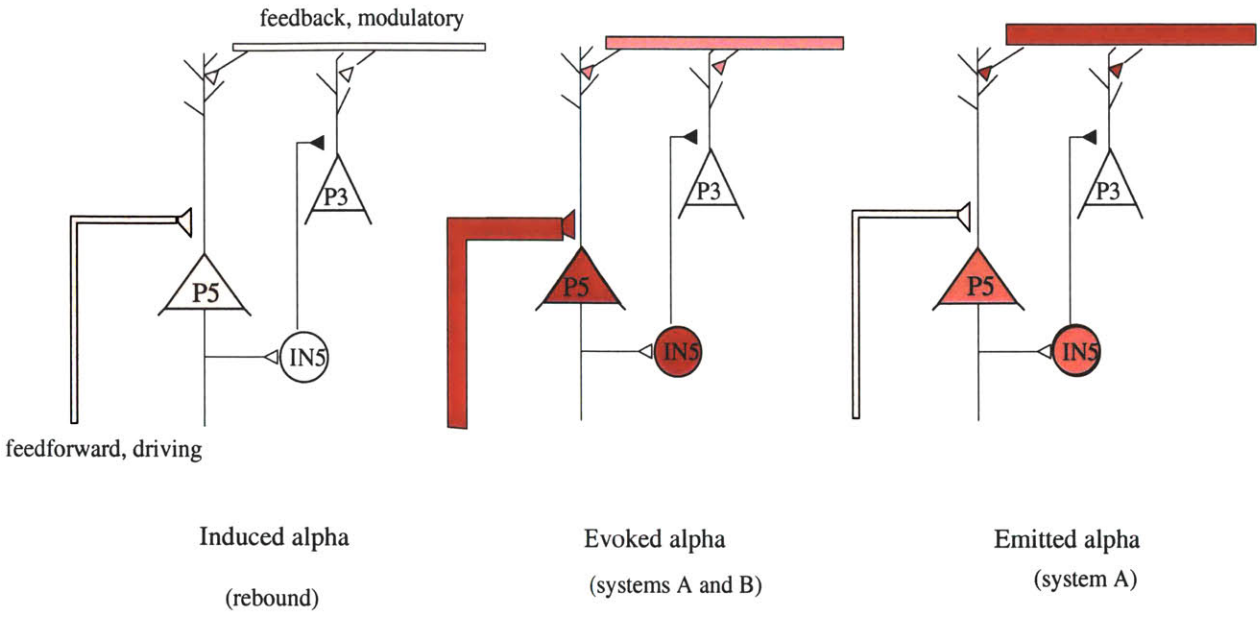

Figure 6-18: Hypothesized mechanisms for different alpha rhythms.

range) among specific neural assemblies and is thus more spatially restricted compared to induced alpha.

C. Emitted alpha range activity is a condition where higher order feedback mechanisms or top-down priming, such as those mediating attention are capable of actively burst-fire many layer 5 pyramidal cells thus improving synchronization between specific neural populations in a time-locked manner. The appearance of emitted alpha rhythms is possibly associated with the ability of a neural system to potentiate thalamocortical sensory systems in preparation for a specific expected sensory stimulus. The 10 Hz range oscillation has been associated with augmenting responses in cortical (Castro-Alamancos et al 1996 [29]) and thalamic systems (Bazhenov et al 1998 [14]) and serves to increase synaptic responses to incoming activity. The improvement in cellular selectivity with training (orientation identification) has been recently demonstrated in monkey primary visual cortex (V1), further corroborating the specificity of activated cellular assemblies with increasing task familiarity (Schoups et al 2001 [198]).

6.2.3 Simulations

In this section we will present minimal model simulations of induced, evoked and emitted alpha activity based on the hypothesized mechanisms of alpha generation.

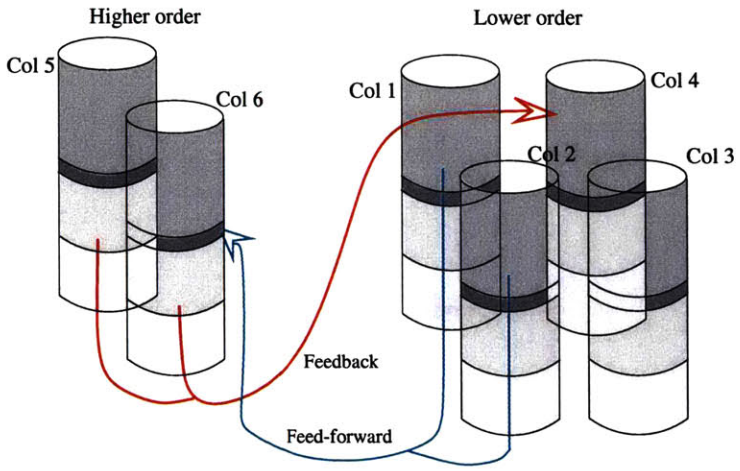

Figure 6-19: Minimal model of interacting hierarchies involved in generation of evoked and emitted alpha rhythms. It is assumed that both higher area (columns 5,6) and lower area (columns 1-4) have a granular layer 4, although this would not affect the simulation outcome

Induced alpha

A four column model is utilized with short-range inter-columnar connectivity assuming a local neural population (axonal delays of 2 ms). Intra-layer connectivity included E-E and E-I connections between cells in layers 2-6 (we also tested I-I connections, but those did not have a salient effect). Interlayer connectivity was the same as outlined earlier in the Chapter 5. Cortical input was simulated as both a randomly injected current to the soma of all neurons as well as a Poisson arriving spike trains of frequency 150 Hz arriving at excitatory synapses of all neurons. The strength of such input synapses were adjusted to give a firing rate of few spikes per second per neuron (as observed in vivo). The specific parameter values are given in the appendix.

Under conditions of low afferent excitation, the soma of layer 5 cells have a relatively hyperpolarized membrane potential ($\approx$ -70 mV). This might occur in vivo under neuronal silence, or rather more realistically, under a strong afference of inhibition onto the cell (dominance of inhibition idea, introduced earlier). Accordingly, and due to the existence of low threshold calcium current I_T and hyperpolarization-activated potassium current I_h, the cells tend to fire single action potentials in the 8 Hz range. This firing will in turn create sufficient depolarization to propagate in other layer 5 cells. The net result is a rhythmic firing of layer 5 cells in the low alpha band which is also propagated to other layers via interlaminar connections.

Evoked alpha

Using the model presented above, an increase in afferent excitation causes important changes in alpha band frequency and power. An increase in activity arriving in the middle layers 4, 5 representing sensory input from specific thalamic nuclei renders the system more excitable and hence more cells are able to fire. However, increase in the

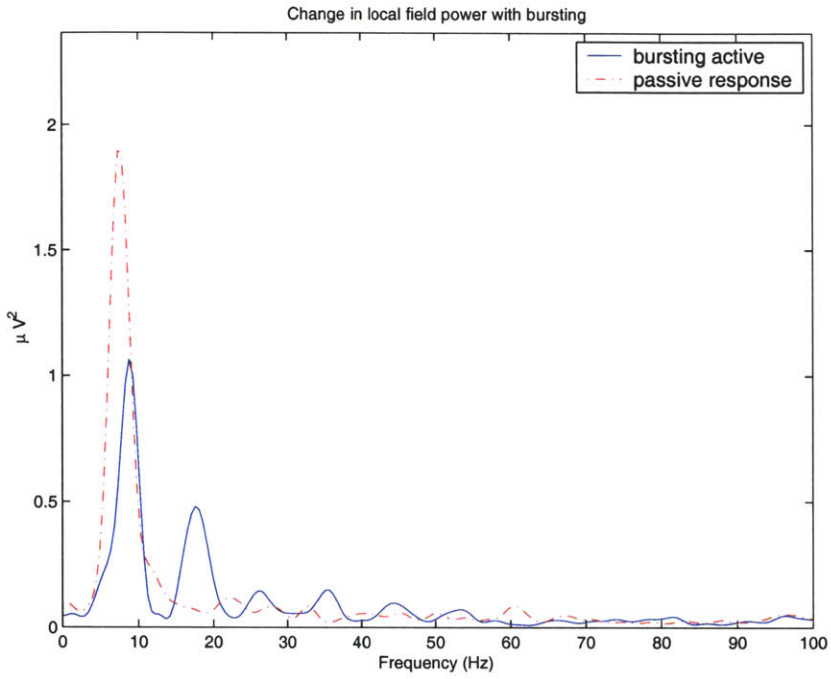

Figure 6-20: Change in alpha power under induced and evoked conditions. An induced alpha is a passive response (dashed lines) of layer 5 cells mainly due to rebound depolarization. Evoked alpha is a bursting response (solid lines) at a higher frequency. It is generated by subsets of neural populations, is characterized by improved noise reduction and a decrease in total alpha band power.

input arriving in superficial layers and targeting apical dendrites of layer 5 cells has a more potent effect. With sufficient input (representing feedback pathways or nonspecific thalamic afferents) can produce dendritic depolarization sufficient to cause specific subsets of layer 5 cells to burst. Thus, the specification of a bursting subset of neurons within a group "enabled" by feedback or nonspecific thalamic inputs is provided by coincident arrival of feedforward or specific thalamic inputs. The bursting subset, in some sense, forms at the intersection of the two aforementioned streams. with layer 5 burst firing representing an "AND" gating mechanism. Finally, the potency of this gate is controlled by dendritic disinhibition (zone C inputs to TL5), as will be described later.

While in a bursting regime, such subset of cells will actually fire at higher rates than the aforementioned induced rate (10-12 Hz bursts compared to 7-9 Hz of single action potentials. This effect is reflected in the total power spectrum of the field potential (figure 6-20). Equally important is the reduction in alpha power in the LFP since burst-firing reduced noise in the system[9] mainly through the action of interlaminar inhibition or the action of LTS interneurons on layer 3 pyramidal cells as well

[9]Noise in neural firing is thought to be response to external activity from neighboring neural populations or distant inputs. Hence it is a distractor since it carries no information about the stimulus

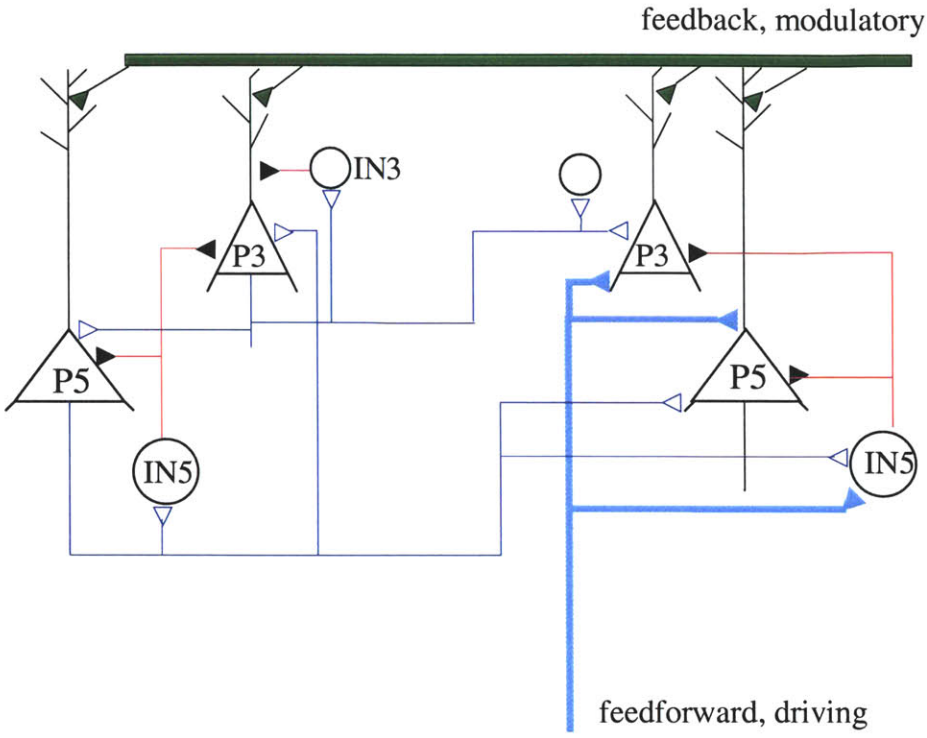

Figure 6-21: Schematic of local connectivity contributing to selectivity. For simplicity, intralaminar connections are drawn on the left only. Afferent inputs on th e right (connections are symmetrical).

as reduced activity in non-bursting columns. This simulation replicates experimental observations of increase of alpha frequency, and reduction in total alpha power in LFP under evoked conditions (discussed earlier).

Bursting in neural selectivity

To better understand the effect of bursting on alpha activity and selectivity of neural populations across hierarchies, we developed a minimal model of 4 columns representing a local neural population and 2 columns representing a higher order neural system (figure 6-19). Long range connectivity follows feedforward and feedback topologies as discussed in chapter 5. Local axonal delays were 2 msec while long-range axonal delays were 12 msec. Within a single area, an individual column consisted of only layers 5 and 3 with the intra-areal connectivity as shown in figure 6-21.

In a sample simulation, columns 1 and 2 were reciprocally connected with columns 5 and 6 of the higher order area. Accordingly, feedback projections are able to initiate bursting only in columns 1 and 2, while columns 3 and 4 are unable to burst-fire. Main results are as follows:

1. Noise reduction: figure 6-22 shows the resultant behavior of the four local columns when two shift into bursting at $t_o \approx 0.8$ sec (Col_1 and Col_2). Unlike the firing behavior prior to t_o, cell firing within each of those columns becomes more

uniform. More importantly, starting from lose synchronization between columns 1-4, *only* columns 1 and 2 lock into an oscillatory mode of firing with both cells in layers 3 and 5 coherently firing. In contrast, non-bursting columns 3 and 4 form a different assembly and which is not coherent with the Col_1-Col_2 group. Finally the synchronization between columns 1 and 2 occurs within 200 msec (at $t \approx 1$ sec) at which point layer 3 cells are well synchronized. It is plausible that this is an example of how evoked alpha activity occurs for the first few hundred milliseconds of an evoked response, and reflects the development of a coherent neural assembly before a switch to higher frequencies occur (via mechanisms yet to be determined, but see conclusions chapter for plausible scenarios).

2. Inter-areal oscillatory coherence: Plotting the spiking cross-correlation across different columns provides a clearer picture of the initiation of alpha band - oscillations. Figure 6-23 plots the correlation in firing between different columns (cross-correlation C). It shows that the resultant periodicity in the alpha range between columns 1 and 2 ($C_{1,2}$) and each of columns 1 and 2 and columns 5 and 6. In contrast, little or no periodic correlation is seen between columns 3, 4 and columns 1,2 or columns 5,6. In the frequency domain, it is seen that the maximum coherence between neural firing occurs in the alpha range and is again appreciable between columns 1 and 2 as well as between columns 1,2 and 5,6 (figure 6-24). Hence inter-areal oscillatory coherence in the alpha band occurs between specific local assemblies and higher order neural systems.

3. Inter-areal delays in the alpha band: while local connectivity results in near synchronous firing of neurons, long-range connections utilized represent significant axonal delay (12 msec). Hence, the inter-areal coherence shows a non-zero delay of cell firing between the two areas (around 8 msec- see figure 6-25). This is qualitatively similar to experimental observations of delays in alpha band coherence between levels in the hierarchy (cat experiments, figure 6-16).

Emitted alpha

The above simulations represented situations in which sufficient depolarization of apical dendrites of layer 5 cells (provided by feedback or top-down inputs) interact with incoming basal afferents (bottom-up inputs) to create topologically specific coherent assemblies. Emitted alpha, it may be argued, is an extreme case of top-down priming where assemblies of layer 5 cells undergo bursting merely due to strong convergent apical dendritic input. One can see how the above results (evoked alpha) can be reproduced for emitted alpha case but the simulations are not currently available.

Summary of simulations

Main results from these simulations are as follows:

1. Induced alpha activity is a characteristic frequency which occurs under low levels of excitation in a cortical column, a state distinguished by rebound behavior

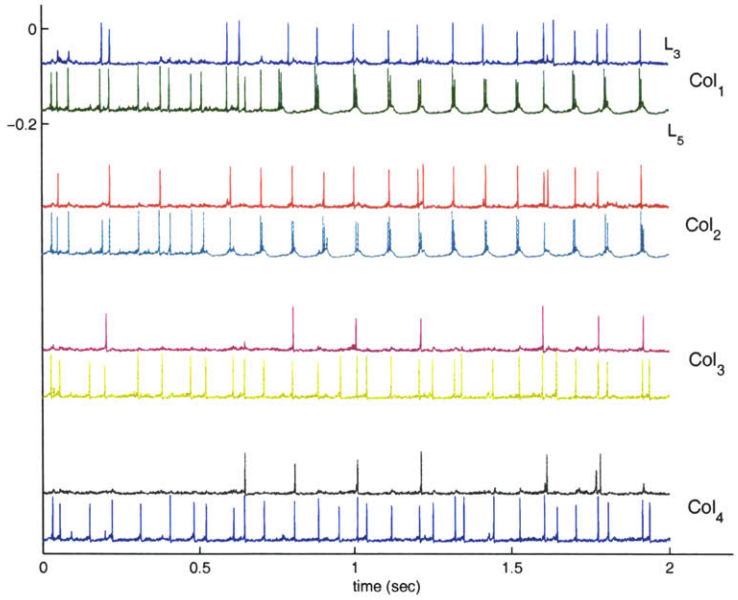

Figure 6-22: Neural selectivity of evoked (or emitted) alpha rhythms within local neural populations. After bursting commences in TL5 cells of columns 1 and 2 at about 0.8 sec, activity in these two columns is closely linked at an alpha band frequency and is dissociated from that in columns 3 and 4

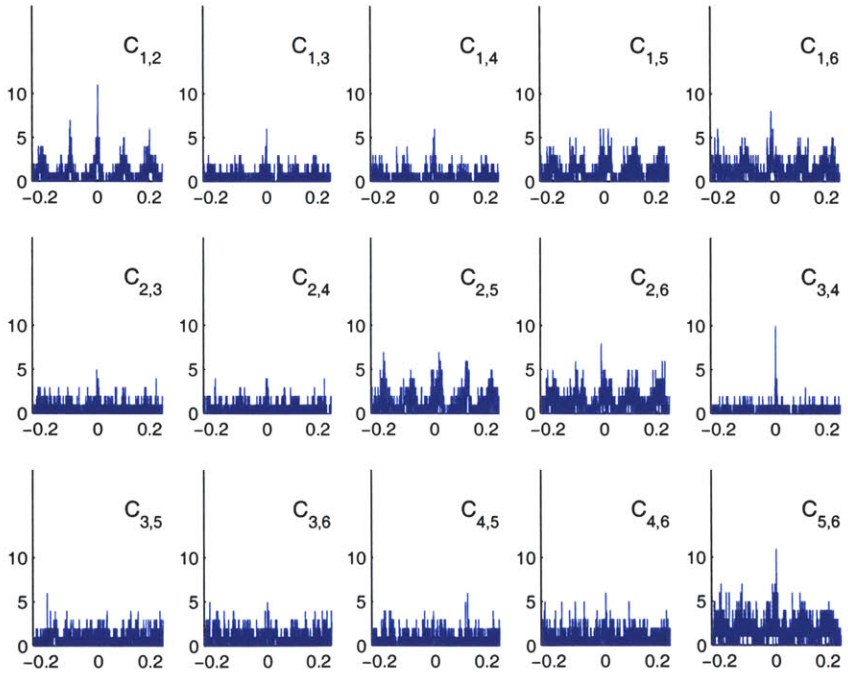

Figure 6-23: Cross correlation of firing patterns in various columns in the model after bursting commences. While periodicity is obvious in $C_{1,2}$ (peak around 100msec), little or no correlation is found in firing of columns 1 and 3,4 ($C_{1,3}$, $C_{1,4}$). Alpha range correlation is also observed between column 1 and columns of the connected higher order area (5 and 6).

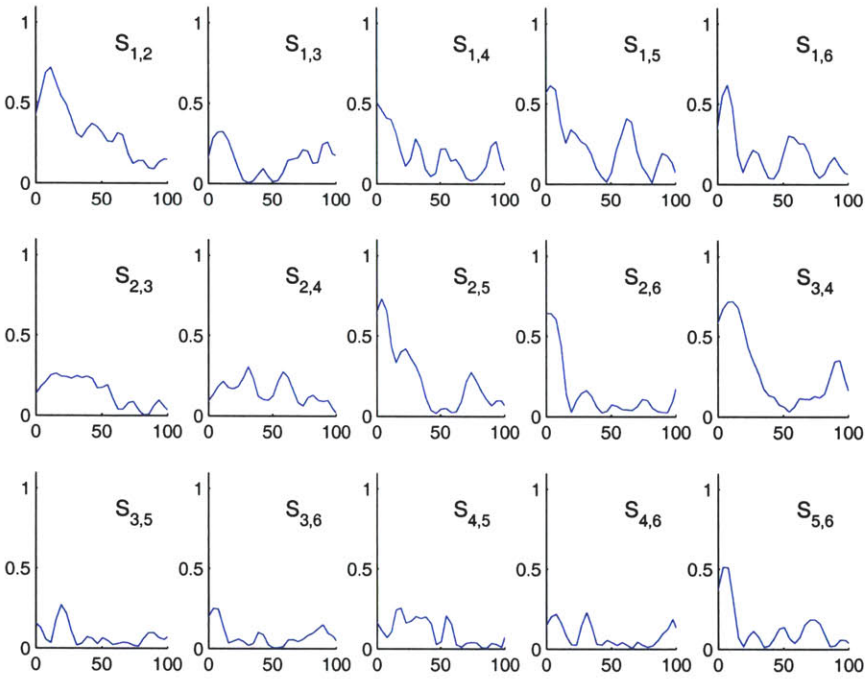

Figure 6-24: Increase in alpha band coherence between specified neural assemblies. Columns 1-4 are within local population limits. Columns 5 and 6 are part of a higher-order system (see text). Note the increased alpha-coherence between columns 1 and 2 ($S_{1,2} > 0.6$) that are responding with bursting to top-down influence. In contrast, decrease in coherence between columns 1, 2 and 3,4 is recorded. Finally $S_{1,5}$ and $S_{1,6}$ demonstrate an increased coherence between the local assembly and higher order assembly

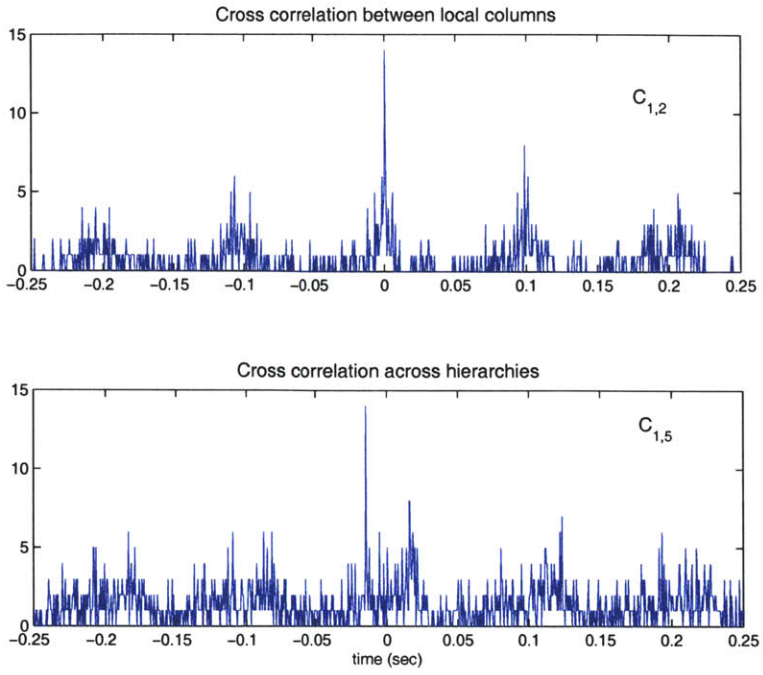

Figure 6-25: Alpha band coherence between hierarchies is not time locked. While local spike correlation at alpha frequency has an average delay of -0.1029 radians (1.6msec, computed from the power spectral density estimate). Spike correlation over hierarchies is +0.51 radians or 8.4 msec.

in layer 5 cells when sufficiently hyperpolarized by virtue of either low input drive or sustained inhibition. The subsequent low-threshold firing of these layer 5 cells will recruits other layers under a low-frequency alpha rhythm (7-9 Hz). In the absence of active recruitment, this can be thought of as a propagating event in the neural tissue.

2. Considering cross-modality experiments, the reduction in alpha power over task relevant areas is due to an increase in general excitation of that area. In the post-cue/pre-stimulus period, layer 5 cells switch from passively oscillating at 10 Hz into a gating mode where the dendritic zone is enabled. This mechanism allows sets the stage for developing evoked alpha oscillations in the transient period after stimulus presentation.

3. Evoked alpha activity is a phenomenon where neural selectivity takes place; that is, local neural assemblies are selectively activated by top-down influence which results in active bursting at 10-12 Hz. This transient phenomenon (1) causes synchronization of activated neural assemblies within a short period (200-500 msec) and (2) decouples activated assemblies from non-selected populations, thus is a mechanism of noise reduction and synchronization. This relates to the transient increased alpha coherence in humans before recognizing meaningful objects.

6.3 High Frequency Oscillations

We discussed in chapter 3 how high frequency activity in neural populations might be related to active processing in various cortical systems. Furthermore, we presented a flurry of experimental and computational investigations into the genesis of high frequency oscillations both at the cellular and network levels (firing and field potentials). These studies showed that such rhythms can be produced in a wide variety of cellular types making it difficult if not impossible to implicate specific types of neurons in producing fast rhythms (see section 3.2.6 for a detailed discussion). Still, an ever increasing body of literature continues to develop on this matter as this research is conducted.

While we will not attempt to make any specific predictions on the functional relevance of high frequency oscillations in our model, we will present how functional alpha oscillations ensuing transiently after a stimulus can develop into high frequency oscillations. In particular, we will discuss how evoked alpha activity might give way to an induced gamma activity within few hundred milliseconds after a stimulus presentation.

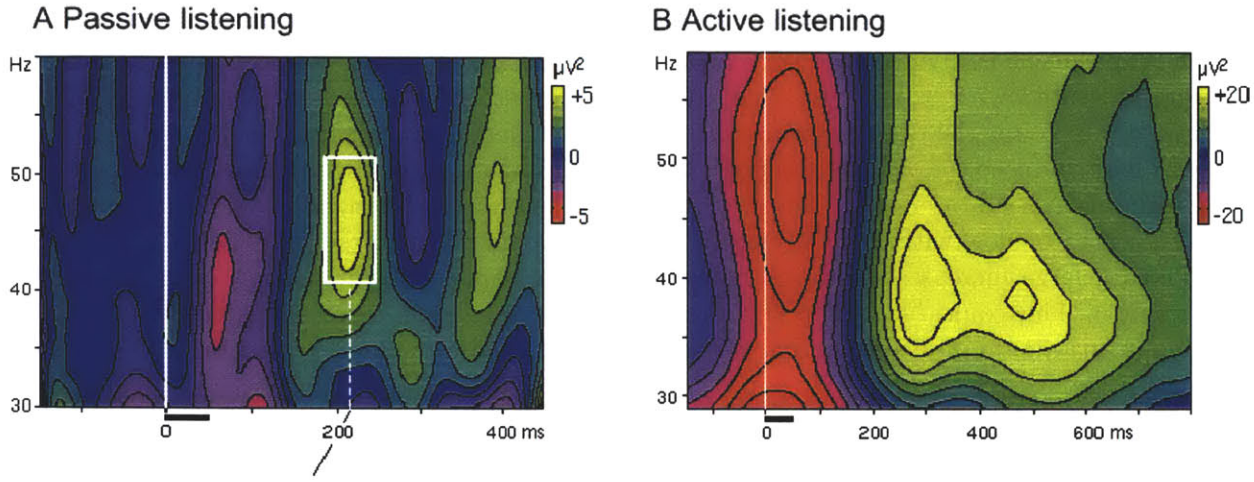

Figure 6-26: Induced gamma oscillations are increased by selective attention in humans. **A:** passive listening. Subject inadvertently listened to binaural stimuli (black bar) while watching a silent movie. Note reduction in power 80 msec after stimulus onset (red) and relative increase at 200 and 400 msec (yellow). **B:** active listening. Large gamma power is apparent compared to passive listening with peak around 300 msec and having a longer duration. Plots are of average time -frequency power distribution over vertex electrode (adapted from Tallon-Baudry 1999 [233]).

6.3.1 Physiological observations on induced gamma activity:

After stimulus onset, the transient evoked alpha activity soon develops into an increase in higher frequency oscillations, usually 100-300 msec post-stimulus. Such gamma range activity was observed in the aforementioned experiments by basar et

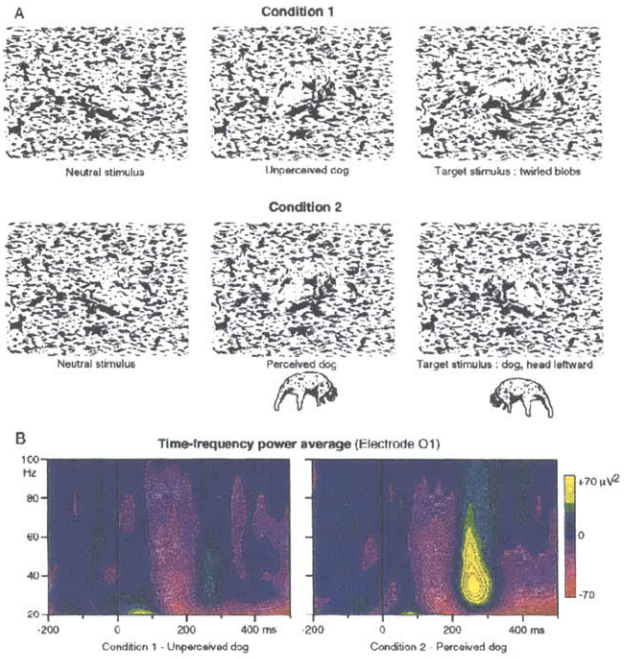

Figure 6-27: Induced gamma activity is enhanced by experience and top-down activation. The experiment is divided into two conditions. In the first (*A, top row*), Naive subjects were presented with 3 pictures. The first two were perceived as meaningless blobs. The task was to count the occurrence of twirl target stimulus (*A, top right*). In this condition, only faint induced gamma is observed, (*B, left*). Subjects were then trained to perceive the dog with head oriented to left or right. In the second condition, their task is to count occurrences of dog with head oriented leftward. Compared to first condition, this task showed a large increase in induced gamma power in response to all stimuli (even neutral stimulus). This could reflect top down activation of the internal representation of the dog. Finally, maximum induced gamma was recorded in response the target stimulus *A, bottom right*).

al in humans (Schurmann and Basar 2001 [201], Basar et al 2001 [13]) as well in the cat experiment (Von Stein et al 2000 [250]). A good review on gamma oscillations in humans is given by Tallon-Baudry and Bertrand in 1999 [233]. Here, the post-alpha high frequency activity is termed *"induced gamma"* oscillation, and is observed to occur about 200 msec after a stimulus onset in various experimental paradigms in sensory systems. *Induced gamma activity is not phase-locked to the stimulus* but its latency jitters from trial to trial [10]. Several properties of this induced gamma activity point to its role in object representation in different brain areas. Of these, we mention:

[10]This definition of induced gamma is similar to that of induced alpha we discussed earlier, that is, it is internally generated by network mechanisms and is not directly aligned with a stimulus arrival. Similarly, evoked gamma resembles evoked alpha in its phase-locking to the stimulus and is repeatable across trials, but will not be discussed here.

1. *Detection tasks:* Induced gamma in the 40 Hz range appeared in scalp EEG recordings, 200 msec after electrical stimulation of the finger in a sensory discrimination task. Also, strength of induced alpha increased 200-400 msec poststimulus in a simple auditory discrimination task.

2. *Feature binding and segmentation:* Induced gamma activity is increased in response to coherent (behaviorally meaningful) versus non-coherent visual stimuli. A short lasting enhancement of EEG in the gamma range was observed around 280 msec after stimulus onset in response to coherent triangle shape stimulus only. Similarly, a peak in induced gamma was observed 230 msec after the presentation of human faces with a much higher response to upright pictures than that for inverted pictures.

   Gamma oscillations might correspond to a successful segmentation of contours from background activity in visual tasks. Gail et al 2000 [83] showed, using intracortical recordings of LFP and multiunit activity in monkey striate cortex, a decoupling in late LFP gamma band activity ($>$ 190 msec latency) recorded from neurons representing figure and ground. This, one can argue, is a direct description of the role of induced gamma activity in binding neural populations into coherent assemblies representing visual features.

3. *Attentional modulation:* Induced gamma activity could reflect increases in attention to presented stimuli. In a passive listening experiment in humans, Tallon-Baudry et al [233] observed a reduction (around 100 msec) of gamma activity power followed by an increase (peaking around 250 msec) in this power compared with pre-stimulus baseline activity (figure 6-26, A) [11]. While actively listening, however, the increase in gamma strength was enhanced and prolonged reflecting active modulation by attention (figure 6-26, B). Experiments on the attentional modulation of intracortical recordings in visual cortex of monkeys provide a qualitatively similar time-line of attentional effects (Mehta et al 2000 [156, 157]). While the initial cortical activity (firing) in response to visual stimulus is unaltered between attentive and passive states in the first 100 msec, this activity is increased considerably 100-300 msec after an attended response.

4. *Internal representation:* Induced gamma activity is enhanced when a trained subject rehearses internally the existence of a stimulus (Tallon-Baudry et al 1997 [232]). In trying to detect a hidden object in a picture, naive subjects who did not perceive the hidden object showed only a weak increase in gamma response around 280 msec post-stimulus (figure 6-27, B left). Once those subjects are trained to perceive and detect the hidden object (dog picture), a much larger induced gamma was recorded, irrespective of whether the hidden object exists in the picture or not. This, they interpret as an improved top-down mediated internal representation of the stimulus.

[11] Similar pattern was observed over the auditory cortex in rats.

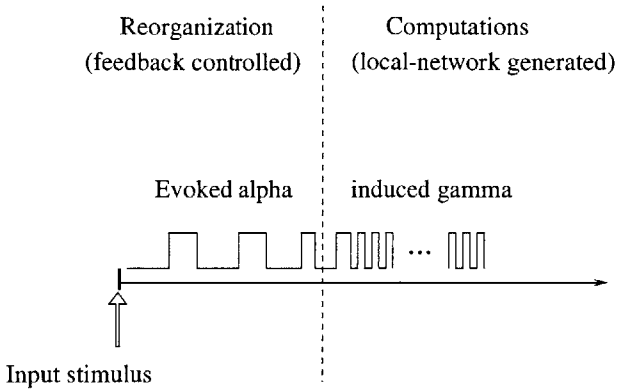

Figure 6-28: Time line for the switch between evoked alpha and induced gamma oscillations. After an input stimulus, evoked alpha oscillations dominate and are characteristic of feedback reorganization of local neural assemblies by higher order input. This will then create novel assemblies, upon receiving sufficient excitation, which oscillate in the gamma band.

6.3.2 Hypothesized mechanism

We will follow up on the role of evoked alpha activity in reorganizing local neural assemblies to propose that this reorganization leads to generation of induced gamma activity in this now coherently-oscillating population. A schematic summary of the post-stimulus activity based on the above observations is given in figure 6-28.

1. A feedforward sensory stimulus to a cortical area arrives in the middle layers and creates an initial map of activation in local cortical columns. This initial map is based mostly on local connectivity within layer 4 (and layer 6) and, as observed in some experiments, might be expressed by a stimulus-locked, short lived gamma activity ($<$ 100msec). The same map is transfered to layers 3 and 5 but creates minimal excitation in the absence of attentional modulation. In particular, tufted layer 5 cells will be able to fire only in single action potentials but not in bursts. At the network level, this might cause occasional periods of short lived gamma activity with no immediate cognitive relevance (passive listening experiment, figure 6-26, A).

2. A top-down, feedback, modulatory input arrives in the superficial layers of the cortex and provides a secondary map of activation. Consequently, TL5 cells receiving both initial feedforward map and the secondary feedback map will burst fire (at high alpha frequeny) with creation of a spatially distributed map in layer 5. As discussed earlier (section 6.2.3), the now-bursting layer 5 population reinforces activity in associated superficial layers populations (P3, within bursting column) while inhibiting the surrounding populations (P3, outside bursting column)[12]. This might be reflected by the decrease in gamma power during 50 -200

[12]Recall that reinforcement is provided by excitatory P5-P3 connections, inhibition by intralaminar P5-P3 inhibitory pathways.

msec period poststimulus in figures 6-26 and 6-27.

3. The reinforced maps of pyramidal cells in superficial layers are now sufficiently excited to fire at a high frequency by virtue of increased excitation. Furthermore, synchronization is achieved at a characteristic gamma-range frequency by virtue of interneurons (Traub-like mechanisms, electric gap junctions among interneurons). This is the period of induced gamma oscillations observed in experiments (as in figure 6-26). Its latency depends on initial conditions in layer 3 cells as well as strength of influence from top-down inputs, and hence is varying. In this period, all cortical layers are engaged in specific computational tasks we will avoid making concrete statements about.

4. Bursting TL5 cells now switch into regular spiking high frequency mode. This can be achieved by either or a combination of the following factors:

   a. The ionic mechanisms leading to burst firing in a TL5 cell are controlled by modulating inputs associated with attention and arousal (such as Norepinephrine NE, and Acetylcholine ACh as observed by Wang and McCormick 1993 [252]). An increase of such neuromodulators leads *to an increase in the frequency of burst firing and a subsequent switch to regular firing mode* (figure 6-29). Furthermore, hyperpolarizing the cell will switch its firing mode from regular back to burst firing. Thus, it is plausible that during the evoked alpha period, such modulating inputs are increased, facilitating higher bursting frequency (high alpha 12-15 Hz) and then switching the firing mode to regularly spiking. TL5 cells in RS mode are then actively involved in local computations at gamma frequencies. Finally, the burst firing mode can be recovered subsequently, as seen in slices, by injecting a negative current which hyperpolarizes the cell. This can occur in vivo by means of active inhibition associated with the basal zone of TL5, as seen earlier during augmenting responses experiments.

   b. The dissociation of basal and apical zones (zones A and B) in a TL5 cell by activation of dendritic inhibition targeting zone C of that cell. Since this zone (apical obliques) lies in the middle layers (lower layer 3, layer 4), it is plausible that the interneurons lying in that zone are contacted by pyramidal cells in layer 3. Consequently, high frequency firing in P3 creates sufficient input to such interneurons, which will then inhibit zone C in TL5 and prevent it from burst -firing.

   c. A bursting TL5 cell can switch intrinsically from bursting to regular-firing mode upon sufficient activation of its apical dendrites (zone A inputs[13], Schwindt et al 1999 [204], see also figure 4-6). This is also plausible since superficial layers are now highly excitable and can exert strong synaptic input to zone A of TL5 cells.

[13]Strong synaptic inputs to zone A are though to cause a plateau Ca^{2+} action potential in the dendrites, as we saw in earlier chapters.

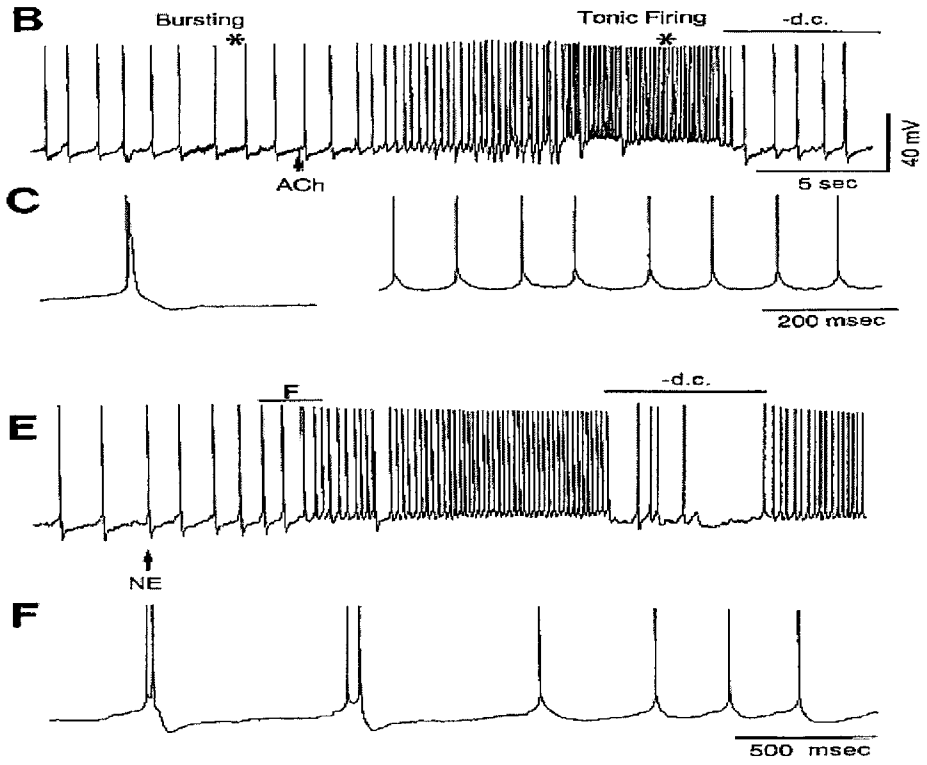

Figure 6-29: Neuromodulators can change the firing mode of large layer 5 cell. B: Intracellular recordings show that injection of acetylcholine (ACh) causes an increase in the rate of rhythmic bursting followed by a switch to regularly spiking mode (asterisks expanded in C). Injection of a hyperpolarizing current negates the effect of ACh and the cell switches back to bursting. E: Similar behavior results by applying Norepinephrine NE to another cell, which increases the rate of doublet firing and causes a switch to RS mode. (figure from Wang and McCormick 1993[252])

5. With TL5 cells in RS mode, these cells are involved in local computations (high frequency) as well as in the output to other areas and deeper systems of the brain. Finally, TL5 cells can switch back to bursting-capable by negating the factors causing mode switching, i.e, either by hyperpolarization caused by inhibitory action at zone B, cessation of inhibitory action on zone C, or decrease of apical input at zone A.

6.3.3 Simulations

The minimal model used in these simulations is the same as that used for the neuronal selectivity example (previous section, see figure 6-19). That is, we utilized 4 columns representing a local cortical area and 2 columns representing a higher order cortical system. Each column was composed of layers 3 and 5 as well as a P5-P3 inhibitory pathway. A schematic of connectivity between two columns is shown in figure 6-30. As a TL5 cell bursts, we assume that the switch to RS mode occurs by action of

inhibitory neurons in the middle layers (zone C) that become active as pyramidals in P3 are engaged at high frequency.

Results

As shown in figure 6-31, TL5 cells in columns 1 and 2 go into bursting shortly after a stimulus due to feedback inputs. Bursting, in turn, will sculpt the activity in layer 3 of the respective columns, but will inhibit layer 3 of other columns from participating in the assembly by virtue of interlaminar inhibition. This is essentially the same behavior we observed in discussing neural selectivity reflected by evoked alpha activity[14].

Shortly after, pyramidal populations P3 cells have received enough excitation by virtue of their recurrent connections as well as feedback from layer 5 to fire more rapidly. This will drive interneurons of the middle layers INC to fire. Since we assumed that INC target zone C of TL5 cells, TL5 will then switch into a regularly firing pattern (around 350 msec after bursting commences). At this time, strong recurrent excitation between P3 as well as feedback from layer 5 will create coherent gamma range firing in columns 1 and 2, but not in columns 3 and 4.

Note also that the period of evoked alpha (200-650msec) is characterized by low gamma frequency content (compare with figure 6-26). It is this decisive period which allows reorganization of relevant cortical assemblies. We predict that the length of such period will decrease with improved task performance, as well as heightened internal expectations.

[14]We will present a more generic explanation of this behavior when we discuss information transfer between cortical hierarchies in the Conclusions chapter, see section 7.2.2.

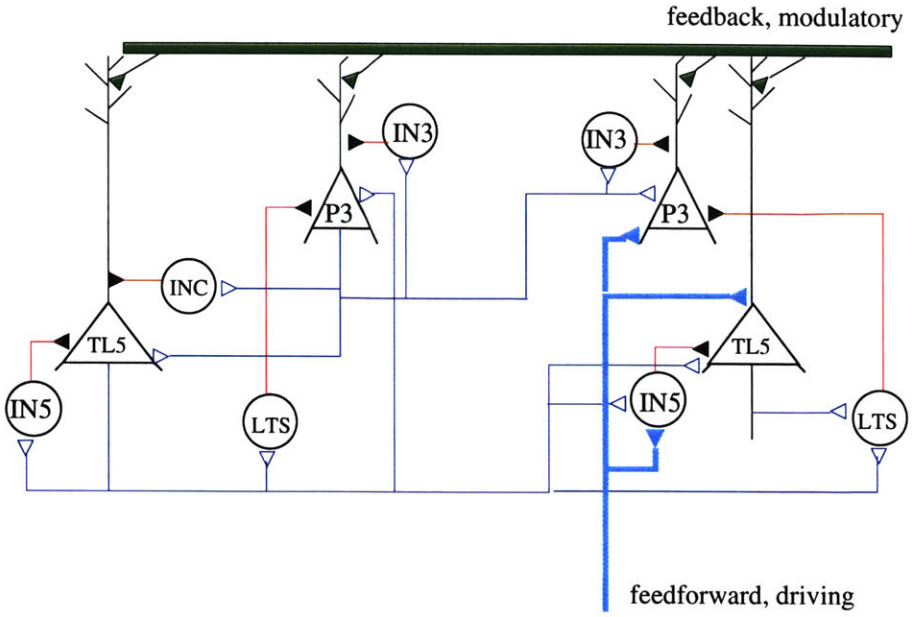

Figure 6-30: Connection diagram between populations in layers 3 and 5 in a local area. We assumed the existence of an inhibitory interneuron INC which is activated upon sufficient excitation in P3. This interneuron provides mid zone C inhibition to TL5, thus causing switch from bursting regularly spiking (see text). Connectivity between columns is symmetrical, although not fully sketched.

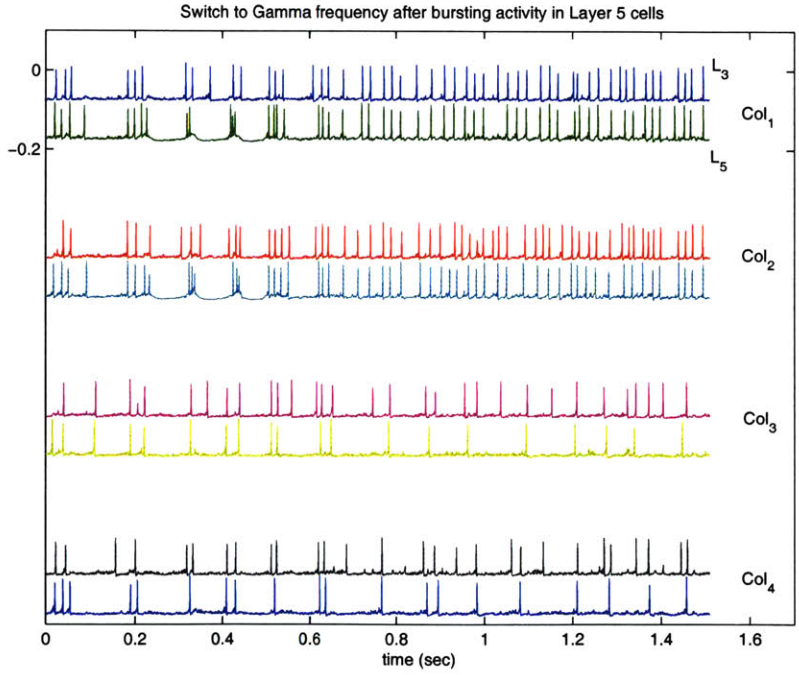

Figure 6-31: Activity in a minimal model of evoked alpha switching to induced gamma firing. While columns 1 and 2 form a neural assembly (coherent firing in the gamma range), columns 3 and 4 are excluded from that assembly, and hence fire at a lower frequency with loose synchrony between layers 3 and 5.

6.4 Slow-wave Sleep Oscillations

The preceding simulations illustrated the functional behavior of layer 5 cells during awake states and their consequences on cortical communications. We will now present the behavior of such cells under states of sleep, and later under the pathologic state of disinhibition.

The experiments of Sanchez-Vives and McCormick provided evidence on the genesis of slow-wave type oscillation even in slices: in a slice preparation of ferret neocortex maintained in vitro, slow wave oscillations were observed when slices were placed in a bathing solution similar to ionic composition in situ (Sanchez-Vives and McCormick 2000, [193]). The oscillations were seen to originate in layer 5 and propagate to layer 6 and then superficial layers 2/3.

The oscillation is characterized by an up state where all cells are active firing action potentials and a down state where hyperpolarization characterized by neuronal silence and decreased excitability occur. This hyperpolarization appears to be a refractory period due to intrinsic mechanisms such as activation of slow potassium conductances (see chapter 3 on oscillations). The slow oscillatory activity is sustained in slices containing layers 5/6 whereas slices containing the superficial layers only generated weak or no oscillations. Furthermore, slices that were less than 0.5mm-1mm in width were still able to generate slow oscillations suggesting that this rhythm may occur within few cortical columns.

Hyperpolarization or depolarization of individual neurons mildly changes the frequency of the slow oscillation in the recorded neuron suggesting that the slow oscillation is a network phenomenon and not due to intrinsic mechanisms. Although the frequency increased marginally when the cell was hyperpolarized ($0.5 \bar{+} 0.15$ Hz depolarized compared to $0.54 \bar{+} 0.13$ Hz hyperpolarized), this might possibly point to the intrinsic behavior of this cell which causes it to recover fast after stronger hyperpolarization due to activation of rebound excitation as observed in augmenting responses.

The slow oscillation exhibited a refractory period for several seconds where the cellular population is disfacilitated and less responsive to excitatory inputs. Although the excitatory neurotransmiter glutamate can evoke slow oscillations in slices alone similar to spontaneously-occurring cycles, application of glutamate immediately following a spontaneous up state significantly reduced the evoked response due to glutamate alone (figure 3-9, repeated here in figure 6-32). This disfacilitation could again be an exaggeration of disfacilitation of augmenting response in layer 5 cells after prolonged depolarization occurs.

Finally, wave propagation in the slice was much slower than that occurring in vivo. This might be due to lack of cortico-cortical connections (and possibly the role of cortico-thalamic connectivity in reinforcing activity).

This case was replicated in a minimal model where the up and down states of a slow wave rhythm can be observed, with layer 5 pyramidals firing action potentials after periods of hyperpolarization.

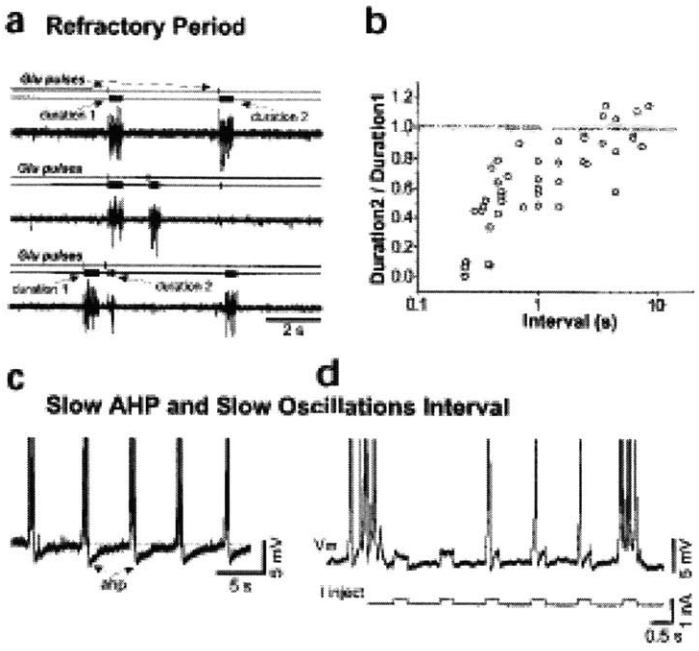

Figure 6-32: Refractory period of slow oscillations in cortical slices where cellular excitability is markedly decreased. A. Application of glutamate causes episodes of cell firing as those occurring spontaneously, the duration of which decreases if inter-application interval is decreased (plotted in B). C. After-hyperpolarization (AHP) occurs in cells after periods of firing. The combined effect of disfacilitation and disfacilitation shows marked decrease in cell response to periodic trains of current after periods of firing, as shown on the right (figure is reproduced from Sanchez-vives and McCormick 2000 [193])

6.4.1 Hypothesized mechanisms

As we have presented earlier, a slow wave sleep rhythm ($< 1Hz$) is characterized by a prolonged period of depolarization (1 sec) where cell firing can be either grouped into spindle, delta or fast rhythms, and followed by a period of hyperpolarization (0.5 sec) of neuronal silence. We will adopt much of the known assumptions on these mechanisms (Timofeev et al 2000 [238], Sanchez-Vives et al 2000 [193], Steriade et al 1993a [216]), and emphasize the role of layer 5 cells.

1. Layer 5 pyramidal cells amplify incoming depolarizing signals, including spontaneous postsynaptic currents (sEPSC), especially through the interaction of low-threshold currents that we observed under hyperpolarization in augmenting responses[15].

2. Layer 5 cell membrane contains ion channels which support persistent sodium current $I_{Na,p}$ (Stafstrom et al 1985 [214]). The existence of such currents non-

[15]A spontaneous postsynaptic current (sEPSC) is a non-induced opening of channels in the cell membrane which caused current influx through the membrane.

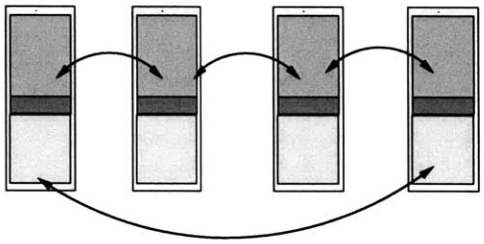

Figure 6-33: Schematic of a chain of 4 connected columns, representing a local region, used to generate slow wave-like patterns

linearly amplifies spontaneous depolarizing events in neural membrane (as suggested by Timofeev et al 2000 [238]). Thus as a consequence, layer 5 cells are more capable of initiating firing in periods of neuronal silence characterized by cell membrane hyperpolarization.

3. While activity is usually initiated in layer 5, it is transfered to superficial layers via layer 5 to layer 3 connections. The latter then provides for propagation of events over large cortical areas and hence provides the neural substrate necessary for perpetuating the ensuing depolarized or up state for prolonged periods of time (one or more seconds).

4. The down state in all cells is due to activation of slow Ca^{+2}-dependent hyperpolarizing potassium currents as well as decrease in synaptic efficacy (Massimini et al 2001 [150]).

6.4.2 Simulations

A minimal model of slow wave sleep generation was developed. A group of 4 columns were connected in a recurrent chain pattern as shown in figure 6-33 with synaptic delays of 3 msec between individual columns replicating local connectivity. Afferent input to each neuron was modeled as a Poisson arriving spikes with constant rate which was adjusted so as no firing was possible in regularly spiking pyramidal cells. AMPA, NMDA and $GABA_A$, $GABA_B$ receptor types were included in each pyramidal cell as outlined in the modeling chapter.

Using synaptic strength presented in the appendix, a slow recurring rhythm of depolarization (neural firing)/hyperpolarization (neural silence) sequences is produced as shown in figure 6-34.

Looking at the neural firing patterns it is seen that layer 5 cells initiate firing after periods of silence in the corresponding columns (figure 6-35) which then propagates to other layers and reinforced by recurrent excitation.

In developing this model, several assumptions were taken as follows.

1. Model scale: since slow wave rhythms are generated by the collective behavior of large neural populations with no or little external afferents, it is impractical to look for a minimal model which replicates observed data faithfully. In particular,

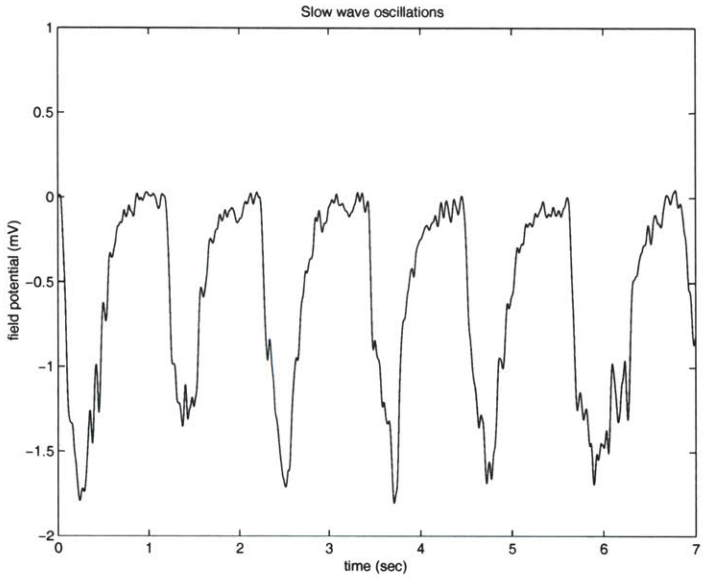

Figure 6-34: Slow rhythmic EEG activity generated by the minimal cortical model.

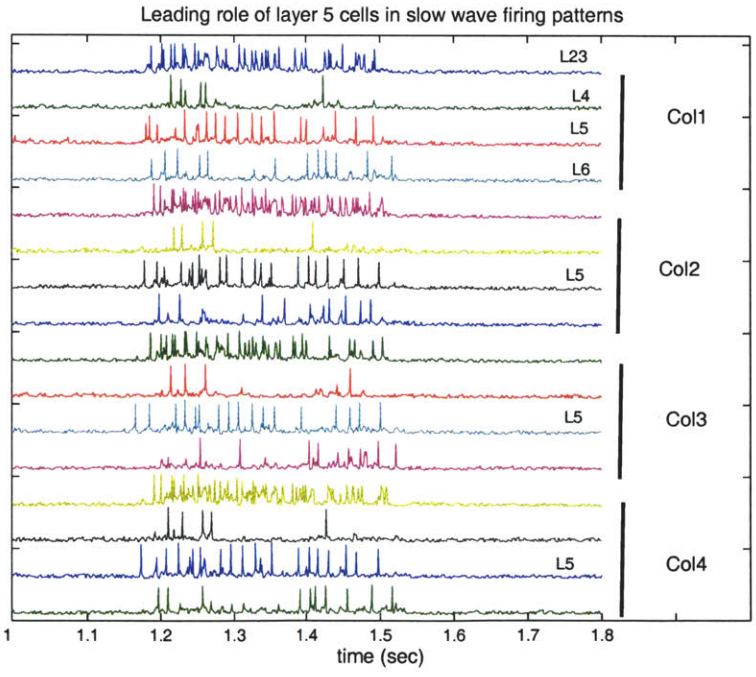

Figure 6-35: Cellular firing the cortical columns in initiated in layer 5 and propagated to other layers.

the ability to initiate a depolarizing phase depends on the probability of layer 5 cells to fire an action potential spontaneously. In a large neural population, therefore, this probability dramatically increases (as was seen in simulations of Timofeev et al). Further, a large neural population can sustain a depolarizing envelop over hundreds of milliseconds since neural tissue is subjected to a large number of synaptic input causing cell membrane to be fairly depolarized over that interval and firing few action potentials over a depolarizing cycle. In a minimal model, we can reproduce this effect only by having individual cells firing much faster, essentially reproducing a collective behavior of a large number of cells. The effect of propagating depolarizing was is recreated by connecting the columns of the model in a circular chain.

2. Ionic currents: while we assume ionic currents to aid in amplifying and diminishing activity in the overall network, only the effects of such currents were included. In particular, persistent sodium currents were not included, rather an afferent input of constant amplitude and rate was injected to each neuron in the model. While such input is unable to fire regular pyramidal cells, layer 5 cells are more excitable under the same input strength and hence will initiate action potentials after periods of silence. Second, the cessation of activity is modeled by a slowly hyperpolarizing current which is an approximation of the composite effect of synaptic disfacilitation and hyperpolarizing currents.

6.5 Seizures due to Neocortical Disinhibition

We will present in this section how our model might explain the pathologic seizure behavior under disinhibition as a obtained in a recent experiment by Castro-Alamancos in 2000 [32]. In this manipulation in rats, and starting from a slow wave sleep stage, neocortical inhibition was blocked in stages, first under fast inhibition blockade ($GABA_A$ antagonists) and then under slow inhibition blockade ($GABA_B$ antagonists). The author obtained extracellular and intracellular data as well as current source density profiles of the emergent activity. The model will show similar qualitative results in agreement with the effect of blocking inhibition in a neocortical group of columns, keeping in mind the limitation of scalability of a small simulated system in terms of synaptic strength, afferent drive and effects of averaging when compared with full-scaled models.

The development of seizure-like patterns of oscillations in the neocortex have been studied extensively by Steriade and others (chapter 3). Such seizure behavior is characterized by what is called paroxysmal depolarizing shifts (PDSs) in cellular potentials. PDS is a phenomenon where, due to excessive excitation into a cell, very fast spiking behavior occurs riding on a highly depolarized membrane potential which leads to spike inactivation (mainly due to Na^+ channel inactivation) and terminating possibly due to intrinsic repolarizing conductances (see figure 6-36). PDSs are reflected in field potential recordings as large amplitude spikes and are usually followed by a wave shape indicating the subsequent hyperpolarization. The propensity of thalamic and neocortical systems to produce seizure-like activity has been reported in slices (Chagnac-Amitai 1989 [36], Calixto 2000 [27]) and in vivo due to disinhibition as well as increased recurrent excitation (mainly through NMDA receptors). An excellent review is given in McCormick and Contreras 2001 [155].

6.5.1 Main physiological observations

The aforementioned experiment by Castro-Alamancos (Castro-Alamancos 2000, [32]) investigates the origins of neocortical synchronized oscillations after disinhibition in vivo. Here, slow wave sleep oscillations in ketamine-anesthetized rats were transformed into a large amplitude 1 Hz spike and wave oscillations after application of BMI, a specific blocker of the fast inhibitory $GABA_A$ receptor type. As seen in figure 6-37, increasing blockade of these $GABA_A$ receptors, the 1 Hz discharges also contained few low-amplitude spikes at 10 Hz (7-14 Hz). Finally, applying $GABA_B$ blockers slows down the 1 Hz oscillation to 0.5 Hz and increments the number of low amplitude 10 Hz discharges that ultimately terminate in a prolonged period of silence. Several important observations resulted from this experiment.

1. The oscillations are cortically generated since they persist with inactivation of the thalamus. While the initial large discharge can occur in either the upper of lower layers of the cortex (24% and 76 % of the time, respectively), *only the lower layers (5,6) could trigger this discharge in the absence of the thalamus*, hence reflecting that thalamic feedback is important for discharges to originate

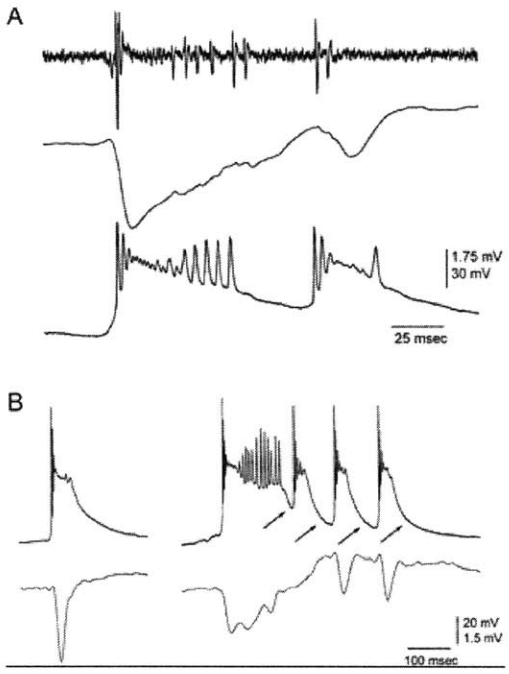

Figure 6-36: Cellular recordings of neocortical activity under disinhibition. *A*, Paroxysmal depolarization Shifts under GABA-A blockade : single unit, field potential, and intracellular recording. *B* PDS under blockade of all inhibition (from Castro-Alamancos 2000).

Figure 6-37: Effect of blocking neocortical inhibitory mechanisms in Ketamine-anesthetized rats. *Trace 1*: slow wave oscillations under ketamine anesthesia. *Traces 2 and 3*: Effect of incrementally blocking GABA-A receptors. *Trace 4* : GABA-B receptors are also blocked in addition to GABA-A receptors (Figure from Castro-Alamancos 2000

in the upper layers (2,3). This initial discharge is propagated from the layer of origin (2,3 or 5,6) into upper layer 5/ layer 4.

2. The subsequent 10 Hz low-amplitude discharges *always* originated in lower layer 5 /upper layer 6, and subsequently jumped to upper layers 2/3. This was confirmed using current source density analysis as well as intracellular recordings. These 10 Hz discharges consisted of PDS bursts at 10 Hz with an increasing repolarizing component that eventually shuts off the bursting due possibly to hyperpolarizing potassium conductances (figure 6-36).

3. The lower layers are maximally sensitive prior to the initial discharge, since depolarization of cells in these layers produced enhanced activity immediately before each PDS. In experiments on seizure propagation, layer 5 was most sensitive to reduction of inhibition in neocortical slices, and at moderate levels of disinhibition, most effective is seizure spread (Telfeian et al 1998 [235]).

4. Disinhibition in the cortex results in different behavior than that in the thalamus. While thalamic application of $GABA_A$ blockers BMI result in 3Hz spike and wave seizures shifting the frequency of slow wave oscillations higher, BMI application in the neocortex does not shift the frequency but rather enhances it by producing large amplitude PDSs at 1Hz. Also, while $GABA_B$ blockers application in the thalamus abolishes 3Hz seizures, it results in an increase of discharges in the neocortex.

6.5.2 Hypothesized circuit dynamics

The proceeding experiment was replicated qualitatively in a minimal model of cortical interaction. Our hypothesis upon which the simulation is based as to how these seizures are generated is the following:

1. The rebound from prolonged periods of silence is due to the high excitability of layer 5 cells. This rebound behavior has been demonstrated in slow wave sleep where L5 cells lead other cells after silence periods (Sanchez-Vives and McCormick 2000 [193]) as well as during augmenting responses. In the current experiment, lower layer cells were shown to initiate activity when the thalamus was deactivated (observation 2 above). This assertion follows our previous arguments on layer 5 excitability, mainly:

   a. Some layer 5 cells are known to have post-inhibitory rebound behavior, and could be highly responsive after periods of inhibition induced by thalamic stimulation.

   b. Layer 5 cells also have a persistent sodium current which amplifies inputs when active (Stafstrom et al 1985 [214]).

   c. Some layer 5 cells were also shown to have strong propensity to burst (so called low threshold bursters), accounting for about 10% of cells in layer 5 pyramidals in rat sensorimotor cortex (Schwindt et al 1997 [202]).

d. Finally, some experiments implied a low level of inhibition in this layer which makes it ideal for amplifying small inputs.

All the above factors make layer 5 a very probable cite of pathologic rhythm genesis under disinhibition. In fact, one genetic model of absence epilepsy in rats demonstrated that layer 5 pyramidals have increased excitability and inward rectification (di Pasquale et al 1997,[65]). Also, Khazaria et al found that some cells in upper layer 5 do not down-regulate glutamate receptors when isolated in slices in vitro unlike other pyramidals of the cortex[16]. These cells might be capable of capable of generating fast excitatory synaptic potentials necessary for the development of synchronous epileptiform activity (Kharazia and Prince 2001 [117]).

2. The rebound behavior in layer 5 cells recruits other cells in different lamina. The recurrent connectivity within layer 5, which extends beyond a single column level, is released from inhibition under $GABA_A$ blockers. Under this condition also, layer 5 to layer 3 connections are mainly excitatory, These two excitatory paths (L5-L5 and L5-L3) create excessive recurrent excitation leading to paroxysmal type events.

3. Subsequently, layer 5 cells have been shown to produce augmenting responses when stimulated at 10 Hz. Large (Intrinsically bursting) layer 5 cells were shown to sustain up to 10 Hz oscillatory behavior, so it possible that these cells, when released from $GABA_A$ inhibition are able to produce and sustain 10 Hz activity. Another variety of lower layer cells described by Steriade as fast rhythmically bursting (FRB) were shown to follow oscillations up to 40 Hz (Steriade et al 1998b [224]). Hence, it is possible that these cells, when released from inhibition, are recruited at the 10 Hz oscillation frequency, with the initial recruitment initiated by intrinsically bursting (IB) cells (sink in upper layer 5 preceding the initiation of 10 Hz discharges), or that these FRB cells themselves have similar mechanisms of facilitation under neuronal silence/hyperpolarization.

4. The cessation of 10 Hz oscillation is due to either Ca^{2+}-dependent hyperpolarizing current, inactivation of persistent sodium current, or disfacilitation of synaptic connections due to decrease in extracellular calcium concentrations, or any combination thereof, with different components playing different roles depending on the level of excitation.

5. With $GABA_A$ receptors blocked ($GABA_B$ inhibition intact), layer 5 cells (IB or FRB) are able to generate bursts for prolonged periods of time. Under high excitation levels, interneurons fire at high frequencies (bursts) which an optimal condition for activation of slow $GABA_B$ inhibition since $GABA_B$ receptors are maximally activated by bursts of activity (see chapter 2, Destexhe et al 1998,

[16]Thus, by holding the density of excitatory connections constant, these cells have higher net excitation in slices which, if left unchecked could lead to unstable positive feedback, or seizures.

1998a [58, 57]). With $GABA_B$ receptors active, a reduction in overall excitation in the network occurs which, combined with increase in hyperpolarizing currents and disfacilitation, will lead to cessation of the 10 Hz oscillations relatively fast.

6. When both $GABA_B$ and $GABA_A$ mediated inhibition is blocked, layer 5 cells continue to oscillate until disfacilitation happens, thus leading to prolonged periods of oscillations. In an epileptogenic cortical model, Curtis et al [50] demonstrated that the PDS is terminated by an after-hyperpolarizing potential (AHP) which is controlled by $GABA_B$ inhibition. Thus, as the latter receptor type is blocked, recurrent PDSs are expected to occur. This is also probable since $GABA_B$ receptor protein was found to be highest in layer V and VI b of rat somatosensory cortex (immunoreactive labeling, Princivalle et al 2000 [184]).

FRB or IB The precise cellular populations in the lower layers that sustain 10 Hz oscillations (7-14 Hz) is debatable. While steriade and coworkers claim that IB cells cannot fire in vivo faster than 7 Hz, some experiments demonstrated that these cells can indeed follow 10 Hz activity in vivo (Castro-Alamancos1996 [29]) and in vitro (Silva et al 1991 [207]). Steriade points to another variety of deep layer pyramidals, the fast rhythmically bursting cells (FRB), to actually follow this rhythm. Whether either scenario is true awaits more experiments; however, we claim that IB type cells play an integral role in initiating these oscillations after prolonged periods of silence.

6.5.3 Simulations

The neocortical model includes 4 interacting cortical vertical units (minicolumns) with all to all connectivity. Interlaminar and Intralaminar connectivity diagram is as presented before for the basic skeleton circuit. Synaptic strengths have been drastically amplified compared to realistic neurons due to the small system size.

The model did not distinguish between the intrinsically bursting large layer 5 cells (TL5, or IB) and the reported fast rhythmically bursting (FRB) cells. Rather, we lumped their behavior into a single cell model (L5,eq in figure 6-38) with equivalent input-output connectivity. That is, we assume *(i)* the IB/FRB network has access to both deep layer inputs (layers 4-6) and superficial layer activity (layers 1-3), and *(ii)* the lack of inhibition merges the behavior of the IB network and FRB network into a single oscillating mechanism.

Summarizing these qualitative simulation results, we note :

1. Starting with a fixed setting of cortical connections and synaptic strengths which showed slow-wave like activity (figure 6-39), we decreased $GABA_A$ synaptic effect. This lead to development of 1 Hz spikes characterized by intracellular depolarizing shifts (figure 6-40, left) and possibly including a few low amplitude discharges at 10 Hz. The initiation of 1 Hz spikes originated mostly in layer 5 and propagated to layers 6, 4 and 2,3 with PDS resulting from large excitation drive and lack of fast inhibition. Such PDSs were large enough to activate

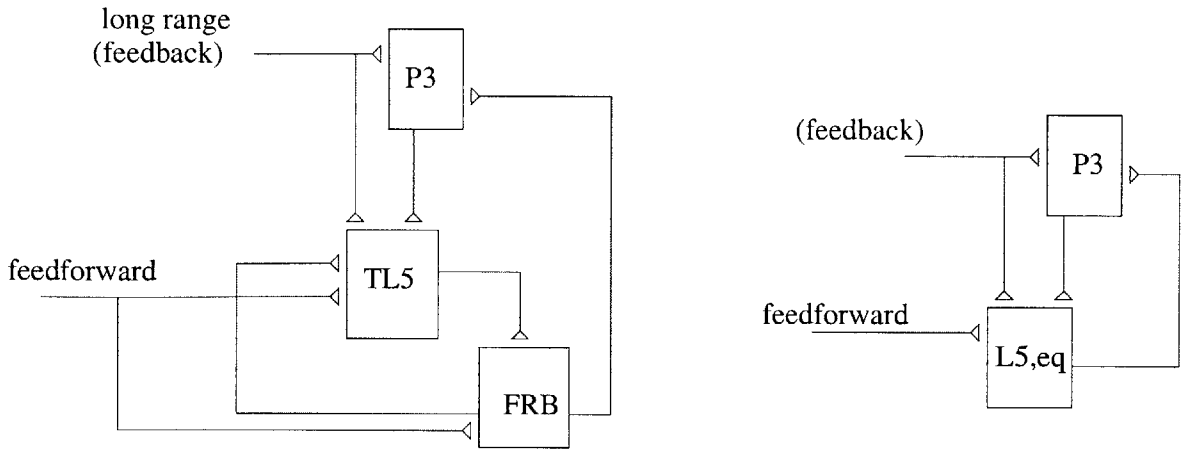

Figure 6-38: Layer 5 cells form a recurrent excitatory network nuder disinhibition which is represented by a layer of equivalent cells (L5,eq). of Simulated effect of neocortical disinhibition. *Left* Major excitatory connections contributing to a seizure under disinhibition. TL5 are large layer 5 cells with apical dendrites extending to layer 1-3. FRB are presumed fast rhythmically bursting cells (Steriade et al 1998) in layer 5 closely connected to TL5 and when released from inhibition fire bursts at 10 Hz

hyperpolarizing currents in regularly spiking cells and render them much less excitable. Subsequently, layer 5 network oscillates at a characteristic resonance of 10 Hz for a short period of time. This oscillation is caused by an interconnected network of large layer 5 cells which burst-fired at or below this frequency (FRB were not modeled but their effect is rather "lumped" to the IB cell behavior). The fast cessation of 10 Hz activity (after a few hundred milliseconds) is due to $GABA_B$ influence which decreases excitability of both upper and lower layer pyramidals, which in turn reduces the bursting behavior of layer 5 IB cells ultimately leading to disintegration of this rhythm under $GABA_B$ influence.

2. With decreasing $GABA_B$ synaptic strength simulating $GABA_B$ blockade, pyramidal cells in all layers are readily excitable in a runaway fashion. Main factors that prevent this from happening: the minimal contribution of NMDA synapses under ketamine anesthesia, the effect of hyperpolarizing potassium currents (as in item 1 above) and the increase in conductance of these cells as the seizure progresses (Neckelmann et al 2000 [168]). The resonance of layer 5 cells is now more sustainable and is capable of driving pyramidal cells in other layers at 10 Hz, which will eventually cessate due to increasing hyperpolarizing currents in regularly spiking cells and decrease in synaptic strength due to disfacilitation (decrease of extracellular calcium concentrations). Note that the frequency of oscillations decreased to around 0.4 Hz as observed experimentally, mainly due to the increased effect of hyperpolarizing currents and synaptic disfacilitation in the network[17].

[17]In the model, this is due to increase in the magnitude of the equivalent disfacilitating current which was calcium dependent.

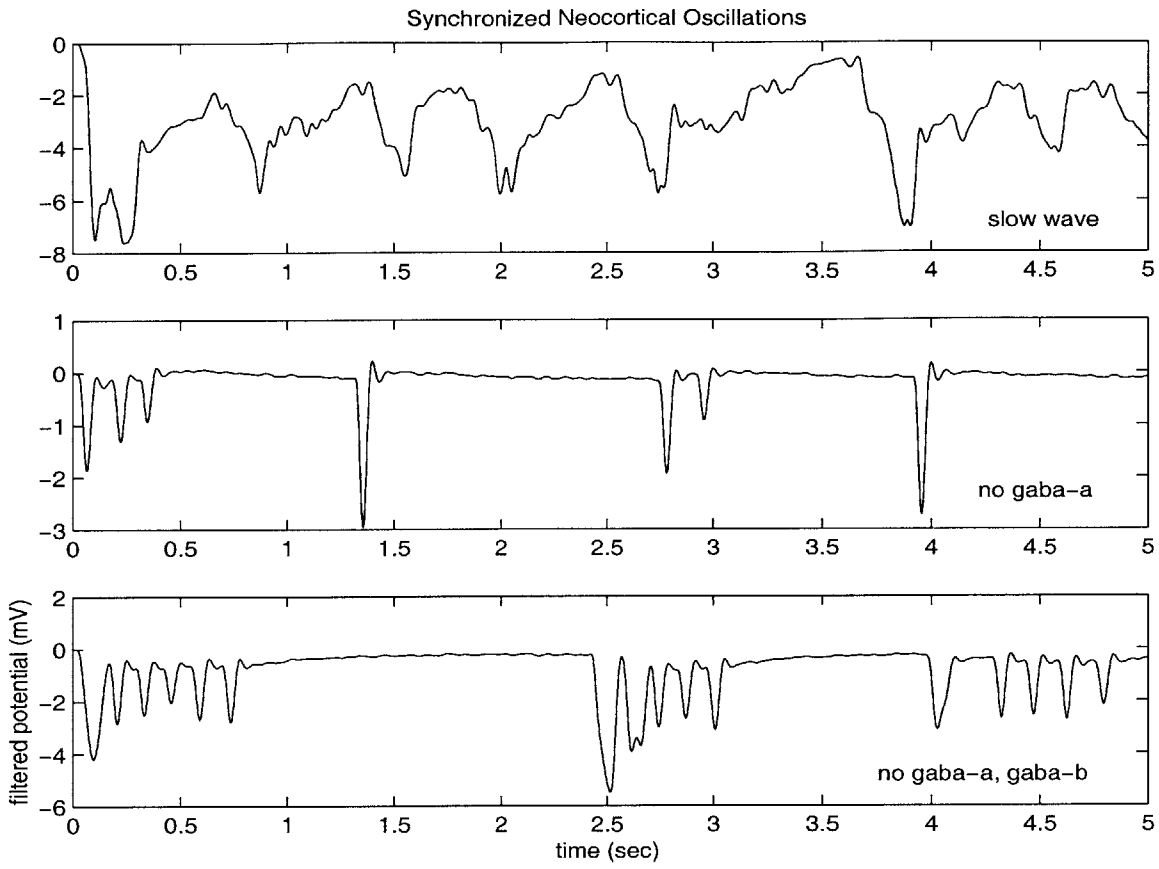

Figure 6-39: Simulated effect of neocortical disinhibition. *Upper trace*, slow wave oscillations with intact inhibition. *Middle trace*, Blockade of fast $GABA_A$ receptors. *Lower trace*, blockade of fast and slow inhibition

6.6 Discussion

The ability of tufted layer 5 cells to burst is dependent upon the amount of facilitation that exists in the proximal dendritic region (system C in figure 4-5). Alternatively, applying inhibition in this layer will decrease the ability of a tufted layer 5 cell to burst. We will investigate next how this inhibition might be kept in check in the above discussed situations. We will then discuss the limitations of the model scale in producing realistic field potentials; the necessity of scaling synaptic strengths; and finally the use of approximations to hyperpolarizing/disfacilitating currents and spontaneous depolarizations.

6.6.1 Control of layer 5 dendritic inhibition

If Tufted layer 5 cells were to maintain a 10 Hz burst firing response, then it is necessary that dendritic inhibition of zone C in these cells is minimal. Since 10 Hz oscillations were initiated in the absence of $GABA_A$ receptors while still maintaining $GABA_B$ receptors, it follows that such inhibition may be mediated mainly by $GABA_A$ connections. In fact, recent experimental work points to higher fraction

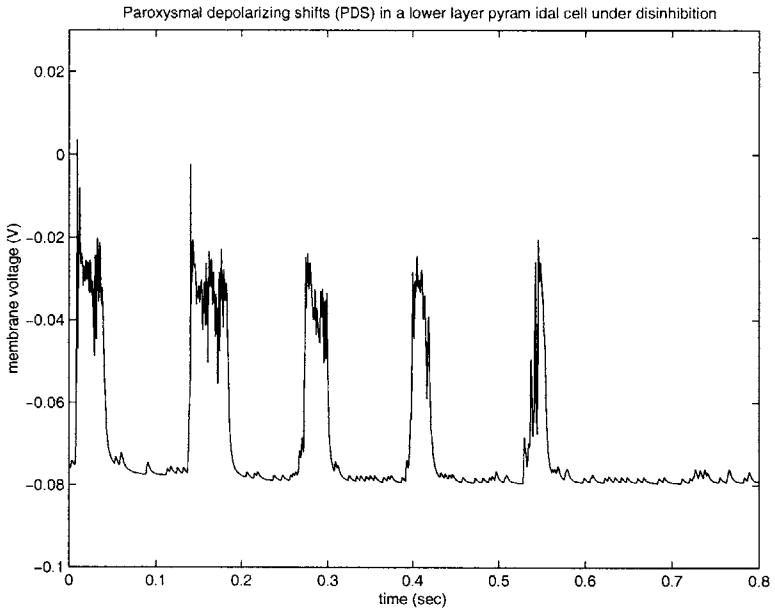

Figure 6-40: Development of paroxysmal depolarizing shifts (PDS) in pyramidal cells in simulated neocortical disinhibition. .

of $GABA_A$ inhibition on apical dendritic tufts of layer 5 cells and more abundant $GABA_B$ onto somatic regions (Eder et al 2001 [69]) which supports this possibility (see also hypothesis). Furthermore, $GABA_B$ receptors were found more abundantly on the feedforward connections in the neocortex, and not on the feedback connections which tend to arborize on apical dendrites in the superficial layers. A recent experiment on temporal lobe epilepsy points to a decreased dendritic inhibition but not of somatic inhibition in an experimental model of epilepsy, further justifying the dendritic action of $GABA_A$ blockers (Cossart et al 2001 [47]). This, we speculate could also be true for the FRB type cells: decrease in $GABA_A$ inhibition is associated with increase in apical dendritic input for these cells (possibly located in layer 3).

If inhibitory action plays such an important role in the genesis of bursting in TL5 cells, then a question begs to be answered: *how is dendritic inhibition controlled?.*

Considering the existence of an interneuron population which targets oblique apical dendrites of large layer 5 pyramidals, then a reduction of their inhibitory influence could be caused by either a direct control input by virtue of secondary inhibitory population, or by a functional modulation of postsynaptic effect which provides a local feedback mechanism that preferentially attenuates higher frequency inputs, mainly depressing elicited IPSPs on pyramidal cells. We will discuss these scenarios next.

Input control of inhibition

The interneuron population that provide synaptic inhibition of apical dendrites of layer 5 pyramidal cells could itself be inhibited by another population of interneurons which act in a complimentary fashion. Examples of recurrent inhibition between two interneuron populations in neocortex are abundant. In layers 2/3 of the rat primary

Figure 6-41: Modulation of inhibitory synapses. *Left* Presynaptic $GABA_B$ receptors ($GABA_BR1a$) depress postsynaptic $GABA_A$ receptors when input stimulus frequency is greater than 2 Hz. *Right* Back-propagating action potentials (B-AP) in pyramidal cells cause postsynaptic $GABA_A$ receptors to depress

visual cortex, Gonchar and Burkhalter 1999 [91] found one class of interneurons that inhibit layer 5 cells and are reciprocally inhibited by other interneurons in that layer [18] . Also, fast spiking interneurons in layer 4 (FS) are reciprocally connected with Low-threshold spiking (LTS) interneurons in the same region. While FS interneurons receive direct input from thalamocortical afferents in layer 4, LTS interneurons do not receive this type of innervation, but are rather inhibited by the FS population. The two types of interneuronal populations seem to respond differently to neuromodulators: while LTS cells become depolarized and could even fire upon Cholinergic stimulation, FS cells are hyperpolarized under the same conditions.

Functional modulation of inhibition

The effectiveness of inhibition elicited on pyramidal cells seems to be modulated by presynaptic mechanisms as well as the activity of the postsynaptic pyramidal cell itself (Figure 6-41).

1. A form of $GABA_B$ receptor act to decrease net inhibition on Tufted Layer 5 cells in a frequency dependent manner, thus allowing such cells to burst-fire and recruit local cortical populations.

   A balance between presynaptic and postsynaptic $GABA_B$ receptors seems to play a role in the effectiveness of $GABA_A$ mediated inhibition [19]. $GABA_B$ receptors are located on both presynaptic and postsynaptic membranes at central nervous system synapses. Presynaptic GABA receptors ($GABA_BR1a$) regulate transmitter release at both inhibitory and excitatory synapses whereas postsynaptic GABA receptors ($GABA_BR1b$) exert a long lasting inhibitory control of the target cell.

   Recently, Deisz has demonstrated that presynaptic GABA receptors can attenuate fast IPSPs ($GABA_A$) in a *frequency-dependent* manner as explained next. As has been shown in many experiments, a strong stimulus delivered to

[18] These cells were identified by immunoreactive labeling (Claritenin immunoreactive)

[19] That is, in addition to their previous role of providing long lasting inhibition, these cells can control how effective fast inhibition is on a postsynaptic target.

a cortical population (mainly through white matter) elicits in pyramidal cells a characteristic initial sequence of small fast EPSP / large fast IPSP (mediated by $GABA_A$ receptors) which is followed by a dominant a long-lasting IPSP, mediated by postsynaptic $GABA_B$ receptors. Delivering trains of impulses in this way, however, has been shown to cause a depression in fast IPSPs in response to subsequent impulses (Deisz and Prince 1999 [56]). Such a depression might actually be caused by a presynaptic $GABA_B$ receptor which acts to reduce IPSPs in a time-dependent fashion: for inter-stimulus intervals of less than 500 msec, IPSPs are reduced to around zero (at 320 msec or shorter intervals), and in some cases, a net depolarization might actually be caused by the impulse train as fast EPSPs dominate. Hence, under such conditions of low-pass filtered IPSP input, strong afferent activity arriving at 3 Hz or higher frequency might produce strong reduction in IPSP efficacy, allowing excitation to dominate (figure 6-41, left).

Furthermore, in piriform cortex, the presynaptic type of $GABA_B$ receptors ($GABA_B$R1a) was found localized on distal apical dendrites of in layer 1a, where as the postsynaptic type ($GABA_B$R1b) was found mostly in basal dendrites and somatic region (Princivalle et al 2000 [185]), which supports the idea that presynaptic $GABA_B$ regulates transmitter release, while postsynaptic $GABA_B$ modulate firing of the cell. Presynaptic $GABA_B$ modulation of inhibition has also been reported by Kapur et al 1997 [108].

Therefore, it is possible that $GABA_B$ mechanisms act to reduce the effectiveness of $GABA_A$ inhibition at particular frequencies and these mechanisms could be located at apical dendritic structures which, when stimulated at 3 Hz or more by strong synaptic afferent, act to reduce net inhibition and promote excitation, allowing tufted layer 5 cells to breakaway from inhibition and burst fire. These cells will then recruit wide populations of cells such as during 10 Hz seizures or augmenting responses.

2. Other presynaptic mechanisms have also been reported to control synaptic efficacy depending on the state of the postsynaptic cell. In the rat neocortex, trains of back-propagating dendritic action potentials in layers 2/3 were seen to cause depression at inhibitory synapses on the dendrites of these cells, possibly through release of glutamate (Zilberter 2000 [270]). This effect was mediated by increase in dendritic Ca^{2+} due to the back-propagation of action potentials from the soma (Figure 6-41,right).

   Back-propagating action potentials in hippocampus have been shown to cause transient depression of inhibitory action in distal dendrites of CA1 pyramidal cells, as well as direct depolarization of these dendrites (Morishita et al 2001 [164]).

   Hence, it is possible that transients in dendritic Ca^{2+} concentration in pyramidal cells of layer 5 reduce the efficacy of inhibition in the dendritic region. Since these Ca^{2+} transients are especially high during bursting (Larkum et al 1999 [132]), dendritic inhibitory control might be quite reduced during burst firing .

3. GABAergic input to pyramidal cells have been reported to unexpectedly cause depolarization in layer 5 pyramidal cells, possibly due to apical dendritic mechanisms (Cerne and Spain 1997,[34]), and after neuronal trauma (van den Pol et al 1997, [245]). In fact, depolarizing effect of $GABA_A$, although related to different mechanisms and time scales, have been reported in the hippocampus where basket interneurons switch their role from inhibition (hyperpolarizing potentials) to excitation (depolarizing potential) in instances when cholinergic inputs are activated, thus transforming the inhibitory role from a filter (of unwanted input noise) to an amplifier of attention signals (Miao-Kun et al 2001 [159]). It is not clear from current evidence whether reported GABA depolarization is due to similar mechanisms or is simply an isolated case.

Summary

To conclude this discussion, we expect that under specific inputs to the cortical column, such as those elicited during augmenting responses, layer 5 cells are released from their apical inhibitory control which enable that latter to incorporate apical inputs and possibly burst-fire. Such release can be either due to an intrinsic attenuation mechanism acting on inhibitory synapses or due to a secondary interneuron population that prevents apical inhibitory interneurons of layer 5 from actively decoupling apical and basal inputs of these cells.

6.6.2 Scale limitations

The ability to replicate EEG data is limited to various degrees by the issue of scale.

Field potentials in a minimal cortical model

The process of averaging currents in few cells can hardly reproduce surface field potentials since the latter is an average over large populations of neurons in a cortical column. Our argument against this limitation is the very fabric of our approach to understanding stereotyped phenomenon of oscillations, such as alpha, slow-wave sleep, and seizures. That is, by using a minimal model of cortical interaction, we argue that such oscillations in cortical field potentials can emerge from specific neural subpopulations and recruitment pathways in neural tissue, and is not the product of an emergent global activity due to spatial filtering or population-averaging over large regions of the cortex. Therefore, by linking rhythmogenesis to specific network and cellular mechanisms at the cortical column level, we claim that field potentials will reflect the cellular behavior and amplify these dominant modes of interactions.

Empirical support comes from many experimental data which found a large correspondence between cellular firing patterns and the oscillatory patterns of th resultant field potential. This was most recently demonstrated in vivo in unanesthetized animals by Destexhe et al 1999 [62]. It is also true for the disinhibition-induced 10 Hz seizure patterns we studied (Castro-Alamancos et al 1999 [31]), spike-and-wave

seizures induced by the thalamus (Steriade et al 1998 [224]), slow-wave sleep (Steriade 1993, Steriade 2000 [216, 217, 221, 227]), and many others.

We also believe that such rhythms are the product of local neural populations if placed in a realistic medium of neuromodulators and afferent activity (base-line excitation). This is true in the case of slow-wave sleep oscillations, which, for the longest time, have been referred to as an "emergent network" phenomenon over large regions of the brain. Not surprisingly, the recent work of Sanchez-Vives and McCormick [193] illustrates that slow waves can be generated in small slices when placed in a physiologically realistic medium.

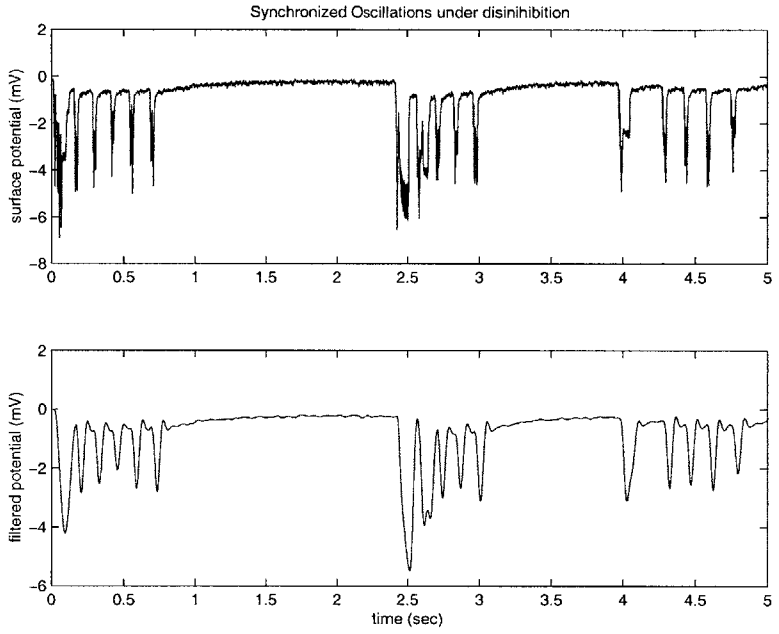

Figure 6-42: Temporal jitter in computed field potentials is due to scale limitations and can be filtered out by population averaging as well as spatial filtering in the medium. *Top:* simulated field potential recordings. *Bottom:* a low pass filtered version of the field potential could signify actual measurements.

Our model uses pointers to specific cellular mechanisms for rhythmogenesis and illustrates the ability of such cells to drive neurons in the direct column, as well as in neighboring columns to produce an emergent activity which *qualitatively* replicates observed field potentials and is thus a minimal effective circuit for oscillation generation.

Accordingly, we expect that with increased model scale, (1) transient, noise dependent, cell-specific firing to be highly *attenuated or filtered* and that (2) emergent network behavior will be further *amplified.*

As an illustration, we included the computed net field potential is a minimal seizure model and a filtered version of it in figure 6-42, right). The filtered version essentially carries the same information about how the EEG might behave when large populations of cells are averaged. As expected, the computed field potential has high degree of jitter due to the baseline synaptic drive and the largely scaled synaptic

strengths.

Synaptic strengths

The synaptic strength (connection weights) between cells are scaled drastically to account for low number of cells in our minimal model. That is, when a presynaptic cell fires, it is able to create a large shift in the depolarization of its postsynaptic targets. In reality, it takes many synapses to produce equivalent postsynaptic potentials. Although this might be thought of as a limitation, one can argue that each cell firing represents an assembly of neurons firing in a similar fashion and targeting a similarly large number of post-synaptic neurons. This was especially exaggerated in the case of seizures since this phenomenon is characterized by enormous depolarizing events in cells due to the firing of a large proportions of pre-synaptic cells targeting a single neurons. Hence, connectivity ratio between the few cells in the model is quite high to reproduce seizure activity. On the other hand, using the same strength to produce slow wave oscillations result in high firing rates in highly coherent cells, resulting in larger amplitude than is expected. This discrepancy could be alleviated as the model scale is increased to include more cells.

Neuronal silence

In the slow-wave oscillations and disinhibition induce seizures, disfacilitation in synapses was not modeled. Also, hyperpolarization currents in regularly spiking cells were of a larger time constant than observed physically and essentially act to reproduce decreased excitability due to both effects. In the case of tufted layer 5 cells, cessation of oscillations was modeled by a lumped hyperpolarizing current model which is dependent on calcium concentrations in the cell (see chapter 5 on models) and which proportionally decrease the strength of synapses between cells (based on experiments by Massimini et al 2001 [150]).

The initial rebound from a period of neuronal silence (as in slow waves) might be caused by persistent sodium currents which act to magnify spontaneous depolarizations in cells. This was not modeled, but rather, we used a tonic Poisson-arriving input to each cell which produces random subthreshold depolarizations (unable to fire a regularly spiking cell, but occasionally able to fire layer 5 cells due to rebound behavior of such cells).

Finally, note that the positive deflections characteristic of a disinhibition-induced seizure is not replicated in the simulated seizure waves (comparing figures 6-39 and 6-37). We believe this to be an issue of approximation and scale: our model cells did not have sufficient hyperpolarizing currents, and as more cells are incorporated to the model, the collective effect is more apparent or amplified in the net field potential.

Chapter 7

Conclusions

The presented work is aimed at producing an outline of a generic effective cortical skeleton circuit which is able to generate different oscillatory activity observed at the level of surface field potentials (in-dwelling electrodes) and scalp -recorded EEG. While many theories have tackled EEG as a gross electrical activity, the wealth of electrophysiological evidence compelled us to look deeper into non-random intracortical mechanisms that can explain observed phenomena. Looking into neural science literature can soon produce a daunting flood of complex behaviors starting at the molecular level where intricacies in calcium utilization change cellular firing properties and ending with psychophysiological experiments where different, sometimes seemingly contradictory EEG patterns are recorded.

Our approach differs from earlier attempts in generic modeling of EEG generation (Lopes da Silva, Nunez, Wright) in that it draws from actual current physiological knowledge of the system, its different constraints and operating regimes, degree of nonlinearity, and connection topologies of involved subsystems.

It also differs from some neurophysiologists' approaches in that it is less tailored to specific cognitive brain function. By using generic cellular models and several guiding principles of a generic cortical neural organization, this thesis attempts to develop a generic outline of an EEG-producing neural circuit incorporating new influx of neurophysiological evidence from disparate sources while keeping in close agreement with currently accepted mechanims contiributing to cognition such as effects of neuromodulators and high frequency synchronization of neural assemblies.

The net result of this effort is embodied in a hypothesis on the gating function of layer 5 cells. The hierarchical binding hypothesis explores features of a proposed generic oscillator in neocortical layer 5 under several vigilance states and argues for its active role in linking two information streams arriving into neocortical computational units. We will now briefly summarize the basic principles of this hypothesis.

Hierarchical circuit

The model describes emergent rhythms based on interaction between three scales of cortical organization (figure 7-1, circuit detail in figures 4-1-4-3).

1. At the lowest scale is the conventional description of a cortical column whose

radial extent is defined by the spatial spread of specific driving inputs arriving at middle layers of the cortex (layer 4 in sensory cortices); synchronization within a cortical column is thus assumed mediated by inhibitory mechanisms such as electrical coupling, and by facilitated interconnections between neurons within the same layer, such as within layer 4 of a sensory area.

2. The next scale is defined by the extent of horizontal connectivity within the deeper layers of the neocortex. This metric surpasses that of a single cortical column to include an assembly of columns up to 1-2mm. We do not attempt to draw a functional equivalence of this *column-assembly scale*, except that neural populations at this level could possibly acquire similar processing capabilities of afferent inputs (produce similar features in a visual segmentation task for example).

3. The final scale describes long-range connections between areas belonging to disparate levels of information processing. That is, while recurrent connections at the previous two scales are those of distributed computation within a single area, the connectivity at this scale is assumed to follow a pattern of ascending/descending fibers along a hierarchical information transfer stream. Accordingly, a system at this scale receives bottom-up or driving inputs that are spatially restricted (columnar level) and top-down or descending modulatory inputs that are more spatially-distributed (column assembly level).

Layer 5 properties

1. *Input amplification*: a subset of layer 5 neurons possesses a high gain amplification property under minimal input excitatory states such as sleep and anesthesia. This amplification occurs both due to internal characteristics of layer 5 cells as well as due to reduced inhibitory gain-control in at least one subpopulation of pyramidal cells in layer 5 under such states.

2. *Intra-layer connectivity*: Layer 5 cells form an extensively-connected network of neurons which goes beyond the functional boundaries of a single cortical column up to the columnar assembly scale.

3. *Intra-columnar connectivity*: At the finest scale of cortical organization, the minicolumn, layer 5 cells are reciprocally connected to key pyramidal cell populations across cortical depth and thus has access and is able to modify the output of both superficial and infragranular (deep) pyramidal cell populations.

4. *Input streams binding*: Some layer 5 cells have two input ports the coupling of which will change the firing characteristics of these cells. While the basal input port is affected by local neural population activity (columnar, columnar assembly scale), the apical input port samples activity from distant neural areas, possibly higher cortical processing regions. An additional control zone acts to selectively enhance or decouple the effect of apical inputs on local cortical activity.

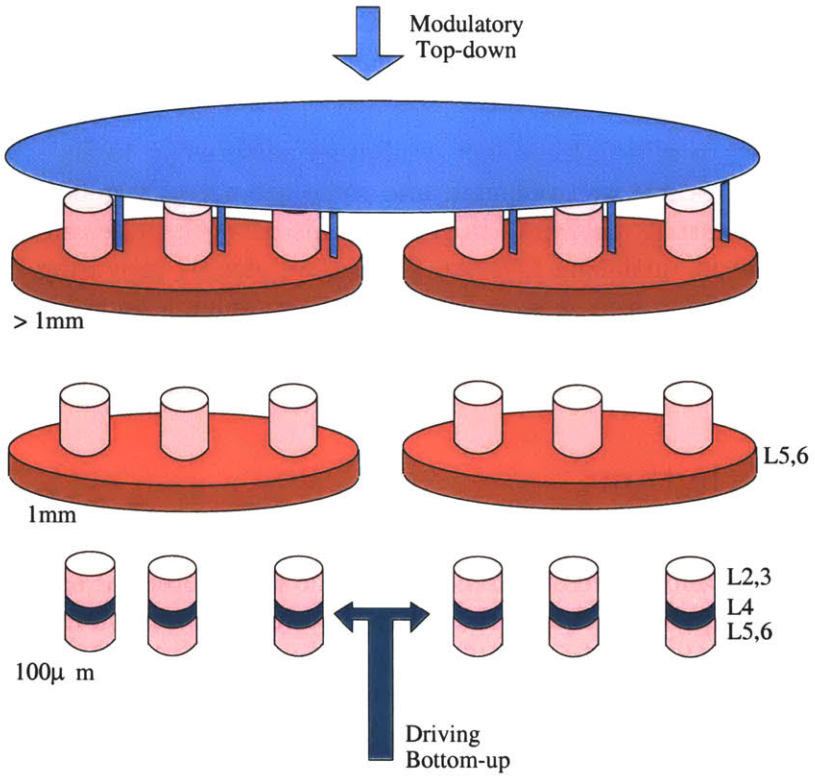

Figure 7-1: Three separate scales are proposed for a hierarchical circuit. The column scale is at the lower end receiving spatially-restricted ascending or driving input. The deep-layer connectivity patterns define the column-assembly scale and the top-down descending inputs arriving from higher structures define the cortical area scale. The role of layer 5 in binding local activity to top-down control is represented by bridge structures at the highest level

5. *Intralaminar inhibition*: An inhibitory pathway from layer 5 to layer 3 pyramidal cells exists and is selectively activated, by virtue of bursting in layer 5, during active cognitive states controlling the output of superficial layers.

Hierarchical binding

Tufted layer 5 cells are argued to actively gate the ability of higher order modulatory control to reorganize local activity at the columnar level. Networks of tufted layer 5 cells extend beyond the columnar level and can accordingly aid in linking columns under matched inputs from driving and modulatory streams into a coherent assembly while decoupling from columns with unmatched inputs. Such reorganization is especially evident during preparatory brain states and also during initial transient periods of task performance.

7.1 Scenario of intracortical slow rhythm generation

We argue that slow-to-middle frequency oscillatory patterns (< 15 Hz) observed across many vigilance states are well reflected and some are actually generated by the behavior of layer 5 recurrent network. In general, this network to be referred to as L5N, participates either in initiating activity (slow-wave sleep), providing baseline oscillatory patterns (alpha activity, sleep delta), or reorganizing local activity based on higher order control (evoked, emitted alpha). Finally, under pathological conditions of disinhibition, L5N can provide for seizure-like patterns in neocortical networks.

7.1.1 Sleep rhythms

As sleep deepens (sleep stages 2-3), cortical areas undergo an increasingly prominent cycle of facilitation and depression reflected in the field potential as slow-wave sleep oscillations with frequency below 1 Hz. After a period of depression characterized by neuronal silence, the high gain amplification property of layer 5 cells is able to initiate rebound activity from hyperpolarized levels. This initial firing will then spread to other cortical layers and be transfered over long distances by superficial layers connections, effectively creating a period of depolarization lasting more than 0.8 sec and is terminated with disfacilitation in the involved neural populations. Disfacilitation creates a period of neuronal silence (around 0.4 sec) which restarts the cycle.

At later stages of sleep (stages 3-4), layer 5 cells become more effective in punctuating delta activity (3-4 Hz) in the cortex. In these sleep stages, intracellular hyperpolarization levels are increased, causing more coherence in thalamic input to the cortex[1]. This coherent activity generates large depolarizing events in tufted layer 5 cells which respond now with strong bursts. Furthermore, inhibitory control in middle layers is decreased due to unknown mechanisms (possibly due to presyaptic $GABA_B$ effects that are maximal at these frequencies, see section 6.6.1). Here, bursting recurs at low frequencies (3-4 Hz) mainly due to increased hyperpolarization[2] as seen in figure3-7.

7.1.2 Awake rhythms

Our hypothesis on generation of slow rhythms during different states of wakefulness was based on two main properties: (1) characteristic properties in individual layer 5 cells as well as in layer 5 network mentioned above, and (2) distinction in the location of input termination and local activity streams into tufted layer 5 cells. The latter is summarized as follows:

[1]The increase in thalamic input coherence has been observed experimentally in thalamic relay neurons, mainly due to stronger rebound in those cells associated with increased firing in reticular neurons, see Steriade 1993 [216]

[2]This contrasts to the burst firing at 7-9 Hz in those cells when injected with current under resting membrane potential

1. Modulatory input arriving at a cortical column from higher-order processing areas have a feedback termination pattern; that is, it tends to target superficial layers 1-2 and possibly layer 5, overlapping with inputs from some thalamic nuclei (e.g. intralaminar, nonspecific) which are known to cause augmenting responses. This input thus accesses the apical modulatory zone A of TL5 cells.

2. Driving input, such as from specific sensory thalamic nuclei as well as from lower order cortical areas, has a feedforward termination pattern; that is, it accesses middle layers and provides for topographically specific excitation of the control zone C of TL5 cells.

3. Local input from pyramidal cells of layers 3 and 6 targets the basal zone B of tufted layer 5 cells. While descending terminations from layer 3 form are restricted to within a cortical column, those ascending from layer 6 are more widely distributed beyond the metric scale of a single column.

Finally, based on electrophysiological experiments by Castro-alamancos et al, we argue that feedback connection patterns are able to elicit augmenting responses in layer 5 cells, but not feedforward connections. Our simulation results demonstrated that the apical dendritic zone of tufted layer 5 cells plays an important role in sustaining 10 Hz augmenting responses observed in experiments of intracortical and callosal stimulation.

Restful inattentive states

During restful wakefulness, wide cortical areas receive minimal excitation from forward sensory streams (e.g. eyes closed) as well as from higher order structures (lack of attention). Under such conditions, layer 5 cells in these cortical areas have the propensity to fire single spikes in the alpha range frequency mainly due to the interplay between low threshold ionic currents (I_T and I_h), which are maximally active at relatively hyperpolarized membrane potentials. Accordingly, a connected network of layer 5 cells oscillates in a broad range of alpha activity (7-10 Hz) with low coherence of firing across long distances. The sustenance of such oscillation within layer 5 is aided by slow NMDA excitatory synapses. Finally, the passive nature of a neocortical system renders a dominance of inhibition in superficial cortical layers, which will thus loosely follow the oscillatory patterns in layer 5 and spread the activity over wide cortical areas by virtue of long range cortico-cortical connections. The L5N oscillator is here broadly tuned to alpha band frequency.

Functional states

During performance of stimulus specific tasks, other types of alpha band oscillations are registered, mainly during preparatory phases of a task (induced alpha), during early stages of responding to a stimulus (evoked alpha) and during states of heightened attention (emitted alpha). The oscillatory behavior recorded under these three states could also be explained by a basic recruiting mechanisms in layer 5 and disparities of input patterns to tufted cells (TL5) in this layer.

1. *Induced alpha* activity is generated in layer 5 under conditions broadly similar to those of restfulness alpha. In this case, there is minimal sensory information input and a general nonspecific excitation by descending or modulatory inputs to task relevant cortical areas. We propose that, since this descending input accesses mechanisms producing augmenting responses, it serves as a preparatory rhythm which facilitates corticothalamic synapses for subsequent stimulus. This is based on experiments that showed an increase in short term plasticity in corticothalamic circuits at alpha band (Castro-Alamancos 1999, Hempel et al 2000 [97]), increase in induced alpha oscillations just before a stimulus occurs in humans experiments (Klimesch et al 1999[120]), and increase in Serotonin levels which facilitates apical zone A of layer 5 cells under novel tasks which require increased attention (Lambe al 2000 [129]).

   The fraction of power in the alpha band (induced alpha) decreases, however, as excitation levels increase further, since layer 5 cells are further depolarized and the effectiveness of ionic currents generating alpha decreases (I_T and I_h). This is observed over task-relevant areas and is denoted as alpha desynchronization which is usually associated with activation of those areas.

2. *Evoked alpha* activity is generated in tufted layer 5 cells that receive both modulatory inputs and feedforward sensory inputs during the transient stages after stimulus onset. In this case, zone A of a TL5 cell is depolarized by virtue of descending or feedback inputs initiating a state of readiness in a large network of layer 5 cells. Feedforward input, however controls the middle zone C which dictates any coupling between this readiness state and local excitatory inputs that drive the basal system B. Thus, only cell assemblies that satisfy this AND relationship of three inputs are able to burst and accordingly synchronize their activity into a coherent pattern. This synchrony, in turn will provide for synchrony of corresponding superficial pyramidal cells in layer 3 by virtue of feedback connections as well as for surround inhibition of "unmatched" cell assemblies by virtue of interlaminar inhibition.

   According to the above hypothesis, the matched TL5 cells will burst and oscillate at high alpha frequency (9-12 Hz) for a transient period of 200-500 msec after which they proceed onto higher frequency associated with actual task performance (induced gamma). This is in accordance with observations on evoked alpha: low-power, sharp-synchrony of high-frequency alpha over spatially limited areas which lasts for up to 500 msec (Schurmann et al 2001, Basar et al 2001 [201, 13]).

3. *Emitted alpha* activity occurs in situations where descending input is large enough to have a driving ability to layer 5 cells too. In this case, spatially limited neural assemblies of TL5 cells undergo bursting and oscillations at high frequency by virtue of this input to zone A (possibly amplified by neuromodulators such as serotonin). Since emitted alpha occurs in situations of increased familiarity and proficiency in a task, we propose that the increased descending input acts to enhance specific cell assemblies (expectation) to quickly respond to sensory

input, thus reducing delays in computational processing time. We finally believe that this is a special functional case where augmenting responses are maximally active, since, as we have argued earlier, feedback connections drive this response which acts to enhance cortico-thalamic pathways.

7.1.3 Seizure-like states

As seen above, the highly interconnected network in layer 5 can initiate and organize oscillatory patterns in neocortical circuits under minimal excitation. It is imperative, therefore, that cortical inhibitory circuits provide a strong gain control for this system for proper operation. Pathological conditions of disinhibition therefore, are expected to generate large excitatory events, expressed as paroxysmal depolarizing shifts and seizure like activity. In particular, a form of spike-and-wave seizure can be initiated at around 10-15 Hz as inhibition is reduced in neocortical circuits. In this case, while the high-gain amplification property of large layer 5 cells could initiate a large spike component, many subtypes of layer 5 and upper layer 6 pyramidals are subsequently entrained due to lack of inhibition and these cells are actively involved in generating the middle frequency (10-15 Hz) oscillation.

7.2 Prediction: The cognitive implications of alpha band rhythms

The presented hypothesis puts emphasis on alpha rhythms as having more functional role than merely idling rhythms of the cortex and proposes an active mechanism of its generation.

In addition to alpha band oscillations observed in visual experiments, it appears that alpha-band rhythms could be part of a generalized middle frequency oscillatory phenomenon which also occurs in other sensory systems. The rolandic mu rhythms of the motor cortex have similar frequency band (10 Hz), are maximal in resting states and are seen to suppress under tactile stimuli. Interestingly, a new study by Klopp et al 2001 using intracranial recordings in human subjects inadvertently showed that alpha band power (7-12 Hz) *actually increases* in early stages of motor response of duration lasting up to 330ms [121]. This recurrent yet-unexplained observation of increased alpha activity, we claim, has roots in assembling local activity based on internal expectation and attention.

7.2.1 Reorganization of local cortical assemblies

We proposed that some alpha band oscillations are correlated with reorganizing local activity based on modulatory influence of higher order systems. Starting from an initial stimulus, one-to-several cycles of alpha-band oscillations will occur with will help define local columnar assemblies before higher frequency computations occur within the selected assemblies, or what is known as induced gamma activity (figure

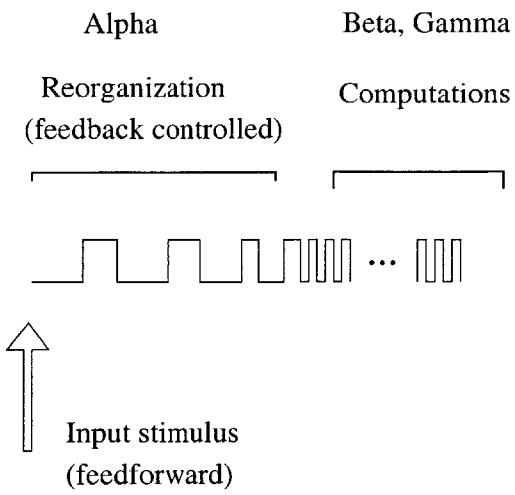

Figure 7-2: Transient evoked alpha precedes higher order computations in a columnar assembly

7-2). A schematic of a possible mechanism generating this phenomenon is shown in figure 7-3 which we will detail next.

The basic cortical circuit of a cortical column is comprised of (i) tufted layer 5 cells (TL5) having the inherent binding mechanism, (ii) low threshold spiking interneurons of layer 5 (LTS5) which provide inter-laminar inhibition in awake states, (iii) generic populations of layer 2,3 cells (P3) which are the library cells, and (iv) a feedback mechanism from deep pyramidal cells (layers 5 and 6) to the superficial pyramidals-schematized by P5. Interactions between cortical columns at the cortical assembly level is provided by both superficial and deep pyramidal connections.

Considering a hypothetical situation where two afferent inputs I_1 and I_2 arrive from sensory streams (feedforward mechanisms). In the initial state under direct feedforward inputs, cellular populations in both cortical columns col1 and col2 are *passive*, that is, there exists minimal firing (at time $t = t_o$) due to both input patterns I_1 and I_2 but which is not sufficient to create meaningful cortical assemblies [3]. Assume further that only input I_2 is the target input as defined by higher order control arriving into layer 1, and that only col1 corresponds to the features of that input I_2 as dictated by this control, that is only column col1 is *enabled*. Our aim is to demonstrate how to cause column col1 to respond only to input pattern I_2 and how column col2, which is not selected will remain in a passive state.

Intracolumnar activity: Assuming that feedback modulation arrives in the second alpha cycle ($t = t_4$), TL5 cells of col1 burst fire. This causes inhibitory cells $LTS5$ to fire since they are assumed to respond vigorously when subjected to burst-like synaptic inputs. In turn, LTS5 firing creates a shunt of inputs in layer 3. Feedback

[3]It might be possible however to create an initial period of gamma oscillations in layers 4 and 6 of the cortex which initially receives the sensory thalamic input; this period was observed and termed phase-locked or evoked gamma activity in some experiments (Tallon-Baudry et al 1999 [233]).

input arriving to P3 from P5 will, however, balance this effect at $t_4 - t_5$. The shunt inhibition will create a decrease in afferent input I1 effect at the following cycle t_6 and accordingly P3 will fire much less in the period $t_6 - t_7$. Again, at $t = t_7$ bursting in TL5 occurs and feedback from P5 will produce sufficient excitation in P3 now corresponding to the target input I_2.

Intercolumnar activity: Since col2 is not selected by higher order control, we should expect that TL5′ cells do not burst at $t = t_4$. Accordingly, populations in this column remain in the passive state. Connections within layer 5 (TL5-TL5′) will however cause LTS5′ to fire creating a shunting effect in P3' which will counterbalance the excitatory drive from P3 (P3-P3′ connection). Further, since P5′ is not activated, no feedback is delivered to P3′ and this population remains passive throughout the alpha cycles.

The above mechanism can be repeated across various enabled cortical columns within a lower order system. Accordingly, one can see how two or more columns could be activated *within two or three cycles of alpha band activity (200-300 msec) which is comparable to the transient period after an input stimulus where evoked alpha is observed.* This activation provides an excitatory drive to selected superficial layer pyramidal cells which could then synchronize based on internal mechanisms (such as inhibition) and proceed to fire at higher levels of activation, presumably creating gamma-band fast oscillations.

How switch to higher frequency might occur: After the transient period of cortical reorganization expressed by evoked alpha, a switch to higher frequency is observed where neural computation occurs in the now-defined columnar assemblies. The resultant high frequency oscillation is arguably related to object representation in sensory systems (termed induced gamma, section 6.3.2). This switch is also reflected in TL5 cells which cease from bursting and start firing in a regular-spiking mode. We discussed earlier possible switching mechanisms as either intrinsic, caused by neuromodulators, or due to active inhibitory control (see 6.3.2). We present here one scenario, mainly that a possible mechanism could be the activation of a group of low threshold spiking interneurons LTS(?) in the middle layers which innervate zone C of a TL5 cell. These interneurons are activated when sufficient firing levels are achieved in the superficial layers after the evoked alpha period (figure 7-4). Subsequently, the inhibitory effect in zone C will prevent a TL5 cell from bursting by decoupling its input zones A and B. This firing mode switch is in agreement with the hypothesized role of bursting in re-organizing local assemblies since decoupling local activity from higher order mechanisms could be yet another way to allow "holding" of developed columnar assemblies under the current computational state.

7.2.2 Information transfer between cortical systems

The presented binding hypothesis is based principally on the existence of two separate streams of information that arrive into a cortical sensory system at distinct input ports

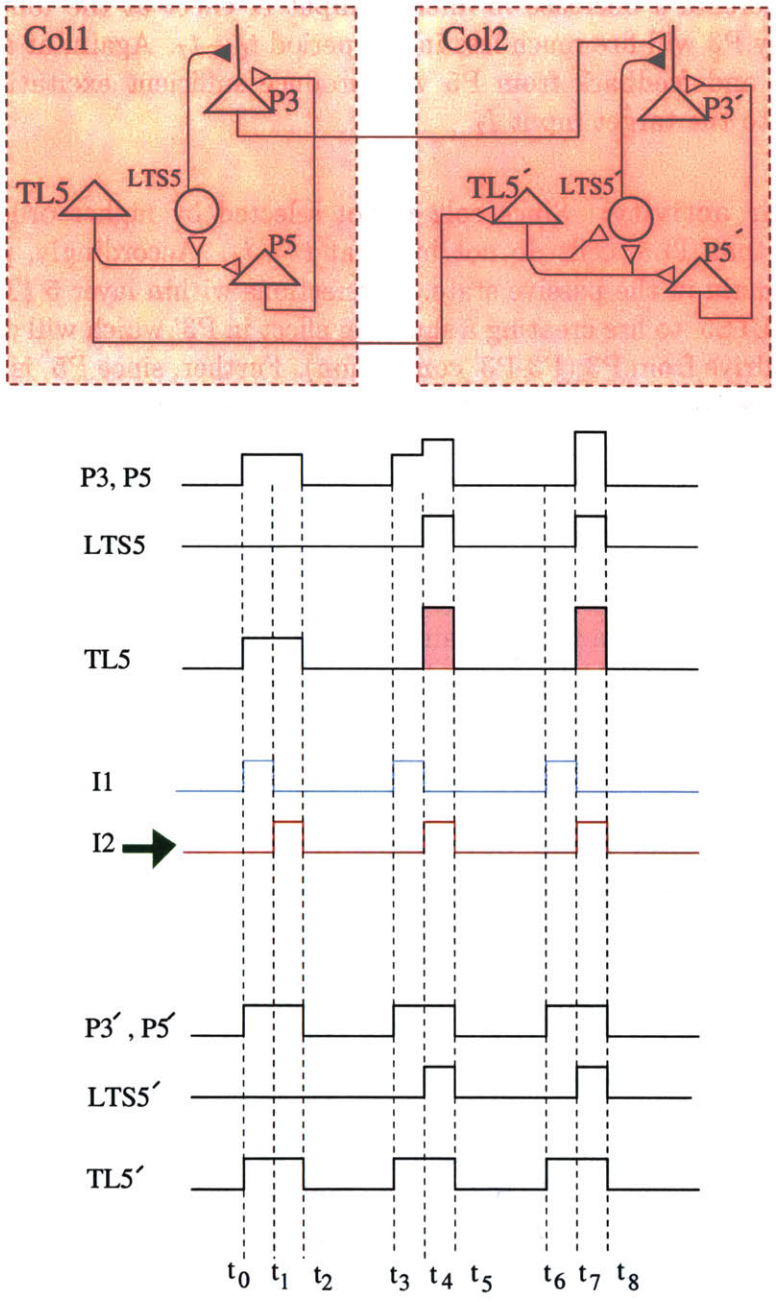

Figure 7-3: Reorganization of columnar assemblies based on tufted layer 5 cell bursting. *Top:* Generic circuit diagram of two columns connected within a cortical assembly. *Bottom:* Time line of activity demonstrating how selected patterns might reorganize activity in column 1 (traces 1-3). Traces 4,5 show two sensory inputs to column 1 with trace 4 being "amplified" by higher order inputs (arrow). Bursting is indicated by red filling in trace 3 of the TL5 cells. Traces 6-8 show how a column which is not selected, and consequently no bursting in layer 5, does not move into higher levels of excitation. See text for details.

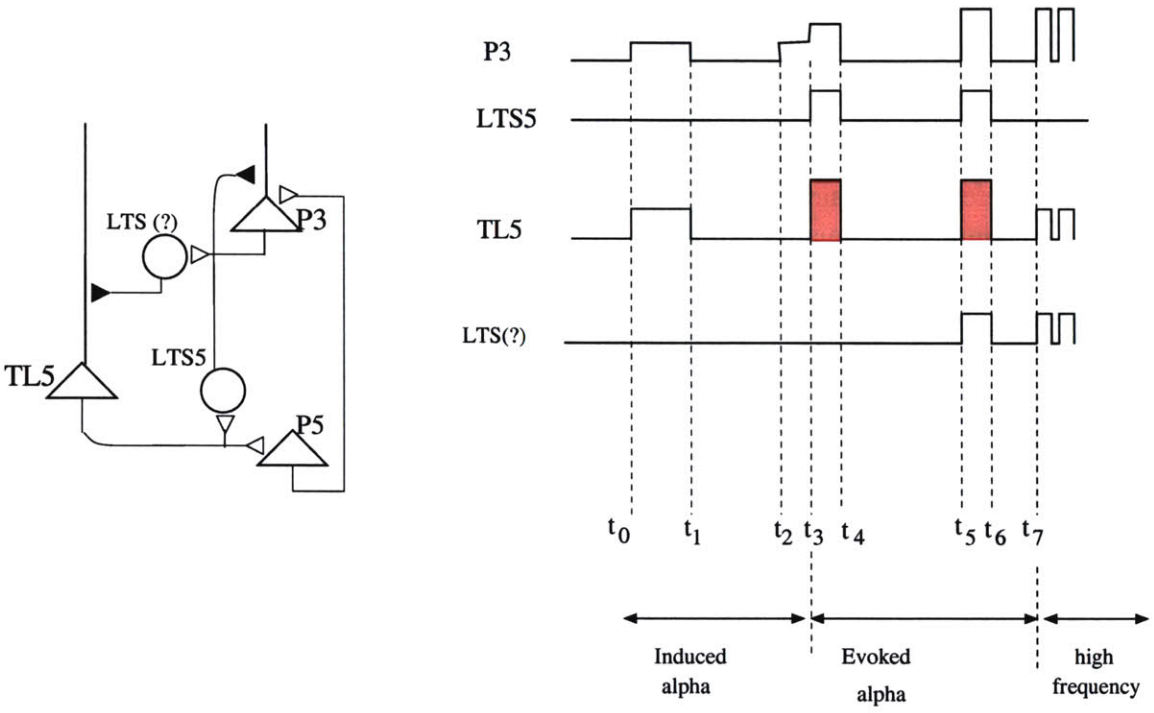

Figure 7-4: Possible mechanisms for switching to higher frequency after an evoked alpha period. *Left:* An unidentified interneuronal population LTS(?) innervates the middle zone C of a tufted layer 5 cell. *Right:* Such interneuron population is activated upon sufficient excitation in pyramidal cells P3 or P5, thus preventing TL5 from burst firing and switching their firing mode to regularly spiking.

and which are bound together in early processing stages by bursting mechanisms of large layer 5 cells. Such information streams appear to exist both within the cortex itself, for example between areas V1 and V2 of the visual system, as well as between the cortex and the thalamus, for example between somatosensory cortex and the thalamic nuclei (VL and VPL). Indeed, recent studies in humans showed increased synchronization in the alpha band (8-12 Hz) between supplementary motor and primary sensorimotor areas during voluntary movements: significant correlation starts $\sim$ 1.4 sec before the actual movement (Ohara et al 2001 [178]).

We believe that such systems play disparate roles in cortical integration as follows.

1. A feedforward stream of information delivers distinct inputs at the functional column spatial scale (see figure 7-1). An input stimulus arriving along such stream is capable of creating an initial response in a cortical functional column as defined by the intracolumnar connectivity patterns within layer 4 and the initial state of that cortical column [4]. This initial response lasts for up to 100 msec before the onset of modification by feedback information streams and other attentional mechanisms. This is supported by experiments on visual attention modulation of neural activity in monkeys where feedforward-based information transfer in V1, V2 and V4 was not changed between attended and ignored stimuli (figure 7-5, Mehta et al 2000 [156, 157]).

2. A feedback stream of information delivers distinct modulatory inputs at the columnar assembly scale which could modify the integration capability of neural populations at the columnar level in response to feedforward input [5]. The effect of feedback information is first observed by a change in the initial activity levels in the cortical column occurring around 100 msec after a stimulus (figure 7-5). Again, this is in agreement with the experiments of Mehta et al which demonstrated that any observable change in population activity for attended visual stimuli happened 100-300msec after a stimulus onset and agrees with a feedback pathway of information transfer, with modulation levels occurring earliest in higher order visual areas (V4), later in V2 and finally V1. We propose that such a time window is initiated by the firing patterns of tufted layer 5 cells (at around 100 msec post-stimulus). Whether TL5 cells fire in bursts or regular spikes implicitly determines whether initially formed patterns are to be amplified and included in a columnar assembly representing certain features of the stimulus or whether such patterns are to be attenuated and decoupled from the representative columnar assembly (as seen in figure 7-3).

New experimental evidence have increasingly pointed to the role of low frequencies in mediated top-down transfer of information in cortical systems. As von Stein discusses in his review, it is possible that alpha and theta rhythms are characteristics

[4]Examples of such streams are the feedforward connections from visual area V1 to V2 and the thalamocortical connection from ventral lateral thalamus VL to somatosensory cortex.

[5]Examples of feedback systems are visual areas V2 to V1 in the cortex, the VPL thalamus to the somatosensory cortex, and intralaminar thalamic nuclei to cortical sensory areas.

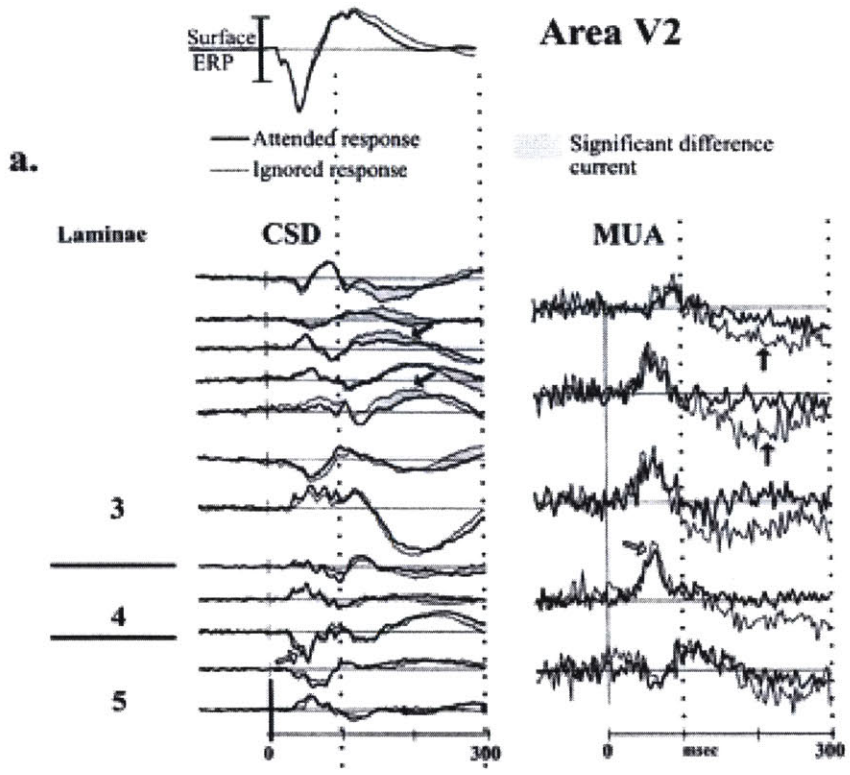

Figure 7-5: Laminar profile of activity modulation in area V2. *Left*: changes in current source density (CSD) in response to attended stimuli (thick lines) versus ignored stimuli (thin lines). Current sinks point downwards. *Right*: changes in multiunit activity (MUA or level of firing, right) under same conditions. Note in MUA plot that observable decrease in depression occurs after 100 msec initial time window and is most obvious in layer 3. Note also that layer 5 is most active around that time (adapted from Mehta et al 2000 [157]).

of cortical integration over long distances especially that alpha rhythms are observed in situations where top-down influence dominates that of bottom-up or feedforward input in sensory areas. Also, there are arguments supporting that the frequency of oscillation involved in integrating information from different cortical systems is dependent on the spatial scale of the involved systems with gamma frequency being for local computations within one system, beta frequency for intermediate distances and alpha/theta for long distances (Von Stein 2000 [250]). Our hypothesis does not contradict such views but rather outlines that such oscillatory frequency, at least in the alpha range, might not only be the by-product of spatial scale but that it is the result of specific cortical mechanisms actively contributing to this information integration. Although premature at this stage, one might also speculate that lower frequency rhythms (theta) arise from similar mechanisms and are simply characteristic "resonance" frequencies of different subsets of layer 5 cells, since, as seen experimentally, this layer have several subpopulations of pyramidal cells extending to different parts of the superficial layer (with some giving longer bursts than others).

7.2.3 Synopsis on role of burst firing

The role of bursting in neural coding have been long debated. Several experiments argue for an active role of bursting in brain functioning, while others dismiss it as being only correlated with non-cognitive states. A main thesis for the importance of bursting is the ability of a high-frequency burst to increase the driving influence of a presynaptic bursting cell on its postsynaptic target and hence to transmit reliably information across unreliable synapses. An interesting review of such evidence is given in by Lisman 1997 [136]. Still, other researchers, although not refuting the ability of a burst to induce strong responses, argue that bursting is more of exception in firing in cortical networks and occurs only in low vigilance states such as sleep. Furthermore, the proportion of bursting cells is more prominent in slices rather than in intact cortical areas (Steriade et al 2001, 2001a [228, 229]), again suggesting the marginal role of bursts.

We believe that *the two regimes of firing, bursting and regular firing, coexist in natural conditions and that each regime have significantly different implications on the ensuing operation of the system.* We base our claim on experimental evidence in layer 5 cells. In these cells, highly specific input sequences by three disparate information streams control whether a cell may burst or not. Furthermore, only burst firing activates both presynaptic and postsynaptic mechanisms at synapses within layer 5 to enhance synaptic coupling and overcome depression, an effect which is not observable under regular firing (Williams et al 1999 [256], see also chapter 4). Finally, some interneurons are able to respond much more readily to burst-like input patterns. Connections onto Low threshold spiking interneurons (LTS), for example, enhance by several fold under fast inputs, and at least one subset of this class is known to exist in layer 5 and are known to be activated in complimentary ways compared to other Fast spiking FS interneuron classes. It might be argued that bursting is a natural way for higher order systems to quickly recruit a large population of neurons in a lower order system, starting from an initial state of low firing. Thus, bursting helps to refine relevant neural assemblies in the lower order system and to drive those assemblies into a state where cognition can proceed, mainly at a high frequency rate of firing.

Our hypothesis is a suggested example of the difference operational regimes indicated by bursting and regularly spiking patterns: while bursts in an awake cortex contribute to reorganization of local activity based on higher order control, regular firing is involved in subsequent local computations occurring at higher frequencies. Thus, the same neural substrate is able to respond differently under different behavioral conditions and to translate this behavioral change into different dynamical state of local activity.

The prominence of bursting during sleep might have yet another functionality. For example, the preponderance of bursting in layer 5 cells at delta frequency during late sleep stages might act to consolidate synaptic connections acquired during awake states, especially that delta sleep occurs immediately before REM sleep where playback of day experiences and memory consolidation occurs. This synaptic strengthening of apical inputs in TL5 cells is especially important to emphasize patterns of

modulatory control of low order sensory areas by higher-order systems.

Finally, the relative decrease in burst firing observed in awake cortex compared to sleep/slice recordings does not contradict the functional relevance of this regime. In fact, while Steriade noted the drop in burst firing cells in awake cats, he also recorded in some instances layer 5 cells bursting at 11 Hz, that is within the alpha range (Steriade et al 2001 [228]). Based on our hypothesized modes of operation in this layer, it is quite possible that only specific subsets of layer 5 cells belonging to now-relevant cortical columnar assemblies are bursting at one instance. Further more, we predict that recording under conditions where active cognition requiring top-down interactions can increase this proportion of recorded cells (which might not have been the case in Steriade's animals). In fact, and assuming that recordings occur in non-attentive states, we expect that most layer 5 cells to be non-bursting, but rather undergoing idling alpha oscillations.

7.3 From neuronal group electric activity to EEG

While our layout of a canonical EEG-generating cortical circuit awaits experimental verifications, the developed ideas open the door for many potential extensions. These include increasing the simulation model scale and incorporating phenomenon-specific knowledge.

With a larger simulation model, one can verify and better replicate EEG waveforms generated in our minimal model exercises. It can also allow for incorporating more detailed dynamics, such as intrinsic hyperpolarizing currents and synaptic disfacilitation observed during sleep and seizures.

Many phenomena can be modeled in more detail and in close simulation- experimental verification loop. For example, the topology of specific sensory systems, such as motor or visual, can constrain local circuits as well as connectivity between hierarchical subsystems of that modality. An interesting phenomenon to explore would be event related potentials (ERPs) in motor cortex and how different areas (primary, supplementary motor ares, etc) contribute to ERP evolution, based on our circuit. Still, global scale phenomena such as anesthesia can be studied by incorporating effects of various drugs on different components in the system (synapses and firing dynamics, for instance).

An integration of our current model with existing models of the thalamus will also provide a more complete picture of EEG genesis under various vigilance conditions. Since our focus was on intra-cortically generated rhythms, our circuit did not explicitly include thalamic circuitry, but rather assumed a net level of excitation over input thalamic streams. Still we incorporated a segregation of thalamic inputs into specific sensory and nonspecific diffuse. Since the termination patterns of such inputs overlaps that of feedforward and feedback pathways in the cortex, it will be very interesting to study the different activation patterns of the specific thalamic nuclei and nonspecific nuclei such as intralaminar and pulvinar [6].

[6]The pulvinar is particularly interesting since it has been implicated in attention (Grieve et al

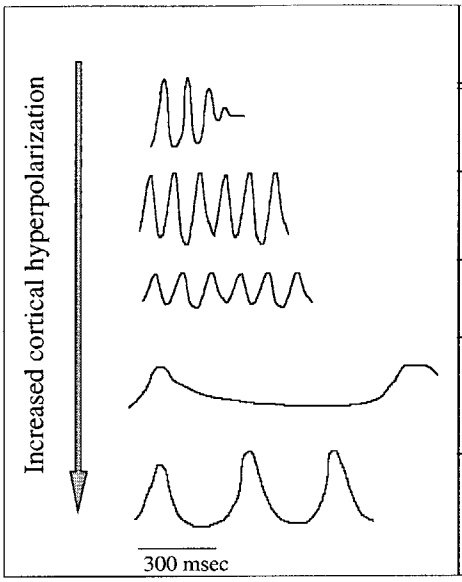

Rhythm	Main cortical inputs	Firing patterns
evoked alpha	bottom-up top-down	bursting
emitted alpha	top-down	bursting
alpha rhythms	non specific	regular spiking
slow-wave sleep	wide range nonspecific	rebound depolarization regular spiking
sleep delta	wide range nonspecific	rebound depolarization and bursting

Figure 7-6: The oscillatory behavior of layer 5 network under different vigilance states

7.3.1 Layer 5 as a network oscillator

The propensity of layer 5 cells to oscillate at slow frequencies (3-10Hz) appears to be a characteristic behavior which dominates in states of vigilance where neuronal hyperpolarization is maximal (sleep delta) or intracortical inhibition is dominant (idling alpha rhythms). In both cases, and due to the wide-spread connections of L5N, neural populations of the cortex follow this rhythm due to lack of afferent excitation.

Furthermore, the layer 5 network oscillator (L5N) might actively participate in cognition by accommodating top-down influence, such as in anticipatory conditions and transiently after an input stimulus. Again, the oscillatory phenomena in other cortical layers mimics that of layer 5 mainly due to the dominance of inhibition in the initial response to sensory input or what has been termed passive nature of sensory cortical areas (Mehta et al 2000 [157]. The functional consequences here are however different: layer 5 oscillator of sensory cortices drives specific cortical assemblies, based on internal expectations, into a cognitive state where high frequency oscillations are dominant. A summary of these observations is given in figures 7-6 and 7-7.

Based on the above, it appears that L5N might behave similarly to the specific thalamic nuclei oscillator. Here, cells oscillate at 7-14 Hz in low vigilance states by virtue of rebound from hyperpolarization, and relay information to the cortex during cognition upon depolarization.

Our final question relates to the generality of layer 5 behavior. While tufted layer 5 cells are found over wide cortical areas, including associational, their role in hierarchical gating is not obvious. Could there exist a general communication scheme

2000 [93], Schroeder et al 2001 [199]) and appears to be closely linked o layer 5 cells (Veinante et al 2000 [248]). The intralaminar nuclei were hypothesized to be involved in context binding while specific thalamic nuclei specify content in the hypothesis put forward by Llinas et al 1994 [134].

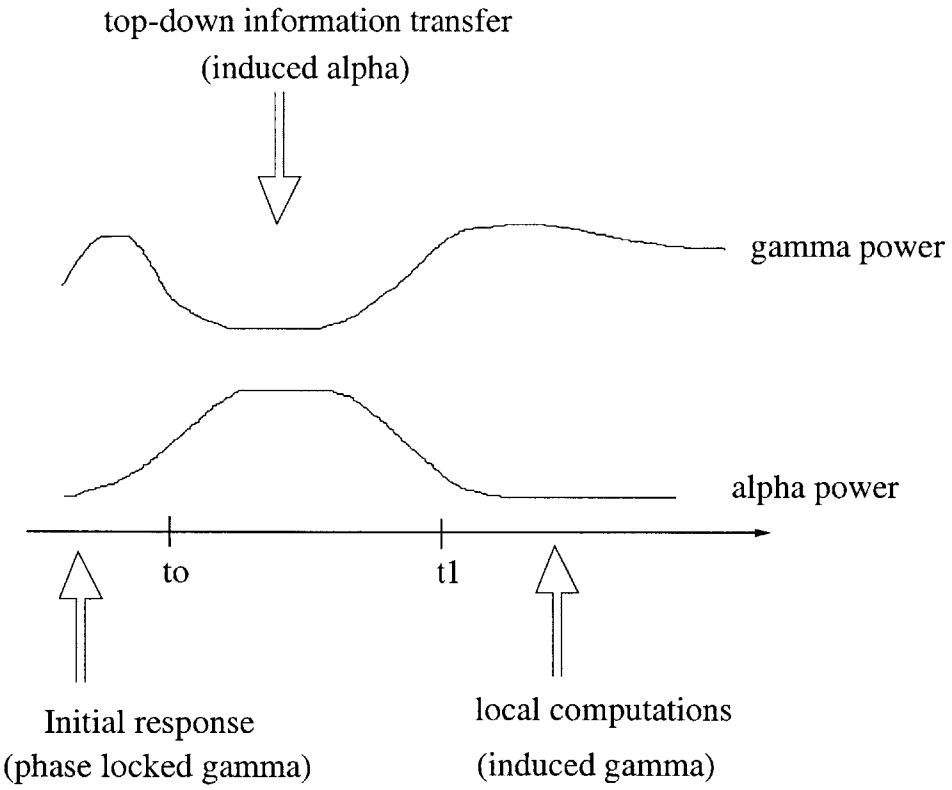

Figure 7-7: Time profile for poststimulus frequencies components in a local field potential and proposed functional consequences. Schematic represents the total power recorded in the alpha and gamma range in the LFP. $t0 = 25-100$ msec, $t1 = 100-300$ msec.

within the cortex which relies on gates that sample information from external inputs and readjusts local activity accordingly? Working memory studies in the frontal cortex seem to provide a preliminary positive answer (Durstewitz et al 2000 [68]). Here, a decrease in external influence and thus holding of local memory patterns is achieved by possibly decreasing the effect of afferent activity in superficial layers where zone A of TL5 cells lie.

Appendix A

General Models of EEG generation

A.1 Wilson Cowan models

The properties of two interacting neural populations depends on two variables:

$E(t)$: the proportion of excitatory cells firing per unit time at instant t;

$I(t)$: the proportion of inhibitory cells firing per unit time at instant t;

The state $E(t) = I(t) = 0$, correspond to low level background, or resting state. In a nut-shell, the value of E and I at times $t + \tau$ starting from time t depends on the proportion of cells which is not in the refractory state (thats is, which are "sensitive") and which also receives at least threshold excitation at time t to fire.

(a) The proportion of sensitive cells is given by

$$1 - \int_{t-r}^{t} E(t')dt' \tag{A.1}$$

This expression is understood by realizing that the integral term represents the proportion of cells that are insensitive due to an absolute refractory period of r *msec.* (An absolute refractory period is the time period after a neuron fires during which it does not respond to input excitation.)

(b) The proportion of cells receiving excitation above firing threshold per unit time is dependent on the average level of excitation $V_m(t)$ and $V_i(t)$ within the excitatory and inhibitory subpopulations (respectively). This dependency is given by a relationship called the subpopulation response function $\mathcal{F}_e(V_m)$ (and $\mathcal{F}_i(V_i)$ respectively). In general, these response functions depend on the distribution of threshold levels over the population and could be well fitted using a *sigmoidal* type function.

In turn, and assuming that individual cells sum their inputs and that the effect of stimulation decays with a time course $\alpha(t)$, then the average level of excitation generated in each cell of a population is obtained as:

$$V_m(t) = \int_{-\infty}^{t} [C_3 E(t') - C_2 I(t') + P(t')]\alpha(t - t')dt' \tag{A.2}$$

where $P(t)$ is the external input to the excitatory subpopulation. C_3 and C_2 are connectivity coefficients representing the average number of excitatory and inhibitory synapses per cell in the excitatory subpopulation. A similar expression can be written for the inhibitory subpopulation

We can now write the proportion of excitatory cells $E(t)$ and inhibitory cells $I(t)$ at time $t + \tau$ as

$$E(t+\tau) = [1 - \int_{t-r_e}^{t} E(t')dt'].\mathcal{F}_e[V_m(t)] \tag{A.3}$$

$$I(t+\tau) = [1 - \int_{t-r_i}^{t} I(t')dt'].\mathcal{F}_i[V_i(t)] \tag{A.4}$$

$$\tag{A.5}$$

where r_e and r_i are the absolute refractory period for the excitatory and inhibitory subpopulations respectively.The above expressions assume that the probability that a cell is sensitive is independent from the probability that it is currently excited above its threshold. Wilson and Cowan argue although this independence might not hold, the above expression is valid for a *richly c connected population* of cells.

After some mathematical manipulations, the authors arrive at a time-coarse grained form of the model equations:

$$\tau_e \frac{dE}{dt} = -E + (k_e - r_e E)\mathcal{F}_e(c_1 E - c_2 I + P) \tag{A.6}$$

$$\tau_i \frac{dI}{dt} = -I + (k_i - r_i I)\mathcal{F}_i(c_3 E - c_4 I + Q) \tag{A.7}$$

$$\tag{A.8}$$

where r_e (r_i) is the refractory period of the excitatory (inhibitory) population. k_e (k_i) is a normalizing constant such that $\mathcal{F}_e(0) = 0$ ($\mathcal{F}_i(0) = 0$). Variations of these equations became benchmark for neural population representations and came to be known as the Wilson Cowan model.

The sigmoidal behavior of $\mathcal{F}_e, \mathcal{F}_i$ introduce nonlinear effects which the authors show to lead to either (1) bistability (low and high activity states) with a hysteresis-like behavior between the two states, or (2) oscillations exhibited by an limit cycle behavior.

A.2 Alpha rhythm models

Elaborating on the above theory, and to obtain an analytical expression for the alpha activity, Lopes da Silva [140] assumed that the *average level of excitation* is

proportional to the *average membrane potential.* Also, the decay function $\alpha(t)$ is substituted by the time function $h_e(t)$ which represents the EPSP (excitatory postsynaptic potential) for the excitatory population and by $h_i(t)$ which represents the IPSP (inhibitory postsynaptic potential). With these changes, equations (A.2) and (inhibitory counterpart) become:

$$V_m(t) = \int_0^\infty [C_3 E(t-t') + P(t-t')] h_e(t') dt' - \int_0^\infty [C_2 I(t-t')] h_i(t') dt' \quad \text{(A.9)}$$

$$V_i(t) = \int_0^\infty [C_1 E(t-t') + Q(t-t')] h_e(t') dt' - \int_0^\infty [C_4 I(t-t')] h_i(t') dt \quad \text{(A.10)}$$

(A.11)

Also, a simplified expression for the proportion of excitatory and inhibitory cells in equation (A.3) neglects the refractory period, that is

$$E(t+\tau) = f_e[V_m(t)] \quad \text{(A.12)}$$

$$I(t+\tau) = f_i[V_i(t)] \quad \text{(A.13)}$$

(A.14)

in which $E(t)$ and $I(t)$ are equivalent to the *impulse density of the subpopulations* excitatory and inhibitory neurons.

In its simplest form, the Lopes da Silva (LS) model consists of a set of simulated neurons called TCR (thalamo-cortical relay) cells which have excitatory interactions and a set of feedback interneurons that provide inhibition of the TCR cells. Each of the TCR cells receives independently as an input $P(t)$, which according the above adjustments is an input *impulse density* $P(t)$ whose value (*impulses/sec*) could be uniformly distributed between two boundaries derived from experimental steady state operation. The EEG activity is then assumed to be proportional to the sum of membrane potentials $V_m(t)$ of all TCR neurons. Accordingly the model output is the excitatory population membrane potential $V_m(t)$.

A lumped model of this interaction is given in figure 1-6. Here $Q(t) = 0$, $C_3 = 0$ and $C_4 = 0$. Also, neuronal subpopulations are neuronal sets, that is cells within the excitatory population do not excite each other but regulate activity though the inhibitory neuronal set. The appropriateness of this model could be tested using power spectral analysis upon expanding the nonlinear $f_E(v)$, $f_I(v)$ terms in a taylor series expansion and taking the random variables $P(t)$, $V_m(t)$, $V_i(t)$, $E(t)$, and $I(t)$ as stationary and described in terms of fluctuations around their respective mean values. For example the input $P(t)$ becomes $p(t) = P(t) - \overline{P}$, $\overline{P}$ being the mean value. Hence, linear filter analysis would apply and resonance characteristics of the system could be studied. The spectral contents of the output signal $V_m(t)$ closely resembled $10Hz$ alpha activity under a specific set of input strength, appropriate $EPSP$ and $IPSP$ time constants, and connectivity strength between the two populations.

From this simple model, a better understanding of how alpha activity is propagated *spatially* was developed in 1982. Staring from the lumped model population

characteristics, the spatially distributed model by Van Rotterdam 1982 [246] was based on the hypothesis that spatial propagation of alpha activity depends on spatial properties of the network. That is, the strength of inhibition/excitation and the resultant dominant resonance frequency depends on the length of inter-neuronal connections.

The model starts with a one-dimensional neuronal chain, consisting of populations of neurons (such as the TCR cells) and interneurons (providing inhibition – figure1-7) and are connected by means of spatially distributed fibers among these populations.The main assumptions involved in this spatially distributed model are:

1. Interconnections between neurons are homogeneous in space. That is, taking a one dimensional chain of interconnected neurons, the connection strength is a function of actual metric distance and not of location within the chain.

2. Inhibitory and excitatory subpopulations Input/output transfer characteristics (EPSP and IPSP) are similar to those chosen in the lumped model (in this instance, $h_e(t)$ and $h_i(t)$ are of second order with $h_i(t)$ more slowly decaying than $h_e(t)$ – see figure A-1).

3. Strength of interconnectivity between subpopulations along the chain decreases exponentially with distance between the two subpopulation. This choice of spatial kernel is motivated by the effective exponential drop of dendritic contacts with other neurons as the dendritic tree spreads away from the neuron cell body.

Hence, and following the terminology presented earlier, Van Rotterdam assumed the canonical circuit to be a simple negative feedback action between the neuronal sets (T_k and I_k). The intra-column and the inter-columnar connection topologies are assumed homogeneous and of exponentially decaying strength away from the minicolumn.

Denoting $C_e(r,l)$ to be the number of excitatory synapses from the r^{th} main cell to the l^{th} interneuron and by $C_i(l,r)$ as the number of inhibitory synapses from the l^{th} interneuron to the r^{th} cell, then :

$$g(r,t) = h_e(t) * p(r,t) - h_i(t) * \left[\sum_{l=-\infty}^{+\infty} C_i(l,r) h_e(t) * \{ \sum_{m=-\infty}^{+\infty} C_e(m,l) g(m,l) \} \right]$$

where $g(r,t)$ is the membrane potential of cell r at time t, and $p(r,t)$ is the corresponding input spike density (or rate) at time t and location r in the chain. As defined before, $h_e(t), h_i(t)$ are the transfer functions between input impulse density to a cell and its post-synaptic potential (excitatory and inhibitory, respectively). Note that the above equation is linear and assumes relationships between fluctuations in input and outputs around an initial operating point (or mean value). Under the assumptions of the model, $h_e(t), h_i(t), C_e$, and C_i are considered as shown in figure A-1. Utilizing the homogeneous interconnection property between neurons, and assuming a continuous chain of neurons, the above equation can be written in the time-space Fourier domain as :

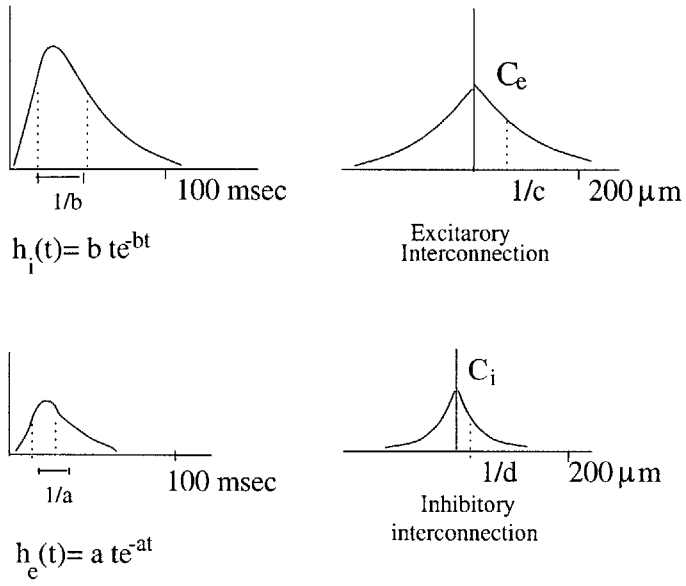

Figure A-1: Transfer Properties of the Spatially distributed model of the local theory.

$$G(jk, jw) = \frac{H_e(jw)}{1 + H_e(jw)H_i(jw)C_i(jk)C_e(jk)} P(jk, jw)$$

where k and w are the spatial and temporal frequencies, respectively.

The alpha rhythm can be obtained from the above model by stimulating the chain randomly in space and time. Since the model is linear, it is sufficient however to excite the chain with a simple harmonic w_o at $x = 0$, or $P(jk, jw) = \delta(w - w_o)$. The oscillatory response of the system above is then studied as roots of the dispersion relation $D_L(jk, jw)$ in

$$G(jk, jw) = \frac{1}{D_L(jk, jw)} P(jk, jw)$$

$$D_L(jk, jw) = \frac{(jw + b)^2(jw + a)^2(k^2 + c^2)(k^2 + d^2) + Q(abcd)^2}{(jw + b)^2(k^2 + c^2)(k^2 + d^2)(1 + Q)a^2}$$

where a,b are characteristic rise times of the EPSP $h_e(t) = ate^{-at}$ and the IPSP $h_i(t) = bte^{-bt}, t \geq 0$, respectively. The postsynaptic potential outputs of h_e, h_i decrease exponentially with distance at characteristic lengths $1/c$ and $1/d$ respectively (see figure A-1). Q is a non dimensional quantity describing strength of coupling between excitatory and inhibitory neurons.

The above dispersion relation has 4 roots forming two branches of a wave phenomenon, one local and another traveling away from epicenters (similar to the rain drop phenomenon in a pool). For the proper choice of c and d, the wave number k of signals propagating into the scalp is low $k < 0.5 - 1.0/cm$ (as higher k is filtered out by the lowpass characteristic of the medium) . For $k = 0$ and $Q < Q_{threshold} = \frac{(a+b)^2}{ab}$, waves in the alpha band are seen to be the least damped among other rhythmic components in the chain which decay around twice as fast. Hence the main frequency

traveling from epicenters is that in the alpha range (11 Hz).

experimental support

The model developed has characteristics that are in qualitative agreement with experiments performed on the visual cortex of a dog where alpha activity could be recorded. This agreement can be seen in

(1) Coherence analysis of recorded EEG (from subdural electrodes) showed that signals in the alpha band were the most correlated as compared to other components of the signal. This agrees with the model prediction that the alpha component is the least damped .

(2) The characteristic lengths $1/c$ and $1/d$ obtained from the model are in agreement with experimental data. Measuring the phase shifts at the alpha frequency in the cortex of four dogs, and using the model to compute $1/c$ and $1/d$ which correspond to this velocity, the calculated figures (160 to 330 μm) are in the same range as the basic physically justified cortical columns (vertical columns of 200-300 μm in diameters).

A.3 Nunez Global model

Unlike the LS theory, the global model neglects local delays due to intra-column connections, but includes activity delays in longer cortico-cortical fibers. Intracortical fibers of the LS theory are both excitatory and inhibitory. The cortico-cortical interactions described here are purely excitatory. Since surface EEG represents average activity at macroscopic scales, the global theory follows the excitatory $l_E(r,t)$ and inhibitory $l_I(r,t)$ action densities (total number of active synapses per unit volume at time t) in a cortical macrocolumn by means of an *assumed quantitative relation* between these densities and action potential firings (figure 1-8,right). The cortical macrocolumns considered here are not restricted in size but should contain sufficient synaptic activity so that the approximations carried are valid.

The main idea behind this theory is that 'the equations linking synaptic activity to action-potential firings $g(r,t)$ follows directly from the idea that synaptic action in a mass of neural tissue is due to action potentials fired from some other location, generally at earlier times'. In figure 1-8,

$$l_E(r,t) = p(r,t) + \int_0^\infty dv \int_s R_E(r,r_1,v) g\left(r_1, t - \frac{|r-r_1|}{v}\right) d^2 r_1 \tag{A.15}$$

$$l_I(r,t) = p_0 + \int_s R_I(r,r_1) g(r_1,t) d^2 r_1 \tag{A.16}$$

where $p(r,t)$ is the excitatory input to the cortex at radius r and time t. The distribution functions $R_E(r,r1,v)$ describe the number density of excitatory cortico-cortical

fibers connecting locations r and r_1 which also have propagation velocity v. The distribution function of inhibitory intracortical fibers $R_I(r, r_1)$ has infinite propagation velocities, as these connections are over short distances (only local). p_o is assumed to be a fixed inhibitory input to the cortex under a given physiological state. Note here that only interactions between columns is considered and not surface-normal interactions within one column (such as between different neocortical layers – hence the integration over surface s) and that equations A.15,A.16 are coupled.

The connection distribution function $R_E(r, r1, v)$ can be thought of as a simplified quantitative topology that is an extension of the inter-column connection topologies defined earlier onto a larger scale. Instead of having cortical columns connecting within a sub-region, the whole sub-region is taken as a cortical macrocolumn and a connection topology between these macrocolumns is drawn (possibly though if as inter-subregional connections).

Linearization of the above equations is performed about some operating point g_o (figure 1-8), writing

$$\delta g = \frac{\partial g}{\partial l_E} L_E + \frac{\partial g}{\partial l_i} L_I \tag{A.17}$$

where $L_E = \delta l_E$ and $L_I = \delta l_I$. Also define the positive definite cortical excitability parameters as

$$Q_E = \left(\frac{\partial g}{\partial l_E}\right)_{g=g_o} \qquad Q_I = -\left(\frac{\partial g}{\partial l_I}\right)_{g=g_o} \tag{A.18}$$

which indicate the responsiveness of cortical columns to excitatory and inhibitory input. Defining G(r,t) to be the fluctuations in $g(r,t)$ around g_o (and similarly for upper case $L_E(.)$ and $L_I(.)$), Equation A.17 is rewritten as:

$$G(r,t) = Q_E L_E(r,t) - Q_I L_I(r,t) \tag{A.19}$$

Hence, the coupled equations (1.4) and (1.5) when linearized now become:

$$\begin{aligned} L_E(r,t) &= \int_0^\infty dv \int_s R_E(r, r_1, v) \left[Q_E L_E \left(r_1, t - \frac{|r - r_1|}{v} \right) \right. \\ &\quad \left. - Q_I L_I \left(r_1, t - \frac{|r - r_1|}{v} \right) \right] d^2 r_1 + P(r,t) \\ L_I(r,t) &= \int_s R_I(r, r_1) \left[Q_E L_E(r_1, t) - Q_I L_I(r_1, t) \right] d^2 r_1 \end{aligned} \tag{A.20}$$

Solutions of the above equations over one-dimension in an infinite medium is first considered and then extended by first applying boundary conditions and then using a 2D surface, and finally using an oblate spheroid.

For the one dimensional system ($r \to x$) the distribution function $R_E(x, x_1, v)$ of excitatory fibers is assumed to be that of N overlapping fiber systems as:

$$R_E(x, x_1, v) = \frac{1}{2} \sum_{n=1}^{N} \rho_n \lambda_n f_n(v) e^{-\lambda_n |x - x_1|} \tag{A.21}$$

where λ_n^{-1} is the characteristic length for the nth fiber system, $f_n(v)$ is the propagation velocity distribution of that system, and ρ_n is the number of synapses per neuron associated with system n.

Similarly, the intracortical fiber connection density is given by;

$$R_I(x, x_1) = \frac{1}{2}\rho_I \lambda_I e^{-\lambda_I |x - x_1|} \tag{A.22}$$

where delays were neglected in this intracortical system.

We can now write in the 2D Fourier domain, after some manipulations,

$$L_E(k, w) = \frac{1}{D_G(k, w)} U(k, w) \tag{A.23}$$

$$D_G(k, w) = 1 - \frac{Q_E}{Q_I} \sum_{n=1}^{N} \frac{\rho_n}{\rho_1} \int_o^\infty \frac{\lambda_n^2 v^2 + jw\lambda_n v}{(\lambda_n v + jw)^2 + k^2 v^2} \tag{A.24}$$

Simplifying further, assume that there is only one excitatory fiber system with finite velocity (N=1, or N is replaced by E), and further that $f_E(v) = \delta(v - v_E)$, (one velocity), then $D_G(k, w)$ has roots with real part γ and imaginary part w_R:

$$w_R^2 = v_E^2 \left[k^2 - \lambda_E^2 B(k)/4\right] \tag{A.25}$$

$$\gamma = -\lambda_E v_E \left[1 - B(k)/2\right] \tag{A.26}$$

where

$$B(k) = \frac{\frac{Q_E \rho_E}{Q_I \rho_I}}{1 - \frac{Q_E}{Q_I} \sum_{n \neq E} \frac{\rho_n}{\rho_I} \left(1 + \frac{k^2}{\lambda_n^2}\right)^{-1}} \tag{A.27}$$

$B(k)$ will be seen to play an important role in controlling the simulated change of state in EEG. If we now close the infinite strip of the cortex to be a loop of length L, then standing waves of discrete wave numbers are forced by the boundary conditions:

$$K_m = \frac{2\pi m}{L}, m = 1, \infty \tag{A.28}$$

Hence from equation A.25, and for B small, the lowest mode has an estimated frequency

$$f_1 \approx \frac{k_1 v_E}{2\pi} \approx 6 - 18Hz \tag{A.29}$$

which is generally consistent with the awake EEG. As B approaches the critical value $2K_m/\lambda_E$, there is an abrupt decrease in the frequency of the kth mode suggesting change from awake to sleeping state. Although the presented linear simplified model has several assumptions, mainly infinite 1-D cortex, single long fiber system which has only one propagation velocity, the theory is later extended to relax each of these

assumptions. Nevertheless, the simple model is seen consistent with EEG phenomena, the experimental support is given next.

experimental support

(1) Alpha rhythm is predicted to occur as a global wave phenomenon which corresponds to the first harmonic of the global system, and which varies inversely with the head size (an experimental survey on 123 subjects showed a mean negative correlation between head size and alpha peak frequency). The theory suggests weakly damped modes of approximate frequency of about $f \approx 2$ to 26 Hz under realistic ranges of cortical radius and propagation velocity, and a relatively small value of control parameter B. As B is increased, different modes in the system are seen to abruptly decrease their temporal frequency at different rates for each mode. This is somewhat similar to different sleep stages: the abrupt decrease which occurs in the dominant EEG frequency to the 1Hz range at sleep onset. In addition some higher frequency components can be observed at different sleep stages. In the context of the global theory, this may be viewed as higher modes that are over-damped at lower B values that break lose and become more apparent at high er values of B. Thus, the model developers claim that B behaves like representing the inhibition from the midbrain, and that the lowpass character of the model matches, at least qualitatively the behavior of the neocortex.

(2) Phase velocity for the global alpha rhythms is predicted to be near the conduction velocity of cortico-cortical fibers at 6-9 m/s. In separate experiments by other workers, alpha activity has been measured at 4-20 m/s and at 7m/s.

(3) Effect of anesthesia on cortical rhythm under halothane: It was seen that by varying the levels of anesthesia (in experiments on eight subjects) different frequencies become dominant and have a global character (appear at all locations on the scalp). In general lower frequencies were observed as intermediate levels of anesthesia are increased. Although the exact effect of halothane on different subcortical structures and brain stem varies, making it difficult to predict how the control parameter B behaves. It is noted that most anesthetics could produce cerebral seizures. They also increase amplitudes of sinusoidal EEG at intermediate levels. Hence, Nunez claims that anesthetics are more likely to increase the excitability of the cortex, and hence increase the control parameter B. If this were the case, Nunez claims, then his model shows that the variations in the observed frequencies matches well (in principle) with dominant frequencies predicted by the (closed spherical surface) model.

A.4 Signal processing techniques in EEG

Understanding EEG signals using engineering tools have been a long-term goal of the medical diagnostics community. This is driven by, first looking for specific signal

features for the purpose of finding correlations between different brain areas, and possibly using an automated classification/detection procedure that will alleviate several man-hours of reading raw EEG.

In extracting features the time-frequency decomposition is a main tool . This included fourier transforms (Duffy 1979, 1981[66, 67], Jando [100] and wavelet decompositions (Schiff 1994 [194, 195, 196]). Other techniques such as nonlinear dynamics, statistical analysis and adaptive segmentation techniques were also applied (Cretzfeldt 1985 [48], Mayer-Kress 1987 [151], Martignon 1994 [149], Von Spreckelsen [249], Stam 1999 [215]) Classification of the features can be done either by, for example, atrifical neural networks (Gabor 1992 [81], Jando 1993 [100], Roberts 1992 [189]) or self-organizing maps (Joustiniemi [104], Gabor 1996 [82]). Still, other methods applied model based parameters, such as attempting to utilize a Lopes da Silva type model to detect seizures in new borns (Roessgen et al 1998 [190].

Appendix B

Neural Diversities in Cerebral Cortex

B.1 Neurons and Synapses

A basic neuron can be described as having a cell body or *soma* and specialized extension for transmission of electrochemical signals, known as the dendrites (input ports) and axons (output port). Dendrites form a branched structure which brings in information (after possible transformation) into the soma while the axons are the output ports which transmit information out of the neurons in terms of action potentials (figure B-1). Neurons are interconnected via synapses which mainly occur between a presynaptic axon of one neuron and a postsynaptic dendrite of another neuron. Synapses are also formed between axons of a presynaptic neuron and the soma of a postsynaptic neuron (axo-somatic), the axon (axo-axonic), as well as between dendrites of opposing neurons (dendo-dendritic). The information transmission at a synaptic junction can be accomplished by chemical or electrical synapses.

B.2 Morphology

Neocortical cells are classified according to the shape of the cell body, their dendritic trees and axonal targets. Cells that have spines on their dendritic trees are called spiny, while those that lack spines are called smooth cells, sparsely spiny cells have a low density of spines.

Spiny Pyramidal cells constitute about 70-80% of neurons in the mammalian neocortex and are called so referring to their somata shape (figure B-2). Their dendritic trees have spiny formation onto which afferent connection are directed, hence the name spiny pyramidals. Pyramidal cells exist in all layers of the neocortex, with their main dendritic trunk usually extending in a vertical direction, towards the neocortical surface (though may well fall short from reaching the surface), giving off first the oblique oblique dendrites, then ramifying in the apical dendrites. Other branching dendrites extend in a region around the layer where the soma exist and these are the basal dendrites. Pyramidal cells of the neocortex have asymmetrical

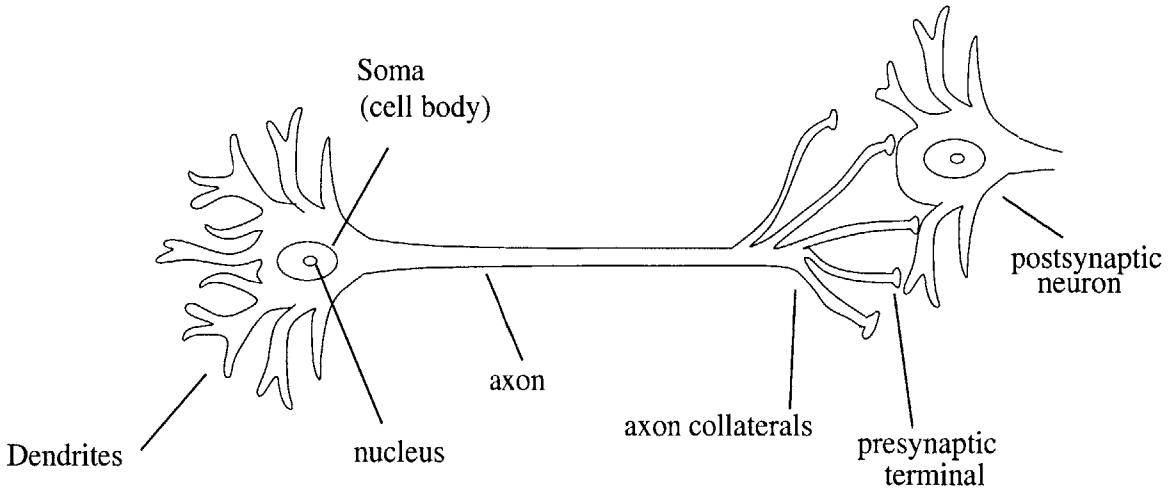

Figure B-1: Basic neuron diagram and its connection. The dendrites are represented as generic structures onto which presynaptic terminals are directed. Axonal output of neurons, or action potentials are transmitted via axon collaterals to postsynaptic targets.

or excitatory axonal projections. That is, they are presynaptic only at asymmetrical junctions mainly to dendritic spines and shafts and rarely to cell body (White [254]). Superficial lying pyramidal cells have myelinated axonal trunks which preserve action potential propagation through an active process thus enabling faithful transmission of information over long distances, while the axonal collaterals are unmyelinated.

Nonpyramidal cells can be spiny, sparsely spiny or smooth according to the density of spines on their dendritic tree. In general, these cells have local axonal ramifications [254], and hence, they tend to be part of the local cortical circuit. Examples of these cells are

Basket cells, whose axonal distributions from nests or baskets around cell bodies and proximal dendrites of pyramidal cells (figure B-2). Their dendrites radiate in all directions, and their axons could run horizontally as far as 1 mm (White [254]). Although their axonal shapes endowed their name, these are increasingly becoming known as interneurons with the classification becoming more functional, that is the cells firing characteristic and synaptic sensitivity. In fact, in later experimentations, Braitenberg and Schuz [22] did not observe basket cells, suggesting that the basket shape is simply due to a convergence of somatic synapes by several smooth neurons.

Spiny stellate cells, which occur exclusively within the middle layers of primary sensory areas if many species. Their dendrites have no defined orientation, with a high density of spines that have similar functional characteristic as those of pyramidal cells. These cells are thought to be specialized form of a continuum of pyramidal cells.

Other cells, such as chandelier, double bouquet and Martinotti are described in the literature with less knowledge of their function.

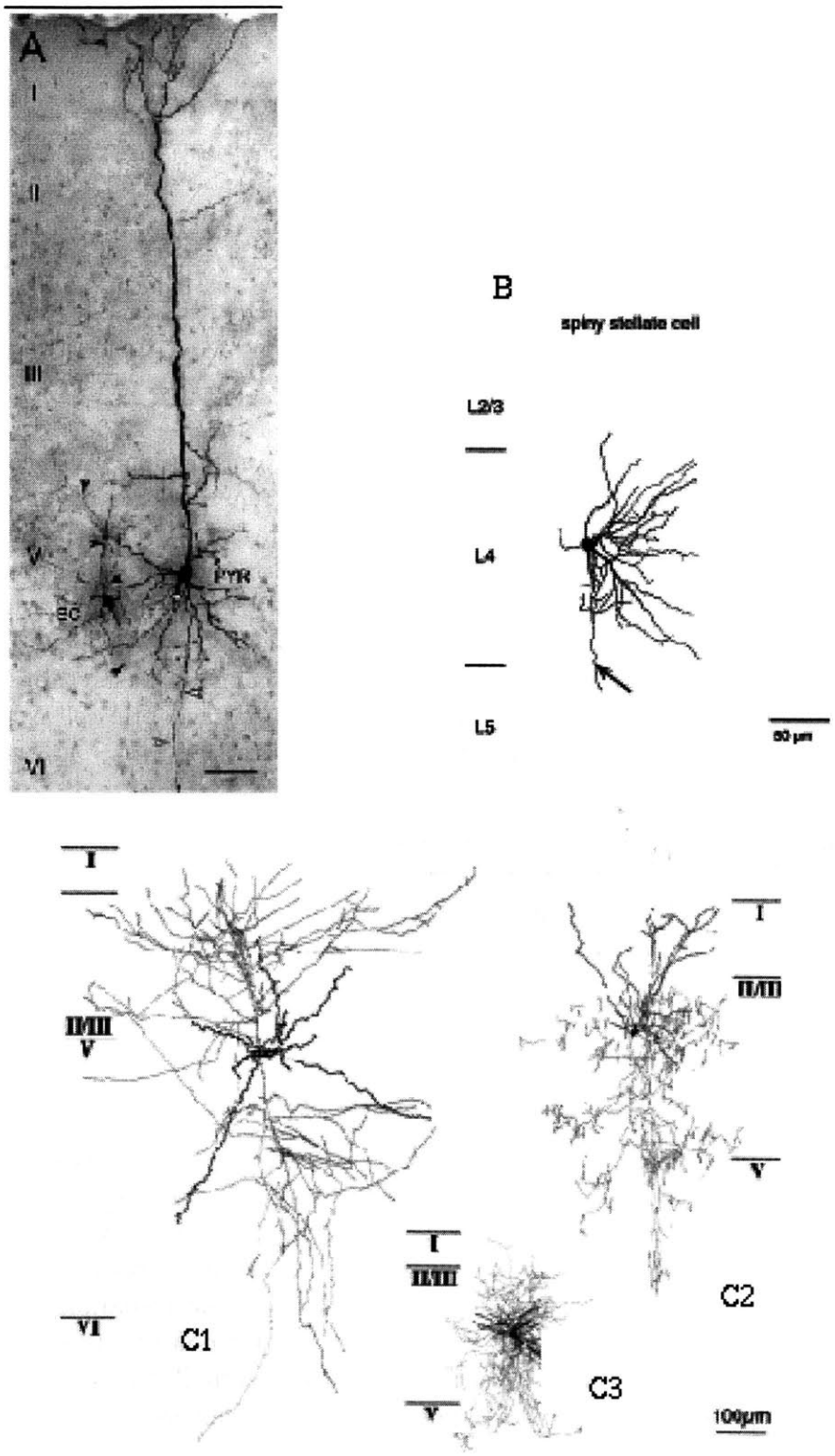

Figure B-2: Sample of neural types in neocortex. Roman numerals refer to laminar location of cells. A: Layer 5 pyramidal cell (Pyr) and a connected basket cell (BC) (in rats motor cortex- from Angulo et al 1999 [7]) scale bar is 100 μm. B: Spiny stellate cell of layer 4 (rat- from Feldmeyer et al 1999 [70]). C1: widely branching interneuron, C2: Chandelier interneuron and C3: neuogliaform cell (rat frontal cortex - from Kawaguchi et al 1998 [116])

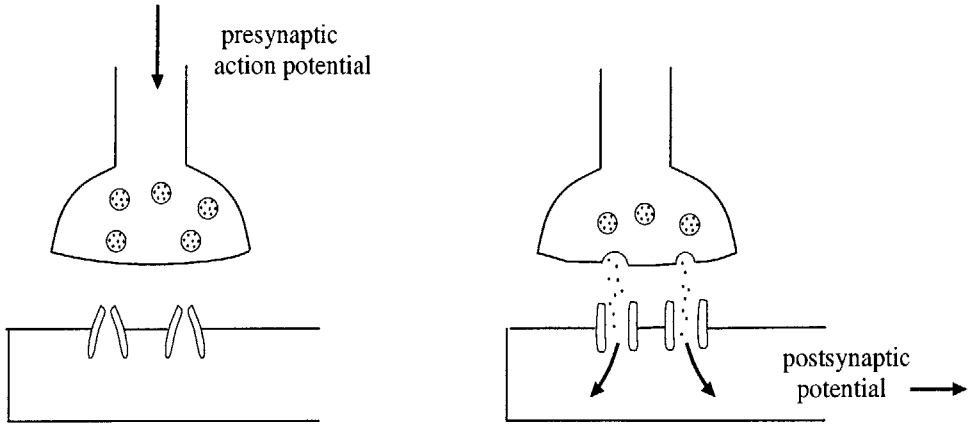

Figure B-3: Diagram for basic direct chemical synaptic transmission. An incoming action potential at a presynaptic terminal causes an influx of calcium in that region causes a migration of vesicles (round bodies) towards the terminal region. The vesicle which contain neurotransmitter molecules inside, will then fuse to that terminal and release neurotransmitter into the synaptic cleft. The neurotransmitter will then diffuse across the cleft and bind with the closed receptors at the postsynaptic side causing them to open (direct) transmission. In general, the neurotransmitter will create a change in postsynaptic membrane potential causing it either to depolarize, increasing the postsynaptic cell excitability, or hyperpolarize, decreasing the cells ability to fire action potentials.

A summarized example of the common types of neocortical neurons is given in table B.1. Included is also the type of neurotransmitter mediating excitation (Glutamate) or inhibition (GABA). The connectivity They are also classified according to their laminar position in the neocortex; this will be discussed in a later section.

B.3 Synapses

A main distinction among classes of neurons is usually made based on the type of synapses they make on their postsynaptic targets. Some neurons mainly spiny pyramidal neurons have asymmetrical synapses and these are excitatory, that is they have a depolarizing effect on the postsynaptic target. Other excitatory synapses are derived from spiny stellate neurons and extracortical inputs. Excitatory connections form 75-80% of total synapses in the neocortex [165]. The remaining synapses are symmetrical synapses; these are usually made by smooth nonpyramidal interneurons and are called inhibitory synapses as they normally contribute to hyperpolarizing their target. In general, synaptic transmission can be either by chemical (figure B-3) or electrical mechanisms.

Direct synaptic transmission between neocortical cells is mostly mediated by glutamate in excitatory synapses and gaba-aminobutyric acid GABA in inhibitory synapses. Afferent modulatory fibers to the cortex from the basal forbrain and brain stem nuclei release other types of neurotransmitters such as acetylcholine, dopamine, serotonin, norepinephrine, or histamine, depending on the system.

Excitatory synapses release the neurotransmitter glutamate which causes changes in the ionic influx in the postsynaptic target, either through membrane depolarization or the action of second messengers. We will avoid talking about biochemical nature of these processes, but instead summarize the net effect on a postsynaptic neuron (see figure B-4). Neurotransmitters bind to postynaptic channels causing influx of ions through those channels across electrochemical gradients with the net effect of either increasing or decreasing the membrane voltage (hence excite or inhibit). Channels can be either voltage-gated or ligand-gated. Ligand-gated channels include AMPA, NMDA , GABA, ACh, and 5-HT receptors.

The effect of a particular receptor on channel opening and closing is usually simplified to represent a net current injection onto the postsynaptic membrane that is voltage dependent

$$I_{syn}(t) = g_{syn}(t - to)(E_{syn} - Vm(t)) \tag{B.1}$$

where g_{syn} describes channel kinetics that come into activation when presynaptic glutamate is released (or an action potential occurs) at time t_o and E_{syn} is the reversal potential of that synapse which essentially affects the ion influx through the channel depending on the voltage gradient at the membrane. More complicated models of the biochemical reactions involved in synaptic activity and which incorporate the rate and availability of neurotransmitters do exist, but will not be discussed here.

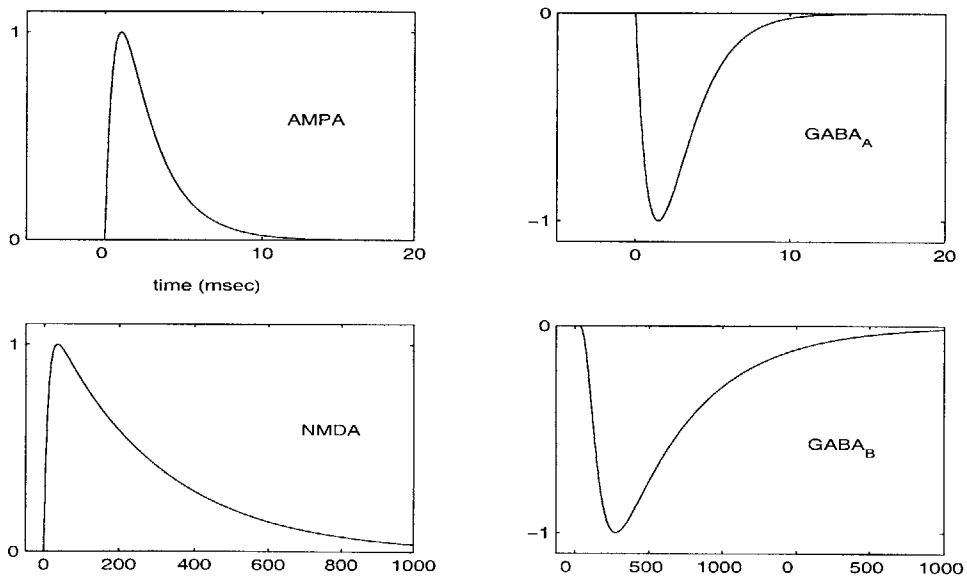

Figure B-4: schematic diagram of the time profile of major synaptic responses

Of the major receptor families, we will mention only those pertinent to our effort.

AMPA receptors mediate fast excitatory synaptic transmission with onset and offset time in the low millisecond range (1-3 msec). They are present in high density at the majority of neocortical synapses.

NMDA receptors mediate slow excitatory transmission through channels that remain open for prolonged periods of time (100-200msec) and are widely abundant in

Table B.1: Common neocortical morphologies (adapted from Mountcastle [165])

Cell type	Transmitter	Terminal type	Targets
Spiny pyramidal	Glutamate	Asymmetric Excitatory	Intrinsic, All cell type Extracortical structures
Spiny nonpyramidal (e.g. spiny stellate)	Glutamate	Asymmetric Excitatory	Intrinsic, Pyramidal Nonpyramidal
Basket cells	GABA	Symmetric Inhibitory	Intrinsic Pyramidal cells
Double bouquet	GABA	Symmetric Inhibitory	Intrinsic Pyramidal cell spines nonpyramidals
Chandelier	GABA	Symmetric Inhibitory	Intrinsic Pyramidal cell (initial segment)
Bipolar	GABA	Symmetric Inhibitory	Intrinsic All cell types

the neocortex. These channels are usually blocked by magnesium ions Mg^{2+} and become active when sufficient depolarization removes this blocking, allowing a coincident presynaptic transmitter release to cause net current influx.

$GABA_A$ receptors are Cl^- selective ion channels that once activated causes an influx of these ions which effectively reduces the voltage gradient across the membrane. The Kinetics of these receptors are relatively fast and play a major role in preventing neocortical neurons from runaway excitation.

$GABA_B$ receptors have slow dynamics mediated by second-messenger proteins. Its activation produces a late EPSP which begins some tens of milliseconds after an afferent volley to the synapse, peaks about 135 msec and may last for 300-400msec, thus overlapping the action of long-lasting excitatory action of NMDA synapses.

Neuronal firing properties

Neocortical neurons are customarily subdivided also by their intrinsic firing behavior, that is, their generation of sequences of action potentials in response to a constant injection of input current to their soma. While this idea is being challenged by an increasing diversity of firing characteristics of different neurons (especially interneurons), as well as within the same neuron under different stimulation patterns, few major firing patterns generally hold.

1. Regularly spiking (RS) cells respond to somatic input by a series of action potentials whose frequency increases with the input current up to a saturation value. For a given level of stimulus, the firing rate can be either uniform over the stimulus (in so called non-adapting cells) or starts with an initial high rate which then adapts to a slower steady-state value (so called adapting regularly spiking cells). RS cells are predominantly pyramidals but could also be interneurons.

2. Fast spiking (FS) cells are characterized by vigorous response to input stimuli at high rates (300-400 Hz) which is possible by virtue of short lived or fast action potentials. These cells are mainly interneurons in the cortex.

3. Intrinsically bursting (IB) cells are seen to produce an initial "burst" of action potentials (2-5 APs) with a high intraburst frequency (100-200 Hz).Subsequently the cell may switch to a regularly firing mode or sustain bursting at a low frequency (6-12 Hz). Pyramidal cells of this characteristic exist in layer 5.

4. Chattering (Ch) cells are characterized by sustaining a high frequency of bursts (30-40 Hz) with interburst frequency of around 300 Hz. These cells were of pyramidal type and observed in the visual cortex of cat (Gray et al 1994 [92]) . Still others saw fast rhythmic bursting (FRB) cells that fire similar sequences of bursts (Steriade et al 1996 [219]).

5. Other firing types exist, these include low threshold spiking (LTS) cells have the ability to fire at relatively hyperpolarized membrane potentials; examples of these cells are interneuronal populations in layers 4 and 5 in rats (Galarreta et al 1999 [84], Gibson et al 1999 [88], Beierlein et al 2000 [15]) as well as pyramidal cells in layer 5 of rat somatosensory cortex (Castro-Alamancos 1996 [29]). Diverse firing behaviors also exist in interneuronal populations, such as late spiking (LS) cells, which respond to a persistent input with a late action potential (Gupta et al 2000 [95]).

Appendix C

Simulation Parameters

C.1 Notation

The parameters of different simulations are in general in close agreement, especially when the same network size is used. Also, some simulations involved layer 5 cells only (augmenting responses); others involved layers 3 and 5 only (alpha selectivity). The general parameter notation is as follows:

g_{xx}	connections within the minicolumn.
$g_{m,n}$	pyramidal cell in layer m and another pyramidal in layer n.
$g_{m,ni}$	pyramidal in layer m to interneuron in layer n
$g^a_{mi,n}$	$GABA_A$ mediated connection between interneuron in layer m and pyramidal cell in layer n
$g^b_{mi,n}$	$GABA_B$ mediated connection between interneuron in layer m and pyramidal cell in layer n
$g_{m,nd}$	pyramidal in layer m to apical dendrite of pyramidal in layer n
$g_{m,ndi}$	pyramidal in layer m to interneurons targeting apical dendrite of pyramidal in layer n
k_{xx}	connections between adjacent minicolumns to form a local circuit, that is, column level. Similar notation follows as above.
$d_{k,m}$	synaptic delay corresponding to $k_{m,-}$. That is, delay in local connections starting from cell m into other microcolumns.
$d_{g,m}$	synaptic delay corresponding to $g_{m,-}$. That is, delay for collaterals of cell m within the minicolumn (set to 0.5-1 msec throughout).

In some instances, such as for alpha selectivity simulations, a cortical column is represented by a single minicolumn and as such g_* represents connections within a column, and k_* represents connections between columns.

For connections over long distances, such as between areas, delay is around 10msec. These connections follow either ascending (feedforward) or descending (feedback) topologies. The notation is as follows:

$K_{ff,m}$ feedforward connection from layer 3 of low-order area to pyramidal in layer m in high-order area.

$K_{fb,m}$ feedback connection from layer 5 of high-order area to pyramidal in layer m in low-order area.

$D_{K,ff}$ synaptic delay in feedforward connections (similarly for feedback delays, D_{K_fb}).

All the synaptic conductances are given per unit in terms of base conductances. For example, if $g_{33} = 0.6p.u.$, and $G_{\text{AMPA,max}} = 3nS$, then the AMPA -mediated connection has a strength $g_{33} = 1.8nS$.

Simulations were performed using Simulink 4.0 with Simulink Accelerator, produced by MathWorks for Windows. Package was installed on a Dell Optiplex GX150 with 1 GHz processor.

C.2 Cellular currents

In the slow-wave and seizure activity simulation, it is argued that a mixture od hyperpolarizing currents, persistent Na^+ current inactivation, and synaptic disfacilitation contribute to the cessation of activity after some period of time (>1 sec). Several experimental evidence also point to the fluctuations in extracellular calcium concetrentations in a similar time scale as a slow-wave cycle of up and down states. A simple way to introduce all these factors, we suggest, is to lump there effect on the total current available to the cell by using a qualitative, calcium-dependent synaptic disfacilitation constant. This was used in layer 5 cells and was especially active during seizure phenomnon

C.3 Simulation scenarios

Slow-wave oscillations

The simulation included 4 cortical minicolumns interconnectd in a closed chain as shown in figure 6-33, and parameters as in table C.1 . Each cell received a random current injecte into the soma uniformly distributed between -0.7 and 0.7 nA. This has the effect of creating, or simulation the appearance of spontaneously-occuring post-synaptic potentials in a cell. This level of base-line excitation, however, does not produce firing in regularly spiking cells; only cells in layer 5 are able to fire occasionally due to their inward hyperpolarization activated currents.

The synaptic connections between cells were drastically scaled to simulate the effect of large populations of cells targeting one given cell. The closed chain connectivity is a way to overcome the size limtation in the model: since the 4 minicolumns are located in a single area, then the delay in synaptic propagation is small, on the order of 2-5 msec. Consequently, as a cell fires, it will drive all of its post-synaptic target neurons within a short period of time. Therefore, a wave of excitation will propagate through the tiny network and terminate relatively quickly, given that all the excitation happens possibly within the refractrory period of a pyramidal cell or

during hyperpolarized periods due to fast inhibition. This can be alleviated by either having extremely high levels of excitation which could cause runaway activity or, more resonably, by having the excitatory wave propagate for relatively long time, which we could achieve if a cell recieves its excitation circularly after the latter passes through the whole chain.

The excitatory wave is minimally dependent on NMDA receptors. Also, when a depolarizing up state is initiated it will circularly propagate, decreasing in magnitude each time, aided by the disfacilitation properties in the network. To approximate this disfacilitation, we increased the time constant of hyperpolarizing current I_H in all pyramidal cells during regularly firing (τ_H = 450msec). Also, the effect of GABA-B receptors counteracted the excitatory influence of NMDA receptors. The compounded influence wasfor the up state to seize, giving way for a period of neuronal silence before another excitatory wave is initiated by layer 5 cells.

Seizures

As mentioned in the simulations chapter, we assume that large layer 5 cells represent the cellular variety which is able to initiate an ictal event as well as sustain the firing at 10-12 Hz. In this case, and due to the lack of inhibition these cells will fire away until hyperpolarizing internal currents as well as synaptic disfacilitation offset the excitatory drive. An equivalent current is used here, and is the same as that utilized in the slow-wave sleep simulation. One limitation to producing large excitatory events is due to scale. Accordingly, excitatory connections were increased drastically to simulate the net effect of a large population of cells driving a local population. This is seen in the parameters table C.2.

Alpha Activity

The model involved 4 columns in one local area and 2 other columns of a higher order area as presented in the main simulation chapter.

Alpha Selectivity

A hierarchical structure similar to that used in the alpha activity simulation is used. A main difference is that only layers 5 and 3 are modeled in this case to illustrate the recruitment by bursting of selected columns. We conducted two sets of simulations. In the first, it is assumed that inhibitory action in one column is a function of both local activity of interneurons as well as that of distant neurons (that is a connection for example $k_{3i,3}$ exists). This can be thought of as a way to increase the local inhibitory tone for a single column instead of increasing inhibitory strength or modeling several local interneurons. Parameters in this case are tabulated in Table C.4. In the second case, only local interneuronal connections were included, as shown in figure C-1. Table C.5 contains the relevant parameters. Note here that $g^{ampa}_{5,LTS}$, $g^{nmda}_{5,LTS}$ represent the AMPA and NMDA-mediate excitatory connections between P5 and LTS. NMDA receptor is utilized to approximate the cumulative sensitivity in an LTS cell for high frequency inputs. Similarly for $k^{ampa}_{5,LTS}$ and $k^{nmda}_{5,LTS}$.

Table C.1: Model parameters for the slow wave (<1 Hz) oscillations simulation

Base Synaptic conductances								*baseline excitation*	
$GABA_{A,max}$		$AMPA_{max}$		$NMDA_{max}$		$GABA_{B,max}$		I_{min}	I_{max}
g_{max}	τ	g_{max}	τ	g_{max}	τ	g_{max}	τ		
33.6	*	12.11	*	1.54	*	27.5	833	-0.7 nA	0.7 nA

Intracolumnar connections											
Layer 3						Layer 4					
$g_{3,3i}$	$g_{3,4}$	$g_{3,5}$	$g_{3,6}$	$g^a_{3i,3}$	$g^b_{3i,3}$	$g_{4,4i}$	$g_{4,3}$	$g_{4,5}$	$g_{4,6}$	$g^a_{4i,4}$	$g^b_{4i,4}$
0.5	0	0.2	0	1	1	0.5	1	0.6	0	1	1
Layer 5						Layer 6					
$g_{5,5i}$	$g_{5,3}$	$g_{5,4}$	$g_{5,6}$	$g^a_{5i,5}$	$g^b_{5i,5}$	$g_{6,6i}$	$g_{6,3}$	$g_{6,4}$	$g_{6,5}$	$g^a_{6i,6}$	$g^b_{6i,6}$
1.2	0.8	0.3	0.8	2	1	0.5	0	0.6	0.8	1	1

Local connections									
Layer 3									
$k_{3,3}$	$k_{3,4}$	$k_{3,5}$	$k_{3,6}$	$k_{3,3i}$	$k^a_{3i,3}$	$k^b_{3i,3}$	$k_{3i,3i}$	$k_{3,5d}$	$d_{k,3}$
1.5	0	0.1	0	1	0.8	0.6	1	0.5	3msec
Layer 4									
$k_{4,3}$	$k_{4,4}$	$k_{4,5}$	$k_{4,6}$	$k_{4,4i}$	$k^a_{4i,4}$	$k^b_{4i,4}$	$k_{4i,4i}$	$k_{4,5d}$	$d_{k,4}$
0.6	1.5	0.1	0	1	0.8	0.6	1	0	3msec
Layer 5									
$k_{5,3}$	$k_{5,4}$	$k_{5,5}$	$k_{5,6}$	$k_{5,5i}$	$k^a_{5i,5}$	$k^b_{5i,5}$	$k_{5i,5i}$	$k_{5,5d}$	$d_{k,5}$
0.6	0.1	1.1	0.4	0.3	0.8	0.6	1	0.1	3msec
Layer 6									
$k_{6,3}$	$k_{6,4}$	$k_{6,5}$	$k_{6,6}$	$k_{6,6i}$	$k^a_{6i,6}$	$k^b_{6i,6}$	$k_{6i,6i}$	$k_{6,5d}$	$d_{k,6}$
0	0.5	0.2	1.5	1	0.8	0.6	1	0	3msec

RS pyramidal					TL5 pyramidal									FS
τ_R	g_T	τ_T	g_H	τ_H	τ_R	g_T	τ_T	g_H	τ_H	g_{H_1}	τ_{H_1}	g_{H_2}	τ_{H_2}	τ_R
4.2	0.1	14	5	450	4.2	2.7	14	9.25	35	1	1.5e3	8	1e3	2.1

Table C.2: Model parameters for disinhibition-induced seizure simulation

Base Synaptic conductances								*baseline excitation*			
$GABA_{A,max}$		$AMPA_{max}$		$NMDA_{max}$		$GABA_{B,max}$		$g_{in,3}$	$g_{in,4}$	$g_{in,5}$	$g_{in,6}$
g_{max}	τ	g_{max}	τ	g_{max}	τ	g_{max}	τ				
25.2	*	15.14	*	0.96	*	55	833	0.2	0.2	0.2	0.2

Intracolumnar connections											
Layer 3						Layer 4					
$g_{3,3i}$	$g_{3,4}$	$g_{3,5}$	$g_{3,6}$	$g^a_{3i,3}$	$g^b_{3i,3}$	$g_{4,4i}$	$g_{4,3}$	$g_{4,5}$	$g_{4,6}$	$g^a_{4i,4}$	$g^b_{4i,4}$
0.8	0	0.2	0	1	1	0.8	1	0.6	0	1	1
Layer 5						Layer 6					
$g_{5,5i}$	$g_{5,3}$	$g_{5,4}$	$g_{5,6}$	$g^a_{5i,5}$	$g^b_{5i,5}$	$g_{6,6i}$	$g_{6,3}$	$g_{6,4}$	$g_{6,5}$	$g^a_{6i,6}$	$g^b_{6i,6}$
0.8	0.8	0.3	0.8	1	1	0.8	0	0.6	0.8	1	1

Local connections									
Layer 3									
$k_{3,3}$	$k_{3,4}$	$k_{3,5}$	$k_{3,6}$	$k_{3,3i}$	$k^a_{3i,3}$	$k^b_{3i,3}$	$k_{3i,3i}$	$k_{3,5d}$	$d_{k,3}$
1.5	0	0.5	0	0.4	0.8	0.6	0	1	2msec
Layer 4									
$k_{4,3}$	$k_{4,4}$	$k_{4,5}$	$k_{4,6}$	$k_{4,4i}$	$k^a_{4i,4}$	$k^b_{4i,4}$	$k_{4i,4i}$	$k_{4,5d}$	$d_{k,4}$
0.6	1	0.2	0	1	0.8	0.6	0	0	2msec
Layer 5									
$k_{5,3}$	$k_{5,4}$	$k_{5,5}$	$k_{5,6}$	$k_{5,5i}$	$k^a_{5i,5}$	$k^b_{5i,5}$	$k_{5i,5i}$	$k_{5,5d}$	$d_{k,5}$
0.6	0.1	1	0.4	0.3	0.4	0.3	0.1	2msec	
Layer 6									
$k_{6,3}$	$k_{6,4}$	$k_{6,5}$	$k_{6,6}$	$k_{6,6i}$	$k^a_{6i,6}$	$k^b_{6i,6}$	$k_{6i,6i}$	$k_{6,5d}$	$d_{k,6}$
0	0.5	0.4	1	0.3	0.8	0.3	0	0	2msec

RS pyramidal					TL5 pyramidal									FS
τ_R	g_T	τ_T	g_H	τ_H	τ_R	g_T	τ_T	g_H	τ_H	g_{H_1}	τ_{H_1}	g_{H_2}	τ_{H_2}	τ_R
4.2	0.1	14	12	700	4.2	2.7	14	9.25	35	1	1.5e3	8	1e3	2.1

Table C.3: Model parameters for Alpha Activity

Base Synaptic conductances								*baseline excitation*	
$GABA_{A,max}$		$AMPA_{max}$		$NMDA_{max}$		$GABA_{B,max}$		I_{min}	I_{max}
g_{max}	τ	g_{max}	τ	g_{max}	τ	g_{max}	τ		
12.6	*	3.03	*	0.77	*	27.50	83.3	-0.1	0.4

Intracolumnar connections											
Layer 3						Layer 4					
$g_{3,3i}$	$g_{3,4}$	$g_{3,5}$	$g_{3,6}$	$g^a_{3i,3}$	$g^b_{3i,3}$	$g_{4,4i}$	$g_{4,3}$	$g_{4,5}$	$g_{4,6}$	$g^a_{4i,4}$	$g^b_{4i,4}$
1	0	0.2	0	1	1	1	1	0.6	0	1	1
Layer 5						Layer 6					
$g_{5,5i}$	$g_{5,3}$	$g_{5,4}$	$g_{5,6}$	$g^a_{5i,5}$	$g^b_{5i,5}$	$g_{6,6i}$	$g_{6,3}$	$g_{6,4}$	$g_{6,5}$	$g^a_{6i,6}$	$g^b_{6i,6}$
1	1.5	0.8	0.8	1	1	1	0	1	0.8	1	1
Other Inter-laminar						*long range connections*					
Intracolumnar			*local*			*Ascending*			*Descending*		
$g_{5,5di}$	$g_{5di,5d}$	$g_{5,3i}$	$k_{5,5di}$	$k_{5di,5d}$	$k_{5,3i}$	$K_{ff,3}$	$K_{ff,5}$	$D_{K,ff}$	$K_{fb,3}$	$K_{fb,5d}$	$D_{K,fb}$
0.6	1	0.5	0.1	0	0.1	1.5	1	10ms	1	3	10ms

Local connections									
Layer 3									
$k_{3,3}$	$k_{3,4}$	$k_{3,5}$	$k_{3,6}$	$k_{3,3i}$	$k^a_{3i,3}$	$k^b_{3i,3}$	$k_{3i,3i}$	$k_{3,5d}$	$d_{k,3}$
1.5	0.1	0.9	0	1	0.8	0.6	1	0.5	4msec
Layer 4									
$k_{4,3}$	$k_{4,4}$	$k_{4,5}$	$k_{4,6}$	$k_{4,4i}$	$k^a_{4i,4}$	$k^b_{4i,4}$	$k_{4i,4i}$	$k_{4,5d}$	$d_{k,4}$
0.6	1.5	0.1	0	1	0.8	0.6	1	0	4msec
Layer 5									
$k_{5,3}$	$k_{5,4}$	$k_{5,5}$	$k_{5,6}$	$k_{5,5i}$	$k^a_{5i,5}$	$k^b_{5i,5}$	$k_{5i,5i}$	$k_{5,5d}$	$d_{k,5}$
0.6	0.3	1.5	0.8	0.6	0.8	0.6	1	0.2	4msec
Layer 6									
$k_{6,3}$	$k_{6,4}$	$k_{6,5}$	$k_{6,6}$	$k_{6,6i}$	$k^a_{6i,6}$	$k^b_{6i,6}$	$k_{6i,6i}$	$k_{6,5d}$	$d_{k,6}$
0	0.9	0.2	1.5	1	0.8	0.6	0	1	4msec

RS pyramidal					TL5 pyramidal									FS
τ_R	g_T	τ_T	g_H	τ_H	τ_R	g_T	τ_T	g_H	τ_H	g_{H_1}	τ_{H_1}	g_{H_2}	τ_{H_2}	τ_R
4.2	0.1	14	3	100	3	2.0	12	10	25	-	-	-	-	2.1

Table C.4: Model parameters for Alpha Selectivity

Base Synaptic conductances								*baseline excitation*	
$GABA_{A,max}$		$AMPA_{max}$		$NMDA_{max}$		$GABA_{B,max}$		I_{min}	I_{max}
g_{max}	τ	g_{max}	τ	g_{max}	τ	g_{max}	τ	-0.1	4
12.6	*	3.03	*	0.57	*	27.50	83.3	(external input, g=1)	

Intracolumnar connections							
Layer 3				Layer 5			
$g_{3,3i}$	$g_{3,5}$	$g^a_{3i,3}$	$g^b_{3i,3}$	$g_{5,5i}$	$g_{5,3}$	$g^a_{5i,5}$	$g^b_{5i,5}$
1	0.6	1	1	1	1.5	1	1

Local connections							
Layer 3							
$k_{3,3}$	$k_{3,5}$	$k_{3,3i}$	$k^a_{3i,3}$	$k^b_{3i,3}$	$k_{3i,3i}$	$k_{3,5d}$	$d_{k,3}$
1.5	0.1	1.5	0.8	0.6	1	0.5	4msec
Layer 5							
$k_{5,3}$	$k_{5,5}$	$k_{5,5i}$	$k^a_{5i,5}$	$k^b_{5i,5}$	$k_{5i,5i}$	$k_{5,5d}$	$d_{k,5}$
0.2	1.0	1.5	0.8	0.6	1	0.2	4msec

Other Inter-laminar					
Intracolumnar			*local*		
$g_{5,5di}$	$g_{5di,5d}$	$g_{5,3i}$	$k_{5,5di}$	$k_{5di,5d}$	$k_{5,3i}$
0.05	1	0.0	0.1	0	2

long range connections									
Ascending					*Descending*				
$K_{ff,3}$	$K_{ff,3i}$	$K_{ff,5}$	$K_{ff,5i}$	$D_{K,ff}$	$K_{fb,3}$	$K_{fb,3i}$	$K_{fb,5d}$	$K_{fb,5di}$	$D_{K,fb}$
1	2	1	2	10ms	1	2	0.9	0	10ms

RS pyramidal					TL5 pyramidal									FS
τ_R	g_T	τ_T	g_H	τ_H	τ_R	g_T	τ_T	g_H	τ_H	g_{H_1}	τ_{H_1}	g_{H_2}	τ_{H_2}	τ_R
4.2	0.1	14	3	100	3	2.0	12	10	25	-	-	-	-	2.1

Table C.5: Model parameters for Alpha Selectivity, figure C-1

Base Synaptic conductances								*baseline excitation*	
$GABA_{A,max}$		$AMPA_{max}$		$NMDA_{max}$		$GABA_{B,max}$		I_{min}	I_{max}
g_{max}	τ	g_{max}	τ	g_{max}	τ	g_{max}	τ	-0.1	4
12.6	*	3.03	*	0.57	*	27.50	83.3	(external input, g=1)	

Intracolumnar connections									
Layer 3				Layer 5					
$g_{3,3i}$	$g_{3,5}$	$g^a_{3i,3}$	$g^b_{3i,3}$	$g_{5,5i}$	$g_{5,3}$	$g^a_{5i,5}$	$g^b_{5i,5}$	$g^{ampa}_{5,LTS}$	$g^{nmda}_{5,LTS}$
0.8	1.2	1.8	1.2	2	1.5	1	1	0.3	0.12

Local connections				
Layer 3				
$k_{3,3}$	$k_{3,5}$	$k_{3,3i}$	$k_{3,5d}$	$d_{k,3}$
0.8	0.1	1.2	0.5	4msec
Layer 5				
$k_{5,3}$	$k_{5,5}$	$k_{5,5i}$	$k_{5,5d}$	$d_{k,5}$
0.2	0.8	1.2	0.2	4msec

Other Inter-laminar						
Intracolumnar				*local*		
$g_{5,5di}$	$g_{5di,5d}$	$g^a_{LTS,3}$	$g^b_{LTS,3}$	$k_{5,5di}$	$k^{ampa}_{5,LTS}$	$k^{nmda}_{5,LTS}$
0.05	1	2	1	0.1	2	0.8

long range connections									
Ascending					*Descending*				
$K_{ff,3}$	$K_{ff,3i}$	$K_{ff,5}$	$K_{ff,5i}$	$D_{K,ff}$	$K_{fb,3}$	$K_{fb,3i}$	$K_{fb,5d}$	$K_{fb,5di}$	$D_{K,fb}$
1	2	0.5	1	10ms	1.5	3	1	0	10ms

RS pyramidal					TL5 pyramidal									FS
τ_R	g_T	τ_T	g_H	τ_H	τ_R	g_T	τ_T	g_H	τ_H	g_{H_1}	τ_{H_1}	g_{H_2}	τ_{H_2}	τ_R
4.2	0.1	14	3	100	3	2.0	12	10	25	-	-	-	-	2.1

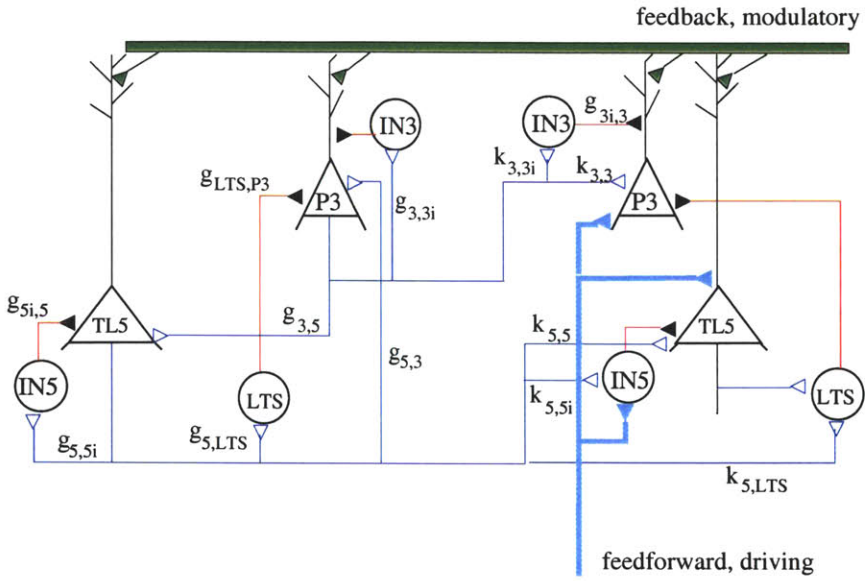

Figure C-1: Local circuit (columnar assembly level) utilized for alpha selectivity simulation

Augmenting response

A circuit diagram of the model used in given in figure C-2. An excitatory input is delivered to the 2 columns on the right hand side (K_{in2} and $K_{in2,i}$) which initiates bursting in those cells. These in turn feedback to the apical dendrites of layer 5 cells in the distant area. Parameters of the model are given in table C.6. Note that in this simulation I_h but not I_t is modeled in layer 5 cells. Addition of the latter will expect to further amplify the augmenting behavior (since it will contribute to cellular depolarization at hyperpolarized membrane potentials).

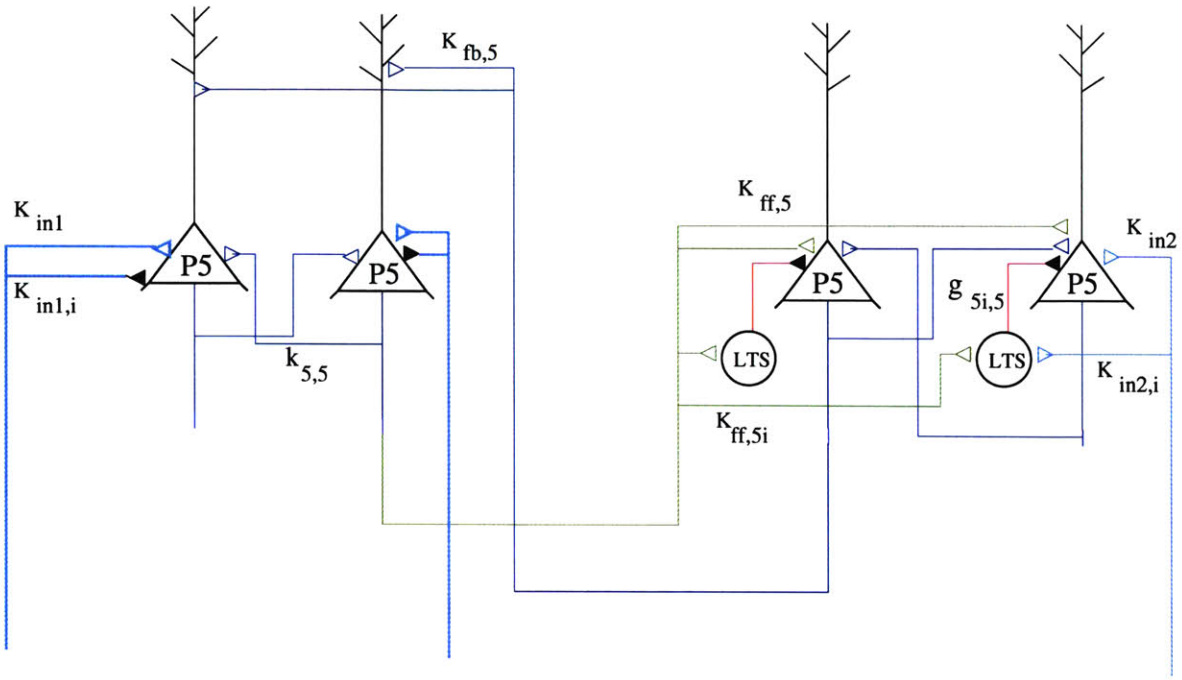

Figure C-2: Schematic of connections between layer 5 cells in an augmenting response simulation

Table C.6: Model parameters for Augmenting Responses

Base Synaptic conductances								*baseline excitation*	
$GABA_{A,max}$		$AMPA_{max}$		$NMDA_{max}$		$GABA_{B,max}$		I_{min}	I_{max}
g_{max}	τ	g_{max}	τ	g_{max}	τ	g_{max}	τ	-0.1	0.1
4	*	6.8	*	0–2.93	*	32.7	50		

Connectivity								
Intracolumnar		*Local*		*Long-distance*				
$g^a_{5i,5}$	$g^b_{5i,5}$	$k_{5,5}$	$d_{k,5}$	$K_{ff,5}$	$D_{ff,5}$	$K_{ff,5i}$	$K_{fb,5}$	$D_{fb,5}$
2	2	0.3	2ms	1.4	5ms	3	1	5ms

External stimulus			
K_{in1}	K_{in2}	$K_{in1,i}$	$K_{in2,i}$
0.49	0.2	0.85	0.3

TL5 pyramidal									FS
τ_R	g_T	τ_T	g_H	τ_H	g_{H_1}	τ_{H_1}	g_{H_2}	τ_{H_2}	τ_R
3	2.7	12	9.25	35	-	-	-	-	2.1

Bibliography

[1] Abeles M, "Corticonics: Neural circuits of the cerebral cortex", Cambridge University Press, 1991.

[2] Achermann P, Borbely AA," Low-frequency (¡ 1 Hz) oscillations in the human sleep electroencephalogram", Neuroscience (1997), 81 (1), pp. 213-222.

[3] Aertsen A et al, "Coupling dynamics and coincident spiking in cortical neural networks", workshop on supercomputing in brain research: from tomography to neural networks, edited by Hermann et al, World Scientific, 1994.

[4] Amzica F, Steriade M, "Cellular substrates and laminar profile of sleep K-complex", Neuroscience, 822(3), pp. 671-686, 1998.

[5] Amzica F, Steriade M, "Electrophysiological correlates of sleep delta waves",Electroencephalography and Clinical Neurophysiology (1998) , Volume 107, Issue 2, pp. 69-83.

[6] Angulo MC, Rossier J, Audinat E, " Postsynaptic glutamate receptors and integrative properties of fast spiking interneurons in the rat neocortex", J Neurophysiology, 82 (1999), pp. 1295-1302.

[7] Angulo MC, Staiger J, Rossier J, Audinat E, "Developmental Synaptic Changes increase the range of integrative capabilities of an identified excitatory neocortical connection". J Neuroscience (1999), 19(5), pp. 1566-1576.

[8] Armstrong-James M, Fox K, Das-Gupta A, "Flow of excitation within rat barrel cortex on striking a single vibrissa", J Neurophysiology (1992), 68(4), pp. 1345-1358.

[9] Azouz R, Gray C, "Dynamic spike threshold reveals a mechanism for synaptic coincidence in cortical neurons in vivo", PNAS (2000) vol 97, No 14, pp. 8110-8115.

[10] Babloyantz A et al, "Evidence of Chaotic Dynamics of Brain Activity During the Sleep Cycle", Physics Letters, Vol 111A, No 3,Sept 1985, pp. 152-156.

[11] Babloyantz A, "From the Single Neuron to the Cortical Networks - A Coherent Model of EEG", Artificial Neural Networks, 2 , pp. 385-390.

[12] Barlow J, "The Electroencephalogram: Its Patterns and Origins", MIT Press, 1993.

[13] Basar E, Basar-Eroglu C, Karakas S, Schurmann M, "Gamma, alpha, delta, and theta oscillations govern cognitive processes", International Journal of Psychophysiology 39 (2001), pp 241-248.

[14] Bazhenov M, Timofeev I, et al, "Computational models of thalamocortical augmenting responses", J. Neuroscience, Vol 18 (16), pp. 6444-6465, 1998.

[15] Beierlein M, Gibson J, Connors B, " A network of electrically coupled interneurons drives synchronized inhibition in neocortex", Nature Neuroscience, Vol 3 No 9 (2000), pp. 904-910.

[16] Bender DB, Youakim M, "Effect of attentive fixation in macaque thalamus and cortex", J Neurophysiology (2001), 85(1), pp. 219-234.

[17] Bernardo LS, "Separate activation of fast and slow inhibitory postsynaptic potentials in rat neocortex in vitro", J Physiol 1994 Apr 15;476(2), pp. 203-215.

[18] Bernardo L, "Recruitment of GABAergic inhibition and synchronization of inhibitory interneurons in rat neocortex", J Neurophysiology 77 (1997) pp. 3134-3144.

[19] Bodenstein G. et al, " Feature Extraction from the Electroencephalogram by Adaptive Segmentation", Proceeding of the IEEE, Vol 65, No 5, May 1977. pp. 642-652.

[20] Bonmassar G et al, "Spatiotemporal brain imaging of visual-evoked activity using interleaved EEG and fMRI recordings.", Neuroimage (2001), 13(6 Pt 1), pp. 1035-43.

[21] Bower J, Beeman D, "The book of genesis", (1998) Second edition, Springer Verlag.

[22] Braitenberg V. and Schuz A, "Cortex : Statistics and Geometry of Neuronal Connectivity", second edition, Springer 1998.

[23] Brumberg J, Pinto D, Simons D, "Cortical columnar processing in the rat whisker-to-barrel system", J of Neurophysiology (1999), 82, pp. 1808-1817.

[24] Bush P, "Compartmental models of single cells and small networks in the promary visual cortex of the cat", PhD dissertation (1995), University of California San Diego.

[25] Buzsaki G, Kandel A "Somatodendritic backpropagation of action potentials in cortical pyramidal cells of the awake rat", J of Neurophysiology, Vol 79, No 3, (1998), pp. 1587-1591.

[26] Callaway EM, " Local circuits in primary visual cortex of the macaque monkey", Annu Rev Neuroscience (1998), 21, pp. 47-74. Review.

[27] Calixto E et al, "Neocortical hyperexcitability after GABA withdrawal in vitro", Epilepsy Res (2000), 39 (1), pp. 13-26.

[28] Castelo-Branco M, Goebel R, Neuenshwander S, Singer W, "Neural synchrony correlates with surface segregation rules", Nature (2000), 405(6787), pp.685-689.

[29] Castros-alamancos, M A, and Connors B, "Cellular mechanisms of the augmenting response: short-term plasticity in a thalamocortical pathway", J of Neuroscience, 1996, (16) pp. 7742-7756.

[30] Castro-Alamancos M and Connors B, "Spatiotemporal properties of short term plasticity in sensorimotor thalamocortical pathways of the rat", Journal of Neuroscience (1996), Vol 16 No 8, pp. 2767-2779.

[31] Castro-Alamancos M, Calcagnotto M, "Presynaptic long-term potentiation in cortico-thalamic synapses", J of Neuroscience (1999), 19(20), pp. 9090-9097.

[32] Castro-Almancos M A, " Origin of synchronized oscillations induced by neocortical disinhibition in vivo", J. of Neuroscience, 20(24), pp. 9195-9206, 2000.

[33] Cauller LJ, Clancy B, Connors BW, "Backward cortical projections to primary somatosensory cortex in rats extend long horizontal axons in layer I", J Comp Neurol 1998 Jan 12;390(2):297-310.

[34] Cerne R, Spain W, "GABA-A mediated afterdepolarization in pyramidal neurons from rat neocortex", J Neurophysiol. (1997), 77(2), pp.1039-45.

[35] Chagnac-Amitai Y et al, "Synchronized excitation and inhibition driven by intrinsically bursting neurons in neocortex", Journal of Neurophysiology, Vol 62, No. 5 (1989), pp. 1149-1162.

[36] Chagnac-Amitai Y, Connors BW," Horizontal spread of synchronized activity in neocortex and its control by GABA-mediated inhibition." J Neurophysiology 1989 Apr;61(4), pp. 747-58.

[37] Chatila M, Milleret C, Buser P. Rougeul A, "A 10 Hz "alpha-like" rhythm in the visual cortex of the waking cat, Electroencephalography and Clinical Neurophysiology (1992), 83, pp. 217-222.

[38] Chen W, Zhang JJ, Hu GY, Wu CP, "Electrophysiological and morphological properties of pyramidal and nonpyramidal neurons in the cat motor cortex in vitro", Neuroscience 1996 Jul;73(11), pp.39-55.

[39] Colrain I, Webster K, Hirst G, " The N550 component of the evoked K-complex: A modality non-specific response?", J Sleep Research (1999), Vol 8(4), pp. 273-280.

[40] Connors B and Amitai Y, "Functions of local circuits in neocortex: synchrony and laminai", in The cortical Neuron (1995), pp. 123-140, ed. Gutnik MJ and Mody I, Oxford University Press.

[41] Contreras D, Steriade M, "Cellular basis of EEG Slow rythms: a study of dynamic corticothalamic relationships " J. Neuroscience, Vol 15 (1), pp. 604-622 , 1995.

[42] Contreras D, Destexhe A, T J. Sejnowski, and M Steriade, "Spatiotemporal Patterns of Spindle Oscillations in Cortex and Thalamus", Journal of Neuroscience (1997), 17 (3), pp. 1179-1196.

[43] Contreras D, Durmuller N, Steriade M, "Abscence of a prevalent laminar distribution of IPSPS in association cortical neurons of cat", J. Neurophysiology, (78), pp. 2742-2753, 1997.

[44] Contreras D, Destexhe, Steriade M, " Intracellular and computational chracterization of the intracortical inhibitory control of synchronized thalamic inputs in vivo"J. Neurophysiology, (78), pp. 335-350, 1997.

[45] R. Cooper, " Comparison of subcortical, cortical, and scalp activity using chronically indwelling electrodes in man", Electroencephalography and Clinical Neurophysiology (1965), 18, pp. 217-228.

[46] Cook E, Johnston D, "Voltage-dependent properties of dendrites that eliminate location dependent variability of synaptic inputs", J Neurophysiology (1999), 81, pp. 535-543.

[47] Cossart et al, "Dendritic but not somatic GABAergic inhibition is decreased in experimental epilsepsy", Nature Neuroscience (2001), Vl4, No 1, pp. 52-62.

[48] Cretzfeldt O , G. Bodenstein, J. Barlow, "Computerized EEG Pattern Classification by Adaptive Segmentation and Probability Density Function Classification. Clinical Evaluation", Electroencephalography and Clinical Neurophysiology, 1985, 60, pp. 373-393.

[49] Creutzfeldt O, "The Neocortical link: thoughts on the generality of structure and function in the neocortex", in Architectonics of the Cerebral Cortex, edited by Brazier and Petsche, Raven Press, 1978.

[50] de Curtis, C. Radici and M. Forti, "Cellular mechanisms underlying spontaneous interictal spikes in an acute model of focal cortical epileptogenesis ", Neuroscience (1998), vol 88, No 1, pp. 107-117.

[51] Dantzker JL, Callaway EM, "Laminar sources of synaptic input to cortical inhibitory interneurons and pyramidal neurons", Nat Neurosci 2000 Jul;3(7), pp. 701-707.

[52] DeFazio et al, " Potassium-coupled chloride cotransport controls intracellular chloride in rat neocortical pyramidal neurons",J Neurosci 2000 Nov 1;20(21):8069-76.

[53] De Gennaro L, Ferrara M, Bertini M, "The spontaneous K-complex during stage 2 sleep: is it the 'forerunner' of delta waves?", Neurosci Lett 2000 Sep 8;291(1):41-3.

[54] de la Pena E, Geijo-Barrientos E, " Laminar localization, morphology, and physiological properties of pyramidal neurons that have low-threshold calcium current in the guinea-pig medial frontal cortex", J Neuroscience, (1996) Vol 16, No 17, pp. 5301-5311.

[55] Deisz RA, Prince DA, "Frequency-dependent depression of inhibition in guinea-pig neocortex in vitro by GABAB receptor feed-back on GABA release", J Physiol 1989 May;412. pp 513-541.

[56] Deisz RA, "The GABA(B) receptor antagonist CGP 55845A reduces presynaptic GABA(B) actions in neocortical neurons of the rat", Neuroscience 1999; 93 (4): pp.1241-1249.

[57] Destexhe A, "Spike-and-wave oscillations based on the properties of GABAb receptors ", J Neuroscience (1998), 18(21), pp. 9099-9111.

[58] Destexhe A, Contreras D, Steriade M, "Mechanisms underlying the synchronizing action of corticothalamic feedback through inhibition of thalamic relay cells", J. Neurophysiology (79), 1998, pp. 999-1016.

[59] Destexhe A, Mainen Z, Sejnowksi T, "Kinetic models of synaptic transmission", in Methods in Neuronal Modeling (2nd edition), MIT Press, 1998, pp 1-25.

[60] Destexhe A, McCormick D, Sejnowski T, "Thalamic and thalamocortical mechanisms underlying 3 Hz spike-and-wave discharges", Prog Brain Res (1999), 121, pp. 289-307.

[61] Destexhe A, Contreras D, Steriade M, "Cortically-induced coherence of a thalamic-generated oscillation", Neuroscience, Vol 92 No 2, pp. 427-443, 1999.

[62] Destexhe A, Contreras D, Steriade M, "Spatiotemporal analysis of local field potentials and unit discharges in cat cerebral cortex during natural wake and sleep states", J. Neuroscience, 19 (11), PP. 4595-4608, 1999.

[63] Destexhe A, Pare D, "Impact of network activity on the integrative properties of neocortical pyramidal neuorns in vivo",J. Neurophysiology (81), 1999, pp. 1531-1547.

[64] Deuchars J, Thomson A, "Innervation of burst firing spiny interneurons by pyramidal cells in deep layers of rat somatosensory cortex: paired intracellular recordings with biocytin filling", Neuroscience (1995), Vol 69 No 3, pp. 739-755.

[65] Di Pasquale E, Keegan KD, Noebels JL, "Increased excitability and inward rectification in layer V cortical pyramidal neurons in the epileptic mutant mouse Stargazer.", J Neurophysiol 1997 Feb;77(2):621-31

[66] Duffy F et al, "Brain Electrical Activity Mapping (BEAM): a Method for Extending the Clinical Utility of EEG and Evoked Potential Data", Annals of Neurology, 1979, Vol. 5, pp. 309-321.

[67] Duffy F et al, "Significance Probability Mapping: an Aid in the Topographic Analysis of Brain Electrical Activity", Electroencephalography and Clinical Neurophysiology, 1981, Vol 51, pp. 455-462.

[68] Durstewitz D et al, "Dopamine-mediated stabilization of delay-period activity in a network model of prefrontal cortex", J Neurophysiology (2000), Vol 83,pp. 1733-1750.

[69] Eder M et al, " GABA-A and GABA-B receptors on neocortical neurons are differentially distributed", Eur J of Neuroscience (2001), vol 13, pp. 1065-1069.

[70] Feldmeyer D et al, " Reliable synaptic connections between pairs of excitatory layer 4 neurones within a single barrel of developing rat somatosensory cortex", J Physiology (1999), 521 No 1, pp. 169-190.

[71] Feldmeyer D, Sakmann B, "Synaptic efficacy and reliability of excitatory connections between the principal neurons of the input (layer 4) and output layer (layer 5) of the neocortex", J Physiology (2000), 525 (1), pp. 31-39.

[72] Fellman DJ, Van Essen DC, "Distributed hierarchical processing in the primate cerebral cortex", Cerebral cortex (1991), 1, pp.1-47.

[73] Fleidervish I et al, "Functionally distinct NMDA receptors mediate horizontal connectivity within layer 4 of mouse barrel cortex", Neuron (1998), Vol 21, pp. 1055-1065.

[74] Foxe J, Simpson G, Ahlfors S, "Perieto-occipital $\approx$10 Hz activity reflects anticipatory state of visual attention mechanisms", Neuroreport (1998), 9, pp. 3929-3933.

[75] Franceschetti S, Sancini G, Panzica F, Radici C, Avanzini G., "Postnatal differentiation of firing properties and morphological characteristics in layer V pyramidal neurons of the sensorimotor cortex", Neuroscience (1998), 83(4), pp. 1013-24.

[76] Freeman W, "Simulations of Chaotic EEG patterns with a dynamic model of the olfactory system", Biological Cybernetics (1987), 56, pp.139-150.

[77] Freeman W, "Mass Action in the Nervous System", Academic press, 1975.

[78] Fries P, Reynolds J, Rorie A, Desimone R, "Modulation of oscillatory synchronization by selective visual attention", Science (2001), vol 291, pp. 1560-1563.

[79] Friston K, "functional integration and connectivity in neuroimaging", workshop on supercomputing in brain research: from tomography to neural networks, edited by Hermann et al, World Scientific, 1994.

[80] Fukanaga K, "Introduction to Statistical Pattern Recognition", Academic Press, 1990.

[81] Gabor A , M. Seyal, "Automated Interictal EEG Spike Detection Using Artificial Neural Networks", Electroencephalography and Clinical Neurophysiology, 83 (1992), pp. 271-280.

[82] Gabor A , R Leach, F Dowla, "Automated Seizure Detection Using a Self-Organizing Neural Network", Electroencephalography and Clinical Neurophysiology, 99 (1996), pp. 257-266.

[83] Gail A, Brinksmeyer H J, Eckhorn R, " Contour Decouples Gamma Activity Across Texture Representation in Monkey Striate Cortex", Cerebral Cortex, Vol. 10, No. 9, 840-850, September 2000.

[84] Galarreta M, Hestrin S, " A network of fast-spiking cells in the neocortex connected by electrical synapses", Nature vol 402 (1999), pp. 72-75.

[85] Galarreta M et al, "Burst firing induces a rebound of synaptic strength at unitary neocortical synapses", J Neurophysiolog (2000), 83: pp. 621-624.

[86] Gernier F, Timofeev I, Steriade M, "Leading role of thalamic over cortical neurons during postinhibitory rebound excitation", Proc. Natl, Acad Sci USA, Vol 95, pp. 13929-13934, Nov 1998.

[87] Ghazanfar A, Nicolelis M, "Spatiotemporal properties of layer V neurons of the rat primary somatosensory cortex", Cerebral cortex (1999), 9 , pp. 348-361.

[88] Gibson J R, Beierlein M, Connors B, " Two networks of electrically coupled inhibitory neurons in neocortex", Nature vol 402 (1999), pp. 75-79.

[89] Gil Z, Amitai Y, "Properties of convergent thalamocortical and intracortical synaptic potentials in single neurons of neocortex", J of Neuroscience (1996), 16(20), pp. 6567-6578.

[90] Gil Z, Connors B, Amitai Y, "Efficay of thalamocortical and intracortical synaptic connections: quanta, innervation and reliability", Neuron (1999), Vol 23, pp. 385-397.

[91] Gonchar Y, Burkhalter A, " Connectivity of GABAergic Calertenin-immunoreactive neurons in rat primary visual cortex", Cerebral cortex (1999), 9, pp. 683-696.

[92] Gray, C.M. and McCormick, D.A., "Chattering cells: superficial pyramidal neurons contributing to the generation of synchronous oscillations in the visual cortex", Science 274,pp. 109-113.

[93] Grieve K, Acuna C, Cudeiro J, "The primate pulvinar nuclei:vision and action", Trends Neuroscience (2000), 23, pp.35-39.

[94] Gulledge A et al, "Dopamine decreases the excitability of layer 5 pyramidal cells in the rat prefrontal cortex", J Neuroscience (1998), vol 18 No 21, pp. 9139-9151.

[95] Gupta A, Wang Y, Markram H, "Organizing principles for a diversity of GABAergic interneurons and synapses in the neocortex", Science, Vol 287 (2000), pp. 273-278.

[96] Hefti B and Smith P, " Anatomy, physiology, and synaptic responses of rat layer V auditory cortical cells and effects of intracellular GABA-a blockade", J of Neurophysiology (2000), 83: pp. 2626-2638.

[97] Hempel C et al, "Multiple forms of short-term plasticity at excitatory synapses in rat medial prefrontal cortex", J of Neurophysiology (2000), 83, 3031-3041.

[98] Huda K, Salunga TL, Matsunami K., "Dopaminergic inhibition of excitatory inputs onto pyramidal tract neurons in cat motor cortex.", Neurosci Lett 2001, 307(3), pp. 175-178.

[99] Huguenard J, McCormick D, "Simulations of the currents involved in rhythmic oscillations in thalamic relays neurons", J Neurophysiology (1992), 68(4), pp. 1373-1383.

[100] Jando G et al, "Pattern Recognition of the Electroencephalogram by Artificial Neural Networks", Electroencephalography and Clinical Neurophysiology, 86 (1993), pp. 100-109.

[101] Jansen B et al, " A neurophysiologically-based mathematical model of flash visual evoked potential", Biol. Cybern 68, 1993, pp. 275-283.

[102] Jones E, "Viewpoint: the core and matrix of thalamic organization", Neuroscience (1998), Vol 85, No 2, pp.331-345.

[103] Jones E, "Microcolumns in the cerebral cortex", PNAS (2000), Vol 97 No 10, pp. 5019-5021.

[104] Joutsiniemi S-L, S. Kaski, T. Larsen, "Self-Organizing Maps in Recognition of Topographic Patterns of EEG Spectra", IEEE Trans. on Biomedical Engineering, Vol.42, No 11, pp. 1062-1068.

[105] Kandel et al, "Principles of Neural Science", third edition, Appleton and Lange, 1991.

[106] Kandel A, Buzsaki G, "Cellular-synaptic generation of sleep spindles, spike-and-wave discharges, and evoked thalamocortical responses in the neocortex of the rat", J Neuroscience (1997), 17 (17), pp. 6783-6797.

[107] Kaneko T et al, "Predominant information transfer from layer III pyramidal neurons to corticospinal neurons", J of comparative neurology (2000), 423, pp. 52-65.

[108] Kapur A, Pearce RA, Lytton W, and Haberly L, "GABA-A mediated IPSCs in piriform cortex have fast and slow components with different properties and locations on pyramidal cells", Journal of Neurophysiology (1997), Vol 78, No 5, pp. 2531-2545.

[109] Karameh F, Dahleh M, "Automatic classification of EEG signals in brain tumor diagnositcs", 2000, ACC proceedings.

[110] Kasper EM, Larkman AU, Lubke J, Blakemore C, "Pyramidal neurons in layer 5 of the rat visual cortex. I. Correlation among cell morphology, intrinsic electrophysiological properties, and axon targets", J Comp Neurol 1994, 339(4), pp. 459-74.

[111] Kasper EM, Lubke J, Larkman AU, Blakemore C., "Pyramidal neurons in layer 5 of the rat visual cortex. III. Differential maturation of axon targeting, dendritic morphology, and electrophysiological properties", J Comp Neurol. 1994, 339(4), pp. 495-518.

[112] Katzenelson RD, " Deterministic and Stochastic Field Theoretic models in the neurophysics of EEG", PhD dissertation, UCSD, 1982.

[113] Kavanagh R et al, "Evaluation of Methods for Three-Dimensional Localization of Electrical Sources in the Human Brain", IEEE Trans on Biomedical Engineering, Vol. 25, No 5, Sept 1978, pp. 421-429.

[114] Kawaguchi Y, "Physiological subgroups of nonpyramidal cells with specific morphological characteristics in layer II/III of rat frontal cortex", J Neuroscience, 15(4), 1995, pp. 2638-2655.

[115] Kawaguchi Y, Kubota Y, " GABAergic cell subtypes and their synaptic connections in rat frontal cortex", Cerebral cortex (1997), pp. 476-486.

[116] Kawaguchi Y, Shindou T, "Noradrenergic Excitation and Inhibition of GABAergic Cell Types in Rat Frontal Cortex". J Neuroscience (1998), 18(17), pp.6963-6976

[117] Kharazia VN, Prince DA, " Changes of alpha-amino-3-hydroxy-5-methyl-4-isoxazole-propionate receptors in layer V of epileptogenic, chronically isolated rat neocortex.", Neuroscience 2001, 102(1)pp. 23-34.

[118] Kitazoe Y, "Theoretical analysis on relationship between neural activity and the EEG", J. Thoer. Biol. (1983), 104, pp. 667-683

[119] Klimesch W, "EEG alpha and theta oscillations reflect cognitive and memory performance: a review and analysis", Brain Research Reviews 29 (1999), pp. 169-195.

[120] Klimesch W, Doppelmayr M, Schwaiger J, Auinger P, Winkler T, " "Paradoxical" alpha synchronization in a memory task", Cognitive Brain Research (1999), 7, pp. 493-501.

[121] Klopp J, Marinkovic K, Clarke J, Chauvel P, Nenov V, Halgren E., "Timing and localization of movement-related spectral changes in the human peri-rolandic cortex: intracranial recordings.", Neuroimage (2001) Aug 14(2), pp. 391-405.

[122] Koch C and Segev eds, "Methods in Neural Modeling. From synapses to networks", 1989, MIT press.

[123] Koch C, Douglas R, Wehmeier U, "Visibility of synaptically indiced conductance changes: theory and simulations if anatomically characterized cortical pyramidal cells", J Neuroscience (1990), 10(6), pp. 1728-1744.

[124] Koch C Crick F, "Some further ideas regarding the neuronal basis of awareness", in Large scale theories of the brain, (1994), pp. 93-109, Cambridge MA, MIT press.

[125] Kohn A et al, " Functional neocortical microcircuity demonstrated with intrinsic signal optical imaging in vitro", Neuroscience (2000), Vol 95, No 1, pp. 51-62.

[126] Kohonen T, "the Self-Organizing Map", Proceedings of the IEEE, Vol. 78, no. 9, Sept 1990,pp. 1464-1480.

[127] Kubota Y, Kawaguchi Y, " Dependence of GABAergic synapse area on the interneuron type and target size", J Neuroscience, 2000, 20(1), pp. 375-386.

[128] Laaris N, Carlson G, keller A, "Thalamic-evoked synaptic interaction in barrel cortex revealed by optical imaging", Journal of Neuroscience (2000), 20(4), pp. 1529-1537.

[129] Lambe EK et al, "Serotonin induces EPSCs preferentially in layer 5 pyramidal neurons of the frontal cortex in the rat", Cerbral cortex (2000), 10:947-980.

[130] Lancel M, "The GABA(A) agonist THIP increases non-REM sleep and enhances non-REM sleep-specific delta activity in the rat during the dark period", Sleep (1997),20 (12),pp. 1099-104.

[131] Larkum M et al, "A new cellular mechanism for coupling inputs arriving at different cortical layer", Nature, Vol 398, 25 March 1999, pp. 338-341.

[132] Larkum M, Kaiser K, Sakmann B, "Calcium electrogenesis in distal apical dendrites of layer 5 pyramidal cells at a critical frequency of back-propagating action potentials", PNAS Vol 96 (25), 1999, pp. 14600-14604.

[133] Larkum ME, Zhu JJ, Sakmann B, "Dendritic mechanisms underlying the coupling of the dendritic with the axonal potential initiation zone of adult rat layer 5 pyramidal neurons", Journal of Physiology (2001), 533, 2, pp. 447-466.

[134] Llinas R, Ribary U et al, "Content and context in temporal thalamocortical binding", in Temporal coding in the brain (1994), G Buzsaki eds, pp. 251-272, Berlin Heidelberg, Springer-Verlag.

[135] Ling Douglas S F, Bernardo L, "Restrictions on inhibitory circuits contribute to limited recruitment of fast inhibition in rat neocortical pyramidal cells", J Neurophysiology 82 (1999) pp. 1793-1807.

[136] Lisman J, "Bursts as a unit of neural information: making unreliable synapses reliable", Trends Neuroscience (1997), 20(1), pp.38-43. Review.

[137] Lopes da Silva F. et al, " Model of Brain Rhythmic Activity", Kybernetik 15,27 (1974), pp. 27-37.

[138] Lopes da Silva F, Van Lierop T, Schrijer C, van Leeuwen S, "Organization of thalamic and cortical alpha rhythms: spectra and coherences", Electroencephalography and Clinical Neurophysiology (1973a), 35, pp. 627-639.

[139] Lopes da Silva F, Van Lierop T, Schrijer C, van Leeuwen S, "Essential differences between alpha rhythms and barbiturate spindles: spectra and thalamo-cortical coherences", Electroencephalography and Clinical Neurophysiology (1973b), 38, pp. 93-96.

[140] Lopes da Silva F et al, "Models of Neuronal Populations: the basic Mechanism of Rhythmicity", in Perspectives in Brain Research, Vol 45, edited by Corner and Swaab, Elsevier, 1976.

[141] Lopes da Silva F, Storm van Leeuwen W, "The cortical source of the alpha rhythm", Neuroscience letters (1977), 6, pp. 237-241.

[142] Lopes da Silva F et al, "The Cortical Alpha Rhythm in Dog: the Depth and Surface Profile of Phase", in Architectonics of the Cerebral Cortex, edited by Brazier and Petsche, Raven Press, 1978.

[143] F. Lopes da Silva, " Dynamics of EEGs as signals of neuronal populations: models and theoretical considerations", Electroencephalography : Basic Principles, Clinical Applications, and Related Fields, third ed., Williams and Willkins, 1987. pp. 63-77.

[144] Lopes da Silva F, "Neural mechanisms underlying brain waves: from neural mechanisms to networks", Electroencephalography and Clinical Neurophysiology (1991), 79, pp. 81-93.

[145] Lopes da Silva F, "Biophysical issues at the frontiers of the interpretation of EEG/MEG signals", in Frontier Science in EEG: Continuous waveform analysis (EEG supl. 45, Editors Dasheiff and Vincent (1996), pp. 1-7.

[146] Magee J, Cook E, "", Nature Neuroscience (2000), 3, pp. 895-903.

[147] Markram H, "A network of tufted layer 5 pyramidal neurons", Cereb Cortex (1997), 7(6), pp. 523-533.

[148] Markram H, Lubke J, Frotscher M, Roth A, Sakmann B., "hysiology and anatomy of synaptic connections between thick tufted pyramidal neurones in the developing rat neocortex", J Physiol (1997), 15;500 (Pt 2), pp. 409-40

[149] L. Martigon et al, " Statistical inference methods for classifying higher order neural interactions", workshop on supercomputing in brain research: from tomography to neural networks, edited by Hermann et al, World Scientific, 1994.

[150] Massimini M, Amzica F, "Extracellular calcium fluctuations and intracellular potentials in the cortex during the slow sleep oscillation", J Neurophysiology (2001), 85, pp. 1346-1350.

[151] G. Mayer-Kress et al, "Analysis of the Human Electroencephalogram with Methods form Nonlinear Dynamics" in "Temporal Disorder in Human Oscillatory Systems", Spinger Verlag, 1987, pp. 57-68.

[152] McCormick D A, Pape H, "Properties of a hyperpolarization-activated cation current and its role in rhythmic oscillation in thalamic relay neurones. Journal of Physiology (1990), 431, pp. 291-318.

[153] McCormick D, Huguenard J, "A model of the electrophysilogical properties of thalamocortical relay neurons", J Neurophysiology (1992), 68(4), pp. 1384-1400.

[154] McCormick D, Bal T, "Sleep and arousal: thalamocortical mechanisms", Annual Review of neuroscience (1997), 20, pp. 185-215.

[155] McCormick DA and Contreras D, "On the cellular and network basis of epileptic seizures", Annual Review of Physiology (2001), 63, pp. 815-846.

[156] Mehta A D, Ulbert I, Schroeder C, "Intermodal selective attention in monkeys. I: Distribution and Timing of Effects across Visual Areas", Cerebral Cortex (2000), 10, pp 359-370.

[157] Mehta A D, Ulbert I, Schroeder C, "Intermodal selective attention in monkeys. II:physiological mechanisms", Cerebral Cortex (2000), 10, pp 359-370.

[158] Melchitzky D et al, "Synaptic targets of pyramidal neurons providing intrinsic horizontal connections in monkey prefrontal cortex", J of comparative Neurology (1998), 390, pp. 211-224.

[159] Miao-Kun Sun, Dennis Dahl and Daniel L. Alkon, " Heterosynaptic Transformation of GABAergic Gating in the Hippocampus and Effects of Carbonic Anhydrase Inhibition", the Journal of pharamcology and experimental therapeutics, Vol. 296, Issue 3, 811-817, March 2001.

[160] Miller M. , "Neural assemblies and laminar interactions in the cerebral cortex", Biological Cybernetics, 75 (1996) 3, pp. 253-261.

[161] Miller M," Cortico-thalamic interplay and the security of operation of neural assemblies and temporal chains in the cerebral cortex", Biol Cybern 75 (1996) 3, pp. 263-275.

[162] Mima T, Oluwatimlehin T, Hiroaka T, Hallet M, "Transient interhemispheric neuronal synchrony correlates with object recognition", Journal of Neuroscience (2001), 21(11), pp. 3942-3948.

[163] Mirabella G, Battiston S, Diamond M, "Integration of multiple-whisker inputs in rat somatosensory cortex", Cerebral cortex (2001), 11, pp. 164-170.

[164] Morishita W, Alger BE, "Direct depolarization and antidromic action potentials transiently suppress dendritic IPSPs in hippocampal CA1 pyramidal cells", Neurophysiol 2001 Jan;85(1):480-4.

[165] Mouncastle V B, "Perceptual Neuroscience, The Cerebal Cortex" , Harvard University press, 1998.

[166] Munoz A, Defelipe J, Jones E, " Patterns of $GABA_BR_{1a,b}$ receptor gene expression in Monkey and human visual cortex", Cerebral cortex, Vol 11 No 2 (2001), pp. 104-113.

[167] Neckelmann D, Amzica F, Steriade M, "Spike-wave complexes and fast components of cortically generated seizures. III. synchronizing mechanisms", J. Neurophysiology (80), 1998, pp. 1480-1494.

[168] Neckelmann D ; Amzica F ; Steriade M, " Changes in neuronal conductance during different components of cortically generated spike-wave seizures.", Neuroscience (2000), 96 (3), pp. 475-485.

[169] Nettleton J , Spain W, "Linear to Supralinear summation of AMPA-mediated EPSPs in neocortical pyramidal neurons", J Neurophysiology (2000), 83, pp. 3310-3322.

[170] Niedermeyer E. , F. Lopez da Silva, "Electroencephalography", Urban and Scharzenberg, 1983.

[171] Nunez P., "Electric Fields of the Brain", Oxford University Press, 1981.

[172] Nunez P, " Generation of Human EEG by a Combination of Long and Short Range Neocortical Interactions", Brain Topography, Vol. 1 Number 3, 1989, pp. 199-215.

[173] Nunez P, "Neocortical Dynamics and Human EEG Rhythms", Oxford University Press, 1995.

[174] Nunez A, Amzica F, Steriade M, " Electrophysiology of cat association cortical cells in vivo: intrinsic properties and synaptic responses", J. Neurophysiology (70), 1993, pp. 418-429.

[175] Oakley J, Schwindt P, Crill W, " Dendritic Calcium Spikes in Layer 5 Pyramidal Neurons Amplify and Limit Transmission of Ligand-Gated Dendritic Current to Soma", J Neurophysiology (2001), 86, pp. 514-527.

[176] Oakley J, Schwindt P, Crill W, "Initiation and Propagation of Regenerative Ca-Dependent Potentials in Dendrites of Layer 5 Pyramidal Neurons",J Neurophysiology (2001), 86, pp. 503-514.

[177] Oka JI, Kobayashi T, Nagao T, Hicks TP, Fukuda H. "GABAA receptor-induced inhibition of neuronal burst firing is weak in rat somatosensory cortex.",Neuroreport 1993 Jun;4(6):731-4.

[178] Ohara S, Mima T et al, "Increased Synchronization of Cortical Oscillatory Activities between Human Supplementary Motor and Primary Sensorimotor Areas during Voluntary Movements", Journal of Neuroscience, December 1, 2001, 21(23):9377-9386.

[179] Petsche et al, "Depth profiles of electrocortical activities and cortical architectonics", in Architectonics of the Cerebral Cortex, edited by Brazier and Petsche, Raven Press, 1978.

[180] Pfurtscheller G et al, " Frequency dependence of the transmission of the EEG from cortex to scalp", Electroencephalography and Clinical Neurophysiology (1975), 38, pp. 93-96.

[181] Pfurtscheller G, "Central Beta Rhythm During Sensorimotor Activities in Man", Electroencephalography and Clinical Neurophysiology, 51 (1981), pp. 253-264.

[182] Pfurtscheller G et al, "Differentiation between finger, toe and tongue movement in man based on 40 Hz EEG", Electroencephalography and Clinical Neurophysiology, 90 (1994), pp. 456-460.

[183] Pfurtscheller G et al, "Event related desynchronization during motor and visual information processing", Even-related Brain Research (EEG suppl.42), Elsevier 1991, pp. 58-65.

[184] Princivalle A et al, "Distribution of GABA(B) receptor protein in somatosensory cortex and thalamus of adult rats and during postnatal development", Brain Res Bull (2000), Vol 52, No 5, pp. 397-405.

[185] Princivalle et al, "Layer-specific immunocytochemical localization of GABA(B)R1a and GABA(B)R1b receptors in the rat piriform cortex", Eur J Neurosci 2000 Apr;12(4):1516-20.

[186] Rappelsberger P et al, "Calculation of Event-Related Coherence– A New Method to study Short Lasting Coupling between Brain Areas", Brain Topography, Vol 7, Number 2, 1994, pp. 121-127.

[187] Reyes A, Sakmann B, "Developmental switch in the short-term modification of unitary EPSPs evoked in layer 2/3 and layer 5 pyramidal neurons of rat neocortex", J Neuroscience (1999), 19(10), pp. 3827-35.

[188] Reyes A, "Influence of dendritic conductances on the input-output properties of neurons", Annual Review of Neuroscience (2001), 24, pp. 653-675.

[189] Roberts S, L. Tarassenko, "Analysis of the Sleep EEG using a Multilayer Network with Spatial Organization, IEE Proceedings -F, Vol 139, No 6, 1992, pp. 420-425

[190] Roessgen M et al, "Seizure detection of newborn EEG using a model based approach", IEEE Trans. Biomedical Eng., Vol 45, No. 6, June 1998, pp. 673-685.

[191] Rougeul-Buser A, Buser P, "Rhythms in the alpha band in cats and their behavioral correlates", International Journal of Psychophysiology, 26 (1997), pp. 191-203.

[192] Salin, Prince, " Spontaneous GABAA receptor-mediated inhibitory currents in adult rat somatosensory cortex", J Neurophysiol 1996 Apr;75(4):1573-88.

[193] Sanchez-Vives M and McCormick D, "Cellular and network mechanisms of rhythmic recurrent activity in neocortex", Nature Neuroscience (2000), Vol 3 No 10, pp. 1027-1034.

[194] Schiff S, "Wavelet Transform for Epileptic Spike and Seizure Detection", Proceedings of the 16th Annual International Conference of the IEEE Engineering in Medicine and Biology Society, 1994, pp. 1214-1215.

[195] Schiff S et al, "Fast Wavelet Transformation of EEG", Electroencephalography and Clinical Neurophysiology, 91 (1994), pp. 442-455.

[196] Schiff S et al, "Wavelet Transform and Surrogate Data for Electroencephalographic Spike and Seizure Detection", Optical Engineering, July 1994, Vol 33 No. 7, pp. 2162-2169.

[197] Schiller J et al, "Calcium action potentials restricted to distal apical dendrites of rat neocortical pyramidal neurons", J Physiology (1997), Vol 505 No 3, pp. 605-616.

[198] Schoups A, Vogels R, Qian N, Orban G, "Practising orientation identification improves orientation coding in V1 neurons", Nature (2001), 412, pp. 549-553.

[199] Schroeder C, Mehta A, Foxe J, "Determinants and mechanisms of attentional modulation of neural processing", Frontiers in Bioscience 6, (2001), pp.672-684.

[200] Schubert D, Staiger J et al, "Layer-specific intracolumnar and transcolumnar functional connectivity of layer V pyramidal cells in rat barrel cortex". J Neuroscience (2001), 21(10), pp. 3580-3592.

[201] Schurmann M, Basar E, "Functional aspects of alpha oscillations in the EEG", International Journal of Psychophysiology 39 (2001), pp 151-158.

[202] Schwindt P, Obrien J, Crill W, "Quantitavtive analysis of firing properties of pyramidal neurons from layer 5 of rat somatosensory cortex", J Neurophysiology (1998), 77, pp. 2484-2498.

[203] Schwindt P, Crill W, "Synaptically evoked dendritic action potentials in rat neocortical pyramidal neurons", J Neurophysiology (1998), 79, pp. 2432-2446.

[204] Schwindt P, Crill W, "Mechanisms underlying burst and regular spiking evoked by dendritic depolarization in layer 5 cortical pyramidal neurons", J Neurophysiology (2000), 81, pp. 1341-1354.

[205] Shao Z and Burkhalter A, "Role of GABA-B receptor mediated inhibition in reciprocal interareal pathways of rat visual cortex", J Neurophysiology 81 (1999), pp. 1014-1024.

[206] Shepherd GM, "The Synaptic Organization of the Brain", Fourth edition, Oxford University Press, 1998.

[207] Silva LR, Amitai Y, Connors B, "Intrinsic oscillations of neocortex generated by layer 5 pyramidal neurons", Science (1991), Vol 251, pp. 432-435.

[208] Singer W, Gray CM, " Visual feature integration and the temporal correlation hypothesis", Annual Review of Neuroscience (1995), 18 , pp. 555-586.

[209] Singer W, "Consciousness and the binding problem", Ann N Y Acad Sci (2001), 929, pp. 123-146.

[210] Sinton CM, McCarley RW, "Neuroanatomical and neurophysiological aspects of sleep: basic science and clinical relevance", Semin Clin Neuropsychiatry 2000 Jan;5(1):6-19

[211] Somogyi P, Tamas G, Lujan R, Buhl E, "Salient features of synaptic organization in the cerebral cortex", Brain Research Reviews (1998), pp. 1-23.

[212] Spain W, Schwindt P, Crill W, "Post-inhibitory excitation and inhibition in layer V pyramidal neurons from cat sensorimotor cortex", J Physiology (1991), 434, pp. 609-626.

[213] Spurston N, "Distant synapses raise their voices", Nature Neuroscience (2000), Vol 3 No 9 , pp. 849-851.

[214] Stafstrom CE et al , "Properties of persistent sodium conductance and calcium conductance of layer V neurons from cat sensorimotor cortex in vitro", J Neurophysiol. 1985, 53(1), pp.153-70.

[215] C. Stam et al, "Investigation of the dynamics underlying periodic complexes in the EEG", Biol. Cybern. 80 (1999), pp. 57-69.

[216] Steriade M, Nunez A, Amzica F, "A novel slow (¡ 1Hz) oscillation of neocortical neurons in vivo: Depolarizing and hyperpolarizng components", J. Neuroscience, Vol 13 (8), pp.3252-3265, 1993.

[217] Steriade M, Nunez A, Amzica F, "Intracellular analysis of relations between the slow (¡1 HZ) neocortical oscillation and other sleep rhythms of the electroencephalogram", J. Neuroscience, Vol 13 (8), pp.3266-3283, 1993.

[218] Steriade M, Contreras D et al, "The slow (¡ 1 Hx) Oscillation in reticular thalamic and thalamocortical neurons : scenario of sleep rhythm generation in interacting thalamic and neocortical networks",J. Neuroscience, Vol 13 (8), pp.3243299, 1993.

[219] Steriade M, Amzica F, Contreras D, "Synchronization of Fast (30-40 Hz) spontaneous cortical rhythms during brain activation", J. Neuroscience, Vol 16 (1), pp.393-417, 1996.

[220] Steriade M, Contreras D, et al "Synhcronization of fast (30-40 Hz) Spontaneous oscillations in intrathalamic and thalamocortical networks" J. Neuroscience, Vol 16 (8), pp. 2788-2808, 1996.

[221] Steriade M, " Synchronized activities of coupled oscillators in the cerebral cortex and thalamus at different levels of vigilance", Cerebral cortex, Sep 1997, vol 7 , pp. 583-604.

[222] Steriade M, Timofeev I, Gernier F, Durmuller N, "Role of thalamic and cortical neurons in augmenting responses and self-sustained activity: dual intracellular recordings in vivo", J of Neuroscience (1998), Vol 18, No 6, pp. 6245-6443.

[223] Steriade M, Contreras D, "Spike-wave complexes and fast components of cortically generated seizures. I. role of neocortex and thalamus", J. Neurophysiology (80), 1998, pp. 1439-1455.

[224] Steriade M, Amzica F, Neckelmann D, Timofeev I, "Spike-wave complexes and fast components of cortically generated seizures. II. extra- and intracellular patterns", J. Neurophysiology (80), 1998, pp. 1456-1479.

[225] Steriade M, Amzica F, "Intracellular study of excitability of the seizure-prone neocortex in vivo", J. Neurophysiology (82), 1999, pp. 3108-3122.

[226] Steriade M, "Coherent oscillations and short-term plasticity in thalamocortical networks", Trens Neuroscience Vol 22 (8), pp.337-345, 1999.

[227] Steriade M, "Corticothalamic resonance, states of vigilance, and mentation", Neuroscience, Vol 101, No. 2, pp.243-276, 2000.

[228] Steriade M, Timofeev I, Gernier F, "Natural waking and sleep states: a view from inside neocortical neurons", J Neurophysiology (2001), 85(8), pp. 1969-1985.

[229] Steriade M, "To burst or, rather, not to burst", Nature Neuroscience (Views), (2001) Jul, 4(7), p. 671.

[230] Stuart G, Sakmann B, "Active propagation of somatic action potentials into neocortical pyramidal cell dendrites", Nature vol 367, No 6 (1994), pp. 69-72.

[231] Swadlow H et al, "Sharp, local synchrony among putative feed-forward inhibitory interneurons of rabbit somatosensory cortex", J Neurophysiology 79 (1998), pp. 567-582.

[232] Tallon-Baudry C, Bertrand O, Delpuech C, and Pernier J, "Oscillatory gamma -Band (30-70 Hz) Activity Induced by a Visual Search Task in Humans", J. Neuroscience (1997), 17, pp. 722-734.

[233] Tallon-Baudry C, Bertrand O, "Oscillatory gamma activity in humans and its role in object representation", Trends Cogn Sci. (1999), 3 (4), pp. 151-162.

[234] Tamas G, Buhl E, Lorinz A, Somogyi P, "Proximally targeted GABAeric synapses and gap junctions synchronize cortical interneurons", Nature Neuroscience, Vol 3 (2000), pp. 366-371.

[235] Telfeian AE, Connors B, " Layer-specific pathways for the horizontal propagation of epileptiform discharges in neocortex", Epilepsia 1998, 39 (7), pp. 700-708.

[236] Thomson A, Deuchars J, "Synaptic interactions in neocortical local circuits: dual intracellular recordigs in vitro", Cerebral cortex (1997),Vol 7 No 6, pp.510-522.

[237] Thomson A and Bannister A, "Postsynaptic pyramidal target selection by descending layer III pyramidal axons..", Neuroscience, Vol. 84 No. 3, 1998, pp. 669-683.

[238] Timofeev I et al, "Origin of slow cortical oscillations in deafferented cortical slabs", Cerebral cortex, Dec 2000, 10, pp. 1185-1199.

[239] Traczy-Hornoch K et al, "Intracortical Excitation of spiny neurons in layer 4 of cat striate cortex in vitro", Cerebral cortex (1999), 9, pp. 833-843.

[240] Traub R.D. et al, "A Mechanism for generation of long-range synchronous fast oscillations in the cortex", Nature, Vol 383 (17) , 1996, pp.612-624.

[241] Traub R, jeffreys J, Whitington M, "Fast oscillations in cortical circuits", 1999, MIT press.

[242] Tsodyks MV, Markram H., "The neural code between neocortical pyramidal neurons depends on neurotransmitter release probability", Proc Natl Acad Sci U S A. (1997), 94(2), pp. 719-23.

[243] Usret W, Reid R, "Synchronous activity in the visual system", Annual review of Physiology (1999), 61, pp.435-456.

[244] Van Brederode J, Spain W, "Differences in inhibitory synaptic input between layer II-III and layer V neurons of the cat neocortex", J Neurophysiology (1995), 74(3), pp. 1149-1166.

[245] van den Pol AN, Obrietan K, Chen G, "Excitatory actions of GABA after neuronal trauma" J Neurosci. 1996 Jul 1;16(13):4283-92.

[246] Van Rotterdam A et al, " A Model of the Spatial Temporal Characteristics of the Alpha rhythm", Bulletin of Mathematical biology, Vol 44, No. 2, 1982, pp. 283-305.

[247] Varela JA, Song S, Turrigiano GG, Nelson SB., " Differential depression at excitatory and inhibitory synapses in visual cortex", J Neuroscience (1999), 19(11), pp. 4293-304.

[248] Vienante P, Lavallee P, Deschenes M, "Corticothalamic projections from layer 5 of the vibrissal barrel cortex in the rat", J of Comparative Neurology (2000), 424, pp. 197-204.

[249] M Von Spreckelsen, B. Bromm, "Estimation of Single-Evoked Cerebral Potentials by Means of Parametric Modeling and Kalman Filtering", IEEE Trans. on Biomedical Engineering, Vol. 35 No 9, pp. 691-700.

[250] von Stein A, Chiang C, Konig P, "Top-down processing mediated by interareal synchronization", PNAS (2000),vol 97, No 26, pp 14748-14743.

[251] Wang Y , F. Yang, "Dynamic Evaluation of Visual Evoked Potentials through Spatial Analysis and Dipole Localization", IEEE Trans on Biomedical Engineering, Vol. 42, No 8, Aug 1995, pp. 762-768.

[252] Wang Z and McCormick D, "Control of firing mode of corticotectal and corticopontine layer V burst-generating neurons by Norepinephrine, acetylcholine and 1S,3R-ACPD", J Neuroscience (1993), 13(5), pp. 2199-2216.

[253] Wang XJ." Fast burst firing and short-term synaptic plasticity: a model of neocortical chattering neurons", Neuroscience (1999), 89(2), pp. 347-62.

[254] White E, "Cortical Circuits", Birkhauser, 1989.

[255] White E, Keller A, "Intrinsic circuitry involving the local axon collaterals of corticothalamic projection cells in mouse SmI cortex", J of comparative Neurology (1987), 262, pp. 13-26.

[256] Williams S, and Stuart G, "Mechanisms and consequences of action potential burst firing in rat neocortical pyramidal neurons", J Physiology (1999), 521 No 2, pp. 467-482.

[257] Williams S, Stuart G, "Site independence of EPSP time course is mediated by dendritic I_h in neocortical pyramidal neurons", J Neurophysiology (2000), 83, pp. 3177-3182.

[258] Williams S, Stuart G, " Backpropagation of physiological spike trains in neocortical pyramidal neurons: implications for temporal coding in dendrites", Journal Neuroscience (2000), 20(22), pp. 8238-8246.

[259] Wilson H and Cowan J, "Excitatory and Inhibitory Interactions in Localized Populations of Model Neurons", Biophysical Journal, Vol 12 1972, pp. 1-23.

[260] Wilson H, "Simplified dynamics of human and mammalian neocortical neurons", J Theoretical Biology (1999), 200, pp. 375-388.

[261] Wilson H, "Spikes, decisions and actions", Oxford University Press, 1999.

[262] Worden M, Foxe J, Wang N, Simpson G, "Anticipatory biasing of visuospatial attention indexed by retinotopically specific α-band electroencephalography increases over occipital cortex", Journal of Neuroscience (2000), Vol 20, RC63 (1-6).

[263] Wright J et al, "Gross electrocortical activity as a linear wave phenomenon with variable temporal damping regulated by ascending catecholamine neurons", Inter. J. Neuroscience, 1987, Vol. 33, pp.1-13.

[264] Wright J and R. Kydd, "The Electroencephalogram and Cortical Neural Networks", Network 3 (1992), pp. 341-362.

[265] Wright J et al, "Simulation of electrocortical waves", Biological Cybernetics, 72 (1995), pp. 347-356.

[266] Wu J-Y, Guan L, Yuang T, "Propagating activation during oscillations and evoked responses in neocortical slices", Journal of Neuroscience (1999), 19(12), pp. 5005-5015.

[267] Xiang Z, Huhuenard J, Prince D, "Cholinergic switching within neocortical inhibitory networks", Science, (1998) vol 281, pp. 985-988.

[268] Yordanova J, Kolev V., "Event-related alpha oscillations are functionally associated with P300 during information processing", Neuroreport (1998).

[269] Zhu J J, " Maturation of layer 5 neocortical pyramidal neurons: amplifying salient layer 1 and layer 4 inputs by Ca action potentials in adult rat dendrites", J physiology (2000), 526 (3), pp. 571-587.

[270] Zilberter Y, " Dendritic release of glutamate suppresses synaptic inhibition of pyramidal neurons in rat neocortex", J Physiol 2000 Nov 1;528(Pt 3):489-96.